PURINERGIC SIGNALLING IN OSTEOBLASTS

Thesis submitted in accordance with the requirements of the University of Liverpool for the degree of Doctor of Philosophy by

Alistair Bond

September 2012

List of abbreviations	
Abbreviation	Unabbreviated word(s)
2PK	Two-pore domain potassium channels
AA	Arachidonic acid
ABC	ATP binding cassette
ADP	Adenosine diphosphate
ALP	Alkaline phosphatase
ALS	Amytrophic lateral sclerosis
AMP	Adenosine monophosphate
ATP	Adenosine triphosphate
BMD	Bone mineral density
BMP	Bone morphogenetic protein
BzATP	O-(4-benzoyl)benzoyl adenosine 5'-triphosphate
Ca^{2+}	Calcium
Ca/CRE	Calcium/cAMP responsive element
cAMP	Cyclic adenosine monophosphate
CFTR	Cystic fibrosis transmembrane conductance regulator
cGMP	Cyclic guanine monophosphate
CNS	Central nervous system
COX	Cyclooxygenase
CREB	cAMP response element binding
CTP	Cystine triphosphate
DAG	Diacylglycerol
DEXA	Dual emission x-ray absorptiometry
DMEM	Dulbecco's modified Eagles medium
DNA	Deoxyribonucleic acid
ECL	Enhanced chemiluminscence
E-NPP	Ectonucleotide pyrophosphatases
ERK	Extracellualr signal-related kinase
FCS	Foetal calf serum
GIP	Glucose insulinotropic polypeptide
GTP	Guanine triphosphate
IGF	Insulin-like growth factor
IL	Interleukin
IP_3	Inositol triphosphate
K^+	Potassium
LAR	Luciferase assay reagent
LDH	Lactate dehydrogenase
LPA	Lysophosphatidic acid
MAPK	Mitogen activated protein kinase
MCS-F	Macrophage colony stimulating factor
NEM	N-ethylmaleimide
NFκB	Nuclear factor κ B
NMR	Nucleotide monitoring reagent
NO	Nitric oxide
NTP	Nucelotide triphosphate
OPG	Osteoprotegerin
PBS	Phosphate buffered saline
PCR	Polymerase chain reaction
PGE	Prostoglandin
PIP_2	Phosphatidylinositol 4,5-bisphosphate
PKA	Protein kinase A
PKC	Protein kinase C

PLC	Phospholipase C
PTH	Parathyroid hormone
PTHR	Parathyroid hormone receptor
RANKL	Receptor activator of nuclear κ B ligand
RNA	Ribonucleic acid
RPM	Revolutions per minute
SOD1	Cu/Zn superoxide dismutase 1
SRE	Serum responsive element
TCF	T-cell factor
TEA	Tetraethlyammonium
TGF-β	Transforming growth factor β
UDP	Uridine diphosphate
UTP	Uridine triphosphate
μCT	Micro CT

Acknowledgements

Firstly a massive thank you to my supervisor, Professor Jim Gallagher, for giving me the opportunity to study is his lab and for his constant support throughout my PhD. Also thanks to my secondary supervisor Prof. Jonathon Jarvis for his help and support throughout the years.

Thanks to my lab colleagues, Craig Kennan, Paul Rothwell, Vicki Waring-Green, Anne Gallagher, Elda Pacheco-Pantoja, Adam Taylor, Hamid Daabo and Firas Al-Ubaidy for your friendship through these years. You have all made it a great environment to work in. Thank you also to Rob Stephenson for his help with the micro ct scanning and analysis, and Dr's John Quayle and Tomoko Kamishima for their assistance in the study of BL-1249 on osteoblasts.

Special thanks to Jane Dillon for her help in the lab, and her friendship and support, and Dr Peter Wilson, again for his help on a day to day basis, but most importantly for all the cups of tea and golf help!

Thank you to all the HARC staff, especially Dr Rhian Lynch, for their support whilst writing this thesis.

Finally, and most importantly, thank you to my Mum, Dad and brothers, David and Keith for all your encouragement throughout my PhD.

Abstract

ATP is now well established as an extracellular signalling molecule and has been shown to play a role in many different tissues including bone. ATP acting on P2 receptors has been reported to cause an increase in osteoblast proliferation, apoptosis, IL-6 production, AA release and a decrease in bone mineralization. It has also been shown *in vivo,* by using KO mice, that ATP can cause both an anabolic and catabolic response depending on the P2 receptor involved, with P2Y2 KO mice showing an increased bone formation whilst P2X7 mice have a decrease in the periosteal bone formation. ATP is released from osteoblasts *in vitro* basally, following trauma to the cell and in response to mechanical strain. This mechanical strain comes in the form of medium displacements, where the medium is taken up in a pipette and then immediately washed over the cells. Work carried out in this thesis looked to refine the experimental procedure of these tests in an attempt to reduce the variation of ATP supernatant measurements following medium displacement experiments. A new experimental procedure has now been implicated that ensures that the luciferase enzyme, used to measure ATP, is kept under constant conditions, the measurements from the wells are taken from the same area and basal levels are measured in each well as it was determined that ATP measurements are not consistent throughout a single well. Further to this a sensitive measure of cell death was developed in order to ensure that the observed ATP release was not due to cell trauma. This used qPCR to measure mtDNA present in the supernatant.

Tests were also carried out to investigate the synergy between ATP and PTH as ATP synergises with PTH to increase the expression of *c-fos* in osteoblasts. *c-fos* is a master regulator gene that causes an increase in osteoblast proliferation and differentiation. It also causes the secretion of RANKL and decreases secretion of OPG, the RANKL decoy receptor, thus osteoclast fusion is also upregulated with an increase in *c-fos* production. Given that ATP is a local hormone that is released by mechanical stress and acts in an autocrine/paracrine manner and that PTH is an indiscriminate system wide hormone this synergy could be one mechanism whereby Wolff's Law is achieved. That is, BMD is increased in areas of higher loading. The mechanism of this synergy is still to be elucidated and is likely to be different between cell types. Experiments on UMR-106 cells has shown that ATP and PTH can cause a potentiation of intracellular calcium release that ultimately leads to increased *c-fos* transcription. In SaOS-2 cells two separate signalling pathways converge on different areas of the *c-fos* promoter to cause an increase in *c-fos.* Work carried out for this project now shows for the first time that ATP sensitises osteoblasts to the action of PTH. Given the short half life of both molecules this increases the likelihood that they do play a significant role in bone remodelling *in vivo*. The mechanism behind this sensitisation appears to be independent of the known mechanisms described above, as it was shown that the sensitisation was conferred in the medium and was not due to ATP break down products ADP, AMP and adenosine. Thus it is likely another, longer lasting, paracrine factor is involved.

BL-1249 is a putative K^+ channel opener and inhibits ATP+PTH induced *c-fos* expression. The inhibition was shown not to be due to BL-1249s effect on K^+ channels. It appears more likely that it acts on the cAMP/PKA pathway to inhibit *c-fos* transcription, as BL-1249 did not decrease FCS induced *c-fos* expression but did inhibit sp-cAMP induced *c-fos* expression. Further to this BL-1249 at concentrations of 100 µM caused a massive increase in cell death to the osteosarcoma cell lines SaOS-2, MG-63 and TE-85, however it had no effect on primary human osteoblasts. The apoptotic effect of BL-1249 is very likely due to the activation of K^+ channels as it has been reported that opening K^+ channels will cause apoptosis through K^+ efflux and subsequent cell shrinkage. This was further confirmed by use of TEA, a K^+ channel blocker, which acted to reverse the effect of BL-1249. Thus BL-1249 can act to decrease osteosarcoma cell number via inhibition of *c-fos* and, via K^+

channels, cause apoptosis. It is still unclear how apoptosis is targeted to osteosarcoma lines however it is likely through BL-1249s effect on *c-fos* expression.

Occasionally the true effect of a gene or protein can only be elucidated when studying it in the context of a pathology. It has been reported that P2X7 can cause astrocytes to be toxic to motor neurones by secreting factors that contribute towards their death. In situations of increased oxidative stress, such as those found in SOD1 -/- mice, this effect can be increased and cause basal levels of ATP to activate the neurotoxic phenotype of the astrocytes. SOD1 -/- mice have also been examined for the bone and muscle phenotypes. They were shown to have a massive reduction in muscle mass with the peak difference being less than 50% their wild-type counterparts, their bones also had a decrease in BMD, a decreased length of their femur and had a decreased stiffness. Given this link between SOD1, P2 signalling and an altered bone phenotype SOD1-/- mice were examined in more detail. μCT scans were used to analyse the bone structure of these mice, however in this study no differences were observed. P2X4 was increased in SOD1-/- calvarial cells whilst P2Y2 was decreased in these cells suggesting that oxidative stress does cause an altered P2 receptor expression and this may change the BMD of bone.

1. Introduction

1.1 Relevance of study in a clinical context

The work carried out in this thesis examines the role of P2 signalling in bone. P2 signalling has been shown to play a role in all bone cell types and can both increase and decrease bone mass. Given the effects of P2 signalling it is reasonable to suggest that with further research treatments could become available that alter the mass of bone. Many diseases are characterised by problems in the regulation of bone mass, for example, rickets, Paget's disease and osteopetrosis, however by far the most prevalent is osteoporosis.

Osteoporosis sufferers have a decreased BMD and as a result have an increased risk of fracture. 3 million people in the UK suffer from this disease despite the fact that there are effective treatments currently available [1]. One of the main treatments available are drugs known as bisphosphonates. These can reduce fracture risk from 25-70% depending on the bone [2]. However patients who are on this can suffer from osteonecrosis of the jaw. Alternatively PTH can be used to treat osteoporosis, however side effects including nausea and vomiting are present. Other treatments include strontium ranelate, selective oestrogen receptor modulators and calcium and vitamin D supplements.

It must be stressed that as well as the side effects that are present with these drugs there are still 250,000 osteoporotic fractures a year in the UK alone [1]. Further to this it has been observed that 13% of osteoporotic fractures are fatal in the following 6 months due to complications [3]. Therefore any studies that examine the regulation and manipulation of bone mass are worth investigating.

1.2 Bone biology

1.2.1 The structure of bone

Bone consists of mineralized type I collagen and a variety of bone cells, osteoblasts, osteoclasts and osteocytes. The collagen fibres are arranged in large sheets known as lamellae, which can be manipulated to form different types of bone. These are trabecular (a.k.a. spongy or cancellous) or compact bone. In compact bone the lamellae are folded to form a tube and surround each other in concentric circles, the innermost of which surrounds a single canal (see Fig 1.1). This canal contains blood vessels which supply the surrounding bone. The supply of bone is aided by the presence of canaliculi (small canals) which are a network of small tunnels that travel in and between the lamellae. They also allow the linkage of the entombed osteocytes which lie between the lamellae. This arrangement of bone is called the Haversian system and is only found in certain areas, mainly cortical areas (see Fig 1.1 (A)). In trabecular bone the lamellae are arranged in a large network of struts that are designed to withstand the application of force from any direction. They are orientated along the lines of stresses and are cross braced to provide support. They do not contain canals in which blood vessels travel, instead the canaliculi open out into the marrow space and therefore can obtain nutrients by diffusion (see Fig 1.1 (B)). As well as being able to withstand forces from all directions the purpose of having trabecular bone is to reduce the weight of the skeleton and also protect the cells in the red marrow.

Fig. 1.1(C) shows the overall macroscopic view of a long bone, in this case a femur. The two ends of the femur contain the trabecular bone and are called the epiphysis, whilst the intervening bone is termed the diaphysis, which is mostly marrow space with compact bone surrounding the edges. It must also be noted that wrapped around the bone is an extra layers of lamellae, called the circumferential lamellae. External to this exists the periosteum which has a fibrous outer layer and cellular inner layer. It actively participates in appositional growth and repair, and separates the bone from the surrounding tissue. It becomes continuous with the joint capsules and allows the attachment of ligaments and tendons. As the bone grows it allows these ligaments and tendons to become interwoven with the circumferential lamellae.

Bone has numerous functions, the most commonly known is that it provides support for the rest of the body to hang upon. As it is articulated it also allows leverage for muscles to act on. The skull, the thoracic cage, the pelvis and the vertebral column all provide protection for organs that reside inside them. As bone consists of mineralized collagen fibres it acts as a store for these minerals to be used when needed, for example during lactation calcium stores will be utilised. The bone also provides for the production of blood cells in the marrow cavity.

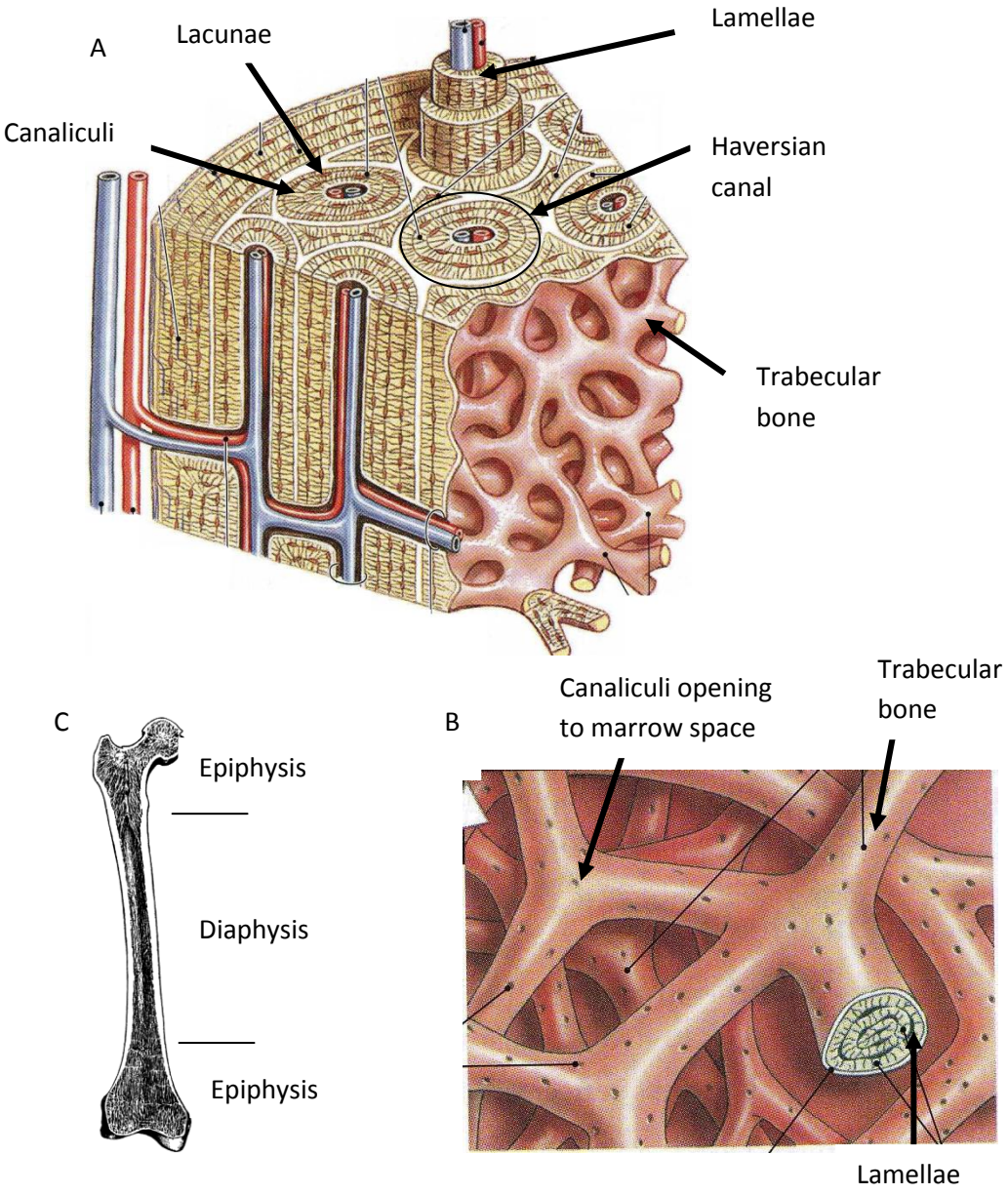

Figure 1.1 The structure of bone. (A) A microscopic diagram displaying the Haversian system. (B) A microscopic diagram of trabecular bone (Martina *et al 2006*). (C) The regions of a long bone (from: *http://etc.usf.edu/clipart/15400/15407/femurxsectn_15407*).

1.2.2 Bone cells

Bone consists of 3 cell types, osteoblasts, osteoclasts and osteocytes. Osteoblasts are the cells that produce bone and are derived from mesenchymal stem cells that are present locally. Osteoblasts can be told apart from other bone cells as they are cuboidal in cross section and can be seen as a layer of cells that line the matrix (see Fig 1.2 (A)). They produce bone individually but work as a group of cells. To form bone a fibrous portion, consisting mainly of collagen I, is secreted, this is termed the osteoid. As well as secreting matrix the osteoblast will also release factors such as alkaline phosphatase (ALP) or matrix vesicles, which contain calcium and phosphate, to aid in the mineralization process. These factors will raise the local concentration of calcium phosphate and promote the formation of hydroxyapatite thus the matrix will mineralize to form rigid bone [4].

As an osteoblast produces mineralized matrix it can become entombed in the bone, unable to make more as the bone will protrude into the osteoblast. When this entombing occurs the osteoblast terminally differentiates into an osteocyte which reside in areas called lacunae (see Fig 1.2(A)). The osteocytes are easily recognisable as they have numerous thin extensions that occupy the canaliculi that expand throughout the bone. They form gap junctions with other entombed osteocytes via their extensions. Through these they are able to pass on nutrients and signal to each other. Osteocytes help to maintain the protein and mineral content of the surrounding matrix and they can dissolve the immediate matrix around themselves to send nutrients into the blood supply. They are also involved in the repair of bone because if released from the lacunae they can de-differentiate into osteoblasts and aid in the formation of new bone [5].

Osteoclasts are responsible for breaking down bone. They are large multinucleate cells due to the fact that they are formed by the fusion of cells derived from the macrophage/monocyte lineage (see Fig 1.2 (B)). To decalcify bone and remove the organic matrix both acid and proteolytic enzymes are needed, both of which are produced and secreted by the osteoclast. To ensure that the hydrochloric acid does not demineralise other areas of bone the osteoclast seals itself against the adjacent bone via way of the clear zone of the osteoclast, which comprises a large amount of cytoskeleton. The

membrane of the osteoclast directly adjacent to the bone matrix is known as the ruffled border as it is highly folded, which helps increase the surface area [4].

The main body of work in this thesis concern the use of osteoblasts, in particular the osteosarcoma cell line SaOS-2. Osteosarcoma cell lines are used due to the fact that they still retain osteoblast phenotypes whilst being immortal and thus practical for use in cell culture work.

SaOS-2 cells are derived from a Caucasian girl aged 11 in 1973 [6]. Their osteoblastic capabilities were outlined in the paper by Rodan *et al* in 1987 [7]. It describes the SaOS-2 cell line as a useful tool in studying human osteoblasts as it produces calcifying matrix in a diffusing chamber. The production of mineralized matrix is, of course, a major indicator of the phenotype of osteoblasts. SaOS-2 cells can produce large amounts of ALP, an enzyme needed for bone mineralization, this is 5-10 fold higher than rat osteosarcoma cells or calvarial cells. Also SaOS-2 cells express parathyroid (PTH) receptors that are linked to adenylate cyclase, a property of bone cells both *in vitro* and *in vivo*. They also express $1,25(OH)_2D_3$ receptors, which are present in human osteoblasts. Finally SaOS-2 cells secrete osteonectin which is another protein associated with bone.

MG-63 cells are a less mature phenotype than SaOS-2 cells. They were obtained from a 14 year old male. They show expression of osteocalcin, bone sialoprotein and decorin, however they do not express ALP [8]. Te-85s were obtained from a 13 year old Caucasian girl. Unlike MG-63 cells they do express the marker of ALP, however they don't synthesise osteocalcin [8].

Due to the fact that SaOS-2 cells were more osteoblastic than MG-63 cells or Te-85 cells the decision was made to carry out the majority of experiments on the SaOS-2 cell line.

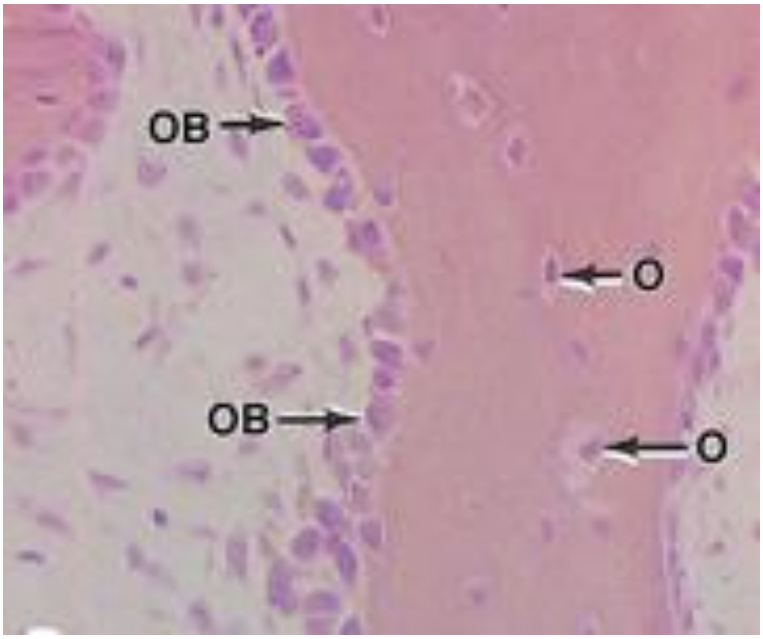

Fig 1.2 (A) A section of bone showing osteoblasts (OB) lining the surface of the bone matrix and osteocytes (O) present in lacunaes. (from:*http://accessmedicine.net/search/searchAMResultImg.aspx?rootterm=osteoblasts&rootID=25306&searchType=1*)

Fig 1.2 (B) A section of bone showing a multinucleate osteoclast in the process of bone resorption. (from:*http://www.lab.anhb.uwa.edu.au/mb140/corepages/bone/bone.htm*).

Figure 1.2 Histological appearance of bone cells

1.2.3 Bone remodelling

Bone is normally thought of as a rather inert substance that once grown to full length stays the same throughout life. This is not true, even once grown, and modelled to its optimum shape, the bone undergoes a constant turnover of resorption and formation called bone remodelling. All this occurs in localized areas throughout the skeleton [9]. There are certain stages in the process of bone remodelling that have been defined (see Fig 1.3). The majority of the time the bone exists in the

resting phase, however upon activation osteoclasts are recruited and will seek to resorb the bone. When finished they will perform apoptosis and the osteoblast precursors will differentiate and begin the process of formation. This is carried out to a certain pre-defined point before the bone enters the resting state again [10]. This process of marrying bone resorption with bone formation is termed 'coupling'. Although not fully understood, it is believed there are a number of reasons why bone undergoes remodelling.

One proposed reason is to maintain the homeostasis of Calcium (Ca^{2+}) throughout the body. However, as stated before, it is the job of the osteocyte to do this and it can be seen that the calcium exchange between blood and bone occurs at the osteocyte interface [10]. Therefore remodelling does not appear to be the main way that the body maintains its Ca^{2+} levels. However, there is evidence that when Ca^{2+} is in extreme need resorption by osteoclasts increases. This is apparent in a number of mechanisms. For example hens that are laying eggs will have increased resorption of their medullary bone. Or stags that are growing their antlers will ultimately have a fivefold increase in porosity due to resorption. Thus in this case, remodelling is allowing the 'borrowing' of Ca^{2+} for use elsewhere, but will eventually be laid down again [10].

This, however, is not the only reason why bone is remodelled, displayed by the fact that individuals experience bone remodelling who have no need to utilise Ca^{2+} so quickly. One theory is that by replacing bone one is simply renewing worn out portions, portions that are perhaps prone to micro cracks or contain stressed fibres. However another reason why remodelling occurs in individuals is due to the strain that is placed upon the bone. Wolff's law states that bone will adapt to the load that has been placed on it [11]. Bones that undergo more strain will adapt in a manner to resist that loading. This is best shown by the fact that the arm that a tennis player uses will have a higher mass than their other arm [12]. The same is true in reverse, bone that is not being loaded will be reabsorbed, which is best seen in the lower bone mass of astronauts [13]. As well as increasing bone remodelling in these areas, the balance between bone formation and bone resorption is also altered. Areas that are loaded will have an increase in bone formation or a decrease in bone resorption. Whilst areas that are not loaded will have a decrease of bone formation and/or an increase in bone resorption [14]. It is also

shifts in this balance that leads to bone diseases, such as osteoporosis or osteopetrosis. To measure the onset of bone remodelling *in vitro* we use the expression of *c-fos* in osteoblasts. *c-fos* is a master regulator gene that when expressed causes activation of osteoclasts through secreted signals and increases proliferation of osteoblasts [15].

The regulation of bone remodelling is extremely complex involving many systemic hormones and local growth factors. To begin with the osteoclast progenitors are recruited from haemopoietic tissues (i.e. the bone marrow or splenic tissues) to the bone site through the blood stream. They reach their destination via specific chemotactic signals [16]. These signals originally come from lining cells on the bone surface before this duty is taken over by the osteoclasts as they are resorbing [17]. Interleukin-1 (IL-1) and IL-6 have been highly implicated as being the signals that are secreted [17]. The osteoclast progenitors will proliferate and then, through interactions with osteoblast stromal cells, differentiate into mature osteoclasts [18]. The osteoclast will recognise that it is on the bone surface by using its integrin receptors, particularly the αvβ3 vitronectin receptor [19] which will bind to proteins like osteopontin. This recognition will allow the osteoclast to polarize its surface to form the clear zone and ruffled border. Osteoclasts are then activated by factors from the osteoblast lineage such as receptor activator of nuclear factor kappa-B ligand (RANKL) and macrophage-colony stimulating factor (M-CSF) [20, 21]. Once resorption has completed the osteoclasts will undergo apoptosis, which in itself highly regulated and can lead to higher resorption if left for longer, or less resorption if instructed to apoptose quickly [17].

Next the reversal phase which lasts around 9 days will occur, where osteoclasts have disappeared and osteoblasts have yet to arrive. Mesenchymal cells will eventually differentiate into osteoblasts and these will secrete the organic matrix and aid in the mineralisation process until the cavity is filled. This takes on average 140 days [10]. Again, like osteoclasts, there is likely to be a chemotactic signal sent out to recruit osteoblasts, or their precursors, to the resorption site. These factors are directly released from bone as it is resorbed. The main one being transforming growth factor β (TGF-β) [22], although type I collagen could also be involved [23]. Similarly released factors, such as TGF-β, insulin-like growth factor-I (IGF-I) and IGF-II will also aid in the proliferation of osteoblasts once

present. IGF-I and bone morphogenetic protein-2 (BMP-2) will cause the differentiation of the osteoblasts [24].

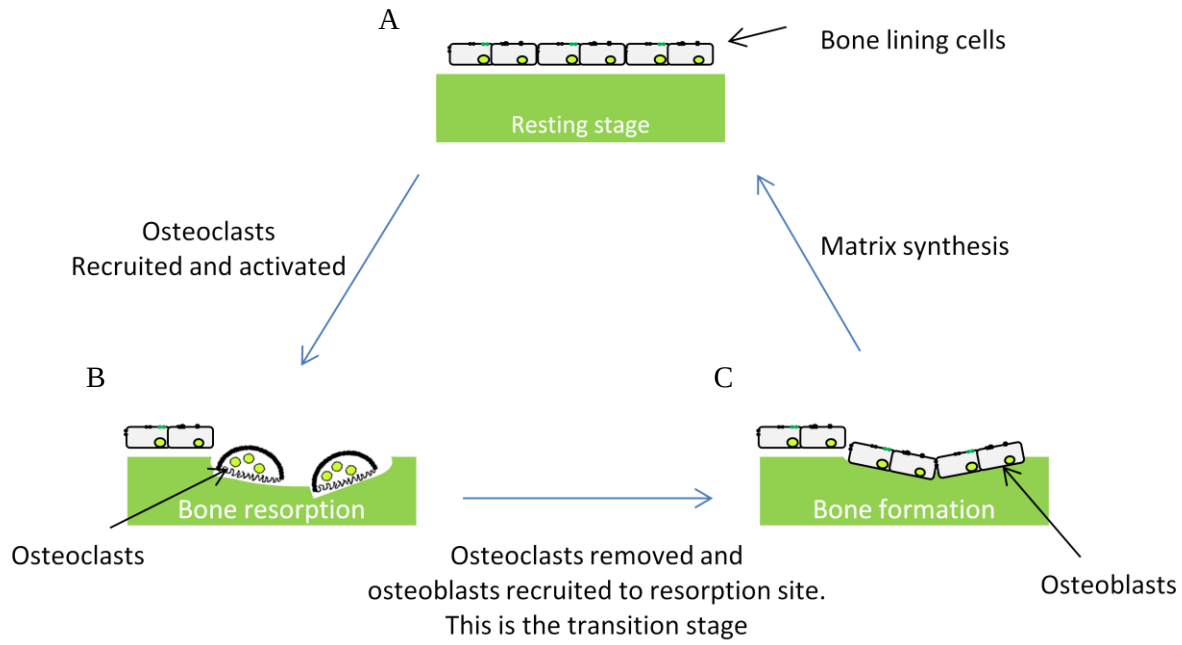

Figure 1.3 The process of bone remodelling. (A) Shows the bone at a resting stage with bone lining cells on the surface of the bone matrix. (B) Shows the cycle at the bone resorption stage. Bone lining cells have removed themselves from the resorbing area and osteoclasts have attached themselves and begun to remove the matrix. (C) shows the final stages of bone formation by osteoblasts. (adapted from:*http://www.lookfordiagnosis.com/mesh_info.php?term=Bone+Remodeling&lang=1*)

1.3 Purinergic signalling

1.3.1 An historical perspective

Adenosine triphosphate (ATP) is the product of cellular respiration and thus is well known as a source of intracellular energy [25]. It is produced from adenosine diphosphate (ADP) and inorganic phosphate under the presence of ATP synthase. The 3 phosphate groups that are attached are used as the sources of energy (see Fig 1.4). For example ATP can be used to phosphorylate signal transduction pathways or it can allow the active transport of compounds into the cell. These processes

convert the ATP back to ADP. Thus there is a continuous cycle of ATP production and breakdown within a cell.

However, although controversial to begin with, it is now widely accepted that ATP also acts as an extracellular signalling molecule. The first evidence showed that injecting 5'-adenosine monophosphate (AMP) into guinea-pig, rabbit, cat and dog heart caused a negative chronotropic effect and dilation of coronary blood vessels resulting in hypotension [26]. Then in 1963 it was shown that adrenergic and cholinergic blocking agents did nothing to prevent the hyperpolarisation of guinea pig taenia coli upon stimulation [27]. By 1972 it was becoming more apparent that there were autonomic nerves that released neither acetylcholine or noradrenalin, these nerves were termed non-adrenergic non-cholinergic (NANC). Evidence began to accumulate that showed the presence of these NANC nerves in the respiratory, cardiovascular and urogenital systems as well as in the gastrointestinal tract [28], thus experiments were undertaken to try to determine the novel neurotransmitter. ATP was identified as being a prime candidate to fulfil the requirements [29, 30] as it can be stored and synthesised in the nerve terminals from where it is released, it is released following stimulation, it interacts with receptors on the post synapse and there is an enzyme/ uptake system present in the synapse. Since then an enormous amount of evidence has been produced to support the purinergic theory (reviewed in [31]).

It also has become apparent that ATP, as an extracellular signalling source, is not limited to the nervous system. For example ATP can alter the tone of local blood vessels in a variety of ways [32], released from a sympathetic nerve it can constrict smooth muscles by acting on P2X receptors, released as part of a reflex it can act on P2Y receptors to constrict the blood vessels and released as a result of shear stress on endothelial cells it causes a further release of nitric oxide (NO) to relax the blood vessels [33]. In the respiratory system ATP acting on P2Y receptors on type II alveolar epithelial cells can cause surfactant secretion and transepithelial chloride secretion [34]. In the urogenital system ATP is released upon bladder distension and can be detected by sensory neurones and thus relayed to the brain [35]. ATP plays a major role in the immune system. It can cause release

of histamine from mast cells resulting in prostaglandin release or can cause killing of intracellular pathogens by inducing apoptosis of host macrophages [36]. ATP has also been heavily implicated as an anti-cancer treatment [37]. This is only a small sample of the reported functions of purinergic signalling since its first concept in 1973 and the list continues to expand to this day.

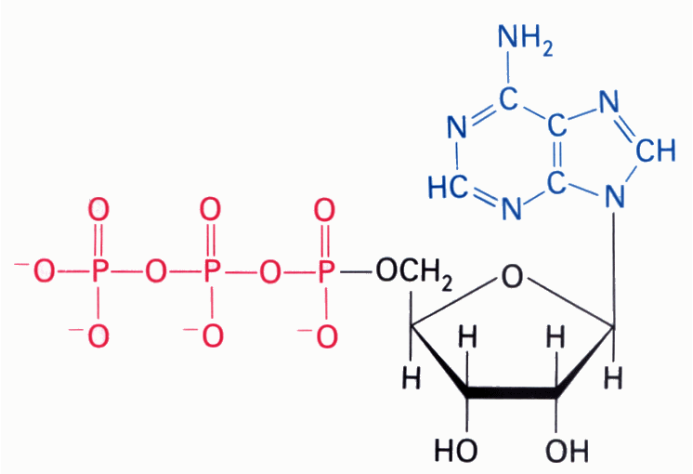

Figure 1.4 Molecular structure of ATP. Showing the 3 phosphate groups in red attached to a ribose sugar (in black). This is attached to the adenine (in blue) to make up the nucleoside adenosine (from: *http://www.bmb.leeds.ac.uk/teaching/icu3/lecture/19/index.htm*)

1.3.2 The classification and structure of P2 receptors

The receptors for purines were first discovered in 1976 [38] and were subsequently split into two types, P1 receptors that bind adenosine and P2 receptors which bind ATP and ADP [39]. In 1985 the first attempts were made to further subdivide the P2 receptors into two groups, P2Y and P2X. At this stage they were named due to their action on smooth muscle cells. P2X receptors would cause a contractile response to ATP, P2Y on the other hand would cause smooth muscle to relax. P2Y was then further subdivided based on the potency of its agonists. P2U responded to both ATP and uridine-5'-triphosphate (UTP) whilst P2T was only responsive to ADP [40]. This classification of P2

receptors did not last, nowadays they are named due to their transduction methods [41]. P2X are ionotropic receptors whilst P2Y are G-protein coupled receptors. There are seven P2X receptors and eight P2Y receptors, which are again named due to their preferential agonist binding.

P2X receptors have both N- and C- terminal domains existing intracellularly, they contain the binding domains for protein kinases. They also have two transmembrane domains, the first being involved with the gating of the channel. A large extracellular loop is present which contains the ATP binding domain, also present is an extracellular hydrophobic domain for possible modulation by cations. To form a complete channel 3 of the subunits are needed, thus a P2X receptor can exist as a homomultimer or a heteromultimer [42].

The P2X1 receptor shows little selectivity for sodium (Na^+) over potassium (K^+) and has a relatively high permeability to Ca^{2+}. It is also a fast desensitization channel, meaning the decline in current, after the initial ATP induced high current, occurs quickly [43]. P2X2 on the other hand is non-desensitizing and is potentiated by protons and low concentrations of zinc and copper. P2X3 is very similar to P2X1 receptors in their fast desensitization, they are predominantly expressed on nociceptive sensory neurones [44]. P2X4 receptors have very high permeability to Ca^{2+} and also notable is the fact that if ATP is left on for several seconds the channel allows the passage of larger cations, such as N-methyl-D-glucamine [42]. P2X5 receptors are most noted for the very small currents that are allowed to pass. Interestingly P2X6 cannot function alone as a homomultimer, it always needs to be present as a heteromultimer. The P2X7 receptors are the most studied and interesting receptors because once activated it can form a large pore. This can be seen by the fact that large dye molecules, such as YO-PRO, are permitted to pass through the cell membrane. Activation of P2X7 also causes the production of membrane blebbing, signalling the onset of apoptosis [42].

As with all G-protein coupled receptors the P2Y receptor N-terminals are extracellular and they have 7 transmembrane domains (α helices). These are connected by 3 intracellular and 3 extracellular loops, with the C-terminus being intracellular. The 7 transmembrane domains are arranged in a circular fashion in the membrane and ligands can either bind here, the extracellular loops, or the tail.

Upon binding the helices of the transmembrane domains undergo a conformational change that leads to downstream signalling (this will be discussed in more detail in 1.2.3). To down regulate the response of G-protein coupled receptors they can either be internalized or can be decoupled from their G-proteins by way of β-arrestin action [45].

There are 8 P2Y receptors in humans, 1,2,4,6,11,12,13 and 14 [46, 47]. The gaps in the numbering is due to non-mammalian orthologs, or receptors that are very similar structurally but have no evidence of binding to nucleotides. The P2Y1 receptors most potent agonist is ADP, it is highly expressed in the brain, prostate gland and the placenta and is insensitive to UTP, UDP, cytidine triphosphate (CTP) and guanine triphosphate (GTP) [48]. The P2Y2 receptors are activated equally by ATP and UTP, the mRNA of the receptor has been shown in numerous cell types [49]. It couples to PLCβ_1 via the $G_{aq/11}$ protein to cause production of inositol triphosphate (IP_3) and diacylglycerol (DAG). It has been shown that P2Y2 activation can cause release of arachidonic acid (AA), prostaglandins (PGE) and NO [50, 51]. Tests which have up regulated the P2Y2 receptor have increased ATP induced activation of the mitogen activated protein kinase (MAPK) pathway, protein kinase C (PKC) and cyclooxygenase (COX) [52]. UTP is the potent activator of P2Y4 receptors, which is most prevalent in the intestine [49]. Its function is best displayed in P2Y4 knockout mice which have been shown to be completely normal except that the epithelia in the intestine is unable to secrete chloride in response to nucleotides [53]. P2Y6 is activated by uridine diphosphate (UDP) [54] and uniquely is very slow at desensitizing and internalizing. P2Y11 is the only receptor to contain an intron in its coding sequence and is dually coupled to phosholipase C (PLC) and adenylate cyclase [55]. P2Y12 like P2Y1 has ADP as a natural agonist, and can cause direct transduction through the N-type Ca^{2+} channels in neurones. Interestingly the knockout of P2Y12 showed the phenotype of one who is on clopidogrel [56, 57], that is, a bleeding phenotype. P2Y13 is activated by ADP and Ap3A and is coupled to a $G_{i/o}$. The P2Y14 receptor is activated by UDP and also couples to $G_{i/o}$ [42].

1.3.3 P2 signalling pathways

P2Y receptors are G-protein coupled receptors thus they are linked to a group of GTPases. These GTPases can bind GTP, in which they are termed 'on', or they can bind to guanine diphosphate (GDP) (off). Once activated, by a conformational change in the receptor, the P2Y receptors will bind GTP, which allows the G_{α} subunit to dissociate from both the receptor and the $G_{\beta y}$ subunit. Both of these subunits can effect downstream pathways [58] (see Fig. 1.5). The type of G- protein that is attached to the receptor determines the signalling pathways it will induce. There are four main types of G-protein, $G_{\alpha s}$, $G_{\alpha i/o}$, $G_{\alpha q/11}$ and $G_{\alpha 12/13}$ [59].

$G_{\alpha s}$ are found on P2Y11 receptors and will cause activation of adenylate cyclase which generates cyclic AMP (cAMP) from ATP. cAMP will then activate protein kinase A (PKA) as binding of cAMP to the regulatory domain of PKA causes dissociation of its catalytic subunits, which are then free to phosphorylate further protein substrates. These proteins cause the transfer of phosphates from ATP to serine or threonine residues on other proteins [60]. There are also some PKA independent properties of cAMP, for example cAMP can cause activation of Ca^{2+} channels. Both P2Y12 and P2Y13 have $G_{\alpha i/o}$ coupled to them which does the opposite to $G_{\alpha s}$ as it inhibits adenylate cyclase from activating PKA and therefore prevents the downstream signalling seen above [61]. $G_{\alpha q11/12}$ is seen on the vast majority of P2Y receptors, 1, 2, 4, 6, 11 and 14. This activates PLC which causes the cleavage of the membrane bound phosphatidylinositol 4, 5-biphosphate (PIP_2). It splits it into two active second messengers, IP_3 and DAG. IP_3 will act on receptors found on endoplasmic reticulum to cause a Ca^{2+} release from its stores which can cause downstream signalling through the calmodulin proteins. DAG will cause activation of PKC, which incidentally can also be activated by Ca^{2+} thus the two pathways can converge. Like PKA, PKC will cause phosphorylation of proteins downstream [62]. There are no $G_{\alpha 12/13}$ proteins linked to P2Y receptors, they activate small GTPases, such as RhoA which generally go on to activate other proteins that are responsible for the cytoskeleton [63].

The P2X receptors, being ligand gated ion channels, are heavily involved in neurones and the activation or inhibition of action potentials. However they are able to raise intracellular Ca^{2+} which can activate MAPK pathways in other non-bone related cells. P2X7 is unique amongst P2 receptors as it has been shown to couple to proteins that can activate downstream pathways [43].

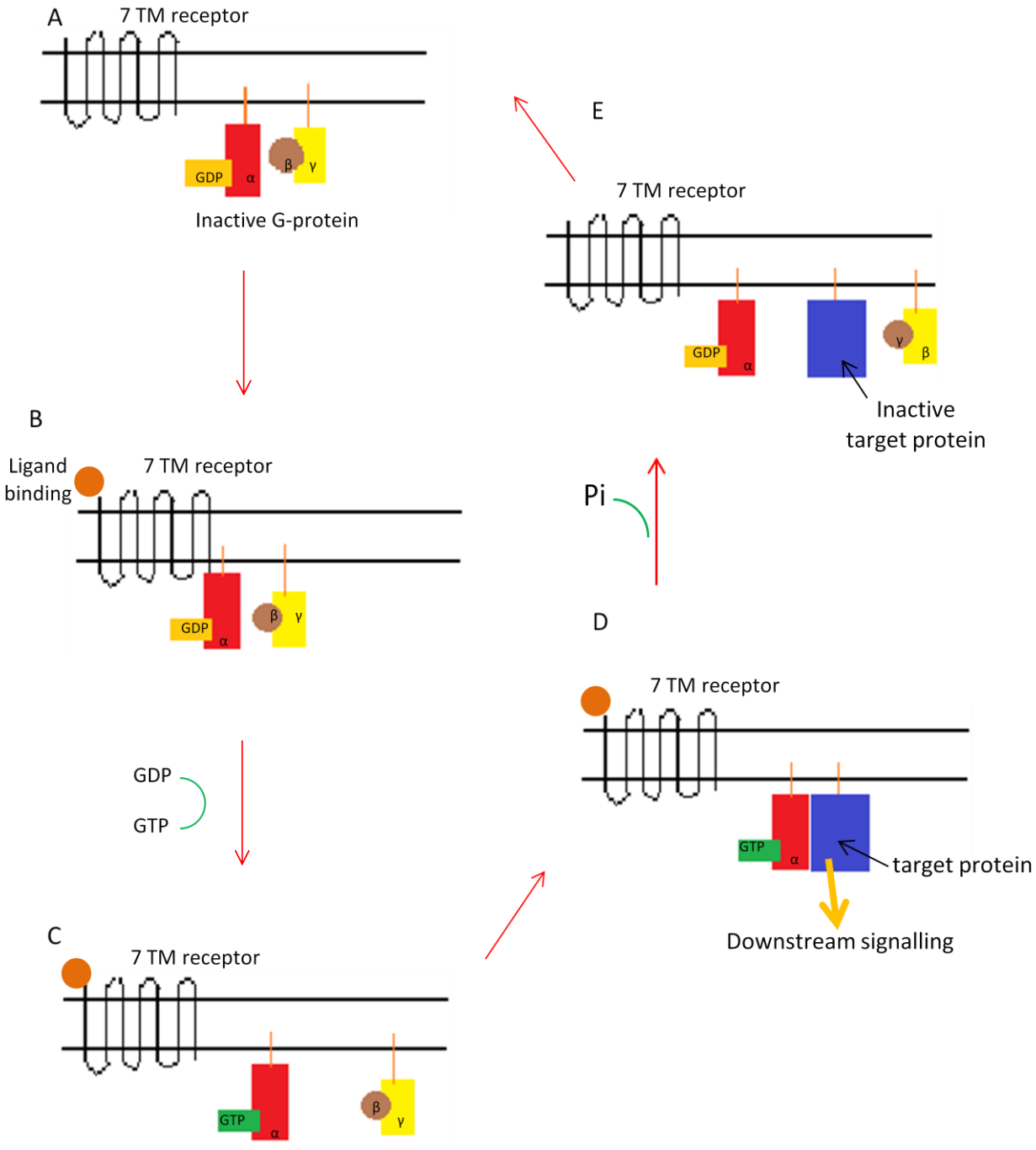

Figure 1.5 Signalling through G protein-coupled receptors. (A) All components of the signalling pathway are shown in their inactive form. (B) The change in conformation of the 7TM receptor on ligand binding brings about the binding of the trimeric G protein. (C) GTP binds and activates the α subunit, which becomes dissociated from the βγ complex. (D) The α subunit binds and activates target proteins, which also act as effectors and propagate the signal. (E) Inactivation of the α subunit via GTPase activity (intrinsic or accessory) results in dissociation from the target protein, which itself becomes inactivated, and formation of the inactive trimeric G protein complex by association with a βγ complex (A). (adapted from :*http://openlearn.open.ac.uk/mod/oucontent/view.php?id=398848&section=3.2*)

1.3.4 Purinergic signalling in bone

SaOS-2 cells express P2Y1, P2Y12, P2X2, P2X4 and P2X7 receptors [64]. MG-63 cells express P2Y1, P2Y2, P2Y4, P2Y6, P2X2, P2X4 and P2X7 receptors. The abundance of P2 receptors in these osteoblast cells go a long way to showing how important P2 signalling is in bone. It should be known that the expression of P2 receptors in osteoblasts is highly dependent on the species it comes from, the differentiation state of the osteoblast and whether it comes from a primary or osteosarcoma cell.

The affect of P2 receptors in bone is still to be completely illuminated, there is a varied response and it often appears contradictory. This is likely due to the fact that there are at least 3 different cell types in bone that are being influenced by nucleotides, All of which can perform different functions at different stages of differentiation and with different concentrations of ATP. This section will look at what is known so far.

When ATP is added to MC3T3-E1 osteoblasts there is an increase in the rate of proliferation [65]. Also there is an increase in the synthesis of deoxyribonucleic acid (DNA) when P2X receptors were specifically activated in MG-63 cells [66]. These would suggest an anabolic response to nucleotides as an increase in osteoblasts will increase bone formation. However, it has also been shown in rat calvarial osteoblasts *in vitro* that treating cells with 1-100μM of ATP or UTP reduced the amount of alizarin red staining, suggesting a decrease of mineralized bone [67, 68]. In fact, what became apparent was that osteoblasts were still secreting collagen to make osteoid but this was not mineralizing [69]. The ALP activity was decreased by 65%. The P2Y4 antagonist, reactive blue 2, failed to stop this inhibition of mineralisation and thus it was assumed P2Y2 was the receptor responsible [69]. P2Y2 knockout mice have a massive increase in cortical and trabecular bone, measured by micro-ct (μ-ct) and by dual-emission X-ray absorptiometry (DEXA) scanning. This backs up the *in vitro* evidence for the role of the P2Y2 receptor [69, 70].

The P2X7 receptor's most potent agonist is 2',3'-*O*- (benzoyl-4-benzoyl)-ATP (Bz-ATP) and if stimulated with a long exposure or with repeated small exposures P2X7 causes the formation of large

cytolytic pores. If stimulated transiently it will open up pores that allow larger non-selective molecules through [71]. This is the case in osteoblasts, with first reports showing apoptosis occuring after membrane blebbing [72]. More recent studies, using lower concentrations of the agonists, have shown that stimulating P2X7 actually increases bone formation and ALP activity, possibly due to an increase in PGE_2 production and lysophosphatidic acid (LPA) [73, 74]. Again knockout mouse models agreed with the *in vitro* work which show P2X7 knockouts have a decrease in periosteal bone formation and cultured osteoblasts had reduced osteogenesis and ALP activity [75, 76]. Thus it seems that the type of nucleotide and the concentration that stimulates osteoblasts will affect the anabolic or catabolic response of bone. There have been other recorded actions of nucleotides. P2X5 activation has caused proliferation [66] and P2Y activation has also been shown to increase IL-6 synthesis [77] and AA release [78].

Another interesting factor is that ATP does not need to act on P2 receptors to have an influence on bone remodelling. This is due to the fact that when ATP is broken down by ectonucleotide pyrophosphatases (E-NPPs) it generates pyrophosphates (PPi) which are inhibitory to bone mineralization. Osteoblasts have been shown to express 3 members of the E-NPP family, E-NPP1, E-NPP2 and E-NPP3 [69, 79]. An interesting study showed that CTP and GTP can be hydrolysed and inhibit bone mineralisation without altering ALP expression at concentrations between 1 and 100 µM. Given that they are only very weak agonists of P2Y2 and P2Y4 this shows that nucleotide triphosphates (NTPs) can exert a dual inhibitory effect via both P2 receptor mediated and PPi production [69].

Osteoclasts also express numerous P2 receptors and thus can be directly stimulated by nucleotides. It has been shown that ATP, and not UTP, can stimulate osteoclast resorption in both human osteoclastomas and in rodent osteoclasts [80-82]. This response acts through the P2Y1 receptors at micromolar ATP, ADP and 2-MeSADP concentrations. Another factor that will be discussed in section 1.3.1 is that nucleotides can stimulate osteoblasts to secrete RANKL and thus can influence resorption indirectly.

The role of the P2X7 receptor in osteoclasts is complex and in contrast to the above. Antagonising P2X7 on osteoclasts that were derived from human peripheral blood appeared to inhibit the formation of osteoclasts [83] and also another antagonist KN-62 caused apoptosis of these osteoclasts [84]. However it has been shown that P2X7 knockout mice have functional osteoclasts, and osteoclasts could be generated *in* vitro using precursors from the same mice [75], Although it has since been shown that these KO mice were not completely null for the P2X7 receptor as a splice variant was still expressed. However this splice variant was only found to be expressed in the salivary gland and the spleen, and therefore may not have had an effect on the reported findings in bone [85]. The importance of P2X7 in bone is in no doubt though; as loss of function polymorphisms in P2X7 have been shown to decrease BMD and cause an increased fracture risk for post menopausal women [86-88]. Activation of P2X7 has also been shown to activate and translocate nuclear factor κ B (NFκB) and PKC, which play a role in intracellular communication, reorganize the cytoskeleton and secrete lytic granules into the resorption lacunae [89-92]. Activation of P2Y6 inhibited the apoptosis of osteoclasts induced by tumour necrosis factor α (TNFα), and was also shown to stimulate and translocate NFκB [93], Thus helping osteoclast survival.

Unlike osteoblasts and osteoclasts there is very little known about osteocytes in relation to purinergic signalling. Although the expression of P2 receptors on osteocytes are yet to be confirmed it seems very likely that they are present as mature osteoblasts express them. There is also some evidence that ATP is released from cultured osteocytes (MLO-Y4) [94].

1.3.5 The release of ATP from osteoblasts and other cell types

It is clear from the amount of P2 receptors that are expressed on bone cells that ATP plays a major role in bone physiology but how does ATP get to the extracellular environment around bone cells? ATP is a well characterised neurotransmitter but there is no evidence that extracellular ATP comes via that mechanism in bone. ATP is released from all cells during trauma and inflammation however it is unlikely that this is the case in osteoblasts. For nucleotides to play a part in bone biology there needs

to be a mechanism for bone cells to release ATP to the extracellular space regularly and in large enough concentrations to activate the receptors. Fig. 1.6 displays the proposed mechanisms of ATP release in osteoblasts. ATP release has been shown in many other cell types (reviewed in [95]) and shows that ATP works in an autocrine or paracrine way. Early results in bone, using a real time detection system [96], showed that ATP was constitutively released from osteoblast cells [97, 98]. SaOS-2 cells have shown ATP basal release that increases in a linear fashion with cell number, with no increase in conventional cytotoxicity markers [64]. The ATP concentration was shown to be in the nanomolar range, however it is likely to be higher closer to the cell surface due to membrane trapping and the fact that the volume of space *in vivo* is smaller. This effect was shown to be true with platelet cells after a study used a membrane anchored luciferase [99].

As described in section 1.1.3 loading plays an important part in bone remodelling. Bone cells, like any other cells, sit in tissue fluid and as such any loading on a bone may transmit itself to the cell membrane in a fluid flow/shear stress manner. It has been shown in HOBIT, SaOS-2 and Te-85 cells that medium displacements cause an increase of extracellular ATP over basal levels [100, 101]. ATP release has also been shown in MC3T3-E1 cells, as well as in SaOS-2 cells, when subjected to a flow of 12 dyne/cm^2 for 5 minutes in a parallel flow chamber [80]. Studies have also been carried out to try to replicate the structure of bone i.e. not to have a monolayer of cells but to have osteoblasts contained in a 3D structure. To do this polyurethrane scaffolds were made and SaOS-2 and Te-85 cells were grown in them. This scaffold could then be put under compressive forces. This did not cause a release of ATP, however when cells in the same scaffold were subjected to fluid flow there was an increase in ATP concentrations, suggesting that fluid flow is the method cells use to detect strain [102].

The mechanism of ATP release in osteoblasts is still to be completely illuminated, though current research suggests 4 main areas that could be responsible for ATP release; these being exocytosis, connexions/pannexins, ATP-binding cassette (ABC) transport proteins or through the pore that is created upon P2X7 activation.

The evidence for ATP being released in vesicles is fairly strong. Using the exocytosis inhibitors, brefeldin A, monensin and N-ethylmalemide (NEM) ATP release in response to fluid flow was inhibited in MC3T3-E1, SaOS-2 and Te-85 cells [80, 103-105]. Also osteoblasts derived from rats release ATP in response to hypoxia which was inhibited by NEM [82]. Furthermore when HOBIT cells have been stained with quinacrine, which binds to ATP, there was a distinct granular appearance that seems to suggest ATP was contained in vesicles and when treated with monensin this staining disappeared [106]. Altering the Ca^{2+} conditions affects the release of ATP, of course an increase in intracellular Ca^{2+} increases exocytosis. For example increasing extracellular Ca^{2+} resulted in a 3 fold increase of ATP release from MC3T3-E1 cells [80], inhibition of Ca^{2+} voltage gated channels inhibited ATP release following shear stress [80] and chelating Ca^{2+} inhibited shear stress induced ATP release from Te-85 cells [81]. It must be noted that in these papers the exocytosis inhibition never completely inhibited ATP release suggesting more than one mechanism may be in place.

There is evidence that gap junctions play a role in ATP release. Gap junctions are well known for their role in cell communication as they join together adjacent cells. Each cell has a hemichannel that attaches to another hemichannel to form a complete gap junction. They allow movement of ions and small molecules between cells [107] and in astrocytes have been shown to permit the movement of ATP [108]. The theory is that if a gap hemichannel opens to the extracellular space ATP could be released via this. Forced expression of connexions (the proteins that combine to create a hemichannel) caused an increase of ATP release in glioma cells [109]. However, this was not the case in HOBIT cells over expressing connexion 43 [100]. Pannexins are a recently discovered protein that also make up hemichannels and have been shown to be involved in ATP release from taste buds in mice and in the retina of cows [110, 111]. These proteins have been shown to be present in osteoblasts but as yet no study has examined them.

ABC proteins are transport proteins that have nucleotide binding sites in them. 3 of the 48 different proteins have been shown to allow ATP transport across the cell membrane. These are P-glycoprotein, cystic fibrosis transmembrane conductance regulator (CFTR), and the sulfonylurea receptor [112].

Interestingly, independent of any purinergic studies, these have been shown to be important in bone. People with Addison's disease, which is characterized by decreased bone mineral density, have been shown to have polymorphisms in the p-glycoprotein gene [113]. CFTR has been shown to exist in primary and MG-63 osteoblasts and studies have shown that it can regulate osteopontin and PGE_2 [114, 115]. No direct link has yet been established yet between ATP release and ABC transporters in osteoblasts.

Activation of P2X7 receptors, when exposed to ATP for long enough, will cause a pore to open which allows large molecules to pass. Astrocytes obtained from P2X7 knockout mice could no longer release ATP, however bone cells from the same mice could still release ATP in response to mechanical loading [116, 117], again suggesting a dual mechanism for ATP release. Interestingly antagonists of P2X7 inhibited fluid flow release of ATP in SaOS-2 cells, but not Te-85 cells, which do not express P2X7 [101].

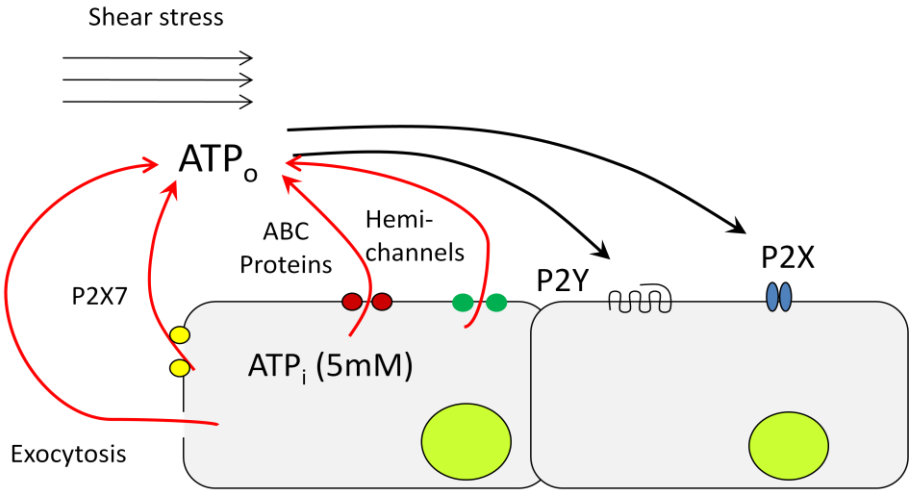

Figure 1.6 ATP release from osteoblasts. This is a diagram of the proposed methods of ATP release from osteoblasts. These being exocytosis, P2X7 proteins, ABC proteins and gap hemi-channels.

1.4 Synergy of ATP and systemic hormones

1.4.1 An overview of PTH

PTH functions to increase the concentration of Ca^{2+} in the blood. It is released from the parathyroid gland, specifically the chief cells, and is the antagonist of calcitonin which acts to decrease Ca^{2+} in the blood. PTH acts on both the PTH receptor 1 (PTHR1), and the PTH receptor 2 (PTHR2). PTHR1 is found in bone and kidney whereas PTHR2 is found in the central nervous system (CNS), pancreas, testis and the placenta. PTH exerts its effect in 3 ways which are described below.

The first being that it causes the resorption of bone via its effects on osteoblasts [118]. Osteoclasts do not express a functional PTH receptor and thus PTH acts on them indirectly through osteoblasts. Upon binding PTH causes the osteoblast to up regulate RANKL and decrease the expression of osteoprotegerin (OPG), OPG is the decoy receptor for RANKL. When RANKL binds to RANK, it causes the fusion of osteoclast precursors to form mature resorbing osteoclasts. This up regulates bone resorption and therefore more Ca^{2+} will be present within the blood stream.

PTH also causes active resorption of Ca^{2+} in the ascending part of the distal convoluted tubule in the kidney and it acts on the intestine to increase the uptake of Ca^{2+}. However, like in bone, it acts on the intestine indirectly. PTH works on the kidneys to increase the levels of 25-hydroxyvitamin D_3 1-alpha-hydroxylase. This enzyme converts the inactive form of vitamin D to the active form which then acts on the intestine via calbindin to cause an increase in Ca^{2+} uptake

The release of PTH is dependent upon the Ca^{2+} levels in the serum, therefore chief cells have Ca^{2+} detecting receptors on them which are G-protein coupled receptors. When Ca^{2+} is present the G_q subunit will activate PLC and ultimately cause release of intracellular Ca^{2+}. Unusually this does not cause release of PTH from their vesicles; instead it causes downstream signals which inhibit the process of PTH release. When no binding occurs PTH is released, which is actually mediated through high levels of magnesium.

Apart from the catabolic function of PTH, in 1985 (*in vitro*) [119] and 1993 (*in vivo*) [120], it was shown that PTH could, under different circumstances, be an anabolic agent for bone. The difference appeared to be how long PTH stimulation occurred for. Prolonged exposure will lead to an increase in resorption, however when only intermittently stimulated, bone formation increases [121, 122]. This is actually in use today as an osteoporosis treatment, once a day injections of PTH will increase bone mass in these patients [123], as well as in ovariectomized monkeys [124]. This anabolic response may result from an increase in osteoblast cell number, either through formation of more osteoblasts from bone lining cells [125], or from an increase in proliferation of already differentiated osteoblasts [119]. PTH has been shown to stimulate the MAPK pathway in numerous cell types including osteoblasts [126-128] and it is likely that through this pathway an increase in osteoblast numbers is observed. However PTH does not act through its normal PKA pathway to activate the MAPK pathway [129, 130], instead it acts through PKC [126]. There is also another argument that the anabolic response is due to a decrease in osteoblast apoptosis. With PTH being shown to either increase or decrease apoptosis depending on which cell type it is being used on [131, 132].

1.4.2 The intracellular signalling pathways induced by PTH in osteoblasts

PTH can have a dual effect on bone. A lot of studies in various labs have attempted to ascertain this mechanism. The PTH receptor is a 7 transmembrane G-protein coupled receptor and specifically belongs to a sub set that contains the calcitonin and secretin receptors. Interestingly, as it is coupled to both $G_{\alpha s}$ and $G_{\alpha q}$ it can signal through both adenylate cyclase and PLC (see Fig.1.7). There have been areas of investigation that suggested PTH exerted its dual effect by acting on different receptors, or splice variants of the same receptor, to start different signalling cascades. While there is a 2nd PTH receptor and others have been claimed to exist, PTHR1 is the only one that has been found to be expressed on osteoblasts [133], although there is evidence that signalling may arise from different splices of this [134].

However it is more likely that the dual response is due to the fact that the PTH receptor can signal to multiple pathways. By activating adenylate cyclase PTH can cause the formation of cAMP, which releases the catalytic subunits of PKA. PKA phosphorylates specific serine residues on certain transcription factors [135]. Also PTH can stimulate the release of intracellular Ca^{2+} via activation of PLC, causing the formation of DAG. DAG activates PKC and IP_3 which leads to the Ca^{2+} release [136]. PTH can also activate additional pathways such as stimulating an extracellular influx of Ca^{2+} either with or without cAMP [137] or with PKC [138].

PTH can activate many transcription factors, but mainly CREB, AP-1 and RUNX2. CREB is phosphorylated by PKA and this leads to the transcription of *c-fos* [139]. *c-fos*, as described earlier, is a master regulator and early marker of bone remodelling. Many kinases are able to phosphorylate CREB but PKA is the vital one in osteoblasts. Recent evidence, however, suggests that GSK-3 plays a large role and that phosphorylation of CREB by GSK-3 may be a necessary pre-requisite for PKA phosphorylation [140, 141].

c-fos itself is a transcription factor that regulates other genes. It is a protein that is a member of the basic/leucine zipper (bZIP) family of transcription factors. In addition to *c-fos*, the expression of other bZIP family members is stimulated by PTH, including c-jun, fos-B, jun-B and fra-1 [142-144]. When *c-fos* heterodimerizes with members of the Jun family it forms a stable complex called AP-1, whose effects can be seen in mouse studies. Overexpression leads to osteosarcomas due to increased proliferation [145] whilst deletion has no effect on osteoblasts, likely due to another member of the *c-fos* family stepping in [146, 147]. But deletion does cause inhibition of osteoclastogenesis, as *c-fos* causes expression of RANKL which will activate the osteoclast [148]. RUNX2 causes transcription of osteocalcin, osteopontin, collagen α1 and α2 and collagenase 3. Again RUNX2 is activated through the PKA pathway. Mice lacking the RUNX2 die before birth due to lack of ossification [149], in humans it has been linked with cleidocranial dysplasia [150].

Through these transcription factors PTH stimulates and inhibits numerous genes. RANKL, MCS-F, IL-6, collagenase 3, *c-fos*, c-jun and osteocalcin are the most noted stimulated genes. It causes inhibition of type 1 collagen, osteopontin, osteonectin, and ALP [135]. Although this suggests that PTH only transcribes catabolic genes this is not always the case. For example collagenase 3 is expressed in rat ossification centres [151], in areas of the rat calvarium that is undergoing modelling [152] and in humans it is expressed during ossification of the ribs and vertebrae [153]. In other words although linked to the resorption of bone it is clear that the resorption is closely coupled with new formation.

The anabolic effect that PTH has on bone is likely due to the fact that there are more osteoblasts present. PKC signalling can activate MAPK signalling pathways that result in the phosphorylation of extracellular signal related kinases (ERK) [126, 128]. For a cell to proliferate faster it needs to reach and progress through the checkpoints of the cell cycle quicker. An active ERK allows progression through the Gap 1 (G1) part of the cell cycle, and thus could explain the increase in proliferation seen *in vitro* in Te-85 cells [154, 155]. In addition to this, PTH treatment can also cause expression of numerous growth factors that will aid in osteoblast proliferation, for example IGF-I, IGF-II, IGF binding proteins and TGF-β [156]. Also the fact that PTH can cause initial resorption means that eventually new bone will form due to the coupling effect.

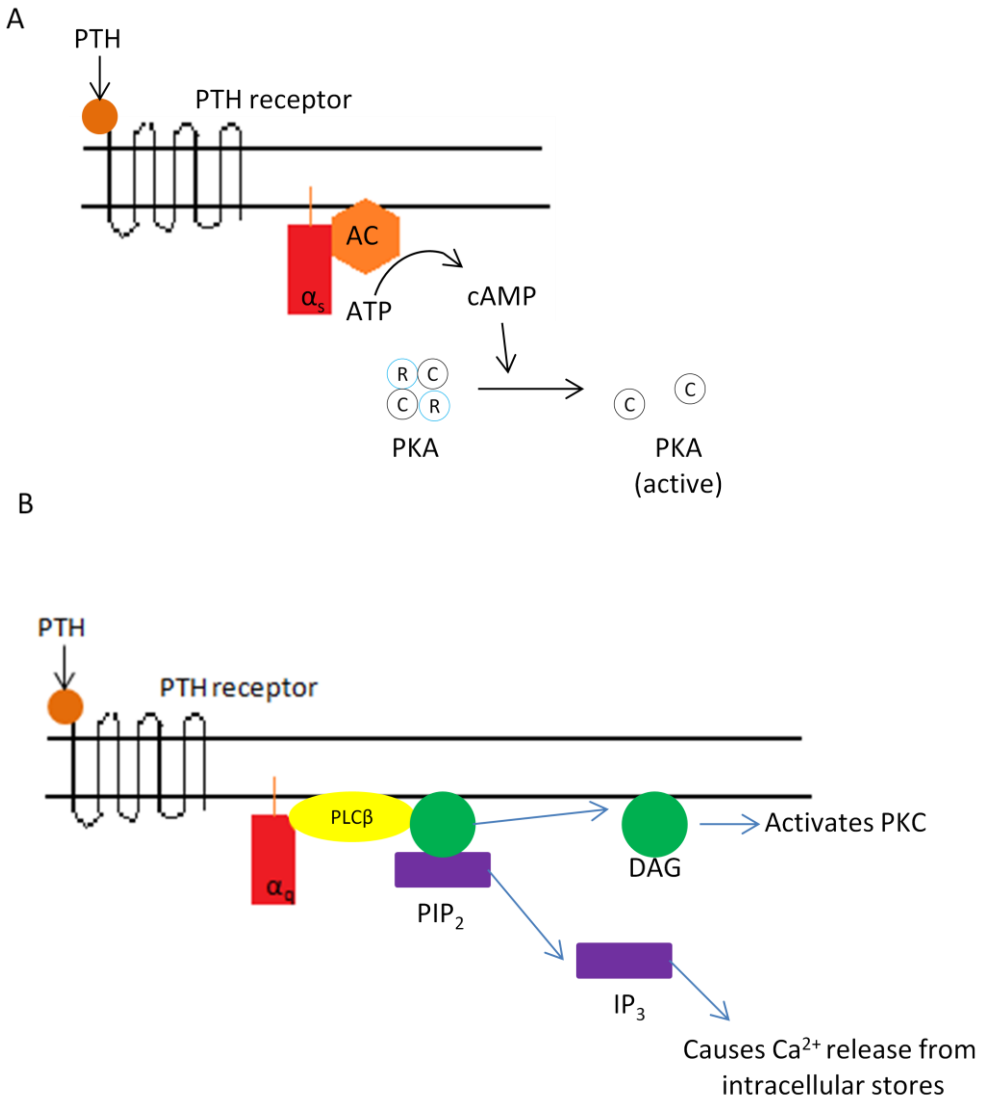

Figure 1.7 PTH signalling in osteoblasts. This diagram represents the two major pathways that PTH can influence. (A) Its attachment to the α_s subunit allows signalling through the adenylate cyclase, cAMP and PKA pathway. (B) Its attachment to α_q allows signalling through PLC and therefore allows the release of intracellular calcium and activation of PKC. (Adapted from *Swarthout JT et al Gene* 2002).

1.4.3 The synergy between ATP and PTH

Studies to determine if ATP and PTH would synergise together in some form on osteoblasts began because of experiments that showed the proliferative effects of growth factors on stromal cells would increase in the presence of nucleotides [65, 157, 158]. PTH acts on osteoblasts *in vivo* to increase cell number, thus it was decided to investigate the effects of this with ATP. It has now been shown that when ATP and PTH are added together on UMR-106 cells, SaOS-2 cells and, importantly, in primary human cells, there is a synergistic increase in *c-fos*. [159, 160]. Acting alone ATP induces a very small amount of *c-fos* whilst PTH can induce a larger response. However, when these two compounds are added together there is a massive increase in the *c-fos* expression. It should be noted that the increase is not simply due to the additive effects of both compounds as it is much larger than this. This phenomenon has implications on how the effect of bone remodelling by PTH is directed to certain, highly loaded, areas. As ATP is released after mechanical stress this synergy may be a mechanism for Wolff's law.

Interestingly how synergy is achieved appears to be different between cell lines. In the rat cell line UMR-106 the synergy is a product of a potentiation of Ca^{2+} release (see Fig.1.8 (A)). It was shown in this cell line that PTH did not act to increase Ca^{2+} release on its own (suggesting that it is not linked to $G_{\alpha q}$), however when added with ATP, acting through P2Y1, there was a massive increase in intracellular Ca^{2+}, having been released from intracellular stores. The method by which PTH aided in the Ca^{2+} release is still unclear. It was shown that it does not act through the expected PKC pathway, which can directly stimulate Ca^{2+} release, but in fact it acts through adenylate cyclase. However adenylate cyclase did not act through PKA, cAMP or cyclic guanine monophosphate (cGMP). What is clear is that the Ca^{2+} potentiation is enough to cause a phosphorylation of CREB and a synergetic increase in *c-fos* expression, shown by the fact that the Ca/CRE (calcium/cAMP responsive element) part of the *c-fos* promoter is all that is needed [160].

In SaOS-2 cells the mechanism is even less clear. Firstly SaOS-2 cells predominantly express P2Y2 receptors and agonist binding, as in UMR-106 cells, did cause an increase in intracellular Ca^{2+}. The authors could find no increase in Ca^{2+} in response to PTH, and concluded that perhaps medium stirring could have caused ATP release, and therefore Ca^{2+} release, in previous studies that showed this. Nevertheless PTH can act on its own to increase *c-fos* in a PKA dependent manner. ATP did not increase cAMP levels; thus is it just acting to increase Ca^{2+}. It was thought that these two pathways could still converge on the Ca/CRE part of the promoter. However truncated reporter promoters showed that this wasn't the case and in fact P2 signalling acts on the serum responsive element (SRE) part of the promoter and therefore the two pathways converge on different parts of the same promoter. The ATP/Ca^{2+} pathway is still undetermined due to the fact it doesn't act through the expected MAPK pathways or through a non-MAPK pathway that could activate T-cell factor (TCF) [159] (see Fig. 1.8 (B)). To complicate matters further the investigations that looked at the SRE promoter were not performed in SaOS-2 cells, but rather UMR-106 cells. This was undertaken before it was apparent that the UMR-106 synergy was due to a potentiation of the intracellular Ca^{2+}. Therefore it appears unusual that ATP acted on the SRE part of the promoter and not the Ca/CRE which it was later shown to do.

A

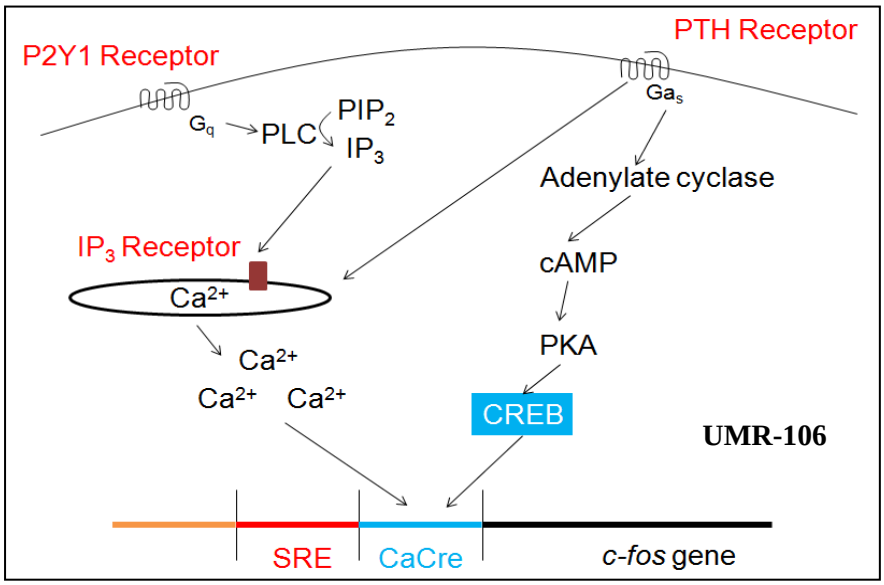

B

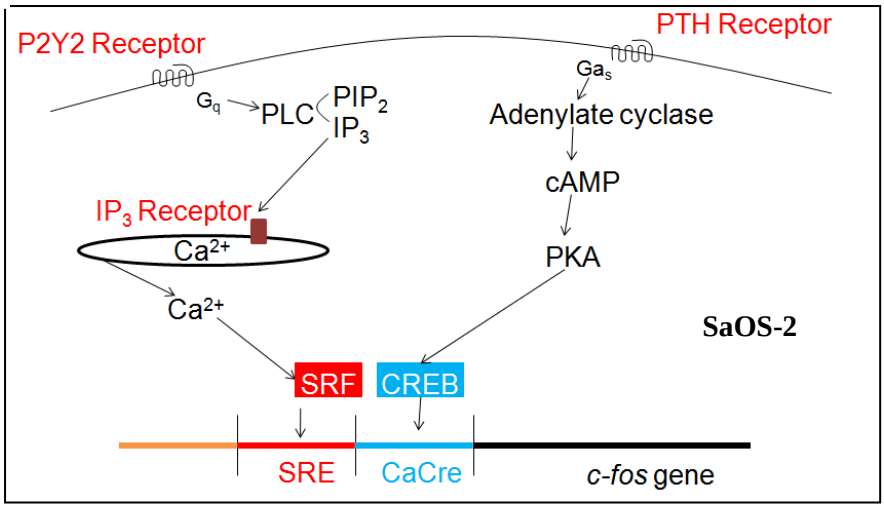

Figure 1.8 Intracellular mechanisms of ATP and PTH synergy in (A) UMR-106 cells and (B) SaOS-2 cells.

(A) Activation of the PTH receptor leads to an increase in *c-fos* production via the G_s subunit. This activates a downstream signalling cascade involving adenylate cyclase, cAMP, PKA, and will result in the phosphorylation of cAMP response element binding (CREB). CREB will then act on the Ca/CRE part of the promoter to cause *c-fos* transcription. When both the P2Y1 and PTH receptors are activated there is a potentiation of Ca^{2+} release from intracellular stores. This increase in Ca^{2+} will also target the Ca/CRE part of the promoter leading to a synergistic increase in *c-fos* transcription. (B) Similar to UMR-106 cells, activation of the PTH receptor leads to an increase in c-*fos* production via the G_s subunit. This activates a downstream signalling cascade involving adenylate cyclase, cAMP, PKA, and will result in phosphorylation of CREB, CREB will then act on the Ca/CRE part of the promoter to cause c-*fos* transcription. However in SaOS-2 cells there is no potentiation of Ca^{2+} release from intracellular stores. Instead, intracellular Ca^{2+} release, as a result of P2Y2 receptor activation, will act on the SRE region of the promoter. However this is not through the classical MAPK pathways involving ERK or TCF. Thus the synergistic increase is achieved through two pathways acting at two different parts of the same promoter.

1.5 The effect of the drug BL-1249 on osteoblast cells

1.5.1 The function of K^+ channels in osteoblasts

K^+ channels allow the flow of K^+ in and out of the cell. As a result of this K^+ channels can influence the membrane potential of a cell, and therefore everything that results from alterations in that. It can also regulate cell volume, osteoblast proliferation, and osteoblast response to hormones.

The membrane potential is the difference in electrical potential from inside of the cell to the outside, due to the different concentrations of ions across the cell membrane. The outside of the cell is more negatively charged as well as having a lower concentration of K^+ ions. Thus if A K^+ channel were to open K^+ would diffuse out of the cell down its concentration gradient. This would hyperpolarise the cell (i.e. make it more negative). By hyperpolarising the cell the voltage gated Ca^{2+} channels are less likely to open, therefore reducing the amount of Ca^{2+} that can enter the cell. Acting in this way osteoblast K^+ channels play a role in osteocalcin and osteoprotegerin production, as well as responses to stress. However voltage gated Ca^{2+} channels do not effect proliferation in these cells so it is unlikely that alterations in the membrane potential caused by K^+ will play a role in increasing cell number via this mechanism.

By allowing the flow of ions in and out of a cell K^+ channels can also influence the water potential of the extracellular and intracellular space. When a cell is forced to swell, by adding a hypotonic solution, the initial response is an influx of extracellular Ca^{2+}. Either this influx of Ca^{2+} or the mechanical stress at the cell membrane causes maxi-K^+ channels to open and therefore K^+ will flow out. As K^+ flows out the water will follow and therefore the volume of the cell can be regulated [161] (see Fig. 1.9).

Because maxi-K^+ channels can be activated by intracellular rises in Ca^{2+} anything that activates IP_3 receptors have the potential to influence K^+ channels. This can be seen in the fact that both PTH and PGE_2 when binding at their respective receptors cause a rise in intracellualar Ca^{2+} and have been shown to open K^+ channels.

K^+ channels also have an influence over the number of cells present which is likely due to its effects on apoptosis. Activating K^+ channels will lead to an efflux of K^+ that will accelerate apoptosis due to cell shrinkage and blocking the K^+ channels will have the opposite effect [162, 163]. Therefore it can be seen there is a strong link between cell volume and apoptosis.

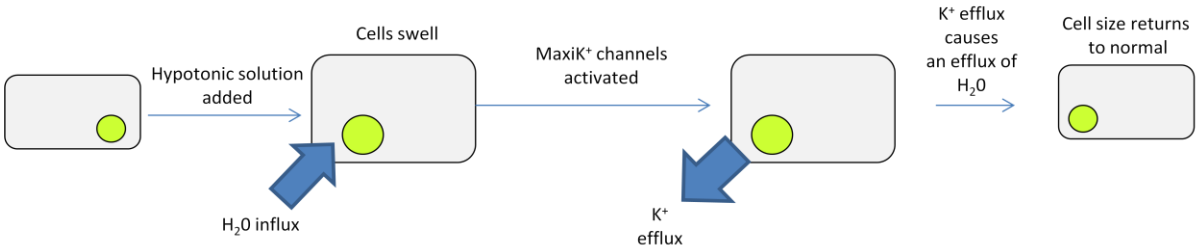

Figure 1.9 Proposed model for volume regulation in cells. This displays the role of maxi K^+ channels in volume regulation, (adapted from: *Weskam M et al membrane biology* 2000).

1.5.2 The expression of K^+ channels in osteoblasts

There are 3 different super families of K^+ channels which are grouped according to their structure (summarised in table 1.1). Channels with 2 transmembrane domains have 1 pore-forming unit and are inward rectifier channels. Channels with 4 transmembrane domains have 2 pore-forming domains and thus are called two-pore domain K^+ channels. Finally, channels with 6 transmembrane domains have 1 pore domain and are voltage gated channels. Due to the fact that 4 pore domains are needed to form a functional channel [164] the voltage gated and inward rectifier channels are tetramers whilst the two-pore domain channels exist as dimers [165]. As they are K^+ channels they all have a conserved region in their pore domain that allows K^+ to pass selectively.

When a cell is depolarised it will activate voltage-gated K^+ channels. By activating these channels the membrane potential will return to its resting state [166], as K^+ comes out of the cell the cell will become more negatively charged. There is a region in these channels that are positively charged

which is important for sensing the membrane potential. Upon activation this will cause a conformational change that will allow K^+ to pass through [166].

Inward rectifying K^+ channels are unusual in that they allow K^+ to flow into the cell whilst still at negative membrane potentials. This is in fact due to magnesium (Mg^{2+}) ions partially blocking the pore [166]. They aid in stabilising membrane potential and help control K^+ transport [167].

Two-pore domain K^+ channels (2PK) are there to allow K^+ to leak out. This is vitally important in setting up the resting membrane potential close to the equilibrium potential of K^+. Uniquely they are insensitive to a lot of K^+ channel blockers and are time and voltage dependent [168]. Of particular interest in this thesis is the TREK-1 2PK. This channel is perhaps the best studied of all the 2PK channels, they are activated by membrane stretch, lower pH, heat and AA [169]. Both PKA and PKC activation cause inhibition of these channels. They have been shown in UMR-106 cells to be important in PTHrP signalling in response to mechanical stress.

There are a number of K^+ channels that have been shown to be expressed in osteoblast cells. These are calcium activated K^+ channels [162], inward rectifying K^+ channels [170], voltage gated K^+ channels, ATP-sensitive K^+ channels (members of the inward rectifying family) [171] and our lab and others have shown the expression of various 2PK channels in osteoblasts (including TREK-1) [169].

Class	Subclasses	Function	Antagonists	Agonists
Ca^{2+} activated	BK Channels SK Channels	Inhibition following stimuli of increasing intracellular Ca^{2+}	charybdotoxin and apamin, tetraethylammonium	1-EBIO, NS309 and CyPPA
Inwardly rectifying	ROMK	Recycling and secretion of K^+ in nephrons	Nonselective: Ba^{2+}, Ca^+	None
	GPCR regulated	Mediate the inhibitory effect of many GPCR	ifenprodil	General GPCR agonists
	ATP-sensitive	Close when ATP is high to promote insulin secretion	glibenclamide and tolbutamide	diazoxide and pinacidil
Two-pore domain	TWIK TREK TASK TALK THIK	Contribute to resting potential	bupivacaine	halothane
Voltage-gated	hERG KvLQT1	Action potential repolarisation. Limits frequency of action potentials	tetraethylammonium, 4-aminopyridine and dendrotoxins	retigabine

Table 1.1 Classes of K^+ channels. (Adapted from Rang, H.P., *Pharmacology*, 2003).

1.5.3. The action of BL-1249 on cells

BL-1249 ((5,6,7,8-tetrahydro-naphthalen-1-yl)-[2-(1H-tetrazol-5-yl)-phenyl]-amine) is a novel drug that was first studied in rat smooth muscle bladder cells [172]. It was proposed to be an activator of K^+ channels due to the fact that voltage clamp studies showed that the current reversed at the K^+ equilibrium potential. Also, as it was insensitive to normal K^+ channel blockers it was assumed it would be a 2PK channel. Finally it was inhibited by Ba^{2+} thus a case was made that BL-1249 was a TREK-1 channel opener [172]. However recent studies in our lab have suggested that this is not the case as it appears that it is voltage dependent due to the fact that the current is larger at 80mV than -120mV. TEA inhibited the current suggesting it is a BK_{ca} channel. Further to its effects on K^+

channels, or due to the effects on K^+ channels, BL-1249 has been shown to strongly inhibit the ATP+PTH induced *c-fos* expression and therefore work was undertaken to investigate this further.

1.6 The role of the superoxide dismutase enzyme in purinergic signalling and bone

1.6.1 Superoxide dismutase 1

Cu/Zn Superoxidedismutase1 (SOD1) is an antioxidant enzyme that is present in every cell of the body. As an antioxidant it acts to prevent the oxidation of other molecules within the cell i.e. it prevents the transfer of electrons or hydrogens between molecules. When oxidation does occur it can produce free radicals, these are molecules that have unpaired electrons in their outer shell which therefore makes them highly reactive. Once formed, they can react with other molecules and start a chain reaction (see Fig 1.10) which can damage a cell. Therefore antioxidant enzymes act to prevent this. Over time, or with deficient antioxidant defences, the accumulation of these chain reactions leads to oxidative stress and cell damage.

SOD1 belongs to a group of three SOD molecules known for their ability to catalyze the dismutation of superoxides into oxygen and hydrogen peroxide. The half reactions are as follows:

$$M\text{-}SOD + O_2^- \rightarrow M^+\text{-}SOD + O_2$$

$$M^+\text{-}SOD + O_2 + 2H^+ \rightarrow M\text{-}SOD + H_2O_2$$

M = Cu^+, Mn^{2+}, Fe^{2+}, Ni^{2+}.

Both SOD1 and SOD3 contain copper and zinc [173] whilst SOD2 contains manganese [174]. SOD1 is found in the cytoplasm, SOD2 is present in the mitochondrion and SOD3 is an extracellular antioxidant enzyme [173, 174].

Free radicals are thought to be one of the causes of ageing as the build up of oxidants over time will cause chain reactions that damage cells. The longer one lives the more free radicals will accumulate.

A lot of age-related diseases have been associated with free-radical accumulation such as diabetes [175], Alzheimer's disease [176], atherosclerosis [177], and arthritis [178].

Interestingly mutations in the SOD1 gene in humans are believed to cause amyotrophic lateral sclerosis [179, 180]. This is a motor neuron disease that affects both the upper and lower motor neurons and is characterized by progressive weakness and muscle atrophy due to lack of stimulation. The full extent of how SOD1 affects this disease is unknown, although it is thought that the build up of free radicals causes an increase in apoptosis signals to the cells.

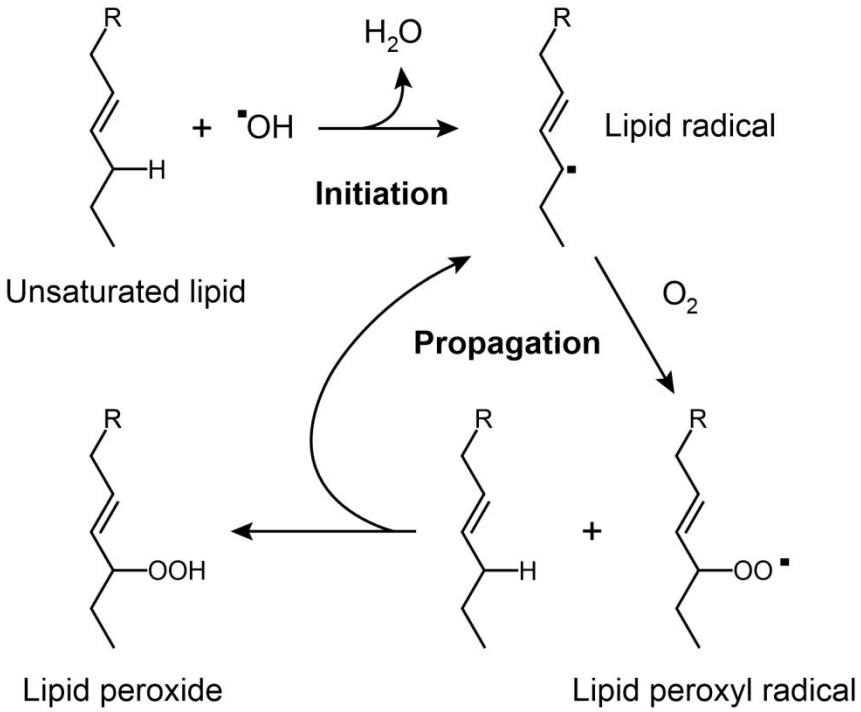

Figure 1.10 Oxidative chain reaction. The first step is initiation. This involves a reactive oxygen species, such as OH^- and HO_2, which reacts with an unsaturated fatty acid to produce a lipid radical. Being a radical it is very unstable and readily reacts with oxygen to form a lipid peroxyl radical. This again reacts with an unsaturated lipid. The product of which is lipid peroxide and another lipid radical, thus the reaction is propagated. (from:*http://en.wikipedia.org/wiki/Lipid_peroxidation*).

1.6.2 The phenotype of SOD1-/- mice

The muscle phenotype of SOD1 -/- mice have age related muscle loss at a young age. At 3-4 months they are 20% smaller than their WT counterparts and by 20 months the hind limb muscles were measured to be 50% less than normal. The proteins, lipids and DNA of these muscles were examined and found to contain higher levels of oxidative damage. These mice are also less willing to do exercise, with a 40% observed reduction in use of their exercise wheel. The older SOD1-/- mice had tremors and were unable to walk properly. From these results it is apparent how crucial an enzyme SOD1-/- is [181].

Tests were also carried out to look at the incidence of cancers in SOD1-/- mice. It was noted that the life span of these mice were greatly reduced and importantly in 70% of these mice there was observed tumour development in the liver. Both benign and malignant tumours were observed. Again these tissues were examined and found to have increased oxidative damage in the cytoplasm and to a lesser extent in the nucleus. The cyclins D1 and D3 were shown to be up regulated in these cells suggesting that it is by this mechanism that the early stages of the hepatocarcinogenesis occurs [182].

There has also been a study performed on bone where 8 month old mice were subjected to bending stiffness and strength tests using a three point bending technique. They were also analysed for bone mineral density (BMD) using µ-ct scanning. It was shown that the length of the femurs were shorter in the SOD1-/- mice, they had decreased BMD and decreased stiffness in them. It was postulated that this was due to oxidative damage and that these mice are therefore ideal for studying age related characteristics in bone [183]. However it is not clear that how the accumulation of these free-radicals directly affects these bones.

1.6.3 P2 signalling and SOD1 mutations

Mutations in the SOD1 gene have been linked to amyotrophic lateral sclerosis (ALS). Further to that some studies have linked the damage these mutations cause with P2 signalling. It is known that ATP, acting through P2X7 receptors, can cause astrocytes to become neurotoxic and secrete factors that contribute to motor neurone cell death [184, 185]. This neurotoxicity is linked to oxidative stress and P2X7 receptor stimulation can cause an increase in peroxynitrite. There is evidence that this P2 signalling is increased in astrocytes that contain the SOD1 mutation. So much so that basal levels of ATP can 'switch on' the neurotoxic phenotype and cause motor neurone cell death. By degrading ATP with apyrase in normal astrocyte neurone co-cultures there was an increase in motor neurone attachment and survival. On cells with the SOD1 mutation, ATP degradation caused a complete inhibition of the astrocyte neurotoxic phenotype. It was proposed that the SOD mutation was causing a sensitisation of the astrocytes to the ATP [186]. This same system has also been proposed in microglia.

1.7 Introduction summary and aims of this thesis

The work in this thesis will attempt to gain further insight in to the role of purinergic signalling in bone.

Firstly work was undertaken to look at the mechanics of ATP release. ATP in the extracellular bone environment is crucial to bone function. However it is not yet known precisely how ATP arrives in the extracellular space. It has been shown to be released from osteoblasts and therefore investigations examined how ATP was released from the osteoblasts.

Investigations were also carried out to look at ATP and systemic hormone synergy in more detail. Firstly to ascertain whether ATP could sensitise osteoblasts to systemic hormones and then what mechanisms were involved in this.

As BL-1249 can inhibit ATP+PTH induced *c-fos* expression it was decided to investigate how BL-1249 was achieving its effect. Firstly to make sure BL-1249 was not killing the cells, then to determine if BL-1249 was acting on K^+ channels, and if not what other function could it be doing to achieve its effects. Also BL-1249s effect on other cell types was investigated to see if the same effect was observed.

Mutations in the SOD1 gene have been associated with ALS. The mechanism by which this occurs is unknown, however a role for P2 signalling has been postulated. The phenotype of SOD1-/- mice show a very distinct loss of BMD and stiffness, therefore given the links in ALS, investigations were carried out to determine whether P2 signalling could explain the observed bone phenotype. This was done via µ-ct scanning and RT-qPCR on the mouse calvarial cells.

The aim of this thesis is to:-

- Determine the characteristics of ATP release from osteoblasts to help gain a clearer understanding of ATP in the extracellular environment.
- Determine if ATP can sensitise osteoblasts to the action of systemic hormones.
- Determine how BL-1249 inhibits ATP+PTH induced *c-fos* expression and if it has the same effect on other cell types.
- Confirm, using μ-CT, the bone phenotype of SOD1-/- mice and to look at the expression of P2 receptors in these mice to determine if there could be a link between the two.

2. Materials and Methods

2.1 Cell culture of osteosarcoma cell lines

The majority of the experiments performed in this thesis were all carried out on the osteosarcoma SaOS-2 cell line. However osteosarcoma cell lines Te-85 and MG-63, and breast cancer cells T74D, were also used in some experiments. All 3 were cultured in the same manner. Cells were defrosted from liquid nitrogen stores and washed using Dulbecco's modified Eagles medium (DMEM, Invitrogen, UK or Sigma-Aldrich, UK). This contained L-glutamine, sodium pyruvate, sodium bicarbonate, 4500 mg/l glucose, 10% fetal calf serum (FCS, Biosera, UK), 50 U/ml penicillin and 50 µg/ml streptomyocin (both from Sigma-Aldrich UK). Cells were then placed with DMEM in 9-cm plates (Falcon, UK) and incubated in a humid atmosphere at 37 ^{o}C and 5% CO_2. To passage cells the DMEM was removed from the dish and the cells washed twice in phosphate buffered saline (PBS), containing sodium chloride 0.28 M, potassium chloride 5.55 mM, disodium hydrogen phosphate 16.4 mM, potassium dihydrogen orthophosphate 2.94 mM and autoclaved distilled water. 2.5 ml typsin-EDTA (Sigma-Aldrich, UK) was added and the cells were incubated for 5-10 minutes. After the cells had lifted 8.5 ml DMEM containing 10% FCS was added to inhibit trypsin. Cells were spun at 1500 revolution per minute (RPM) for 1 minute and resuspended in DMEM (amount being dependent on where cells were being placed, i.e. 9 cm dish, 6-well plate, 96 well plate etc, all obtained from 'Falcon UK'). This was the standard procedure as outlined in [187]. For the majority of experiments plates were seeded when cells were at 90% confluence and always to the same dilution. This ensured that cell numbers were comparable between experiments. Where cell counts were used these will be referred to in the relevant result sections.

2.2 Preparation and culture of primary cells

SOD1-/- and WT C57BL/6 Mice were kindly donated by Prof. McArdle. To obtain calvarial cells the head of the mouse was removed and placed in 70% ethanol for 2 minutes. The head was then placed in a 9 cm dish containing PBS, where the soft tissue was removed. Facial bones were removed and calvarium was cut into small pieces. Bone chips were placed in DMEM and incubated in the same conditions as outlined in section 2.1. To passage cells the bone chips were removed and placed in a separate 9 cm dish containing DMEM, and then dissected into smaller pieces.

MA-16 cells were kindly given to me by Mrs Jane Dillon. These are taken from the proximal end of a tibia. They were cultured in the same way as the cell lines in section 2.1.

2.3 RNA reverse transcriptase

Cells were lysed in 1 ml tri-reagent (Sigma-Aldrich, UK) and left to stand at room temperature for 5 minutes. 0.2 ml of chloroform (Sigma-Aldrich, UK) was added and shook manually for 15 seconds. Samples were then left to stand for 15 minutes at room temperature. To separate the mixture into protein, DNA and ribonucleic acid (RNA) the samples were centrifuged at 12000 G for 15 minutes at 4^{o}C. The top RNA layer was removed and 500 µl of isopropanol (Sigma-Aldrich, UK) was added to it. Samples were mixed and then stood at room temperature for 15 minutes before centrifuging at 12000 G for 10 minutes at 4^{o}C to obtain a pellet of RNA. The Pellet was washed in 75% ethanol, and centrifuged at 7,500 G for 5 minutes at 4^{o}C. The ethanol was then removed and the pellet was air dried for 10 minutes. The pellet was then dissolved in 50 µl DNAase and RNAase free H_2O (Sigma-Aldrich, UK) and treated with DNAase to remove unwanted DNA. 10 µl of DNAase buffer and 25 µl of the DNAase was added. This was incubated in a water bath for 2 hours at 40^{o}C before deactivating the DNAase at 70^{o}C for 15 minutes. Spectral absorption at 260/280 nm, using a Helios UV-visible spectrophotometer (Thermo Scientific, UK), was run to detect the quality of the samples. Absorbtion readings at 260 nm were divided by 280 nm to find out the ratio between nucleic acid quantity and protein quantity. Anything below a ratio of 1.7 was rejected as not being of sufficient quality. Samples

were transcribed using superscript II (Invitrogen, UK). 1µl oligo$(dt)_{12-18}$ primers (500 µg/ml) (Sigma, UK), 1µl dNTP's at 10 mM (Lorenza Biochemie, Germany) and 5 µg of RNA was added to 12 µl H_2O. This mixture was incubated at 65^oC for 5 minutes before being quick chilled on ice. Then 2 µl DTT and 4 µl first strand buffer (both from Sigma, UK) was added to the mix and heated to 42^oC for 2 minutes. The reverse transcriptase, superscript II, was added at 42^oC for 50 minutes and finally deactivated by heating to 70^oC for 15 minutes. Samples were stored at -20 ^oC until ready for real-time quantitative PCR to measure DNA concentrations.

2.4 Real-time quantitative polymerase chain reaction (qPCR)

qPCR was performed using the iCycler IQ (Bio-Rad, UK). cDNA samples were diluted 1:10 in DNAase and RNAase-free H_20 (Sigma, UK). 2 µl of cDNA, 0.5 µl forward primer and 0.5 µl reverse primer (Invitrogen, UK) at a concentration of 20µM, 7.5 IQ SYBR Green Supermix (Bio-Rad, UK) and 4.5 H_20 was used to make a total reaction volume of 15 µl. The cycle program was then set up and was as follows: 95^oC for 3 minutes to denature and then 40 cycles of 60^oC and 95^oC each lasting for 30 seconds a time; this was to allow annealing and denaturing respectively. Following on from this, a melt curve protocol was run which consisted of increasing the temperature from 55-95^oC, stepping up 0.5^oC each time, and reading for 30 seconds, thus giving 81 total readings. This is run to ensure that the products that were being amplified were the right length and that they contained the correct G-C content to confirm that the correct product was being amplified. To calculate the relative expression of these genes they were compared to a β-actin which acts as a housekeeping gene. Thus using x = ct value of β-actin and y = ct value of gene of interest we can calculate the relative expression of each gene using the formula: Relative gene expression = $2^{(ctx\ -\ cty)}$ [188]. Once the relative gene expression has been obtained the fold change between the genes was calculated and displayed on graphs. The efficiencies of each reaction were calculated using 'LinReg PCR' software [189]. If values obtained using this program were outside 1.8 to 2.2 then the reaction was discarded. A value of 2 being the most efficient as this signifies a doubling of dsDNA with each cycle. Discarding efficiencies outside this range allowed for reactions to be compared in analysis.

For each sample that was analysed there were 3 repeats of that single sample, an average was then taken.

2.5 Primer design

In designing the primers the considerations listed here [190] were taken into account. These being that the primers should be maximum 22 bases long, the G-C content should be no more than 50%, the product should range between 100 and 150 base pairs, the primer annealing temperature should be 50-62^{o}C and finally, primers should span different exons. To design primers, three online free websites were used 1) to obtain a list of possible candidates using the parameters listed above, 2) to ensure no DNA folding occurred at possible primer binding site and 3) to makes sure that primers did not form secondary structures at the annealing temperature.

The first website that was used is called Primer 3 and can be found at http://www.frodo.wi.mit.edu/primer3/. To obtain the list of possible primer candidates the sequence of DNA to be analysed was inserted and the following parameters were defined; the product size as 100-150bp, the primer size to be between 18-22 base pairs, the annealing temperature as 50-60 ^{o}C and the primer GC content between 20-50%. The list of candidates must then be manually checked to ensure that they span exons before moving on. Once a primer has been selected from this list it was taken to the next site, DNA mfold, found at http://www.mfold.bioinfo.rpi.edu/cgi-bin/dna-form1.cgi. Here the candidate sequence was entered along with the Na^{+} concentration at 50 mM and the Mg^{2+} at 3 mM. This website will then show any secondary structures that occur at the annealing temperature. Thus it was possible to determine if primer binding was likely to occur. Finally the candidate primer was input into a website known as beacon designer. This can be found at http://www,premierbiosoft.com/qOligo/Oligo.jsp?PID=1. To proceed the nucleic acid concentration was put in at 500 nM, the monoion concentration was entered at 50 mM and the free Mg^{2+} concentration was entered at 3 mM. This website ensured there would be no dimerisation or folding of the primers during PCR. Primers were obtained as desalt purified and HPLC purified. A stock

solution of 100 µM was made up using DNAase and RNAase-free H_2O. Aliquots were made up to 10µM and stored in -20^{o}C.

Gene	Sequence (5'-3')		Anneal Temp	Product size (BP)
RANKL (human)	Fwd	ATCCCATCTGGTTCCCATAAA	62	150
	Rev	ATGTCGAAAGCAAATGTTGG		
OPG (human)	Fwd	GGCAACACAGCTCACAAGAA	65	144
	Rev	GGTTAGCATGTGCAATGTGC		
mtDNA (human)	Fwd	ACCACCTCTTGCTCAGCCTA	60	107
	Rev	CATGGGCTACACCTTGACCT		
β-actin (human)	Fwd	GGACCTGACTGACTACCTC	61	135
	Rev	GCCATCTCTTGCTCGAAG		
β-actin (mouse)	Fwd	ATTGCTGACAGGATGCAGAA	59	124
	Rev	TGATCCACATCTGCTGGAAG		
Osteocalcin (mouse)	Fwd	TGAGGACCATCTTTCTGCTCA	60	127
	Rev	ACCTTATTGCCCTCCTGCTT		
SOD1 (mouse)	Fwd	TGGTGGTCCATGAGAAACAA	60	104
	Rev	AATCCCAATCACTCCACAGG		
ALP (mouse)	Fwd	CAAGCCCAAGAGACCTTGAA	60	109
	Rev	TTACTGTGGAGACGCCCATA		
Col1A (mouse)	Fwd	TGTTCAGCTTTGTGGACCTC	59	141
	Rev	TCAAGCATACCTCGGGTTTC		

Table 2.1 Primer sequences used in this thesis

2.6 Measuring *c-fos* levels in SaOS-2 cells

SaOS-2 cells were obtained that had been transfected with a luciferase reporter gene attached to the full *c-fos* promoter. Thus whenever the *c-fos* promoter was activated it would cause transcription of luciferase (see Fig 2.1). To create the reporter named pfoslucneo1 the pUC19fosluc1 (obtained from Dr L. Runkel) was subcloned into pSV2neo from the fragment of *c-fos* promoter that was wanted, -721 to -1, (accession number M16287) and linked to the luciferase gene. Although different *c-fos* promoters have been used, all work carried out in these investigations concerns the use of the full *c-fos* promoter. The final step was created by transfection of pfoslucneo1 into SaOS-2 cells using lipofectamine (Invitrogen, UK). To culture cells the procedure from section 2.1was used. However, in addition, G-418 disodium salt solution (Sigma, UK) was added to a final concentration of 50 µg/ml to select for stably transfected cells. This ensured the signal remained high through multiple passages, although cells were no longer used after 15 passages.

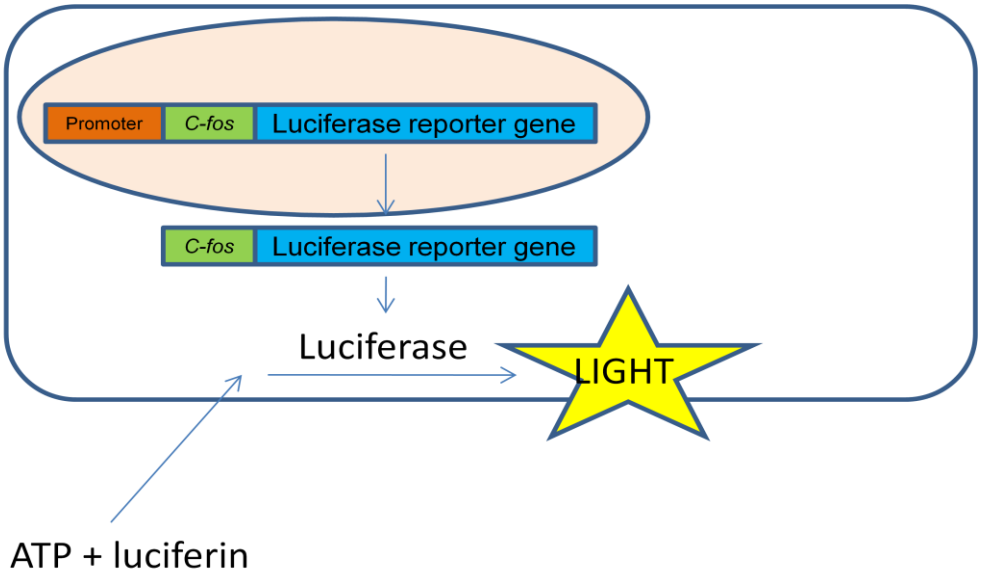

Fig 2.1 Production of light from *c-fos* reporter cells

To perform *c-fos* assays cells were passaged as outlined in section 2.1 and seeded into 96 well luminometric, white, plates (Falcon, UK). The outside wells of the plate were left empty as they produce inconsistent readings in the luminometer. The cells were then grown until 90% confluence.

When ready, cells were serum starved by first washing x2 in PBS, then adding DMEM medium with penicillin, streptomyocin and L-glatamine. The cells were serum starved for 24 hours. Following on from this the cells were treated with reagents, mostly by adding them to the top of the well to prevent any ATP release, and then gently rocked to diffuse the compounds. One important factor when treating plates was to spread treatments across the length of the plate. This is because there was a gradual decreasing signal in the luminometer readings across the plate. After treatment, which could range from 18 hours to 4 hours the cells were again washed twice in PBS. Lysis reagent (Promega, UK) was prepared by diluting 1:5 in double distilled, autoclaved H_2O. A final PBS wash was removed and 20 µl of this solution was added to the wells and stored overnight at -20^{o}C. The following morning luciferase assay reagent (LAR, Promega UK), containing luciferin, was allowed to defrost. 20 minutes before reading, the plate was taken out of freezer to reach room temperature. To read the plate the luminometer injection system was first subjected to a wash cycle of ethanol, water, ethanol and air. It was then primed with the LAR. Plate was read at a 2 second delay and 10 second incubation time. Upon completion the injection system was again flushed with ethanol, water, ethanol and air. Files were stored as excel files and then resorted following randomisation of treatments in the plate.

2.7 Protein extraction for Western blot analysis

Lysis buffer contained 2 ml of 1M trizma HCl (20mM), NaCl 250 mM, EDTA 3 mM, EGTA 3 mM and 500 µl Triton x 100 (0.5%) was made up to 100 ml with double distilled, autoclaved water. pH was then adjusted to 7.6 and stored at 4^{o}C. For every 1ml lysis buffer used 10 µl of protease inhibitors was added just before the extraction of the protein.

To extract the protein the confluent Petri dishes were firstly chilled on ice and supernatants were removed. Then 500 µl of the above lysis buffer solution (containing the protease inhibitors) was added to the dishes, which were left on the ice for a maximum of 5 minutes. To obtain the cells from the bottom a cell scraper was used. The cells were then added to a 1.5 ml eppendorf. This cell lysate

was then centrifuged in the megafuge 1.0R (Heraeus, UK) at 13,000 G for 10 minutes. This was performed at a temperature of 4^{o}C. The supernatant was extracted and placed in a fresh eppendorf and 500 µl of sample buffer was added. Mixed sample and then was heated to 98^{o}C for 10 minutes on heat block before storing the protein extract at -20^{o}C overnight.

2.8 Western Blotting of phosphorylated CREB

10% resolving gel was made up, consisting of 3.3 ml of 30% acrylamide, 2.5 ml of resolving buffer 100 µl of 10% SDS, 3.97 ml H_2O, 100 µl of 10% ammonium persulfate and 5 µl tetramethluethylenediamine (TEMED). After the 2 glass plates were set up in the casting tray the above solution was vortexed and immediately added between the plates. A space was left at the top to allow for the stacking gel. To ensure a clean line between the two gels a layer of isopropranol was added, this also prevented the resolving gel from drying out. Stacking gel was made up by adding 1.3 ml of 30% acrylamide, 2.5 ml of stacking buffer, 100 µl of 10% SDS, 6 ml H_2O, 100 µl of 10% APS and finally 10 µl TEMED. Water was then added to rinse once the isopropronal had had been drained off. Now the stacking gel was loaded into the space that was left and a comb inserted to make a space for the loading wells. Then the apparatus was put in a clamp and transferred to a gel tank. The running buffer made up to 2 L with water consisted of 60 g Trizma base, 288 g glycine and 20 g SDS was poured into tank. Combs were then removed and the molecular weight marker, and all the protein samples that were used, were loaded into the wells. For 1 hour a charge of 120 V was applied to the samples.

To transfer the proteins across to the nitrocellulose membrane, the membrane, and the filter papers were first cut to the correct size. They were then completely soaked in H_2O and transfer buffer. After this the plates were extracted from the tank and the stacking gel was scooped out. Carefully the resolving gel was taken out of the plates and the nitrocellulose membrane was placed on top. This was smoothed out and any bubbles were flattened out using a plastic pipette. The membrane and gel were then placed between two filters on either side and a wet gauze on top of that. These were all tightly clamped together. Then placed in gel tank and transfer buffer (Trizma base 25 mM, glycine (192 mM

and 300 ml of methanol was made up to 1.5 L with water) was poured in to surround it. Ice was packed outside to keep the temperature low. This time 110 V was applied to the gel for 1 hour.

The next stage involved the addition of primary and secondary antibodies. Firstly, Tris buffered saline Tween-20 was made up to 1 L by adding H_2O, 20 mM Trizma base, 127 mM NaCl and 1 ml of Tween-20 (0.1%). The pH was then made to 7.6. Then using the coloured ladders on either side the membrane was cut to size. To prevent unspecific binding the membrane was placed in 5% skimmed milk (Marvel) TBST for 2 hours prior to the addition of the anti-phospho CREB polyclonal rabbit primary antibodies (Millipore UK). Primary antibodies were then diluted 1:200 in milk and incubated overnight with the membrane in the fridge at 4^oC. In the morning 3 x 10 minute washing were performed following removal of any unbound primary antibody. The anti-rabbit horseradish linked secondary antibody was used in 1% milk at a dilution of 1:5000. This was then incubated at room temperature for 90 minutes. Again 3 x 10 minute washed were performed. ECL (enhanced chemiluminescence) was then made up using 50% reagent 1 and 50% reagent two and stored in darkness until added to membrane for a maximum of 1 minute. ECL was then removed and the membrane put in cling film before adding to the hypercassette (Amersham Biosciences, U.S.A). This was secured in place by using tape.

Development of film was carried out in a dark room. The hyperfilm (Amersham biosciences, U.S.A) was placed at the front of the film and the hypercassete closed. The film was exposed to membrane for 5 minutes, and then a second film was exposed for 30 seconds. Film was then rinsed in water, fixed and rinsed in water again. When the film was dry it was placed against the membrane in order to draw on the molecular sizes of the band.

2.9 Measuring ATP in supernatants

20 mls of EDTA (Sigma-Aldrich, UK) was added to a vial of nucleotide monitoring reagent (NMR) and this was stored in 1 ml aliquots at -20^oC until ready for use. The NMR consisted of the firefly luciferase enzyme and its substrate luciferin. In the presence of ATP these react with each other to

form oxyluciferin, AMP and PPi. Further to this light is produced, which is very easy to measure in a lab environment (see Fig 2.2). Before any ATP measurements were performed the NMR was pipetted out into the plastic luminometer tubes. These tubes were placed on ice. After experiments had been performed the 100 µl of medium was taken out of the wells and placed in the labelled tube containing NMR. These could be left on for at least 30 minutes without any adverse effects to the reaction. The reaction was at a dilution of 1:10. The tubes were then placed in the luminometer and read. The samples were read 5 times and a mean taken

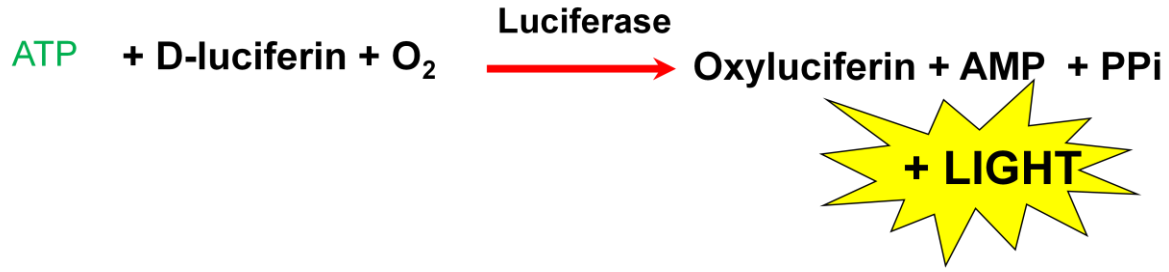

Fig 2.2 The chemical reaction of ATP with luciferin to produce light

The protocol for the measurement of ATP in supernatants was altered during this investigation in an attempt to reduce variation between measurements. This process is described in detail in chapter 3. The final method for measuring ATP is as follows; ATP measurements were performed in HEPES buffered medium to ensure the reaction in Fig 2.2 was carried out at the same pH. Furthermore the samples were loaded into the luminometer and left for 4 minutes to allow the temperature to increase to room temperature and get maximum and consistent readings between experiments. The location in each well where the samples were taken from was also kept exactly the same. This was achieved by using holes drilled into the lid of the plates. This ensured that the pipette tip not only sampled from the same place but also, as it got stuck in the lid, it also sampled from the same depth, see Fig 2.3.

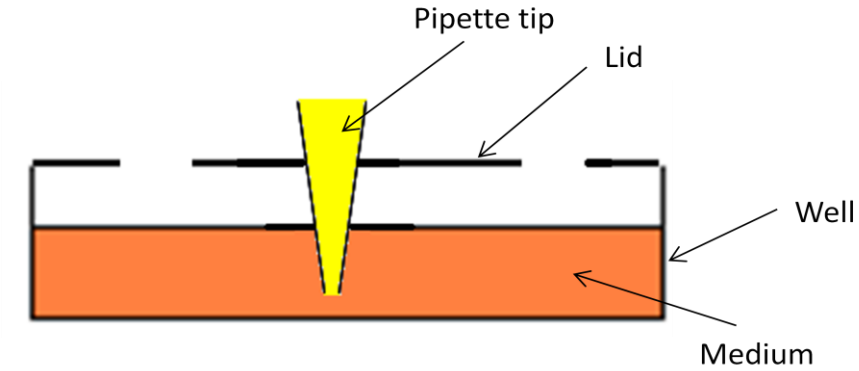

Fig 2.3 6-well lid used to sample medium

2.10 Fluid perturbation techniques

3 methods of fluid movement were tested to examine ATP release. The first of these being medium displacements. To displace the medium 25-50% of the total medium was taken up from the centre of the well in the pipette. The pipette was then moved to the side wall of the well and dispensed against it, so as to minimize any blowing off of cells from the bottom (see Fig 2.4 (A)). Plate vibration was also attempted. This involved placing the plate on the 'micromix 5' (DPC, UK). Three functions could be altered on this vibrating platform. The amplitude of the vibration, which ranged from 0 to 10 (relative units), the frequency of the vibrations, which ranged from 5Hz to 30Hz and the amount of time the plate was left on the platform (see Fig 2.4 (B)). The third method involved the use of an orbital rocker, the type that is generally used a laboratory for incubating membranes with antibodies. The Stuart scientific plate rocker was used in this case (see Fig 2.4 (C)). Two variables were used in the testing. These being the revolutions per minute (RPM) of the rocking, and the amount of time the

plate was rocked. Following on from these methods the medium was sampled from as outlined in section 2.11.

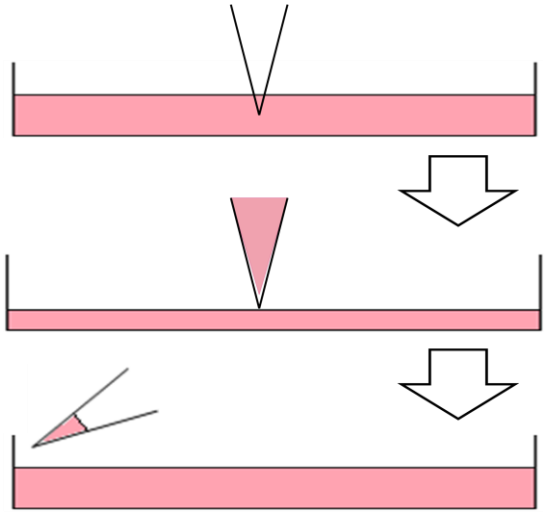

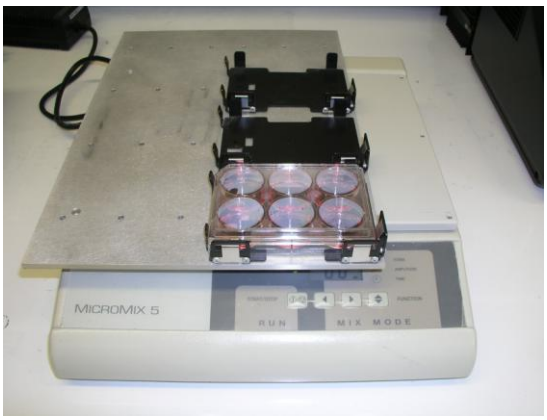

Fig 2.4 Different methods of fluid perturbation. (A) medium displacement (B) plate vibration and (C) plate rocking

2.11 Cell count

Medium was removed from cells and washed twice in PBS. For 24 well plates 0.5ml trypsin was added. These were placed in the incubator at 37^{o}C for 5-10 minutes, depending on if the cells had been lifted. Once ready 1ml of DMEM supplemented with 10% FCS was added to the wells. This was them mixed thoroughly to allow an even distribution of cells. 10µl of cell suspension was added to 10µl of trypan blue (Invitrogen, UK). Again this was mixed well and 10µl of this was placed in a disposable haemocytometer (Lilly, UK). To count the cells the end four large corners were used (see Fig 2.5) and an average taken. The total cell number within the well was then calculated.

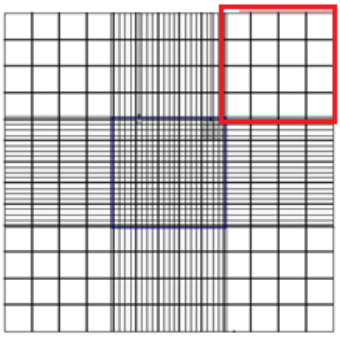

Fig 2.5 Haemocytometer grid. Area marked in red is an example of one of the four corner squares and the blue area is representative of the centre square.

2.12 Micro ct analysis

The knee joint of each mouse was dissected out and placed in phosphate buffered formal saline (PBFS). These were scanned in Sheffield University using a Skyscan Desktop µCT' (Kontich, Belgium). The specimen was placed in the machine using a plastic straw packed with clingfilm to ensure the specimen did not move during scanning. The scan was limited to proximal tibia and fibula. The x-ray source was operated at 49 kV and 200 µA with a 0.5mm aluminuium filter. The CT images were captured every 0.5^{o} through 180^{o} rotation of the bone. The scans were then reconstructed using the provided Skyscan software (SkyScan NRecon) at a threshold of 0.0-0.16. Upon reconstruction the images were made into stacks using imagej (available free to download from

http://rsbweb.nih.gov/ij/). Using this software it was also possible to line the bone in a vertical manner which is necessary for accurate analysis.

To analyse the data the software CTAn (Skyscan) was used. This software allowed a region of interest to be created within the bone and allows the user to determine the threshold limit for the trabecular and cortical bone. Once completed the software will measure the selected parameters and transcribe the data into a notepad file (.rtf). This can them be copied to a spreadsheet to analyse the data.

2.13 Statistical analysis

The statistical analysis carried out in this thesis used the software package Stats Direct (StatsDirect Ltd). As results were observed to be normally distributed analysis of variance (ANOVA) and Student t-tests were used depending on the number of means. For experiments that had more than two means a one-way analysis of variance, with a Tukey post test, was used. When two means were being compared an unpaired, two tailed Student t-test was carried out to determine significance. The significance level was set at $P<0.05$ for both ANOVA and the Student t-test. Star symbols were used in graphs to represent significance. One star represents $P<0.05$, two stars represent $P<0.01$ and three stars represent $P<0.001$. Results are presented as either mean ± standard error or mean ± standard deviation. Sample number for each graph is presented in the figure legend.

3. The release of ATP from osteoblast cells

3.1 Introduction

The field investigating ATP release from cells has risen alongside purinergic signalling. The first evidence of ATP release came during the early years of purinergic study, and was shown in neurones by Holton and Holton [191] in 1954. This was followed up by studies, outlined in the Introduction, that showed ATP release coincided with depolarisation of frog nerves and muscle [192], and which showed similar depolarisation in nerves that were non-adrenergic and non-cholinergic [29]. As well as in neurones, it is now apparent that ATP release, like purinergic signalling, is incredibly widespread. For example: vascular cells [193-195], astrocytes [109], glial cells [196], Sertoli cells [197] and chondrocytes [198] have all been shown to release ATP in response to stimuli. How cells achieve ATP release is also diverse, they include mechanical stimulation (shear stress, deformation etc), hypoxia, acidosis and osmotic damage [95]. Osteoblasts also release ATP, which was first discovered in 1998 by Bowler *et al* [199]. Furthermore it was also shown that ATP is released from osteoblasts is response to mechanical stimulation.

The importance of purinergic signalling and, therefore ATP release, in bone is shown in the wide variety of functions that are attributed to it. It has been implicated in increased osteoblast proliferation [200], decreased bone mineralization [69], increase in osteoclast activity and fusion [201] and finally it also aids the release of other mediators, for example LPA [202].

Initially the focus of this chapter was to specifically investigate how ATP was released by SaOS-2 cells. Is it by exocytosis, ATP binding cassettes, P2X7 receptors or gap hemichannels? All of which have been implicated in other cell types [203]. On initial investigations, it became apparent that investigating the mechanism behind ATP release would not be feasible, because the variation seen in these experiments were massive. For example, some experiments would have relative large concentrations of ATP after 1 medium displacement, whilst other experiments would have very little or no ATP after 1 medium displacement. It also even became apparent that the ATP concentration was not consistent across a single well, in some areas of the well ATP concentrations would be 10

times higher than other parts. Of course this issue would make it impossible to study how ATP was released, as altering the conditions to determine how ATP release was affected would be of little use if levels fluctuated as much as they did. Therefore much of investigation looked at decreasing this variation such that future investigators will be able to carry out experiments knowing that they are standardised.

3.2 Methods

3.2.1 ATP measurement

To measure ATP NMR containing luciferin and luciferase was used. How this works is outlined fully in the Material and Methods, briefly they are able to react in the presence of ATP to produce light which can be measured. Before experiments, 10 µl NMR was pippetted into luminometer tubes and placed on ice. This was to ensure that it would not react with the ATP before it was placed in the luminometer. The majority of experiments carried out in this chapter use the technique of 'medium displacements' to create fluid shear stress over the cells. This involves taking medium from the well, usually a third of the volume of medium, and then dispensing it against the side wall to ensure that cells on the bottom were not blown off. Caution was taken to ensure that the pipette tip did not touch the bottom of the well and thus damage cells. Other experiments used plate vibrators and orbital rockers to cause fluid movement.

Once the cells had been treated 100 µl of medium was taken off and placed in the NMR. The samples were then read and a calibration curve was used to determine the concentration of ATP.

3.2.2 Investigating ATP release

To investigate the release of ATP a number of chemicals were used. These included ATP, NEM, HEPES buffered medium and potassium (all obtained from Sigma-Aldrich, UK). Whilst investigating the release of ATP from osteoblasts cultured on different substrates dentine disks, which were cut from walrus and glass coverslips (BDH, UK) were used

3.2.3 Using mtDNA as a measure of cell death

This technique was developed as lactate dehydrogenase (LDH) is not a sensitive enough measure of cell death when measuring ATP in a supernatant. This is because ATP is also released when cell death occurs and can be detected in smaller quantities than LDH. To detect mtDNA in the supernatant

primers were specifically designed to recognise repeats on individual mtDNA chromosomes. This combined with the fact that there are 2-10 copies of the chromosome in one mitochondria, and cells have on average 200 mitochondria per cell means this is an extremely sensitive test. In theory it should be able to recognise one single cell, whereas LDH cannot distinguish between 200 cells. The test simply consists of adding the supernatant, possibly containing cell debris, to the real time PCR reaction, which has the mtDNA primers in it. A calibration curve was constructed by lysing known number of SaOS-2 cells, then diluting this to create a series of solutions containing known cell numbers. These can be plotted against the threshold value that is produced in the real time PCR reaction.

3.3 Results

3.3.1 Standard curve for luminometer measurements, and ATP half life *in vitro*.

Fig 3.1 outlines the calibration curve that is used to determine the concentration of ATP *in vitro*. Then, given that ATP half life data *in vitro* appears to be different from laboratory to laboratory (unpublished) steps were taken to measure it again and it was found to be 9 minutes. This graph is shown in Fig 3.2.

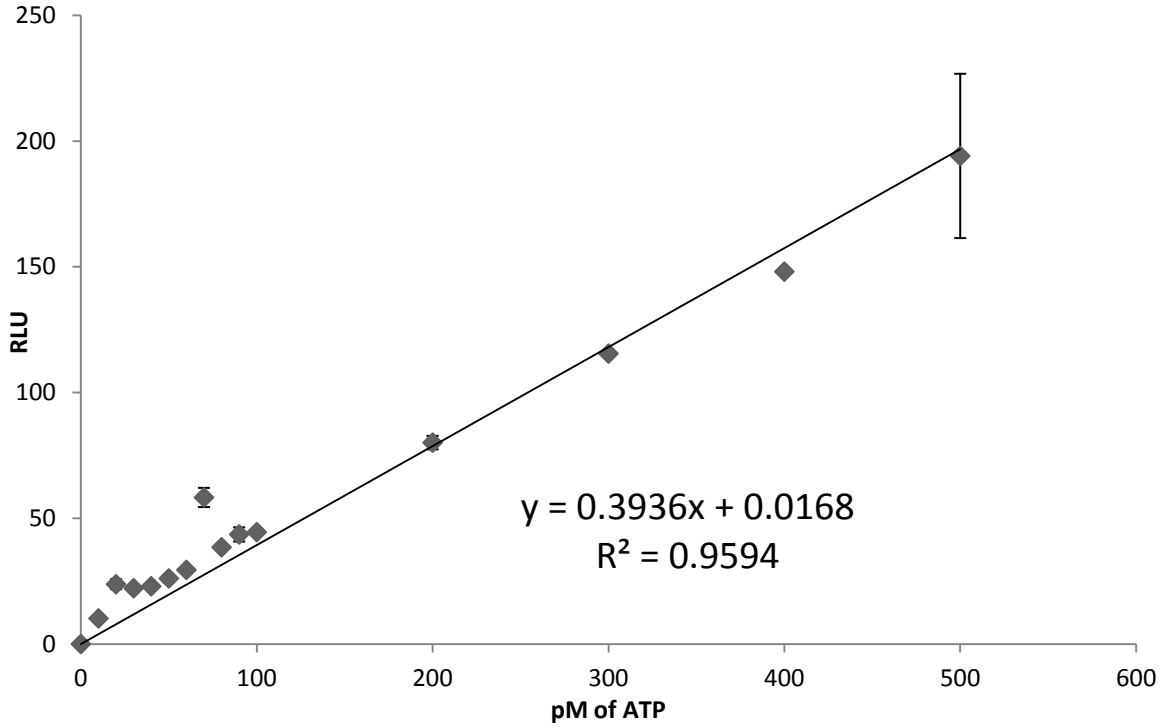

Figure 3.1. Calibration curve comparing ATP concentrations to RLU in the Berthold tube luminometer. Known concentrations of ATP were made up from 0 to 500 pM and read in the Berthold tube luminometer. Relative light units were recorded, plotted against pM ATP and a linear trend line was fitted. n=6. Error bars = S.D.

Fig 3.1 shows the calibration curve for ATP concentrations compared to the relative light units produced by the Berthold tube luminometer. A linear trend line was fitted to the graph as $R^2 = 0.9594$ and thus was a good fit. The equation to find pM ATP (x) is x= (y-0.0168)/0.3936.

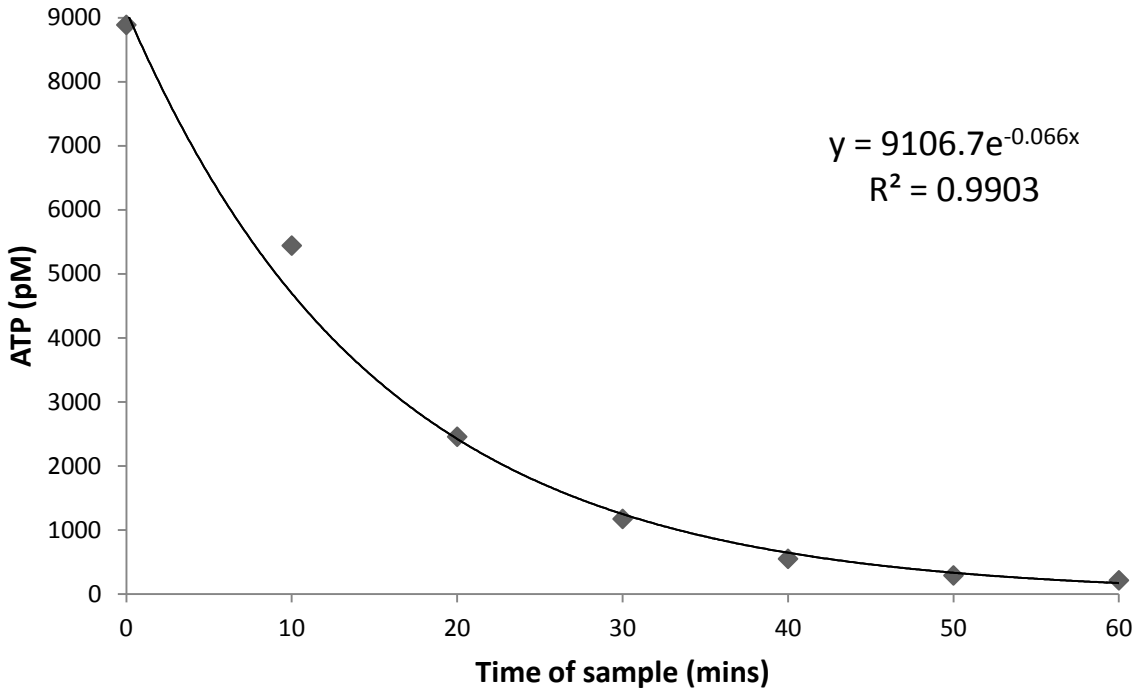

Figure 3.2. The half life of ATP in a SaOS-2 cell culture. 500 nM ATP was added to the medium, left for 30 minutes and then a 100 µl sample was taken every 10 minutes from the supernatant. An exponential line was fitted. n=1.

The experiment shown in Fig 3.2 was carried out to determine the half life of ATP *in vitro*. ATP was dissolved in medium to 500 nM and then added to the wells. A period of 30 minutes was left until the first sample was taken to ensure the cells had stopped releasing ATP. A sample was taken then, and every subsequent 10 minutes. It shows the ATP half life is 10.5 minutes.

3.3.2 SaOS-2 cells release ATP when subjected to medium displacements

Fig 3.3 shows experiments were SaOS-2 cells were subjected to medium displacements and then the ATP concentration in the medium was measured. It can be seen that medium displacements caused an increase in ATP presence within the medium. However there was massive variation between repeats A), B) and C).

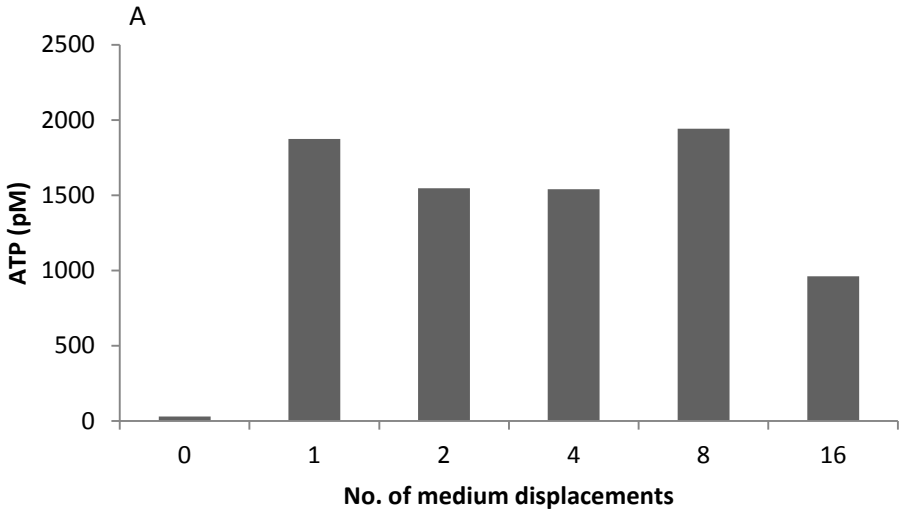

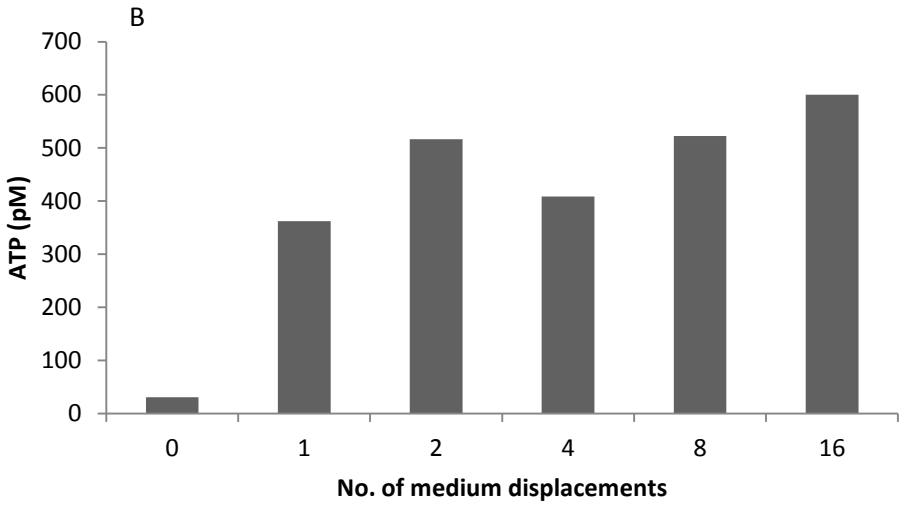

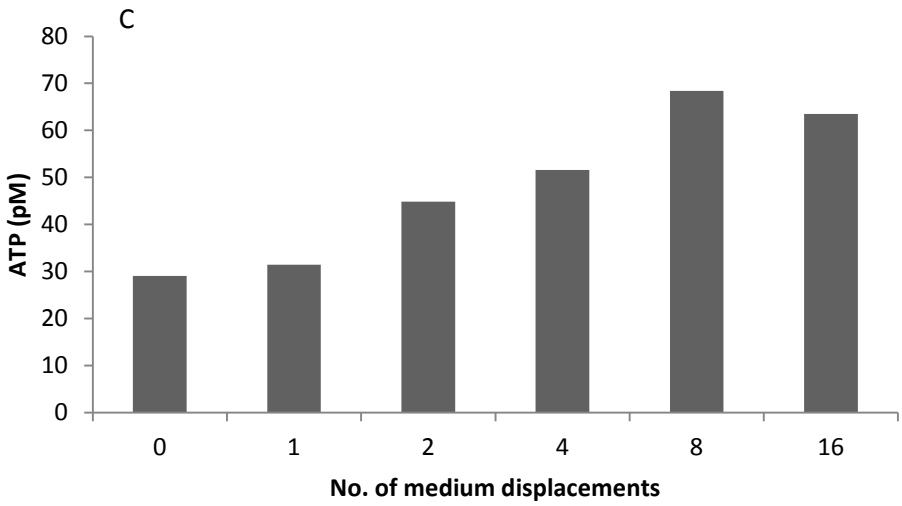

Figure 3.3. (A, B and C). ATP concentrations in SaOS-2 supernatants after medium displacements. Medium displacements were performed in different wells and then sampled from to measure for ATP.

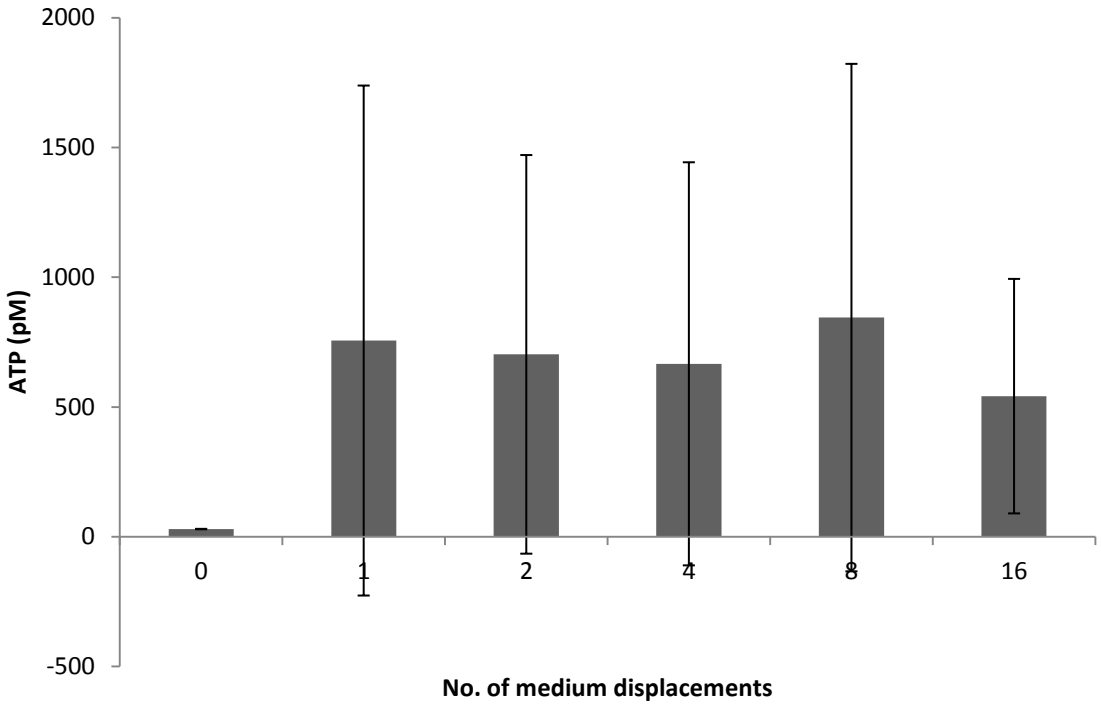

Figure 3.3 (D). ATP concentrations in SaOS-2 supernatants after medium displacements. Medium displacements were performed in different wells and then sampled from to measure for ATP. n=3. Error bars = S.D.

Fig 3.3 A), B) and C) represent the standard medium displacement experiments. They have been displayed separately to show the difference in pattern between each experiment. Fig. 3.3 D) shows the mean of all 3 experiments. These figures show that, as there was ATP present within the medium prior to medium displacement, ATP is constitutively released from SaOS-2 cells. Further to this Fig 3.3 shows that there is an increase in ATP present within the medium following medium displacements. However, there is high variation between experiments (note the different y-axis on each graph) and furthermore there is not a consistent pattern between experiments i.e. in C) the graph ascends to 8 medium displacements before levelling off at 16 medium displacements. However, in A) the graph peaks at 1 medium displacement and then descends before peaking again at 8 medium displacements, with 16 medium displacements having the lowest value. As stated in the Introduction this made investigations into what causes ATP release difficult and therefore attempts were made to reduce the variation.

3.3.3 The effects of temperature and pH on luciferase

Currently the experiments were performed in serum free medium to prevent excess breakdown of ATP due to ATPases present in the serum. However the experiments required the plate to be out of the CO_2 incubator, and thus the medium became alkaline due to the partial pressure of $C0_2$. Therefore, during an experiment, taking an early sample from the supernatant meant it was more acidic than taking a later sample. To test if this had a large effect on luciferase a solution of ATP was measured at different pH's. This would determine if the length of time the plate was out of the incubator contributed to the high variation. Fig 3.4 shows that it does have an effect, showing the need to keep the pH the same between tests.

Further tests were carried out on the kinetics of the enzyme, in the next case the effect of temperature was determined. A solution of ATP was kept on ice in NMR, as with all tests that are carried out, then placed in the tube luminometer and measured straight away and every subsequent two minutes. This was an important test to carry out, because in large batches samples loaded first would be warmer than those loaded last. So this test was carried out to determine how much of a difference that made to the light readings and if, because of this, future experimental methods needed to be changed. Again Fig 3.5 shows that leaving the sample for 4 minutes causes a large difference in the light readings given off. Therefore in future all samples were taken off the ice for the same period of time.

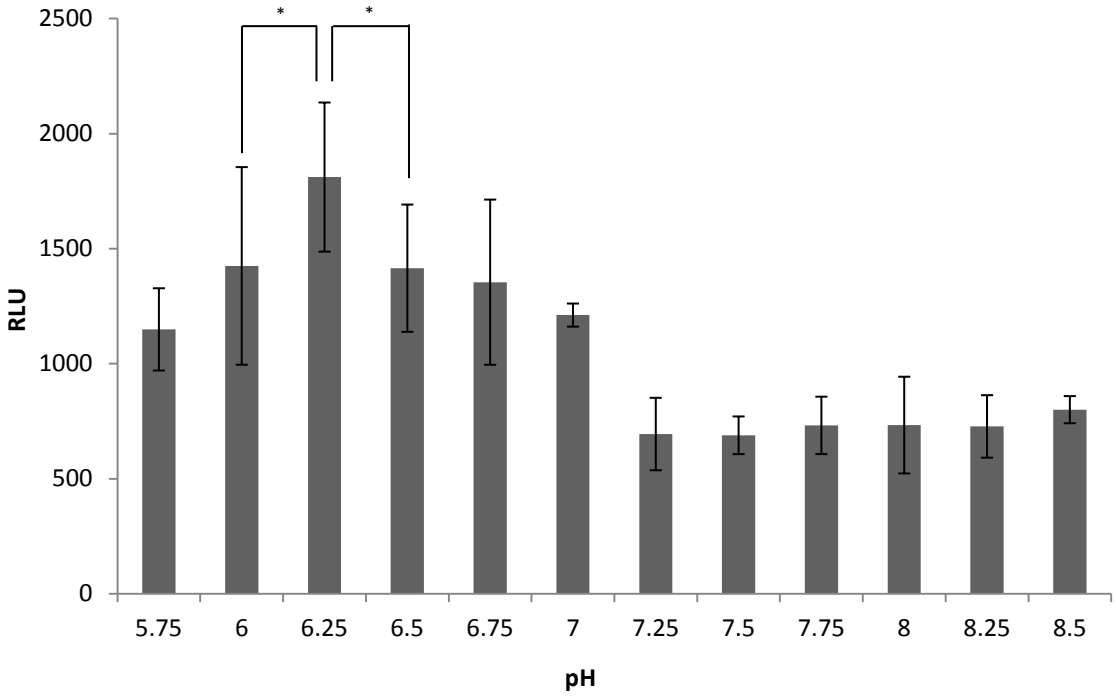

Figure 3.4. 2 nM ATP measured at different pH levels. 2 nM of ATP was made up and then the pH of the solution was adjusted. 3 measurements of 100 µl was taken from each solution and measured in the luminometer. n=3. Error bars = S.D.

This graph shows that 6.25 is the optimal pH for the luciferase enzyme as is produced the most light. A difference in the pH of 0.25 can make a large difference to the light reading with 6 and 6.5 being significantly different to 6.25. This outlines the importance of keeping the pH of the luciferase enzyme constant through different experiments. Following these results it was determined to now carry out all ATP release experiments in HEPES medium. HEPES is an organic chemical buffering agent and so does not need the presence of CO_2 to carry out its buffering properties. Thus it can be kept out of the incubator for a lengthy period of time and still maintain the same pH. Therefore measurements of ATP at the start of a long experiment will be comparable to measurements of ATP at the end of an experiment.

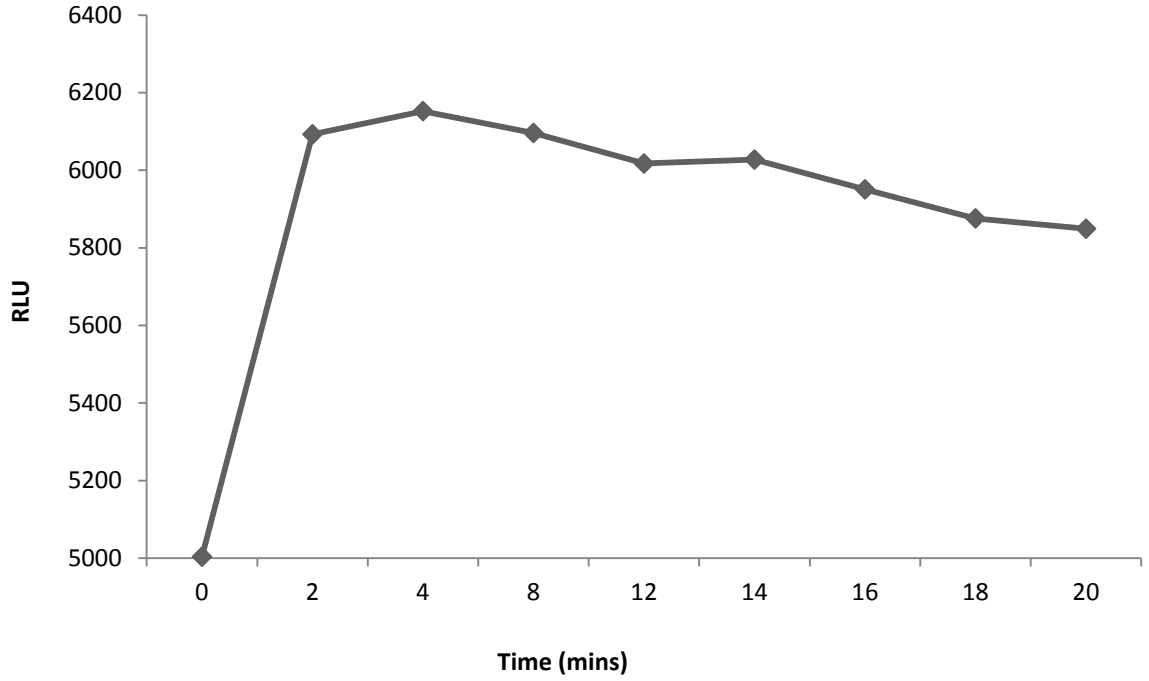

Figure 3.5. The effect of time on ATP measurement. The 10 nM sample of ATP was taken off ice, placed in the tube luminometer and then had light measurements taken every 2 minutes. n=1.

This graph shows that samples measured immediately produce less light than samples that have been left to warm up at room temperature. The same sample that initially measured 5000 light units now read 6100 light units 4 minutes later. This difference is equivalent to 3 nM ATP using the calibration curve. Following on from the peak at two minutes there was a slight increase to 4 minutes followed by a steady decline in the light units that were produced, reaching 5900 after 20 minutes.

This experiment emphasises the need to perform ATP measurements at the same time, previous to this samples were placed into luminometer and measured straight away. However the time it takes to load the samples and measure will differ between experiments with lots of samples and experiments with few samples. Therefore samples placed in the luminometer to start with would warm up by the time loading had finished which would contribute towards the variation that was seen in, and between, experiments. From this point onwards only small sample sets of 5 were placed in the luminometer and then left for 4 minutes before being read. The other samples would remain on ice to be loaded later on.

3.3.4 ATP release following plate vibration

In addition to reducing the variation by altering the conditions of the luciferase enzyme, tests were carried out to standardize the fluid perturbation technique to a more consistent method. Firstly by using a plate vibrator, shown in Fig 2.4 (B), the specifications of which were described in Material and Methods. This machine was able to alter the frequency the plate was vibrated at, the amplitude of the vibration and the time the plate was vibrated for. This was shown, at this stage of investigation, to cause release of ATP, although a lot of variation was encountered.

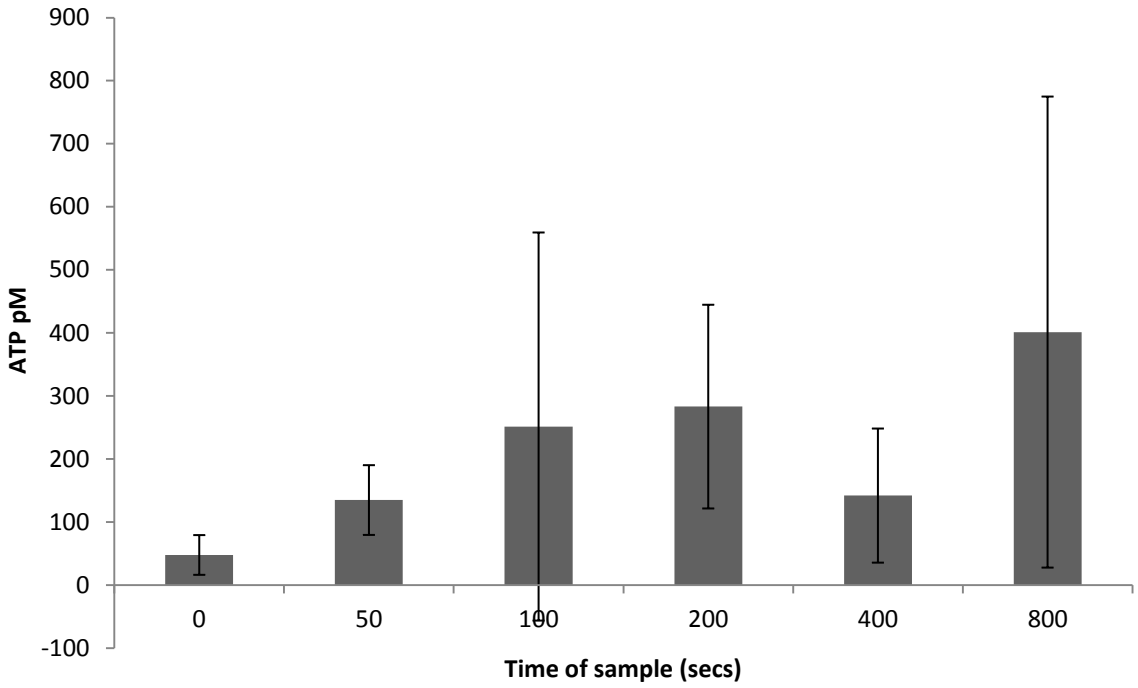

Figure 3.6. Concentration of ATP in SaOS-2 supernatants after plate vibration. SaOS-2 cells were vibrated at 15 Hz for 800 seconds. 100 µl samples were taken from separate wells, before vibration, after 50, 100, 200, 400 and 800 seconds of vibration. n=3. Error bars = S.D.

Fig 3.6 shows that vibration appears to cause a release of ATP from the SaOS-2 cells into the medium. After vibration, for any amount of time, there was an increase of ATP levels in the medium. This peaks at 800 seconds, which has an average of 350 pM (+/- 385 pM S.D.). These increases, however, were not significant because the variation between experiments was large. Also again note that SaOS-2 cells secrete ATP constitutively with basal levels at 47.6 pM (+/- 42 pM S.D.)

3.3.5 ATP readings within a single well

Despite the changes that had so far been applied there was still high variation in experiments. Fig 3.7 shows a test where multiple readings were taken from the same well as it had been assumed, until now, that ATP within a well would diffuse and give similar readings across the well. The experiment showed that multiple samples of ATP from within a well gave different readings.

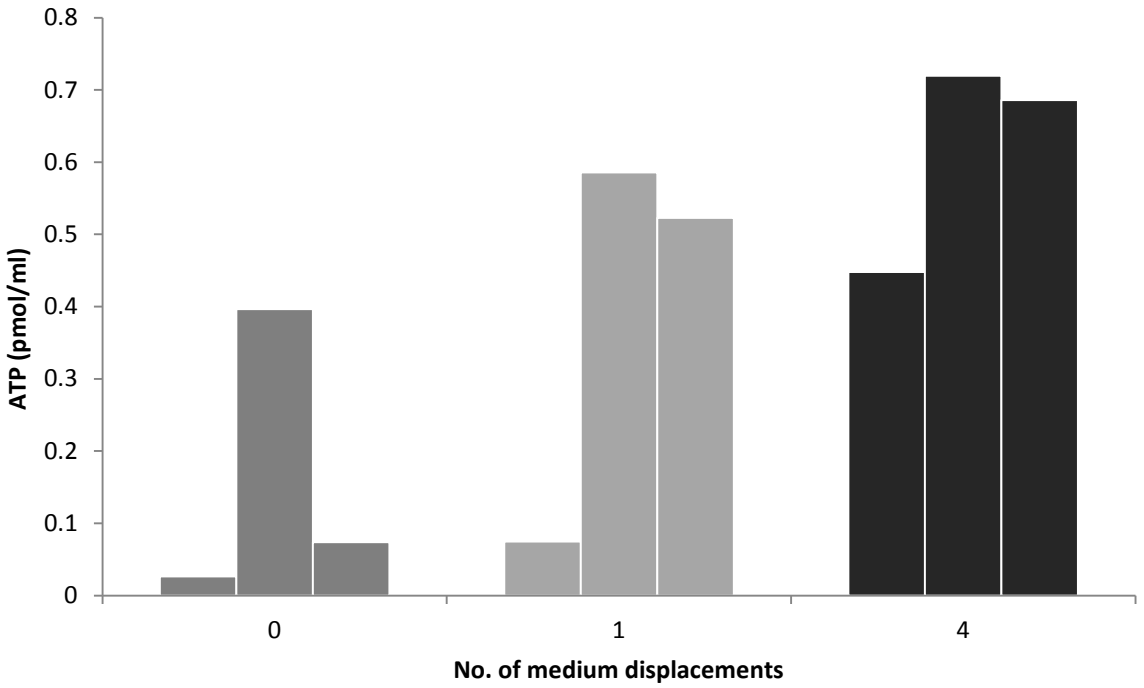

Figure 3.7. The concentration of ATP from different areas of the same well after SaOS-2 cells were subjected to plate vibration. At each time point 3, 100 µl, samples were taken from the same well in different areas. Plate vibration was at 5Hz and amplitude of 7. n=1.

This experiment (Fig 3.7) takes one well and samples 3 times from it in different areas. 3 samples were taken before vibration, 3 samples were taken after 1 minute of vibration and 3 samples were taken after 4 minutes of vibration. It shows that an increase in the time of vibration caused an increase of ATP present in the medium. However, the major point of this experiment is the fact that there appears to be high variability within a single well, this was present even before the plate had been vibrated. At this stage it was believed that ATP was being released in individual bursts and that is why sampling from different parts of the well would give different levels of ATP. This was believed to be why there was high variability between experiments.

3.3.6 Changes implemented to measuring ATP in a supernatant

Given that basal levels of ATP were different in different parts of the well, and that basal levels were different between experiments, even with comparable cell numbers, it was decided to change how ATP was read. From now on, where possible, 3 samples of ATP were taken from each well before manipulation (medium displacement or vibration) then a further 3 samples were taken after manipulation. This would allow an average reading of ATP in the well, before and after mechanical stimulation, as well as being able to calculate a percentage difference.

Further to this, another tool was implemented in an attempt to reduce the variation between experiments. This entailed the use of using, for a 6 well plate, a 6 well plate lid with small holes drilled into it for the pipette tip, there were 3 holes for each well. This is again outlined in more detail in the Material and Methods, but briefly, using these holes for the pipette tip allowed 3 advantages: firstly it allowed the samples to be taken from the exact same area of the well each time, a must, given the variation in a well. Secondly it allowed samples to be taken from the same depth, as it is likely that more ATP would be present near the cells that release them, thus sampling from the top of the well may give different results from sampling near the cells. Finally, it also prevented the pipette tip hitting the bottom of the well which had previously ruined a lot of experiments as this would likely damage the cells and release ATP. Fig 3.8 shows the first experiments using the new methods.

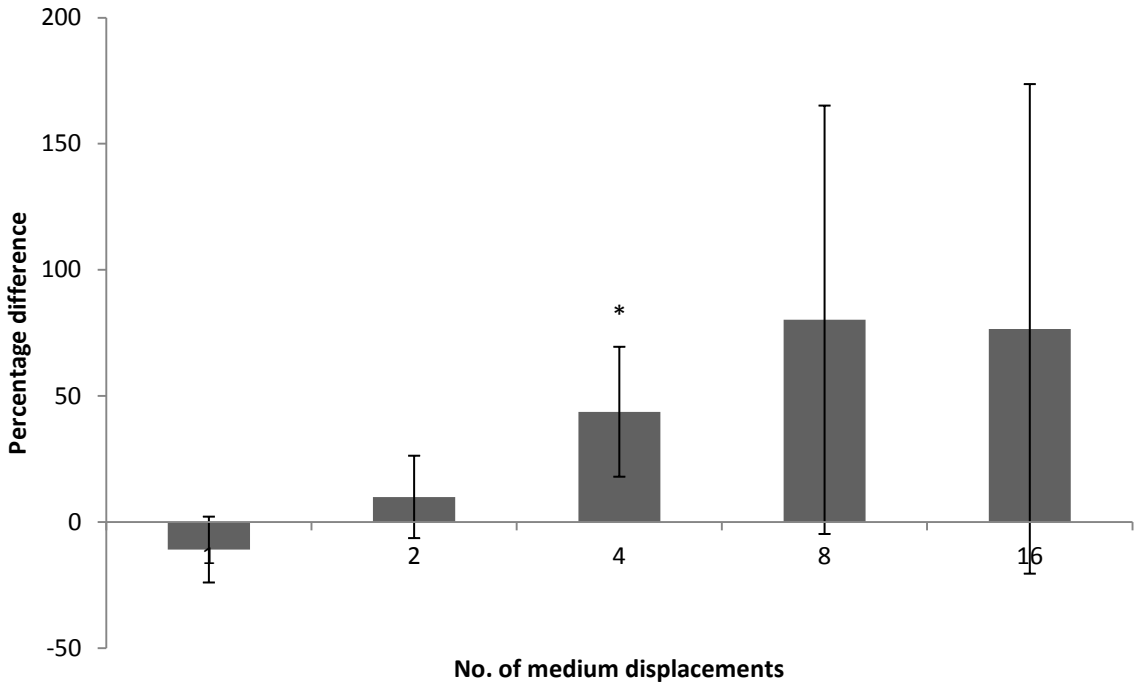

Figure 3.8. The percentage difference of ATP concentrations in SaOS-2 supernatants before and after medium displacements. 3 samples were taken before and 3 samples were taken after medium displacements using the lid with holes in. n=6. Error bars = S.D.

This experiment was performed using all the changes listed above. That is, it was performed in HEPES medium with 3 measurements taken before and 3 measurements taken after, the lid with holes in was used and samples were measured at the same temperature. As samples were taken before and after the percentage difference was calculated. The graph shows that in this instance, because of the high variation in the other results, only 4 medium displacements caused an increase in ATP as it was the only significant result ($p>0.05$).

3.3.7 Medium displacements using a multi-channel pipette

The next experiment attempted to standardize medium displacements by using a multi-channel pipette, this would ensure that the force being applied was the same between different wells. Fig 3.9 shows an experiment that took 3 samples from 4 wells, then these 4 wells were displaced at the same time using the multi-channel pipette and 3 samples were taken after. The percentage difference of these was calculated. Again, this used the lid with holes in to sample, it was performed in HEPES medium and the samples were left for 4 minutes before reading.

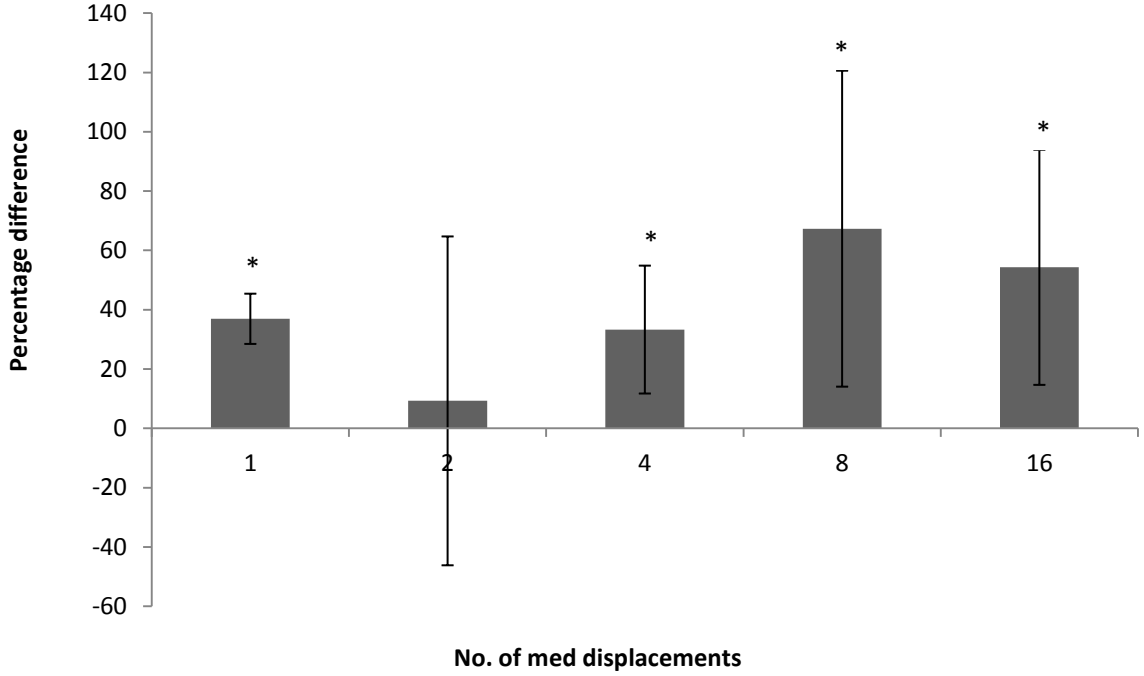

Figure 3.9. ATP released after SaOS-2 cells were subjected to medium displacements using a multi-channel pipette. 3 measurements were taken from each well before, then wells were displaced using a multi-channel pipette, then 3 samples were taken after. Percentage difference was calculated. n=4. Error bars = S.D.

The results show once again that medium displacements cause an increase of ATP within the medium. The highest difference being that of 8 medium displacements with a 67% increase (+/- 49% S.D.), the lowest being 2 medium displacements having a 9% increase (+/- 59% S.D.). However, a multi-channel pipette did not cause a decrease in the variability that was seen nor did it give a consistent pattern between experiments.

3.3.8 ATP concentrations in SaOS-2 supernatants following plate vibration and plate rocking experiments

The changes that had been implemented were tested on the plate vibrator in an attempt to reduce variation. Again these changes being that the was experiment performed in HEPES, samples were left for 4 minutes before reading, sampling was carried out using the 'sampling' lid, taking 3 samples from each well and taking before and after plate vibration measurements. On this occasion the time the plate was vibrated for remained the same at 2 minutes, as was the amplitude at 7, but the frequency was altered between plates with frequencies of 5Hz, 16.5Hz and 30Hz. The results in Fig 3.10 show that there is no release of ATP following vibration of the plate.

Given the apparent lack of ATP release after vibrating another method of fluid perturbation was looked at. This time the plate was placed on an orbital rocker (Fig 3.11.), on which the time or the RPM could be altered between tests. All the conditions listed above for the vibration experiment were kept the same for this. Again no ATP release was observed.

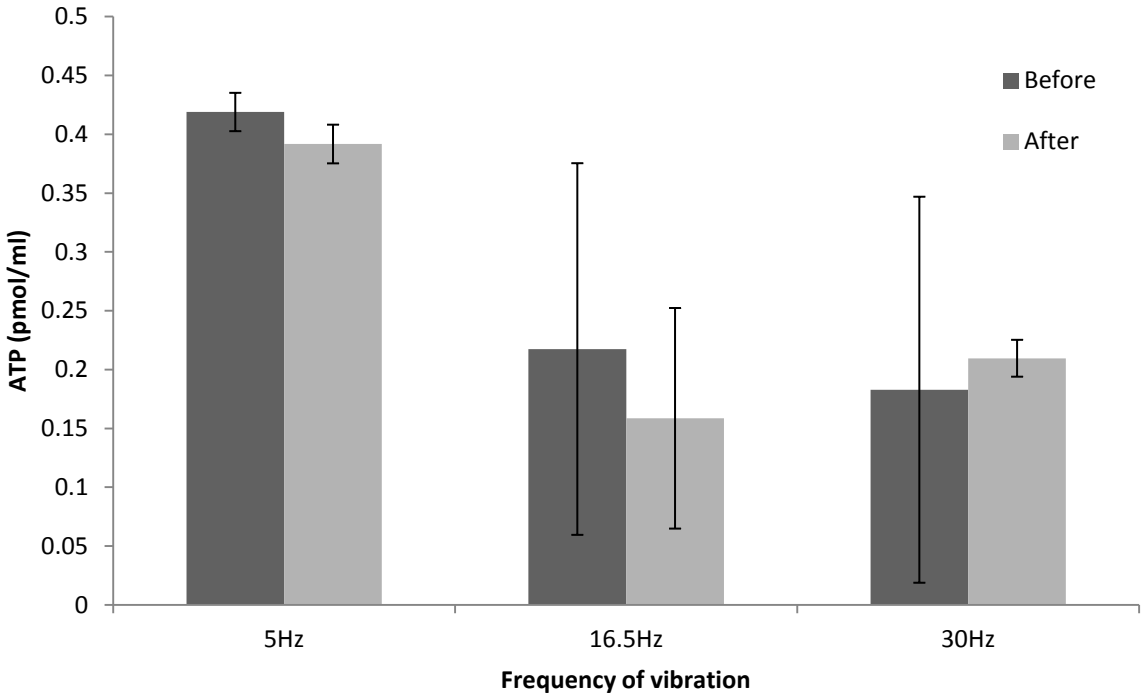

Figure 3.10. Concentration of ATP in SaOS-2 supernatants taken before and after vibration. Before the plate was vibrated 3 samples of 100 µl of the supernatant were taken from each well. Cells were then vibrated for 3 minutes and 3 samples were taken after. n=3. Error bars = S.D.

Fig 3.10 shows the ATP concentration in the medium before and after the SaOS-2 cells were vibrated. In each case, 5 Hz, 16.5 Hz and 30 Hz, there was no significant difference between ATP concentrations after the cells were vibrated. Again it should be noted the need to perform before and after measurements as there is a large difference in basal levels between wells, with the 5 Hz wells averaging 0.4 pmol/ml (+/- 0.01 pmol/ml S.D.) and both 16.5 Hz and 30 Hz averaging 0.2 pmol/ml (+/- 0.16 pmol/ml S.D.).

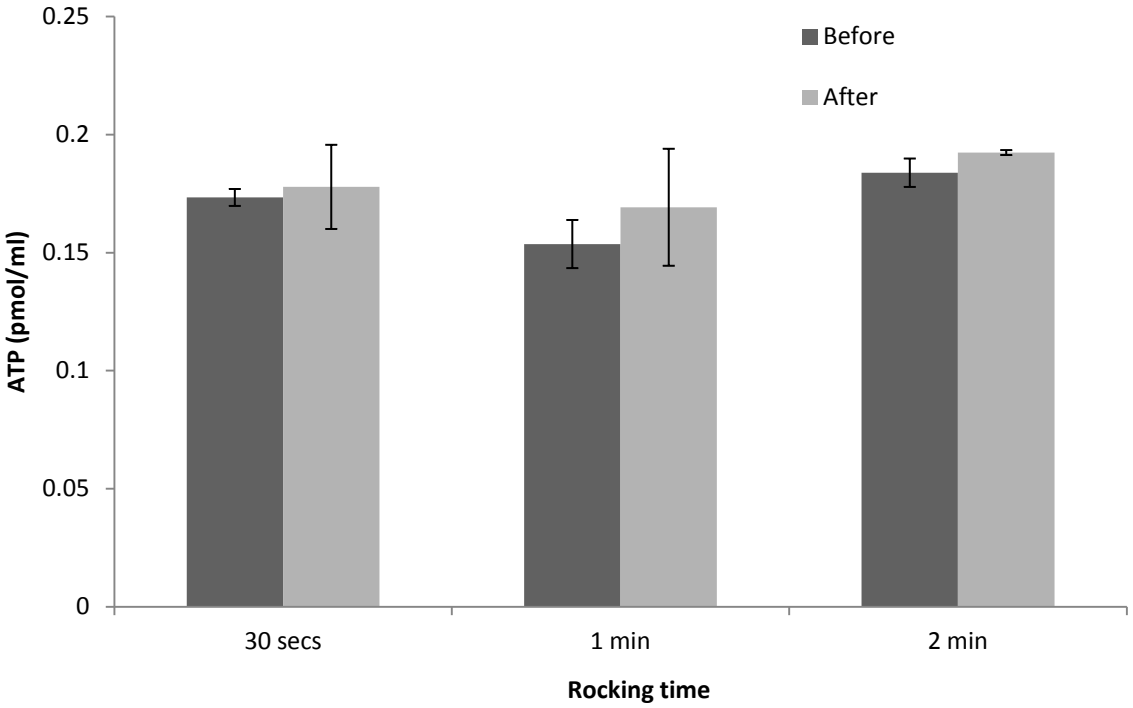

Figure 3.11. The concentration of ATP in SaOS-2 cell supernatant before and after the plate underwent orbital rocking. 3 samples were taken before, then plates were subjected to orbital rocking at 30 RPM, then 3 samples were taken after orbital rocking. n=3. Error bars = S.D.

This graph (Fig 3.11) shows an experiment where 6 well plates, cultured with SaOS-2 cells, were placed on an orbital rocker and rocked for different periods of time. All were rocked at 30 RPM. Again samples were taken before and after from the same area (using the lid with holes in) and the average calculated. The lengths of time were chosen as they were comparable to how long it takes to perform medium displacements. Fig 3.11 shows that there was no significant difference of ATP in the medium before and after the plate was rocked. This was the same for all lengths of time that the plate was rocked for.

3.3.9 Using mtDNA to determine cell number in a supernatant

Given the apparent lack of ATP release with plate vibration or orbital rocking it was now decided to re-examine the possibility of medium displacements causing cell membrane damage and thus releasing ATP via that mechanism. It has been shown previously by using LDH measurements that no cell death was occurring and that ATP was being released through normal physiological means (not published). However it was thought, given results on the plate vibrator and the plate rocker, that this needed to be re-examined in more detail. A new, more sensitive, measure of cell death was developed using mtDNA. Multiple mtDNA can be present in one mitochondria and cells on average contain 200 mitochondria. On top of this primers were developed that recognised highly repeated sequences on the mtDNA, thereby making it a very sensitive test. Also it can tell if live cells have been lifted off the bottom, and therefore contributing towards the ATP in the sample.

Firstly, as described in the methods part of this chapter, a calibration curve was calculated to compare amounts of mtDNA to cell number, either damaged of floating in supernatant. Then cells were subjected to medium displacements, plate vibration or plate rocking. The samples that were taken from them were measured for ATP, then placed in a PCR reaction with the primers for mtDNA to determine the ct value and thus the cell number. This would attempt to determine if the high levels of ATP in medium displacements were due to damaged cells or cells being lifted off the bottom. Fig 3.13 shows that there was more cell debris in the supernatant following medium displacements.

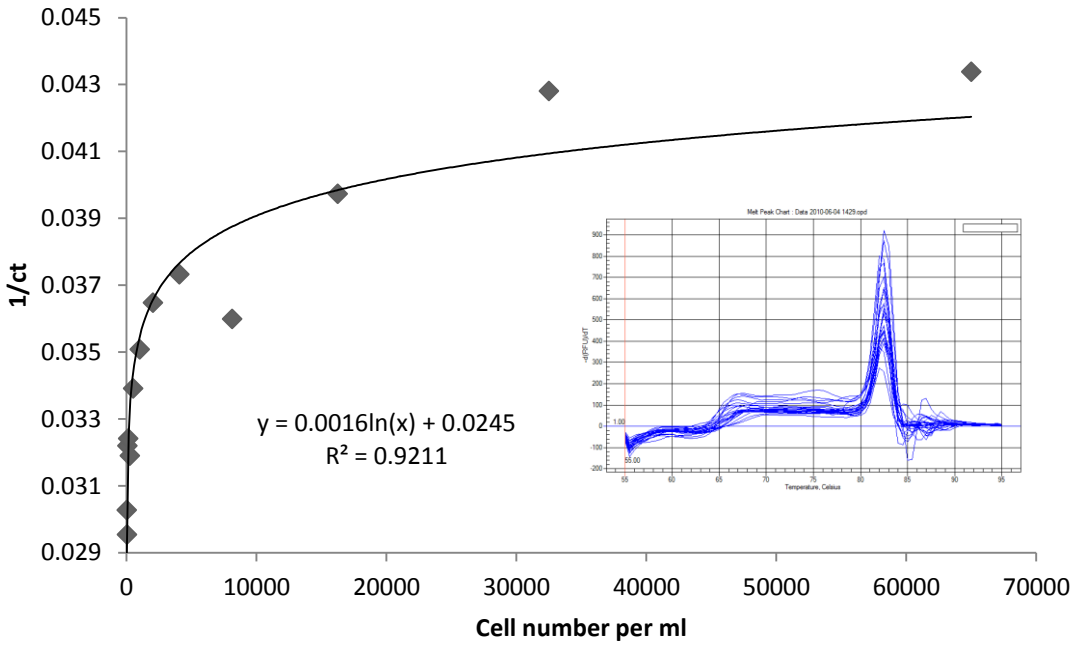

Figure 3.12. (A) Calibration curve comparing 1/ct value for number of cells in PCR reaction. Cells were grown to confluence and then lysed using H_2O. Cell lysate was then subjected to a series dilution and placed in a PCR reaction containing mtDNA primers. The cell number was determined by counting cells in a sister well. n=1**(B) melt curve of the mtDNA primer amplified product.**

This graph (Fig 3.12) is the calibration curve that is used for future experiments concerning the examination of SaOS-2 cytotoxicity.

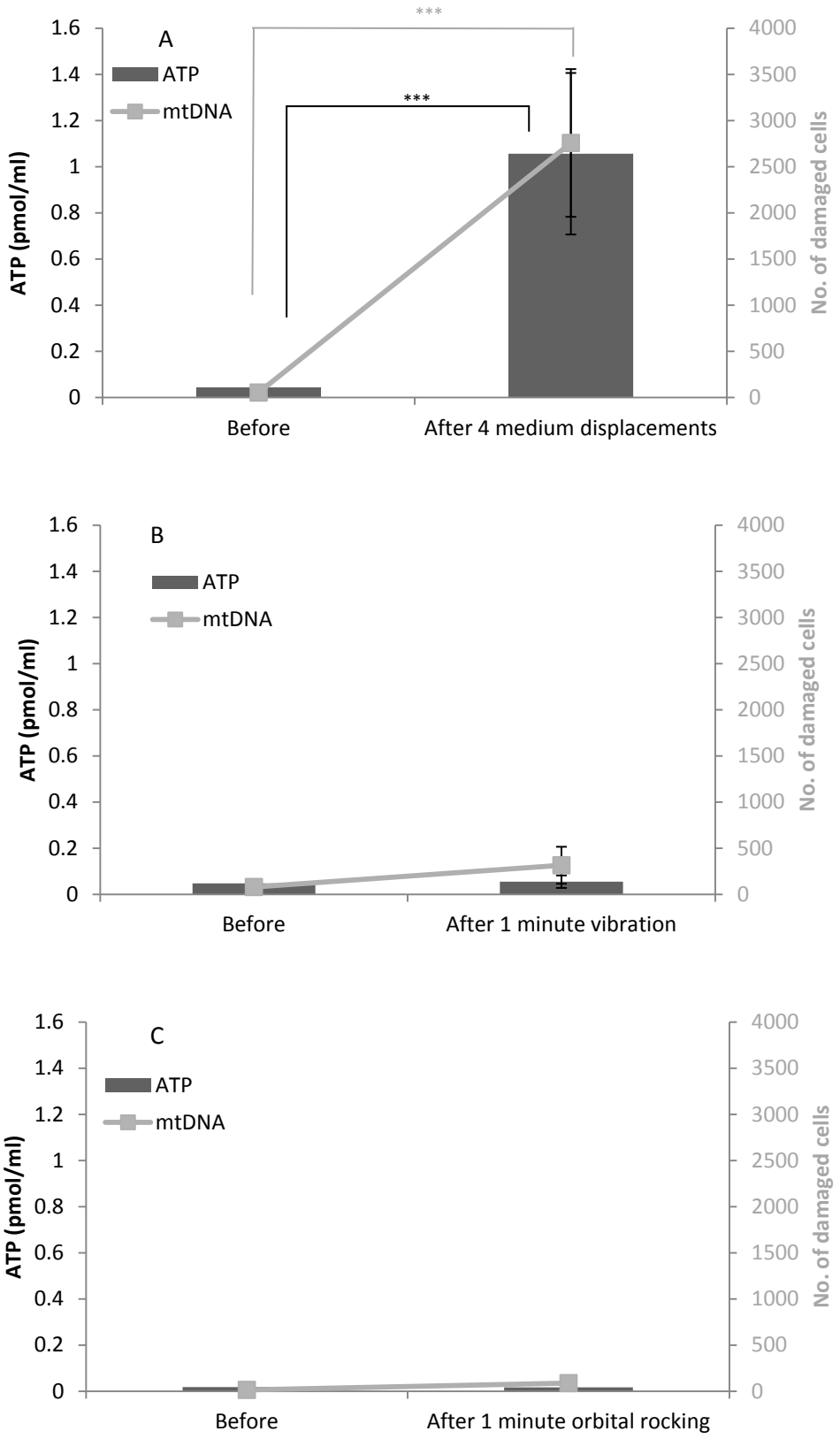

Figure 3.13. ATP and mtDNA levels in the SaOS-2 supernatant following A) medium displacements, B) plate vibration and C) orbital rocking. Samples were taken before treatment, then plates were subjected to displacement, vibration or rocking. Samples were then taken after to measure the change in ATP. These samples were stored in -20^{o}C and added to a PCR reaction to test for mtDNA. n=3. Error bars = S.D.

These results show that medium displacements cause an increase of ATP in the medium. With 1 pmol/ml ATP (+/- 0.35 pmol/ml S.D.) after displacements compared to basal levels of 0.04 pmol/ml ATP (+/- 0.01 pmol/ml S.D.), this difference was significant. Again both rocking the plate and plate vibration caused no increase of ATP in the medium. There was an increase in mtDNA in the medium following medium displacements, which was significant, measuring 2756 total damaged/floating cells (+/- 800 cells S.D.). The vibration and rocking did not have a significant increase of mtDNA in the medium, with measurements of 314 total damaged/floating cells (+/- 200 cells S.D.) compared to 79 total damaged/floating cells for vibration (+/- 12 cells S.D.) and 86 total damaged/floating cells (+/- 8 cells S.D.) compared to 13 total damaged/floating cells for plate rocking (+/- 2 cells S.D.).

3.3.10 Inhibition of exocytosis prevents increases of ATP within the media

Given the knowledge that there is increased mtDNA in the medium the question was whether the cells were being damaged on the bottom and releasing ATP, or whether the medium displacements were lifting cells off the bottom, and therefore being taken up with the sample and measured for mtDNA. The next test, Fig 3.14, looked at using NEM, an exocytosis inhibitor that has been used previously to stop ATP release in response to medium displacements [10, 204]. It was examined alongside mtDNA presence in the medium. If NEM did not cause an inhibition of ATP release and there was mtDNA in the medium then it would be likely that medium displacements were causing an increase in ATP via damaged cells. However if mtDNA did increase and NEM inhibited ATP release then it is likely that medium displacements, as well as releasing ATP, also cause cells to be lifted off the bottom, and therefore contribute to variation.

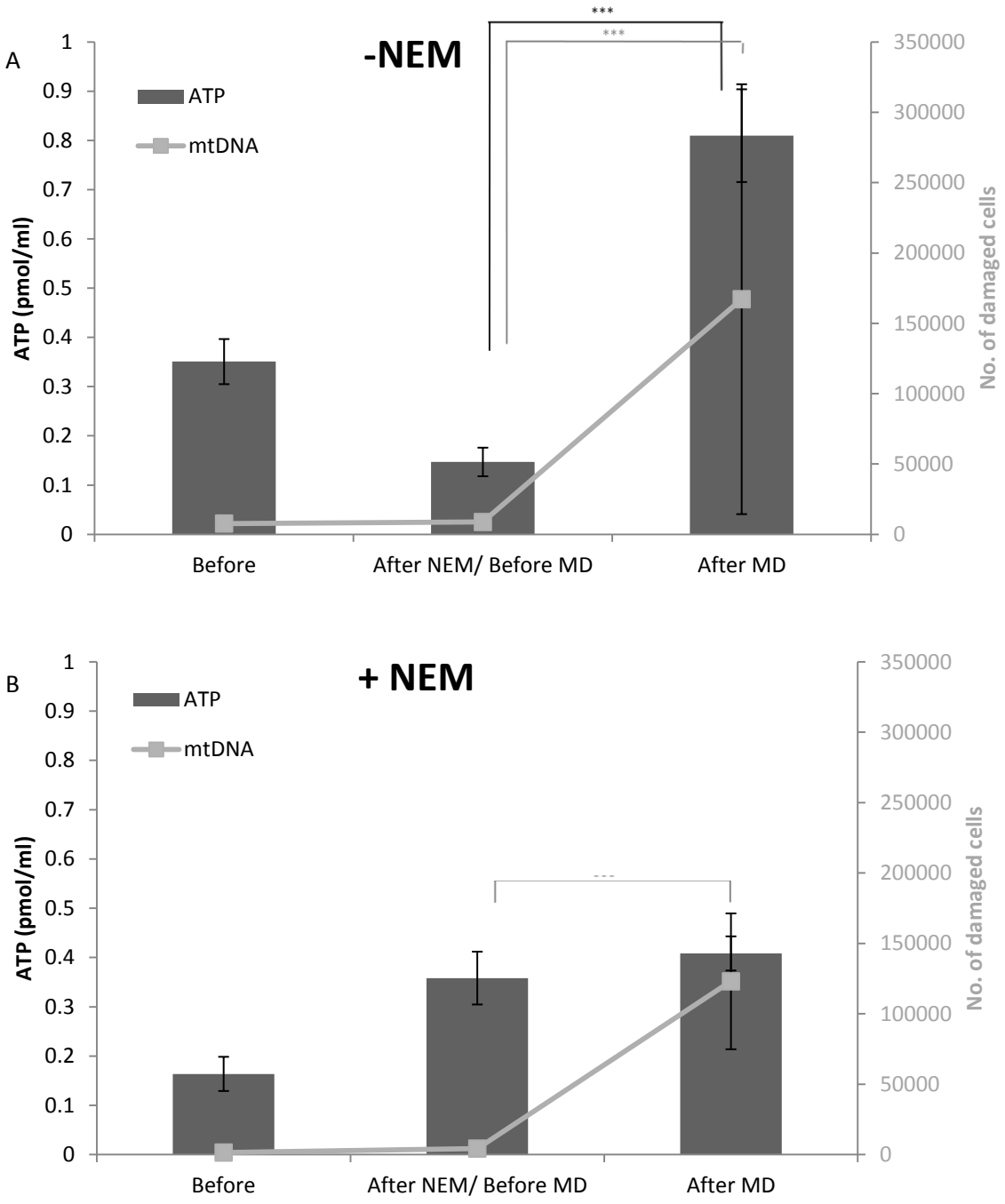

Figure 3.14. ATP and mtDNA concentration in the medium following medium displacements with NEM. SaOS-2 cells were used. 100µl sample was taken for ATP and mtDNA measurement. Then cells were treated A) without or B) with NEM then incubated for 2 hours before a further sample was taken for analysis. Finally medium was displaced 4 times and a final sample was taken. n=6. Error bars = S.D.

Fig 3.14 A) shows a decrease of ATP present between the before treatment and the time controlled second sample which is likely due to normal variation. After 8 displacements the amount of ATP present within the medium increased and this was significant to both previous samples. The mtDNA

in the medium was similar for the before NEM and time controlled sample. Following displacements there was a significant difference between the amount of mtDNA before displacements than after, with measurements being the equivalent of 160,000 damaged cells (+/- 150000 cells S.D.). B) shows a significant increase between levels of ATP following treatment of NEM, reaching 0.36 pmol/ml (+/- 0.07 pmol/ml S.D.), and before medium displacements, which was measured at 0.16 pmol/ml (+/- 0.03 pmol/ml S.D.). Interestingly the ATP did not increase following medium displacements which was read at 0.41 pmol/ml (+/- 0.03 pmol/ml S.D.). Finally, B) shows no change in levels of mtDNA before and after treatment of NEM. However following on from medium displacements the mtDNA measured in the medium was equivalent to that of 123,036 damaged cells, and this was significantly different compared to before the medium displacements began.

3.3.11 Time course of ATP release and ATP diffusion times

Now what follows are experiments that examined the characteristics of ATP release and the diffusion rate of ATP, both of which would contribute to the variation seen. Firstly ATP was measured at different time points after the displacing to determine if the ATP was released in a short burst or a more prolonged release. Fig 3.15 shows an increase of ATP in the medium up to 60 seconds later and Fig 3.16 shows an increase up to 2 minutes later.

Fig 3.17 is a graph that displays the slow diffusion rate of ATP within medium. This was set up as it was found surprising how the ATP concentration was different in different areas of the well. To do this medium was placed in a small plastic trough, usually used for multi-channel pipettes, and a small volume but highly concentrated amount of ATP was added at one end. The final solution would be 10 μM. The area where the ATP was added was noted and samples were taken 2, 4, 6 and 8 cm away and the ATP concentrations were measured in those areas.

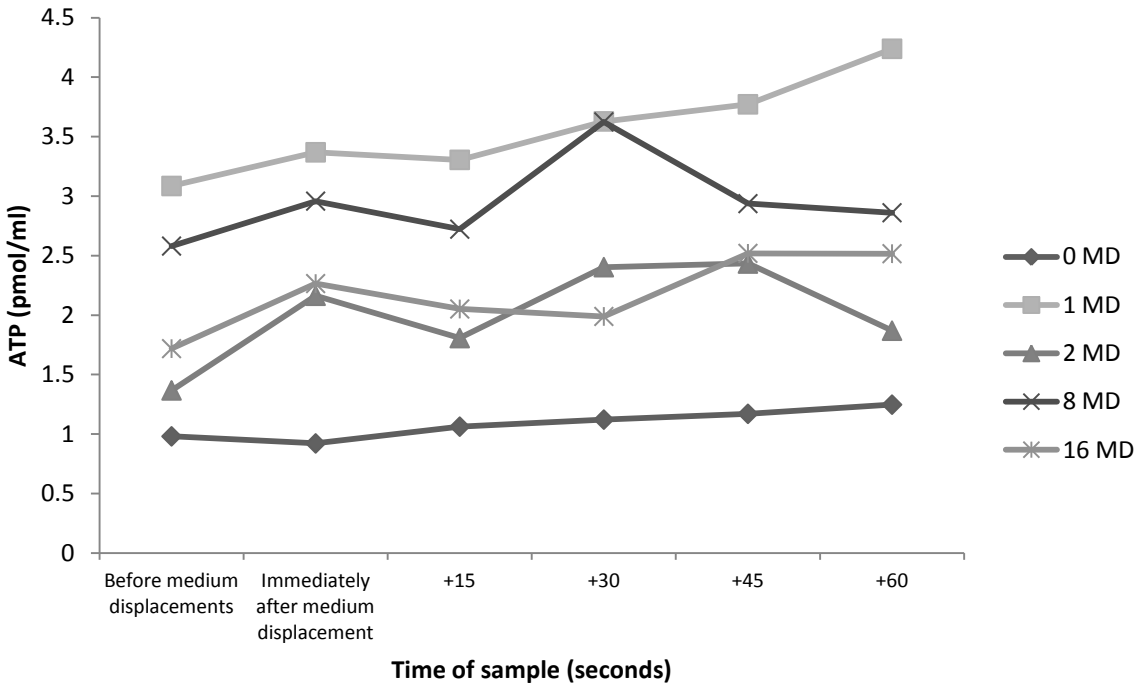

Figure 3.15. Concentration of ATP in SaOS-2 supernatants following medium displacements measured at different time points for 1 minute. Medium was sampled from before, immediately after medium displacements (MD) and every subsequent 15 seconds. Samples were taken from same area. n=1.

This graph shows that levels of ATP are still increased in all cases 1 minute after medium displacements. The highest being 1 medium displacement which has an increased to 4 pmol/ml ATP. Again it also shows the difference in basal levels of ATP even though they have the same number of cells in each well. It can be seen that even though samples were taken from the same area the levels increased and decreased considerably.

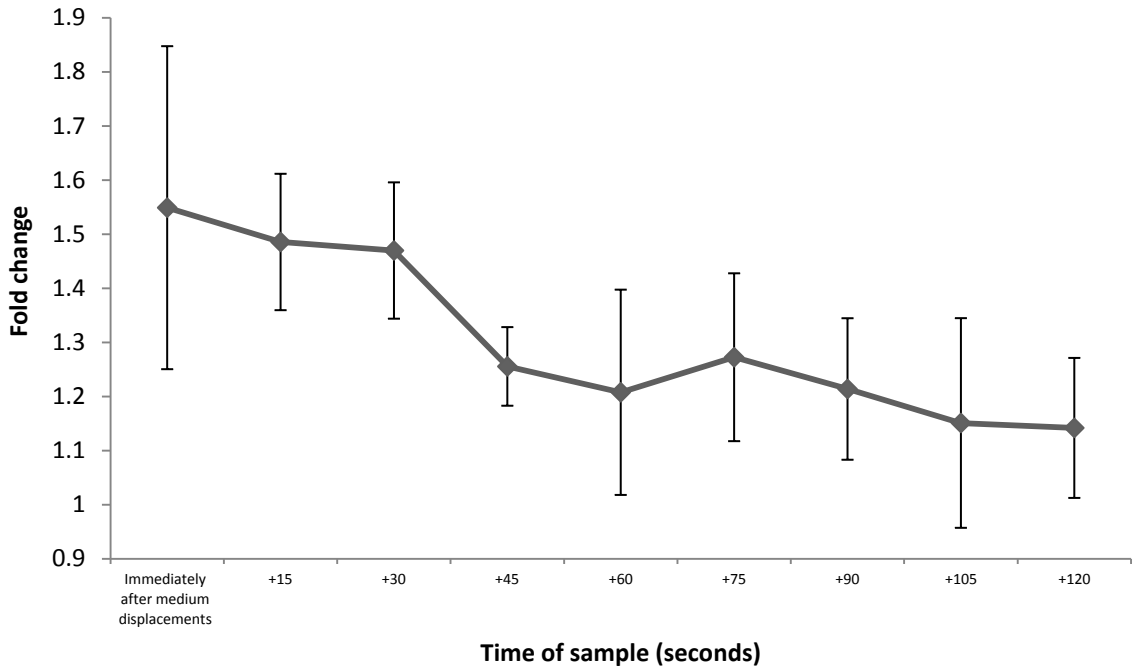

Figure 3.16. Concentration of ATP in SaOS-2 medium following medium displacements, measured at different time points for 2 minutes. Tests were sampled before medium displacements then they were displaced 4 times and immediately sampled from. Samples were then subsequently taken every 15 seconds for 2 minutes. Data is represented as fold change compared to basal levels. n=3. Error bars = S.E.

The result in Fig 3.16 shows that again medium displacement causes an increase in the amount of ATP present within the medium. It shows the largest measurement is immediately afterwards, which is the time that the medium is normally sampled from in experiments in this thesis. After 2 minutes there is no significant difference between any of the measurements.

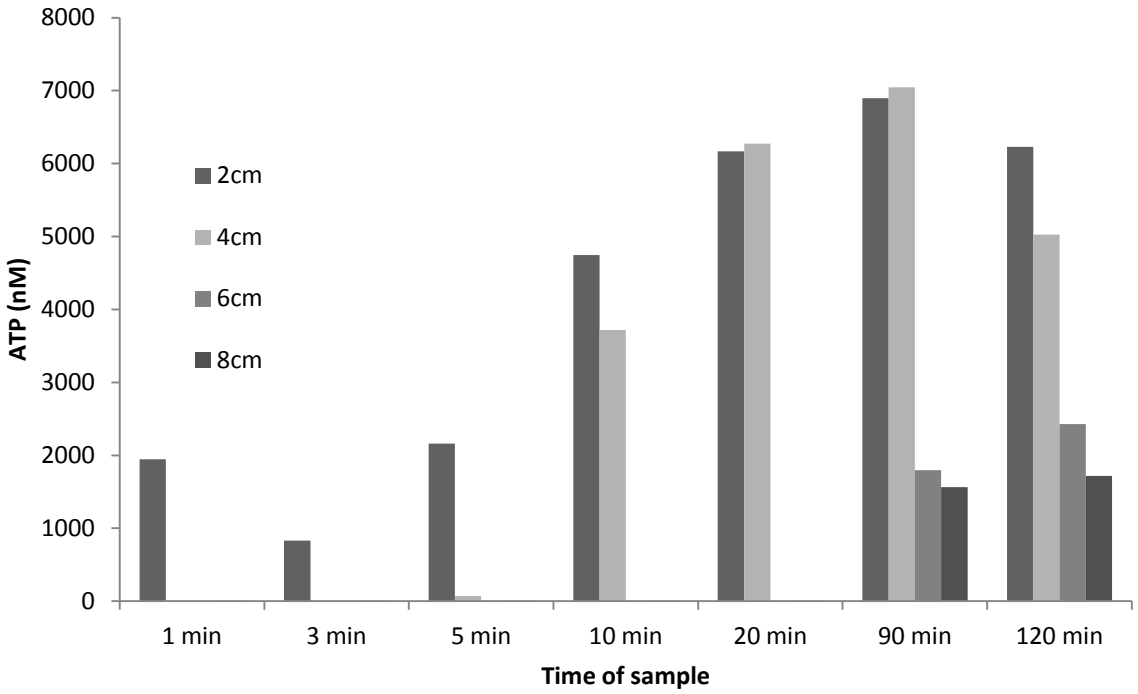

Figure 3.17. ATP concentrations at different locations following ATP addition, measured over a period of 120 minutes. A highly concentrated small volume of ATP was added to a trough of HEPES medium to a final solution of 10 µM. The solution was not mixed. Then at 1, 3, 5 10, 20, 90 and 120 minutes following ATP addition samples were taken 2, 4, 6 and 8cm from where the solution was added. n=1.

This graph demonstrates the diffusion time of ATP in HEPES medium. The concentration at the 2 cm point peaks at 90 minutes with 7000 nM which then falls off at 120 minutes. There is very little ATP near the 4 cm mark until 10 minutes at which point 4000 nM was recorded. Then this increases to 90 minutes before falling off. It takes 90 minutes before any ATP is detected at the 6 and 8 cm points, both measuring 2000 nM, which then increase slightly at 120 minutes.

3.3.12 The effect of substrate on ATP release

The final set of experiments examine the impact on ATP release of the substrate the SaOS-2 cells were cultured on. Firstly ATP release on dentine was compared to plastic, shown in Fig 3.18. Then ATP release on dentine was compared to cells cultured on glass cover slips, Fig 3.19. Finally some tests were run to determine if, like pyrophospahtes, ATP binds to dentine, shown in Fig 3.20 and Fig 3.21.

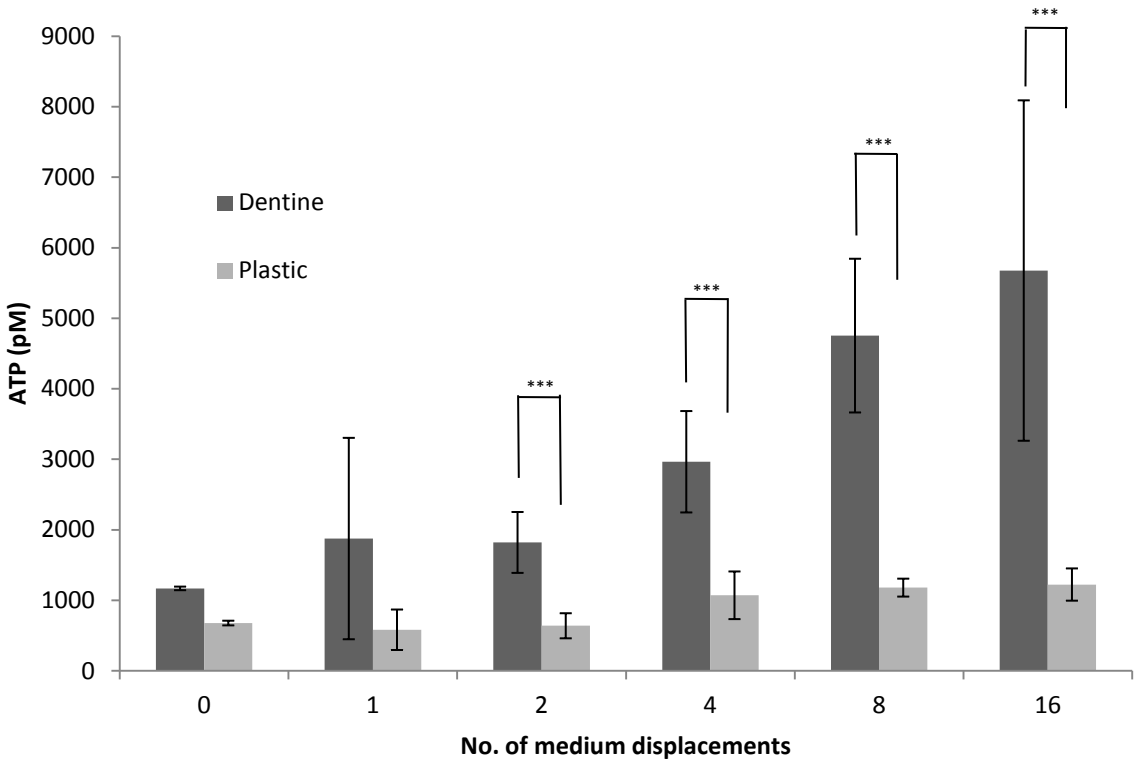

Figure 3.18. ATP concentrations following medium displacements of SaOS-2 cells cultured on dentine and plastic. n=10. Error bars = S.D.

Fig 3.18 shows that SaOS-2 cells cultured on dentine have a larger constitutive release of ATP than that of SaOS-2 cells cultured on plastic. Both substrates had an increase of ATP release compared to 0 medium displacements. The plastic substrates highest measurement was 16 medium displacements, which was 1224 pM ATP (+/- 112 pM S.D.) and was significant compared to basal levels of ATP on plastic. The dentine substrates highest measurement was 5676 pM ATP (+/- 2323 pM S.D.), again this was significant compared to basal levels of ATP on dentine. Importantly, for all measurements of medium displacements, the ATP concentration in the medium on dentine was higher than that of its equivalent cultured on plastic. Apart from 1 medium displacement these were all significantly different.

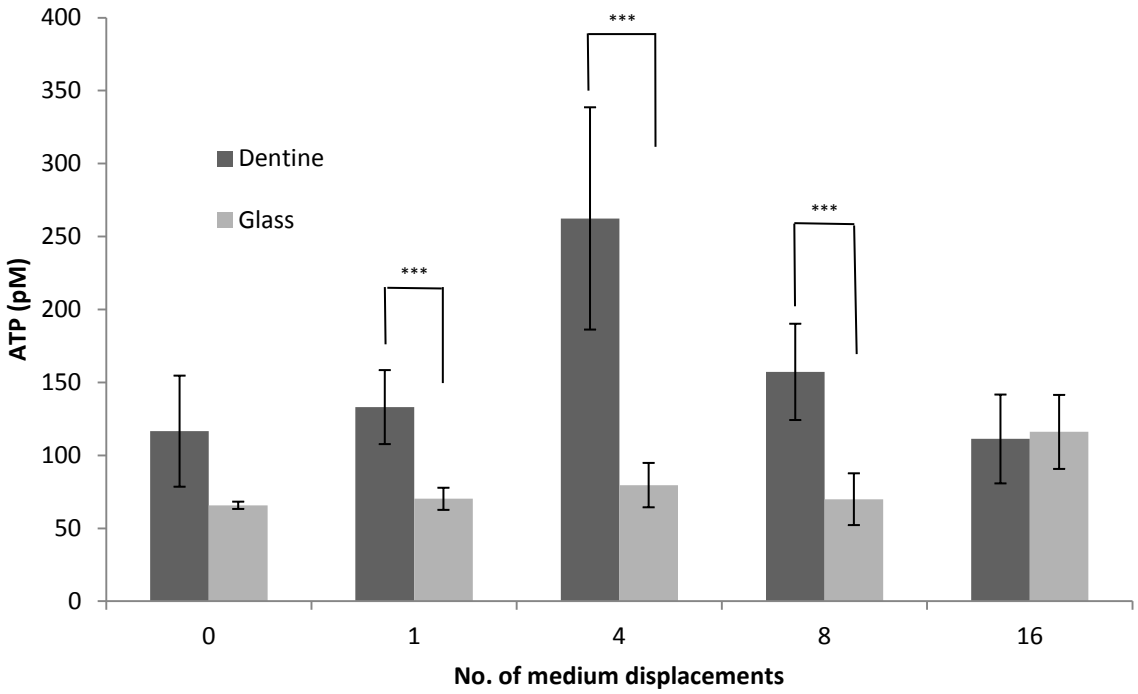

Figure 3.19. ATP concentrations following medium displacements of SaOS-2 cells cultured on dentine and glass. n=10. Error bars = S.D.

This data (Fig 3.19) shows that SaOS-2 cells cultured on dentine appear to release more ATP constitutively than those cultured on glass cover slips, however this was not significant. Medium displacements performed on glass caused an increase of ATP release only at 16 medium displacements, with a concentration of 116.05 pM ATP (+/- 24 pM S.D.), which was significant compared to basal levels. Again medium displacements caused an increase in ATP when SaOS-2 cells were cultured on dentine, however only 4 medium displacements, which measured 262 pM ATP (+/- 83 pM S.D.) was significant compared to basal levels. As is the previous experiment the levels of ATP on dentine were higher after medium displacements, except for 16 medium displacements where levels on both substrates were comparable.

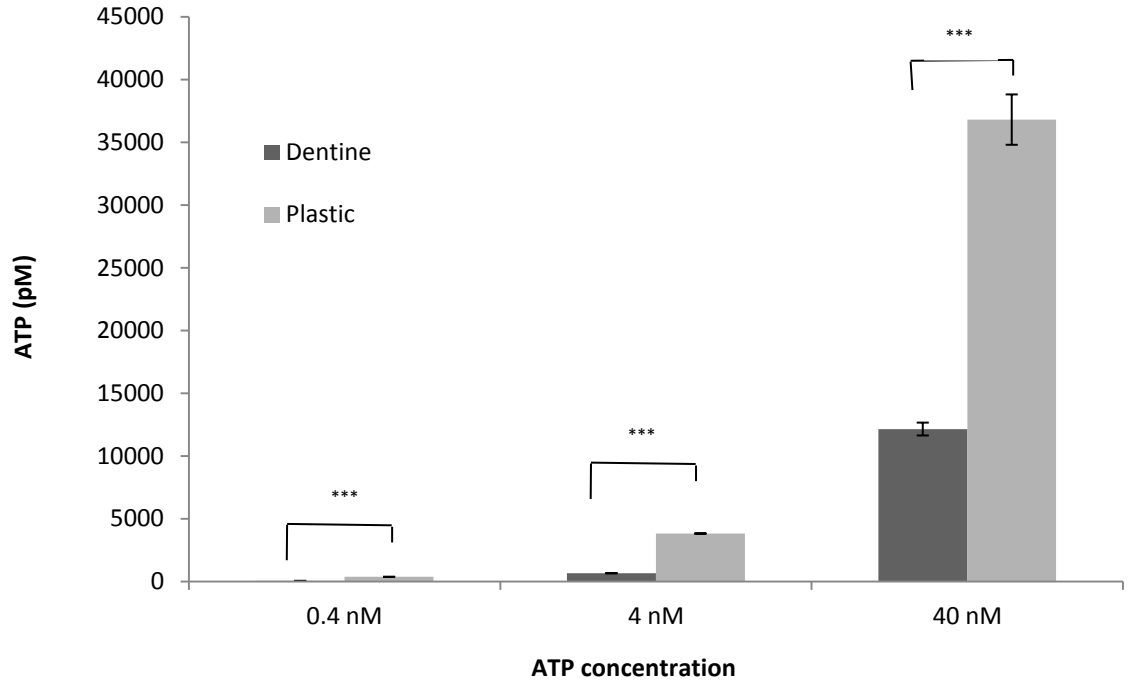

Figure 3.20. ATP concentration following ATP addition to a supernatant overlying an acellular dentine disk. After adding ATP the wells were left for 2 minutes before taking a 100 µl sample which was then measured for ATP concentrations. n=8. Error bars = S.D.

Fig 3.20 shows an experiment to test whether ATP binds to dentine wafers. 40 nM, 4 nM and 0.4 nM were each added to a well containing a dentine disk and one without. Then samples were taken to measure for ATP. The graph shows that in all cases there was more ATP present in wells that did not contain dentine disks and these differences were significant.

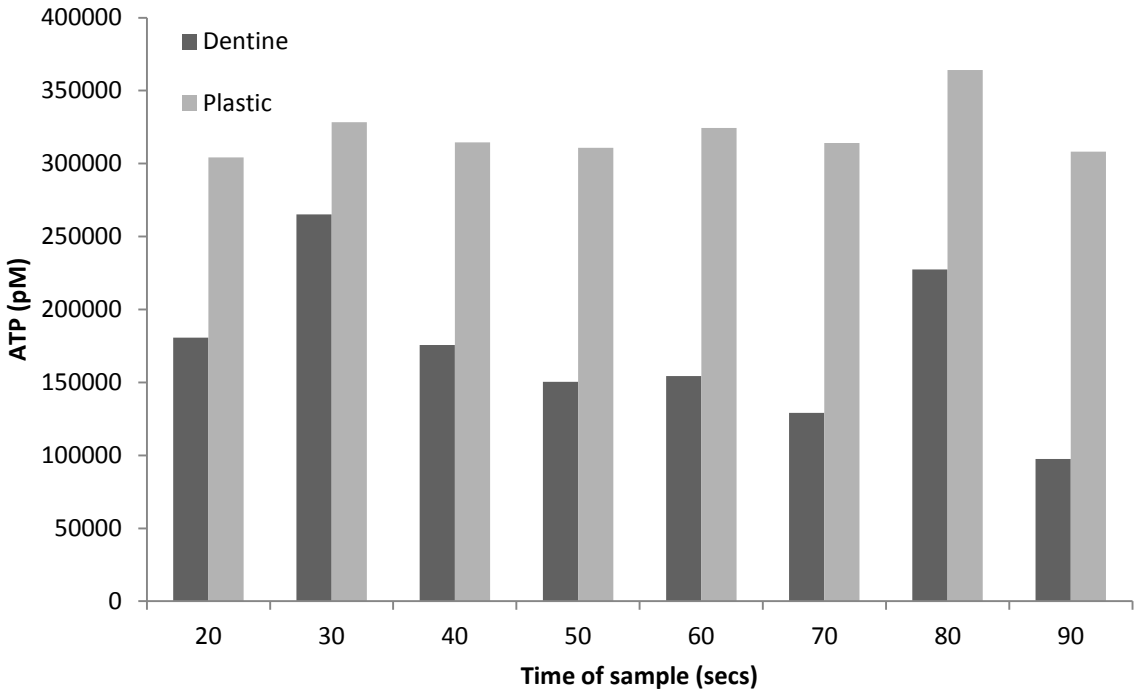

Figure 3.21. ATP concentration following ATP addition to a supernatant overlying an acellular dentine disk. 35nM ATP was added to wells with or without a dentine disk at the bottom. Starting at 20 seconds, and then at 10 second intervals, samples of the supernatant were removed and measured for ATP. n=1.

Fig 3.21 shows that in all cases there was a larger amount of ATP present in wells that did not contain any dentine disks. As this experiment was only run once it was not possible to test for significant differences between them. However if added together, such that n=8, then there is a significant difference between dentine and plastic. Further to this it can be seen that apart from 30 seconds and 80 seconds there is a general decline between wells, after 20 seconds there is 180 nM ATP and after 90 seconds there now is only 98 nM ATP in the supernatant.

3.4 Discussion

The main focus of this chapter was to investigate the current methods of measuring ATP in an attempt to reduce variation. When comparing *in vitro* cell loading models in the literature it is apparent that shear stress caused by fluid flow appears to be the dominant way that osteoblasts detect strain. When using a flow-loop apparatus system to create shear stress NO and PGE_2 were upregulated in mouse MC3T3-E1 cells and rat UMR-106 cells [205] which ultimately lead to an increase in cox-2 and *c-fos* gene expression.

Hydrostatic compression uses pistons to deliver compressed air into an enclosed tissue culture chamber to increase pressure. However as well as increasing hydrostatic pressure it will also cause a shearing force where the cell attaches to the substratum. Given that continuous hydrostatic pressure had no effect on the cell but intermittent pressure did it is likely that effects seen from hydrostatic pressure models are due to the shear stress that the cell is undergoing [206].

Uniaxial stretch is believed to closely represent what is present *in vivo*. Cells are cultured on a silicone membrane and then stretched which causes both tension and compression to cells. Once again this will cause shear stress through movement of the cell culture media. This however can be negated by just stretching the silicon membrane and leaving it stretched. It was reported that when stretching was combined with fluid shear there was an increase in osteopontin expression whereas when cells were merely subjected to uniaxial stress there was no increase in osteopontin production [206].

Cells have numerous ways of detecting mechanical stimulation through different types of mechanoreceptors, and the broad spectrum of these may account for a cells ability to detect different stimuli and act accordingly. These mechanoreceptors include intergrins, focal adhesions and numerous ion channels.

Integrins are present on the cell membrane and attach to the extracellular matrix. Thus any deformation of the ECM will transmit itself to the cell via these integrins. Furthermore they can influence cell signalling through their b subunit which is present intracellularly [207].

Another characteristic of cells that undergo mechanical stress is that they will reorganise their cytoskeleton, which amongst other things, will allow them to upregulate their focal adhesions in these areas. Focal adhesions attach both the ECM and the intracellular cytoskeleton. Signalling through focal adhesions causes an upregulation of b-catenins which act on the wnt signalling pathway [208]

Various ion channels have been shown to be involved in mechanosensation. The main ones being gadolinium sensitive stretch activated cation channels, mechenosenstive calcium channels to a lesser extent voltage gated cation channels. By altering the flow of ions into or out of a cell they can influence various intracellular pathways [207].

The first preliminary experiments are shown in Fig 3.1 and concern the production of a standard curve for the relative light units, measured by the tube luminometer, compared to the amount of ATP that was present. This standard curve was used for subsequent experiments and can be used for future investigations. Also the half life of ATP was examined as this appears to be different between laboratories, in this case a half life of 10.5 minutes was calculated. From here some initial experiments were carried out looking at ATP release after medium displacements (Fig 3.3). It quickly became apparent after looking at the repeats, including the unpublished observations of previous investigators, that there were massive differences between each experiment, thus making it hard to measure the effect that changing conditions would have on the amount of ATP release. Therefore experiments were undertaken to try to reduce the variation that was seen so that future investigations could be carried out in the knowledge that the tests were standardized.

The activity of the luciferase enzyme was investigated, beginning with the effect of pH on luciferase. Up to this point all experiments had been carried out in serum free medium which was used to prevent excessive breakdown of ATP. This is buffered in a 5% CO_2 atmosphere, thus when the plate was outside the incubator having tests run on it the medium would gradually become more alkaline. It can be seen in Fig 3.4 that the optimal pH for the luciferase enzyme is 6.25, either side of this there is a massive difference in its activity. It matters not that 6.25 is reached in each experiment just that each experiment was the same, therefore all experiments after this were carried out in HEPES buffered

medium, allowing them to proceed outside of the incubator and still be buffered. Also, as luciferase is an enzyme its activity is dependent on the temperature. All samples from experiments before now were placed on ice with NMR to slow the reaction, these samples were then loaded in the tube luminometer and measured for ATP. However in some tests a few samples would be loaded and in others many samples would be loaded. The samples loaded first would begin to warm up and Fig 3.5 shows that the difference between 0 minutes of warming and 2 minutes of warming was very large. Therefore samples loaded at the end would be colder and thus give off lower light readings. This will undoubtedly have contributed towards variation. Again from this point onwards samples were only loaded in to the tube luminometer in sets of 5 and left for 4 minutes before reading.

As well as looking at the luciferase enzyme as a source of reducing the variation different methods of fluid perturbation were investigated, one of these being plate vibration. Simply, a plate was loaded onto a vibrating platform, the frequency, the amplitude and the time it was left could be altered. The plate was vibrated for different lengths of time and the medium was sampled. Fig 3.6 shows the result of such a test. It seemed, at this point of the investigation, that vibrating the plate caused a release of ATP into the medium, as all vibrating conditions causing a higher reading of ATP in the medium, 800 seconds being the highest at 400 pM. However, even with this standardized fluid perturbation method there was still large amounts of variation in the tests causing the changes to be insignificant.

Next it was attempted to reduce the variation and get a consistent pattern by sampling multiple times from the medium after testing to get a more accurate average. Fig 3.7 shows that interestingly the concentrations within a 6-well plate in different points were largely different. This was the case even with constitutive ATP release. Therefore, as had been done up until now, by only sampling from one place in each well there was a possibility you could sample from a relatively high concentration, perhaps in the 0 medium displacements, or sample from a relatively low concentration in another well. This will have created large variation, and more so, inconsistent patterns between experiments. Due to this discovery three changes were made to future experiments, the first being that 3 samples were taken from within a well. Secondly, because basal levels were different between wells and in the same wells, samples were now taken before and after experiments. Finally, a device was used to

ensure that samples were taken from the same place and from the same depth. This was simply a 6-well plate lid that had small holes drilled into it, 3 for each well. This allowed the pipette tip to get stuck at the same depth for each sample, as well as sampling in the same place before and after.

Medium displacement experiments following all the above rules i.e. performed in HEPES medium, samples read at same temperature, taking before and after treatment samples and taking 3 samples from the same place still did not cause a decrease in variability. Fig 3.8 shows that medium displacements did cause an increase in the amount of ATP present but in this test only 4 medium displacements was significant. Therefore the above changes were also tested using mechanical methods of fluid perturbation, and thus not prone to human error. These being the vibrating table, as described previously, and the orbital rocker, which can rock the plate at a given RPM for a given amount of time. Both of these methods, after all the changes that had been made to reduce variability, showed no increase in the amount of ATP present within the medium. This ruled out the earlier experiment in Fig 3.6 that appeared to show an increase of ATP with vibration. It is likely that basal levels in these wells were higher and therefore appeared to show an increase in vibration that wasn't there.

Because of the lack of ATP increase following vibration or rocking it appears that either osteoblasts can only react to the specific fluid flow of medium displacements or previous studies on osteoblast cell damage in response to medium displacements was not sensitive, or accurate enough. One final test was carried out to finish looking at different methods of fluid perturbation. This was by using a multi-channel pipette, which should cause the exact same fluid flow force between wells. This again did cause an increase in the amount of ATP present within the medium, but interestingly failed to reduce the variation, suggesting that perhaps inherent human error involved in pipetting with the same force wasn't as big a contributory factor as thought.

Given the possibility that previous cytotoxicty tests were not sensitive enough to account for the release of ATP, work was undertaken to produce a more sensitive test. This came in the form of mtDNA detection. A damaged cell will release its contents, include its mitochondria into the

extracellular environment, therefore detecting mtDNA is a sensitive method of measuring cell damage because the primers could be designed to recognise multiple repeats on one mtDNA, there are many copies in one mitochondria and given that an osteoblast is an active secretory cell there are a higher than average amount of mitochondroia in one cell. This makes it much more sensitive than LDH and therefore should give a more accurate reading. Further to this the test needed to account for live cells that may have lifted off the bottom and therefore sampled with the medium. This test allowed for this, as any live cell placed in a PCR reaction would immediately burst and release its mitochondria into the PCR reaction. Firstly a calibration curve was made to allow the ct value for any supernatant to be compared to the number of damaged/lifted off cells. The main tests were carried out after medium displacements, after plate vibration and after plate rocking, again these showed that ATP concentrations only increase in the medium following medium displacements and not in response to vibration and rocking. But it can also be seen that the levels of mtDNA in the medium displacement were significantly higher than it was before, whilst there was only a small insignificant increase in mtDNA following vibration and plate rocking experiments. Therefore at this stage it appeared that either medium displacement causes cell damage and ATP is released in that manner, or ATP is released normally but cells can be lifted off the bottom and measured in the luciferase reaction and therefore can cause variation between experiments.

Next attention was turned to a previous experiment that examined the effect of NEM on ATP release. NEM inhibits exocytosis and in previous experiments it was shown to inhibit the release of ATP [30, 31]. This may indicate that ATP is released in response to fluid flow via vesicles. Also, importantly, it does confirm that ATP is released through normal physiological means and therefore was used to determine if the mtDNA results were a product of cell damage or of cells being lifted off the bottom. The results show that in this case NEM did not appear to inhibit the basal release of ATP, however there was no increase in ATP in the medium following on from medium displacements. Despite that there was still an increase in mtDNA. The results show that ATP increases are inhibited by NEM after medium displacements. Thus it is unlikely that medium displacements are damaging the cells and

that, in fact, cells are being lifted off the bottom, being taken up in the sample and may contribute towards the ATP measurement. This is therefore another factor in the ATP variation that is observed.

Experiments were also undertaken to look at the characteristics of ATP release and of ATP behaviour *in vitro*. Up until this point, after medium displacements were carried out, the medium was sampled from immediately after displacements had finished, so it was decided to take samples at given time points after medium displacements. Fig 3.16 shows that following on from medium displacements there were increased levels of ATP for 2 minutes. If only a short release of ATP was occurring then these levels should have decreased due to the breakdown of ATP. This suggests that, for example, peaks shown at 4 and 8 medium displacements could have just been a result of 2 medium displacements that have taken time to release all the ATP. The graphs also show the variation from a single point in time. However for the first time there does appear to be patterns in a medium displacement experiment as it appears that after an initial peak there is a small decrease in all repeats before levels increase again (Fig 3.15). There is some evidence that ATP causes ATP release, and this may be what is being seen here [18]. Nevertheless it is clear that the sampling time of medium is vital as different times give different levels of ATP and therefore this constitutes a further source of variability.

Finally, the diffusion time of ATP in medium was examined. This was due to the fact that the ATP concentration was different in different parts of the well. It was always assumed that any release of ATP would quickly spread throughout a well, but these results suggested differently. To do this, an experiment was set up where ATP was added to one end of a trough and then different, measured out, parts of the trough were sampled at different times. It can be seen in Fig 3.18 that even after 2 hours of diffusion the ATP had not yet managed to travel the full 8 cm. This therefore explains why different parts of the well are so different if ATP is only being released in bursts periodically across the cells.

The rest of this results chapter examine the characteristics of ATP release, specifically the effect of culture substrate on ATP release. SaOS-2 cells were cultured on either glass coverslips, dentine or

plastic and subjected to medium displacements. Fig 3.18 shows that when cultured on dentine the constitutive release, and release after medium displacements, is larger than when cultured on plastic. The low levels of ATP compared to other experiments is because the cells were cultured in a 96 well plate and therefore less cells were present. This was similar for glass compared to plastic, although it must be said that only one medium displacement was greater than basal levels (4 medium displacements). Also results appear to show that ATP binds to dentine, shown by the fact that the same concentrations of ATP gave different light readings after being placed on plastic or dentine, and over time the light levels decrease in the dentine well, presumably as more ATP binds. This is likely due to the two oxygen atoms which will bind to Ca^{2+}, in a similar manner to bisphosphonates. Therefore the above results, where ATP release is higher with dentine, is likely to be a severe underestimation of the amount of ATP that is present as a lot of it binds to the dentine. There are numerous reasons why ATP release may be higher on dentine than on other surfaces. For example, the extracellular matrix that dentine presents to the cell may change the phenotype of the cells to one that secretes more ATP [209]. Alternatively, the morphology of the SaOS-2 cells may change when cultured on dentine as they have been recorded as having extra extensions. This may alter how fluid flow passes over the cell and it is possible, knowing how osteoblasts only detect specific types of fluid flow, that this increases the ATP release. The dentine disks that are used in these systems are roughened and again this may alter how fluid passes over the surface as a whole, and therefore may affect how the cells perceive it [209].

To conclude, the ATP experiments outlined in this chapter provide a more detailed knowledge of the characteristics of ATP release and how best to measure that release for an accurate assessment. If further investigations take into account these changes then standardised experiments can be carried out to get a more detailed and accurate assessment of ATP release in osteoblasts.

4. Characteristics of ATP synergy with systemic hormones

4.1 Introduction

ATP synergises with PTH to increase the expression of *c-fos* in osteoblasts [159, 160]. *C-fos* is a proto-oncogene and thus plays a major role in proliferation and differentiation [210]. In addition, through its expression in osteoblasts, it plays a role in bone resorption, and due to the coupling effect, bone remodelling. When transcribed it becomes part of the AP-1 transcription factor along with c-Jun, thus becoming part of a heterodimeric protein. As part of AP-1 it effects the transcription of many genes, for example it increases the expression of RANKL and decreases the expression of its decoy receptor, OPG [211]. These changes in gene expression increase osteoclastogenesis and therefore increase bone resorption. In a healthy homeostatic system, an increase in bone resorption will allow an increase in bone deposition when the osteoclasts have finished [212]. Thus when ATP and PTH signal to osteoblasts the rate of bone remodelling in these areas is increased compared to PTH signalling to the osteoblasts alone.

ATP is released locally from osteoblast cells in response to mechanical stimulation. The initial experiments in this chapter investigated others factors that synergised together to increase *c-fos* expression. To determine this, the gene coding the luciferase protein was attached to the *c-fos* promoter and was used in this, and all, *c-fos* measurements. Firstly medium displacements and PTH were tested to determine if they synergised together, then experiments were carried out to confirm that glucose insulinotropic polypeptide (GIP) synergised with PTH. GIP is a hormone that is released from the GI tract in response to food absorption, its major function is one of insulin regulation, however the receptors were also discovered on osteoblasts [213]. It is presumed that the synergy between GIP and ATP exists as a way of only allowing bone remodelling to occur if nutrients are available. Finally tests were carried out to look at whether supernatant taken from resorbing osteoclasts could synergise with PTH, as certain factors released from osteoclasts can recruit and activate osteoblasts. Although all of them have yet to be elucidated PDGF-BB is an example of one [214, 215]. Thus it was looked at

whether the presence of PTH would enhance the action of these factors and further stimulate *c-fos* in the osteoblasts.

Experiments also examined if ATP and PTH need to be at the osteoblast cell membrane simultaneously for synergy to be observed. Fig 3.2 shows ATP half-life at approximately 9 minutes at low concentrations (<500nM), although this has been observed as low as 2 minutes by other researchers, PTH measurements *in vivo* have shown a half life of approximately 4 minutes. Given that ATP has such a low half life tests were carried out to determine if ATP could sensitize osteoblasts to PTH, or vice versa.

4.2 Methods

4.2.1 *c-fos* assays. These were carried out using the transfected SaOS-2 cells, as described in the Materials and Methods. Cells were seeded until 90% confluent and then serum starved for 24 hours prior to experiment. In experiments that used PTH (Bachem, Switzerland) 1 nM was used and added to the cells for 4 hours. 10 µM of GIP (Sigma-Aldrich, UK), ATP, AMP (Sigma-Aldrich, UK) or adenosine (Sigma-Aldrich, UK) was used in experiments. The length of time the cells were treated for varied in, and between, experiments. 50% of the medium was displaced for the medium displacement experiments. The human resorbing osteoclast supernatant was provided by Mrs Jane Dillon.

4.2.2 Real-time PCR. This was used to determine mRNA levels of RANKL and OPG following ATP time course experiments. Cells were treated with 1 nM PTH for 18 hours before mRNA was extracted, during this period they were incubated at 37^{o}C and 5% CO_2. ATP was used at a concentration of 10 µM and was added to the experiments at different time points.

4.3 Results

4.3.1 Synergy of ATP with systemic hormones

The experiments shown below are investigations into what compounds synergise with PTH or ATP. Fig 4.1 confirms that ATP synergises with PTH to increase *c-fos* transcription, suggesting an activation of bone remodelling [148]. In Fig 3.4 ATP is released in response to medium displacements, thus the experiment in Fig 4.2 was carried out to determine whether PTH added together with medium displacements caused synergy to be observed. Fig 4.3 confirmed previous experiments in that it showed a synergy between ATP and GIP. During the bone remodelling process osteoclasts will provide signals that recruit and activate osteoblasts. Thus Fig 4.4 tested whether these factors contained in osteoclast supernatants, induced a synergistic response with ATP [10]. Interestingly the results showed an increase in *c-fos* when osteoclast supernatant was added, but it did not synergise with ATP.

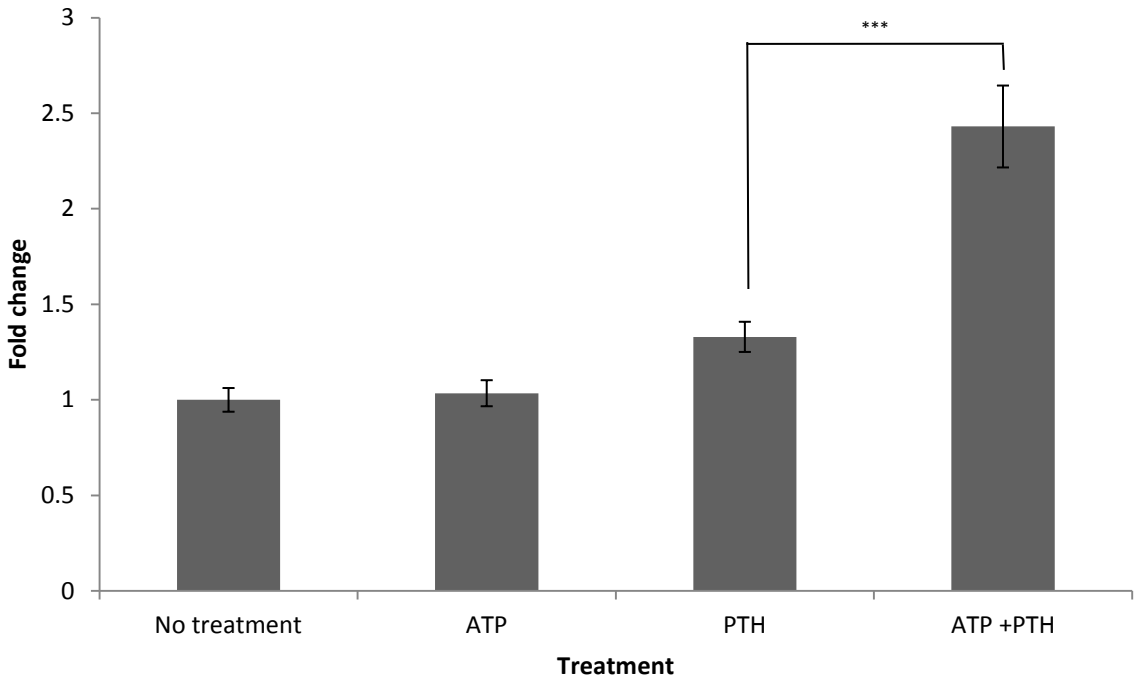

Figure 4.1. The effect of ATP and PTH stimulation on *c-fos* transcription in SaOS-2 reporter cells. The data are represented as fold changes compared to no treatment. Concentrations of agonists were 10 µM ATP and 1 nM PTH. n = 12. Error bars represent S.E.

In Fig 4.1 10 µM of ATP caused no increase of *c-fos* levels over basal expression. PTH (1 nM) caused a 1.25 fold increase. By co-treating the cells with ATP and PTH the fold change reached 2.5 (+/- 0.02 S.E.) which is greater than the sum of PTH and ATP together. The ATP + PTH treatment is significant to PTH treatment alone ($p<0.001$).

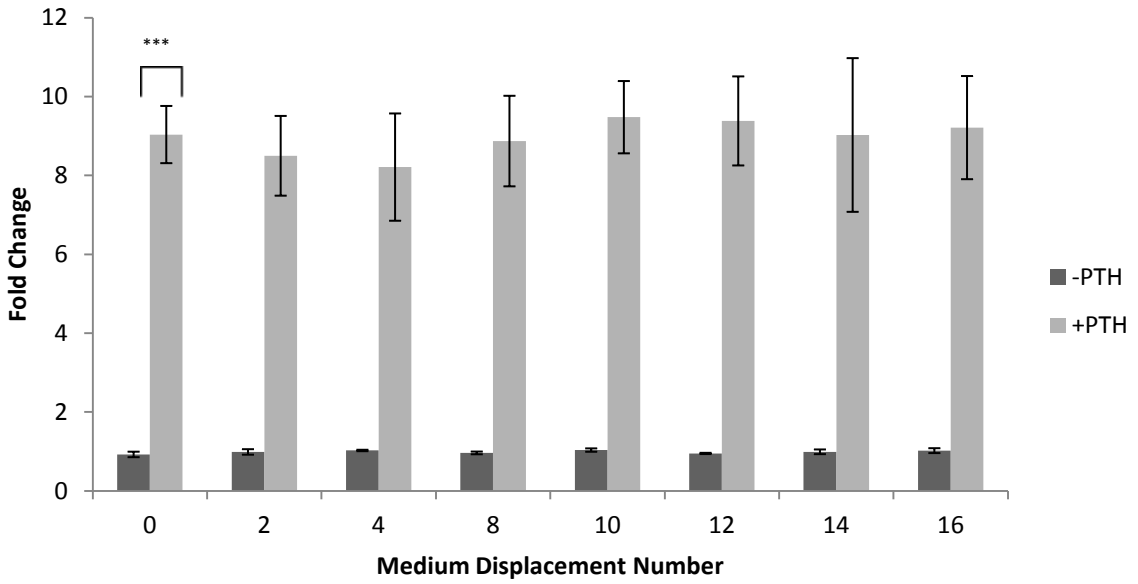

Figure 4.2. The effect of medium displacements with and without PTH treatment on *c-fos* transcription in SaOS-2 reporter cells. Results are represented as fold change compared to medium alone control treatment –PTH. PTH was used at a concentration of 1 nM. n = 6. Error bars represent S.E.

Medium displacements alone did not cause an increase in *c-fos* expression. PTH addition caused a 9 fold increase (+/- 0.7 S.E.) of *c-fos* compared to basal levels (0 medium displacements) **(**$p<0.001$). Medium displacements with PTH caused no significant increase in *c-fos* expression compared to PTH alone.

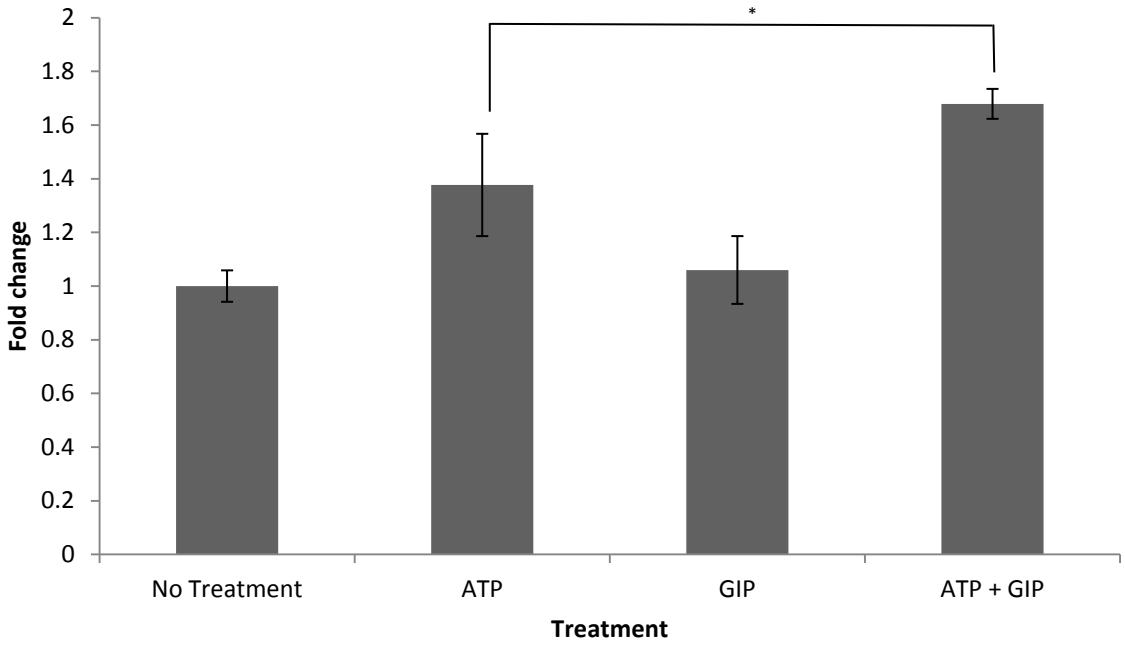

Figure 4.3. The effect of ATP and GIP stimulation on *c-fos* transcription in SaOS-2 reporter cells. Results represent fold changes compared to no treatment. Treatments were 10 µM ATP, 10 µM GIP and both ATP and GIP together. n = 2-6. Error bars represent S.E.

This graph (Fig 4.3) shows ATP caused a 1.3 fold increase in *c-fos* transcription compared to no treatment. 10 mM of GIP was insufficient to cause an increase in *c-fos* levels. When the cells were co-treated with ATP and GIP a synergistic effect did occur, with a 1.6 (+/- 0.05 S.E.) fold increase over no treatment, which was significant compared to ATP treatment alone ($p<0.05$). This increase was not simply due to addition of ATP + GIP, as 1.6 fold is larger than these two combined.

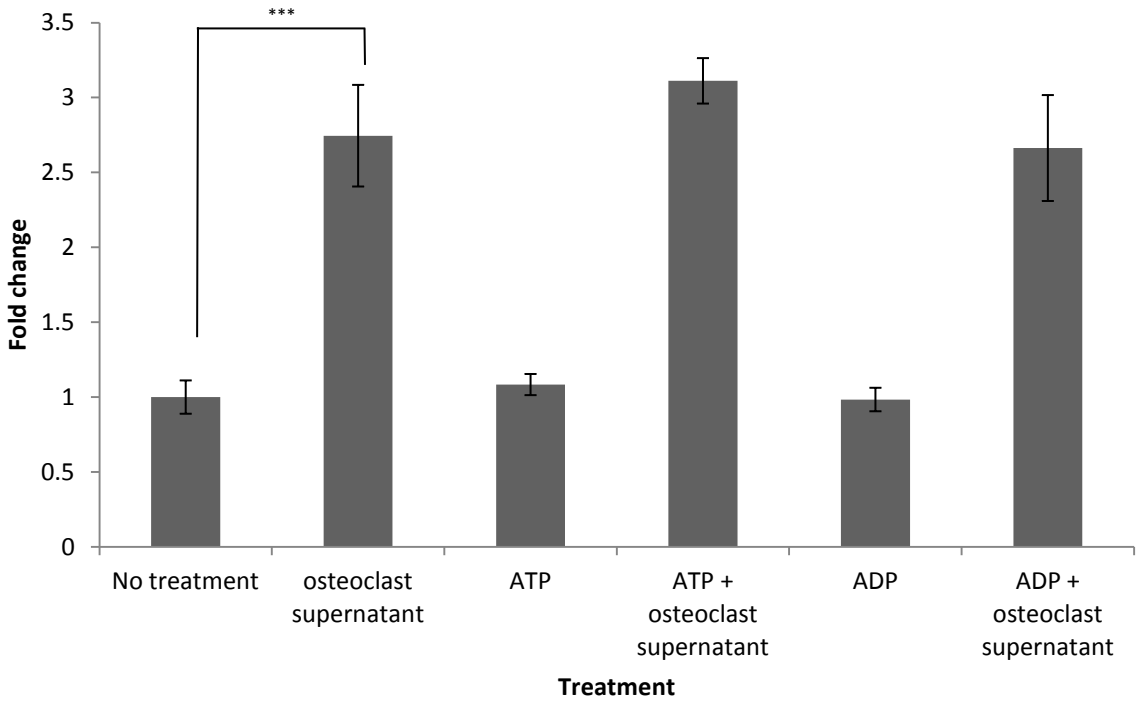

Figure 4.4. The effect of resorbing human osteoclast conditioned medium treatment of SaOS-2 reporter cells on *c-fos* transcription. Results represent fold changes compared to no treatment. Cells were treated with supernatants taken from osteoclast cultures (generated from osteoclast precursors using MCS-F and RANKL) and ATP (10µM) or ADP (10µM). n = 6. Error bars represent S.E.

Fig 4.4 shows that adding medium to the SaOS-2 reporter cells that had been removed from resorbing osteoclast cultures caused a 2.55 fold increase (+/- 0.5 S.E.) of *c-fos* transcription and this was significant compared to no treatment ($p<0.001$). Adding the osteoclast supernatant and then treating with ATP or ADP had no effect over adding the osteoclast supernatant alone.

4.3.2 ATP sensitises osteoblasts to systemic hormones

This section looks at the effect of adding ATP before PTH to see if it could sensitise the osteoblast to the effect of PTH. Fig 4.5 A) shows ATP addition up to 30 minutes before PTH, B) shows ATP addition up to 3 hours before PTH. Fig 4.6 A) shows ATP addition up to 9 hours before PTH and B) shows ATP addition up to 18 hours before PTH. The results show that ATP can be added 9 hours before PTH and still have a synergistic increase in *c-fos* production, furthermore adding it 1 to 3 hours before appeared to be more beneficial than adding it at the same time. Fig 4.7 shows a similar experiment were ATP was added from 1 to 9 hours before GIP, in this case no synergy was observed suggesting ATP does not sensitise the osteoblasts to GIP. Fig 4.8 shows the sensitisation effect of ATP in respect to its effect on RANKL and OPG. RANKL is released from osteoblasts and causes activation of osteoclasts to their mature bone resorbing phenotype [216]. OPG is the decoy receptor for RANKL and as such a decrease in OPG would result in an increase of bone resorption/bone remodelling [216].

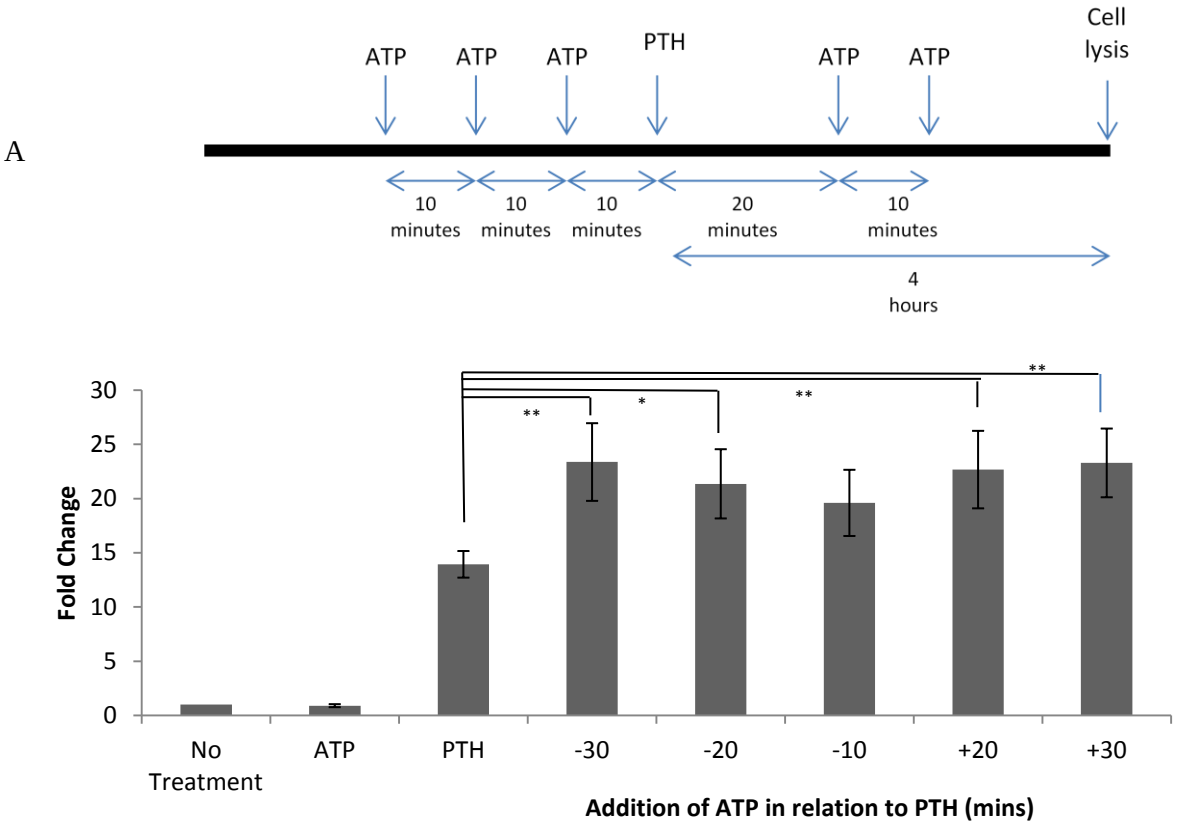

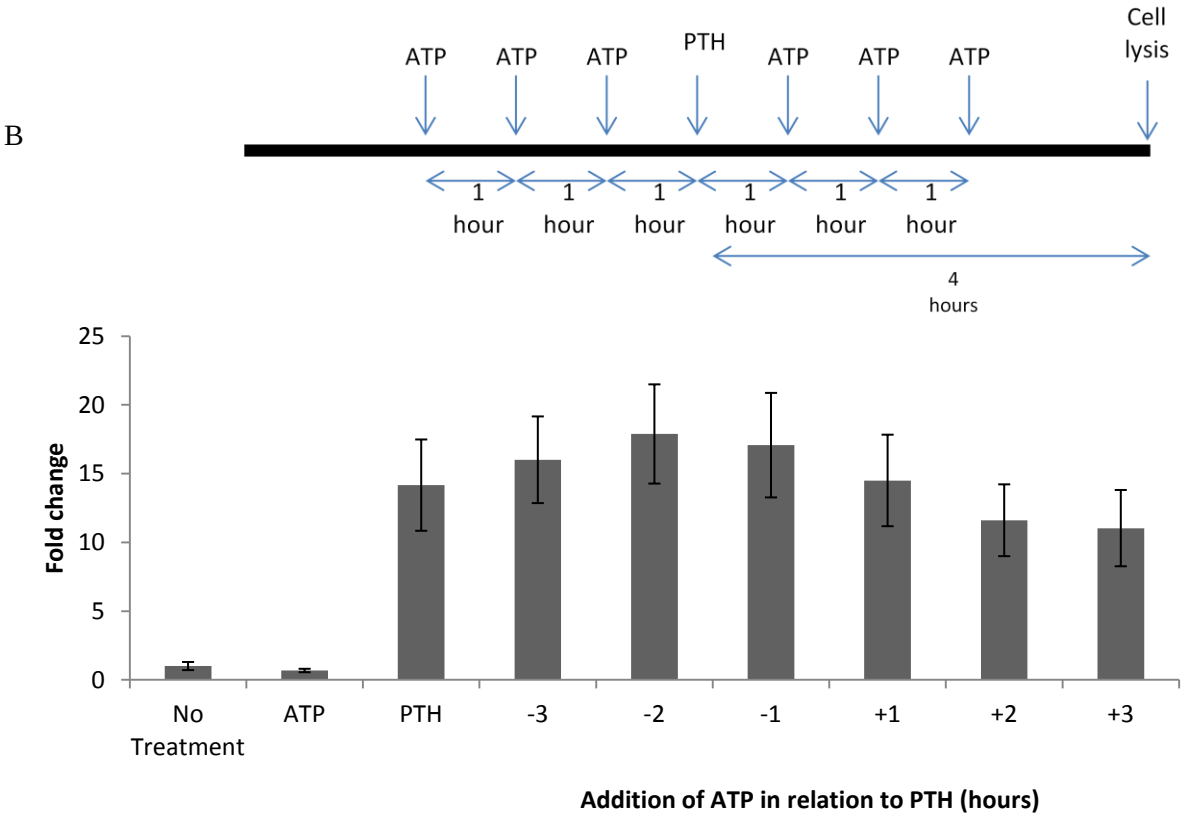

Figure 4.5. The effect of adding ATP before and after PTH on *c-fos* transcription in SaOS-2 reporter cells. Results represent fold changes in compared to no treatment. PTH (1 nM) was added for 4 hours before cell lysis, however the time of ATP addition varied between treatments. A) Displays ATP addition from 30 minutes before to 30 minutes after PTH. B) Shows ATP addition 3 hours before and after PTH addition. n = 6-10. Error bars represent S.E.

A

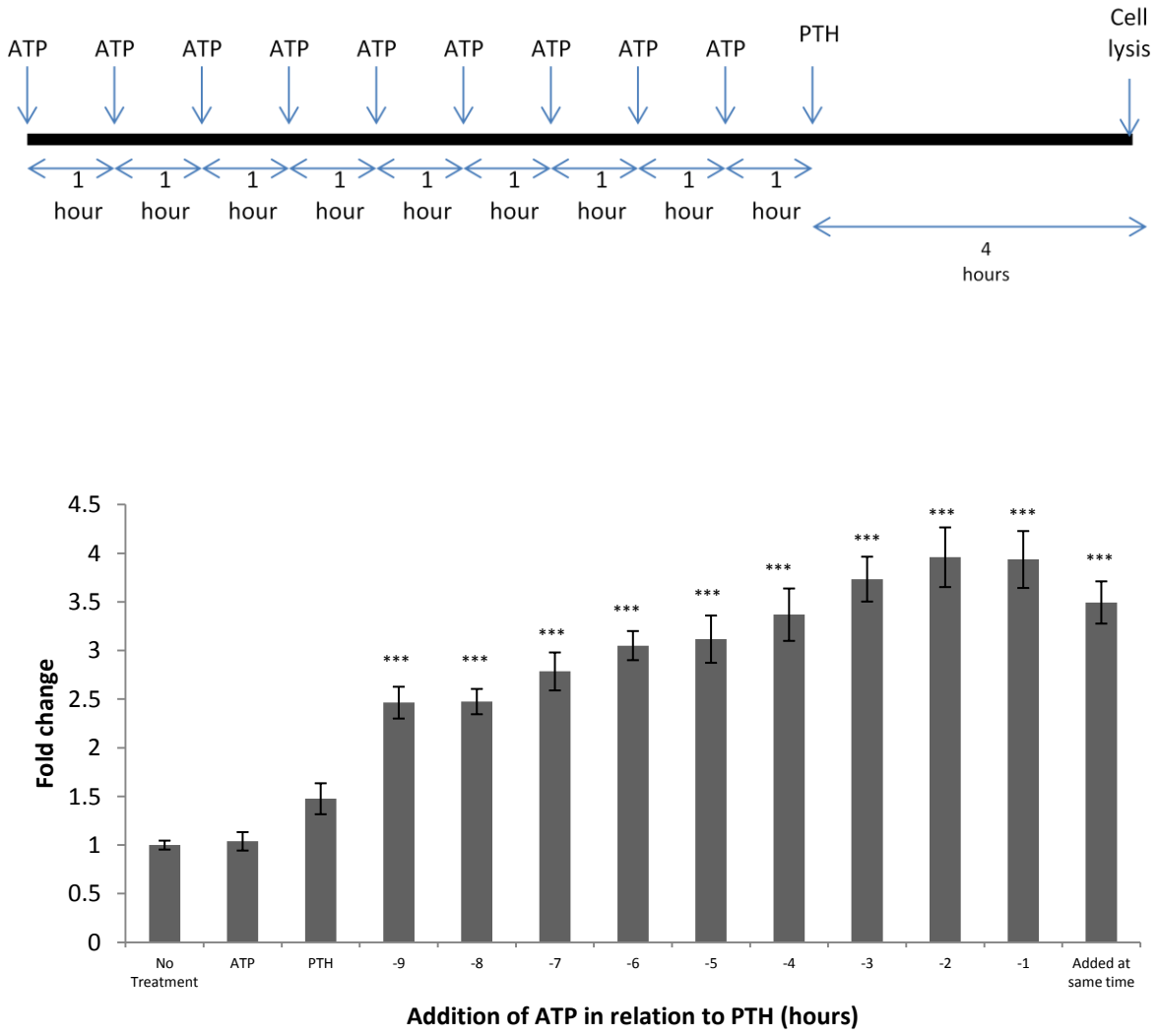

Figure 4.6 (A). The effect of adding ATP before PTH on *c-fos* transcription in SaOS-2 reporter cells. Results represent fold changes compared to no treatment. PTH was added for 4 hours before cell lysis. ATP addition was from 1 hour to 9 hours before PTH. n = 2-10. Error bars represent S.E.

B

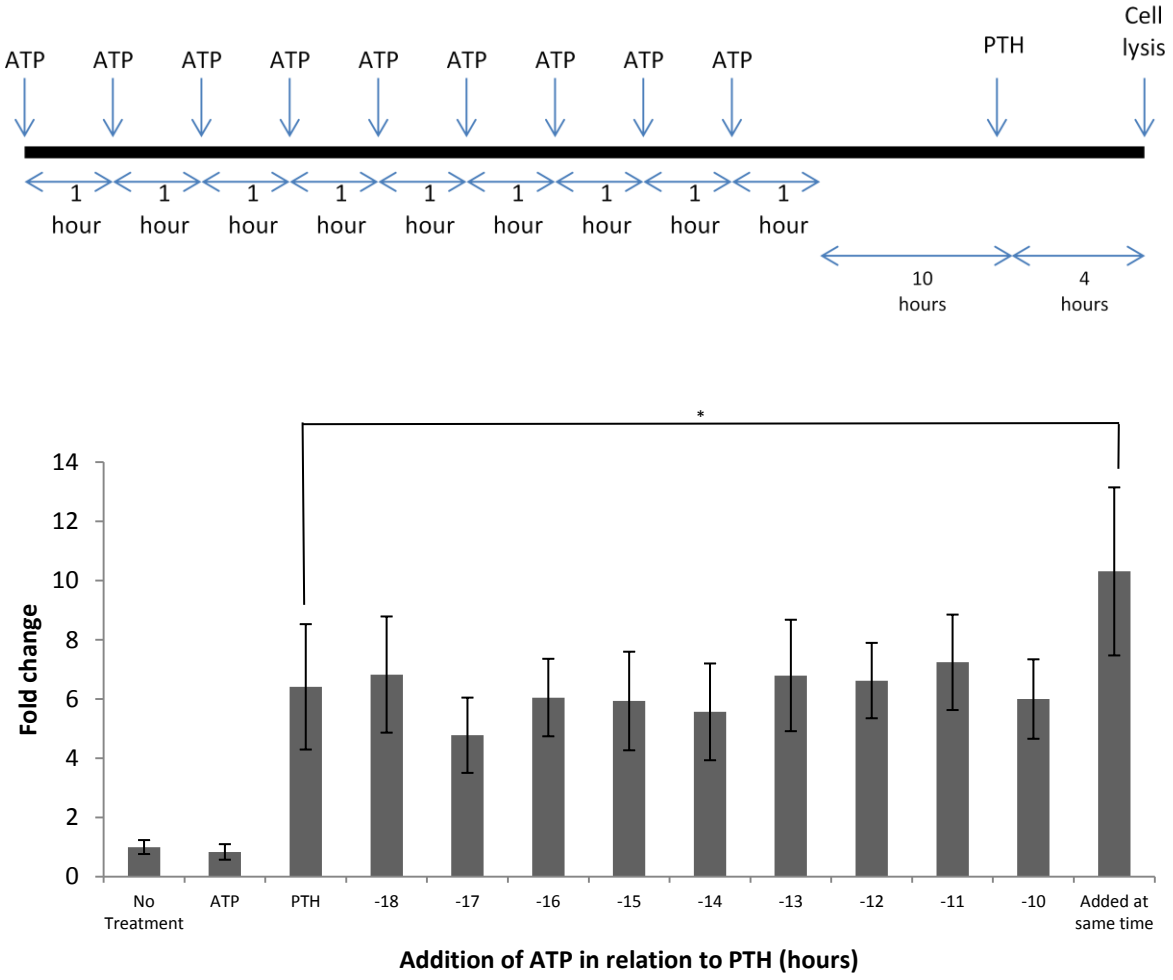

Figure 4.6 (B). The effect of adding ATP before PTH on *c-fos* transcription in SaOS-2 reporter cells. Results represent fold changes compared to no treatment. PTH was added for 4 hours before cell lysis. ATP addition was 10 hours to 18 hours before PTH addition. n = 2-10. Error bars represent S.E.

Fig 4.5 A) shows that ATP did not increase basal levels of *c-fos*. When ATP was added up to 30 minutes before and 30 minutes after PTH there was a higher *c-fo*s expression than PTH alone ($p<0.001$). B) Shows a further experiment that extended this time course where ATP was added 3 hours before and 3 hours after PTH addition. When ATP was added 3, 2 and 1 hour(s) before PTH there was still synergy observed, whilst adding ATP an hour after PTH shows no synergistic action. In Fig 4.6 A) the time course was again extended from 1 to 9 hours and synergy is observed in all treatments which were all significant ($p<0.001$) compared to PTH alone. In fact, in this case, synergy appears to be higher when ATP is added 1 to 3 hours before PTH than when ATP is added at the same time as PTH. B) The time course was extended from 10 to 18 hours with synergy was observed in these cases. Taken together the data suggests that ATP can be added 9 hours before PTH and still cause a synergistic expression in *c-fos*, even though ATP only has a half life of 9 minutes. Therefore ATP must be causing an action intra- or extracellularly that is longer lasting and can synergise with PTH.

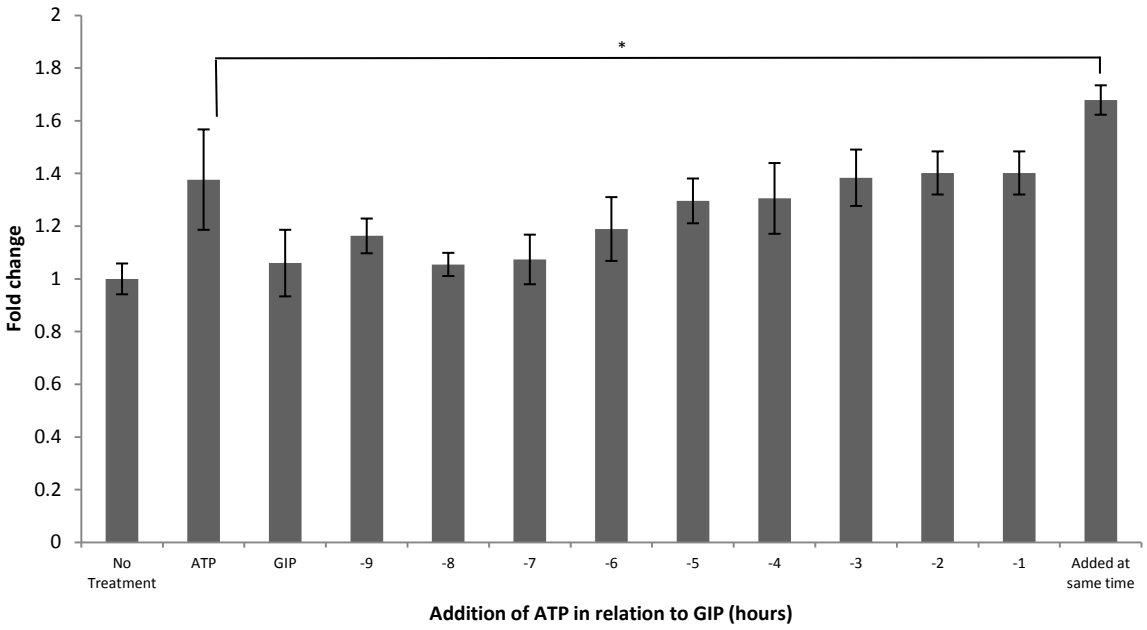

Figure 4.7. The effect of adding ATP before GIP on *c-fos* transcription in SaOs-2 reporter cells. Results represent fold change compared to no treatment. GIP (10 µM) was added for 4 hours before cell lysis. ATP (10 µM) was added from 9 hours to 1 hour before GIP at increments of 1 hour. n = 2-6. Error bars represent S.E

Fig 4.7 Shows 10 µM ATP caused a 1.4 fold increase (+/- 0.19 S.E.) over basal levels of *c-fos* and a slight increase was observed with GIP over basal levels, but this was not significant. When ATP and GIP were added at the same time it caused a 1.6 fold increase (+/- 0.02 S.E.) over basal levels and this was significant compared to ATP ($p<0.05$). ATP that was added 9 to 1 hours before GIP did not cause any increase over ATP alone.

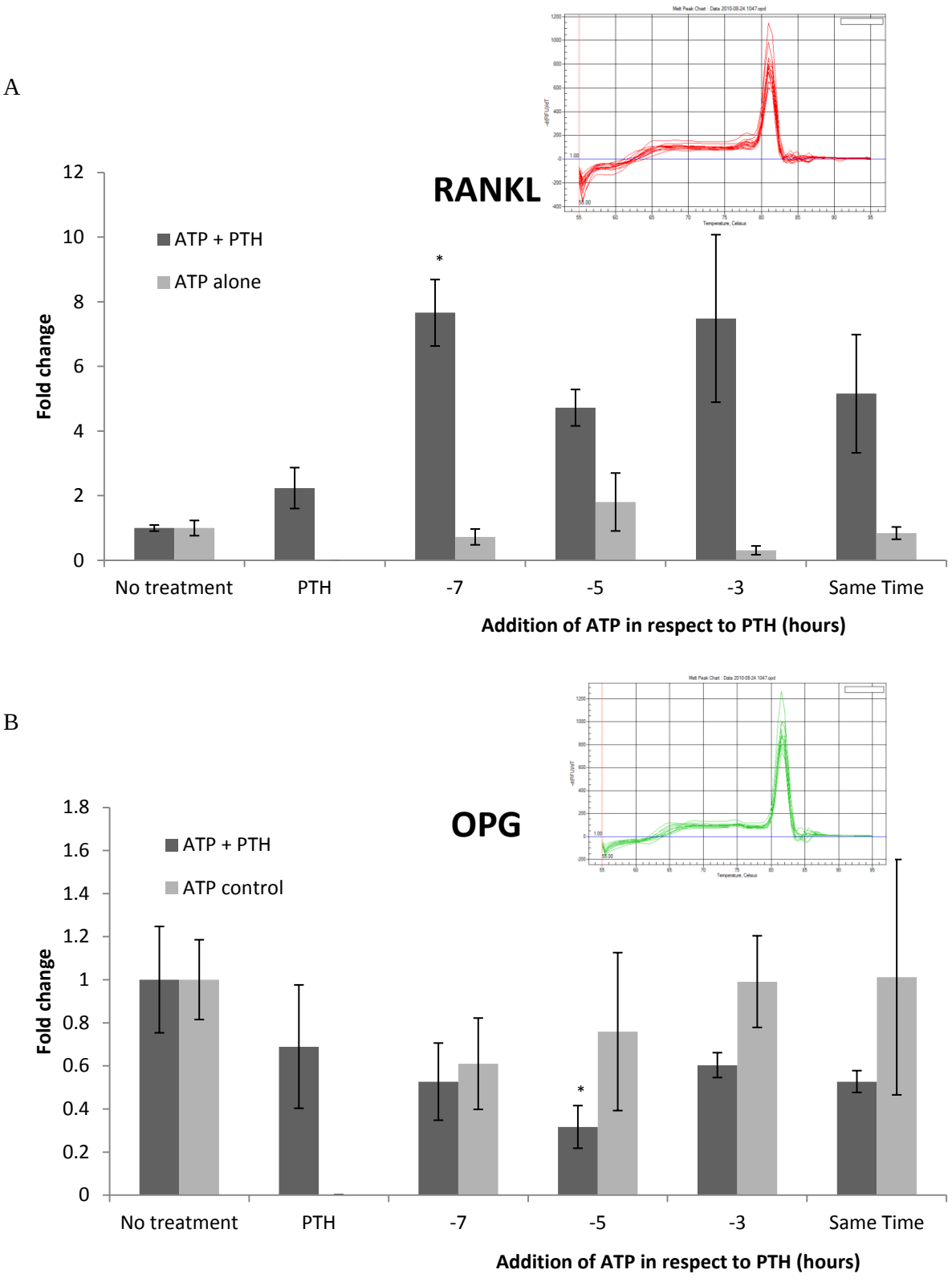

Figure 4.8. The effect of adding ATP before PTH on mRNA expression of RANKL and OPG in SaOS-2 cells. Results represent fold changes compared to no treatment. Following PTH treatment cells were left for 18 hours before cell lysis, Graphs are of A) RANKL and B) OPG levels in SaOS-2 cells. 1 nM PTH was used and 10 µM ATP was added at different time intervals. A control, of ATP that was added at the same time intervals, was also run. n = 4. Error bars represent S.E. The inlaid graphs represent the melt curves of the amplified products.

Fig 4.8 shows that when cells are treated with PTH (1 nM) an increase in RANKL production is observed. When ATP (10 μM) and PTH are added together a further, synergistic, increase is observed. Furthermore when 7 hours before PTH there is a significant increase in RANKL expression which is larger than ATP + PTH added together at the same time control of adding ATP without PTH at the same time points was carried out to ensure the increase in RANKL wasn't due to a longer exposure of ATP. It can be seen that apart from a small insignificant increase at the -5 hours time point that ATP alone did not cause an increase in RANKL expression.

Figure 4.8 B) shows PTH (1 nM) treatment reduced the expression of OPG. Treatment with ATP (10 μM) and PTH at the same time reduced this further. Treatments where ATP was added 5 hours before PTH showed a larger decrease than ATP and PTH added simultaneously. However in this experiment it should be noted that when ATP alone was added for the same time period as the 5 and 7 hour treatments a similar decrease in OPG expression was observed. When ATP was left on for the same period, 3 hours before and at the same time as PTH there was no decrease in OPG levels observed.

4.3.3 ATP sensitisation is mediated extracellularly

The next step was to determine whether the sensitization was conferred intracellularly or extracellularly. Is it something within the cell that ATP activates that is able to still increase *c-fos* when PTH is added hours later, or does ATP cause something to change within the medium that is still present when PTH is added? Firstly ATP was added to the medium then, after a certain time period, the medium was replaced with fresh serum free medium (Fig 4.9). It shows that in wells where medium was taken off and replaced there is no synergy, suggesting a factor in the medium is responsible for the synergy.

The next experiment, shown in Fig 4.10 (B), looked to provide further evidence that the sensitization effect came from the medium. ATP was added to one set of wells and left for two hours. This medium was then moved (and the wells were replaced with fresh serum free medium) over to a new set of wells where PTH was added. PTH was also added to the replaced medium (design shown in Fig 4.10 (A)). A parallel test was also run, where the medium that was removed after two hours was measured for ATP. This was to check the half life results in this system. Controls of ATP alone, PTH alone, ATP + PTH added at the same time and ATP added, but not removed, before PTH was added were run.

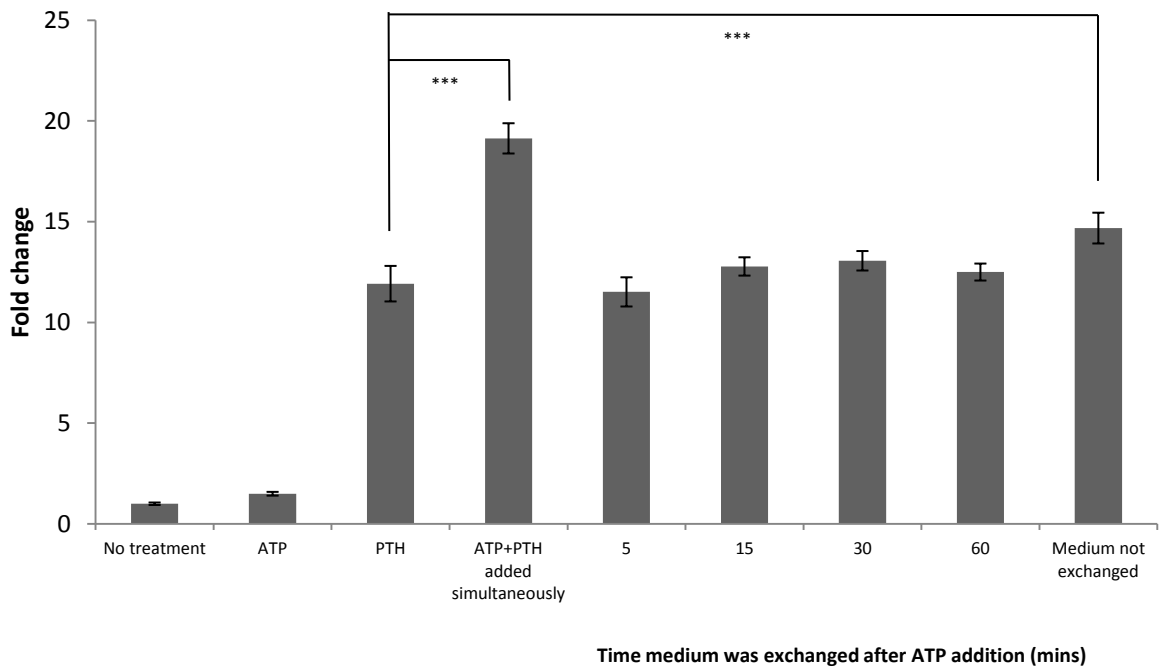

Figure 4.9. The effect of ATP addition before subsequent medium change on *c-fos* transcription in SaOS-2 reporter cells. Results represent fold changes compared to no treatment. ATP (10 µM) was added 2 hours before the addition of PTH (1 nM). Then to different sets of wells the medium was taken off and replaced with non-treated serum free medium. This occurred 5, 15, 30 and 60 minutes after the addition of ATP. n= 6. Error bars = S.E.

These data shows that PTH caused an 11 fold increase (+/- 0.7 S.E.) of *c-fos* transcription over basal levels and that ATP + PTH added simultaneously caused a 19 fold increase (+/- 0.8 S.E.). In wells where the medium was not exchanged a 14 fold increase was observed (+/- 0.8 S.E), both of these were significant to PTH alone ($p<0.001$). Removing the medium, and therefore any factors left in it, at any stage caused no increase in *c-fos* levels over normal PTH levels, suggesting PTH is the only treatment acting on these wells.

A

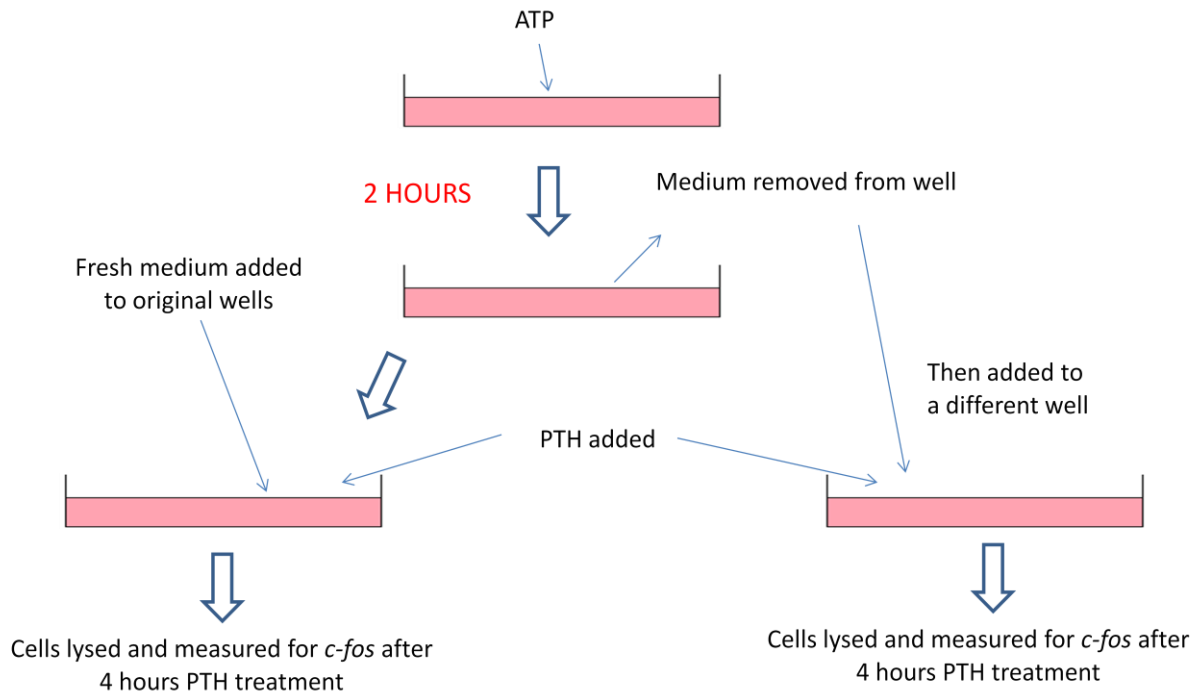

Figure 4.10 (A). Diagram of the design for the experiment shown in Fig. 4.10 (B). ATP was added to wells and left for 2 hours. Medium was then removed and added to separate untreated wells. The original wells had fresh serum free medium added to them. PTH was then added to both sets of wells for 4 hours before cell lysis and *c-fos* measurements.

B

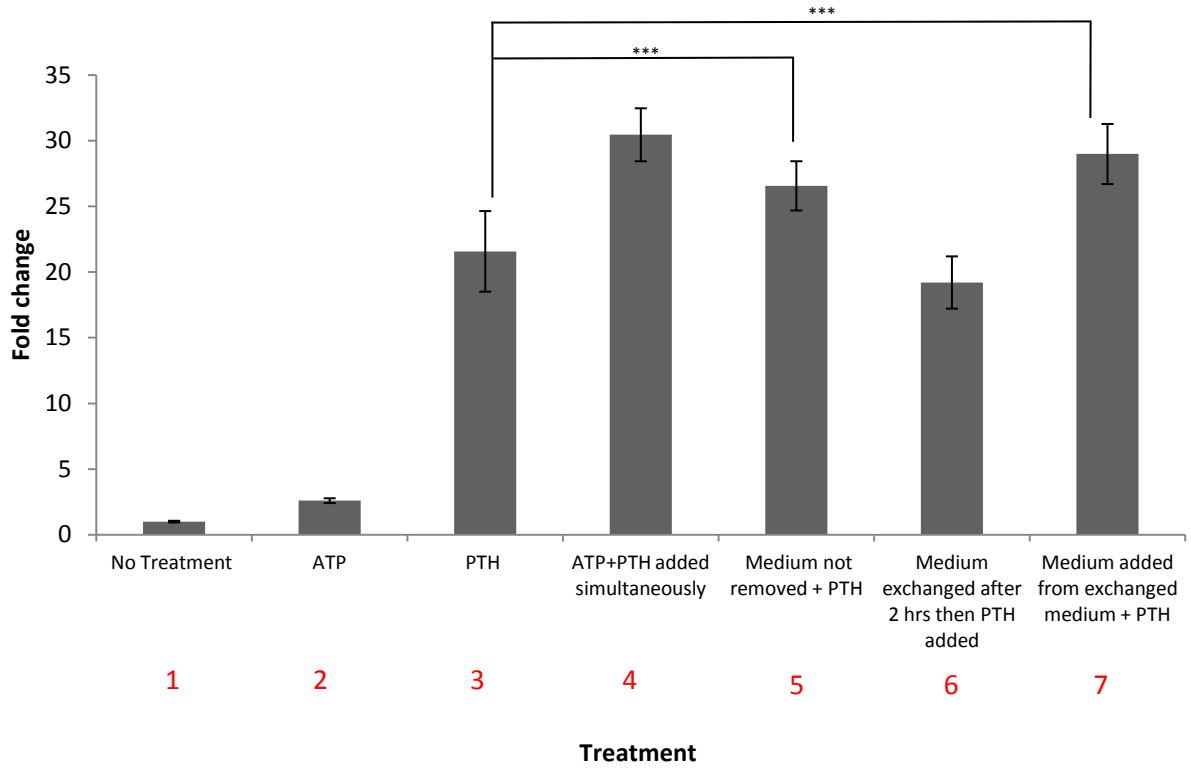

Figure 4.10 (B). The effect of ATP addition and subsequent removal of supernatant to parallel wells on *c-fos* transcription in SaOS-2 cells reporter cells. Results shows fold changes compared to no treatments. To treatments 5 and 6 ATP (10 µM) was added 2 hours before PTH (1 nM). Following the 2 hour incubation medium from 5 was added to 6 and PTH was added to it. Fresh medium was added to 5 and PTH added. PTH then added to treatments 4, 5 and 7. Finally ATP was added to 2 and 4. n = 12. The error bars represent S.E.

In Fig. 4.10 PTH caused a 21 fold increase (+/- 4 S.E.) over basal levels and ATP + PTH synergised to cause a 30 fold increase over basal levels (+/- 2 S.E.). Treatment 5, where ATP was added 2 hours before PTH, produced a 26 fold increase (+/- 2.7 S.E.), which was significant compared to PTH alone ($p<0.001$). Treatment 7, where medium from wells that were treated with ATP 2 hours before, then moved to separate wells where PTH was added, caused a 28 fold increase (+/- 3.3 S.E.). This was significant compared to PTH alone ($p<0.001$). The cells that had the medium taken from them, and then treated with PTH did not have an increase in *c-fos* levels compared to PTH alone. Finally a parallel test was run were the medium was measured for ATP after being taken off after 2 hours. This gave a mean ATP reading of 80nM.

4.3.4 Sensitisation is not due to low concentrations of ATP or ATP break down products

Fig 4.11 shows that 10 μM of ATP is needed to cause synergy with PTH. Given that there was only 80 nM of ATP for the experiment shown in Fig 4.10 this would suggest that ATP at low concentrations is not causing the synergy. Furthermore Fig 4.12 and Fig 4.13 show that AMP and adenosine (the break down products of ATP) do not synergise with PTH. In fact they appear to inhibit the action of PTH on *c-fos*.

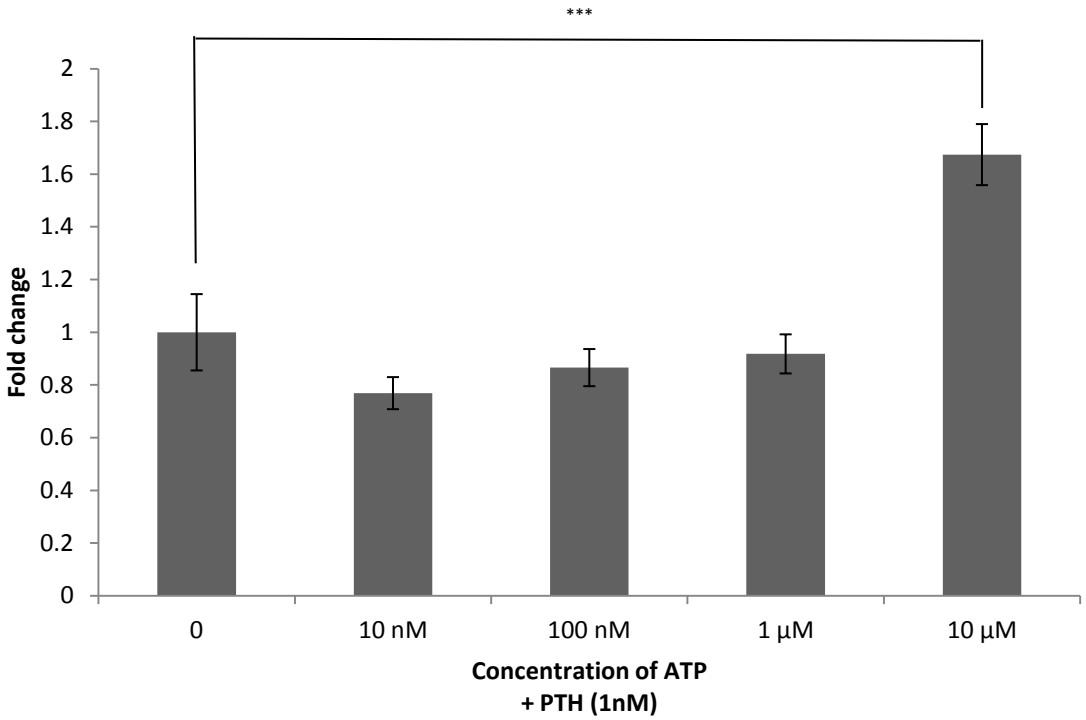

Figure 4.11. A dose response curve comparing *c-fos* transcription in SaOS-2 reporter cells with different ATP concentrations when added alongside PTH (1 nM). Bars represent fold changes compared to PTH (1 nM). n = 6. The error bars represent S.E.

Fig 4.11 shows that concentrations of ATP up to 1 µM show no synergy with PTH as there is no significant difference between 10 nM, 100 nM and 1 µM compared to 0 ATP. Whereas 10 µM ATP causes synergistic expression as seen by its significance compared to PTH alone ($p<0.001$).

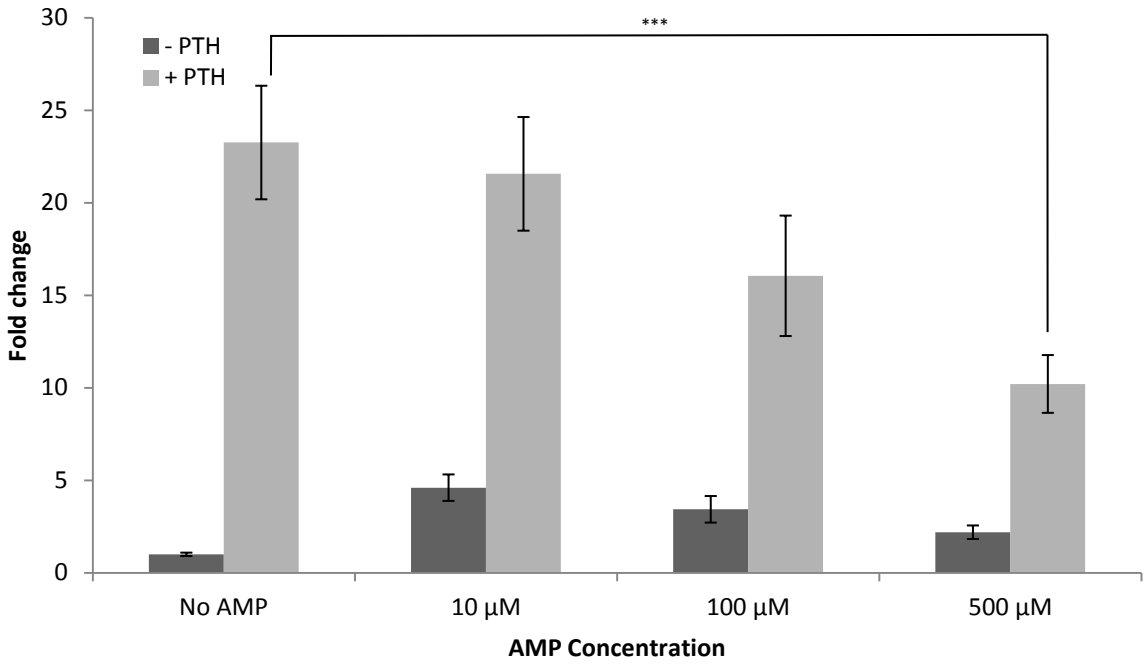

Figure 4.12. A dose response curve comparing *c-fos* transcription in SaOS-2 reporter cells with different AMP concentrations when added with or without PTH (1 nM). Results represent fold changes compared to no AMP and no PTH. n=6. Error bars = S.E.

Fig 4.12 shows a 23 fold increase (+/- 3.3 S.E.) in *c-fos* with the addition of PTH. When added together with 10 µM and 100 µM AMP there was a decrease in *c-fos* levels compared to PTH. 500 µM AMP caused a 50% inhibition of PTH, which was significant ($p<0.001$). 10 µM and 100 µM of AMP alone increased basal levels 5 (+/- 0.6 S.E.) and 4 fold (+/- 0.7 S.E.) respectively although this increase was not significant.

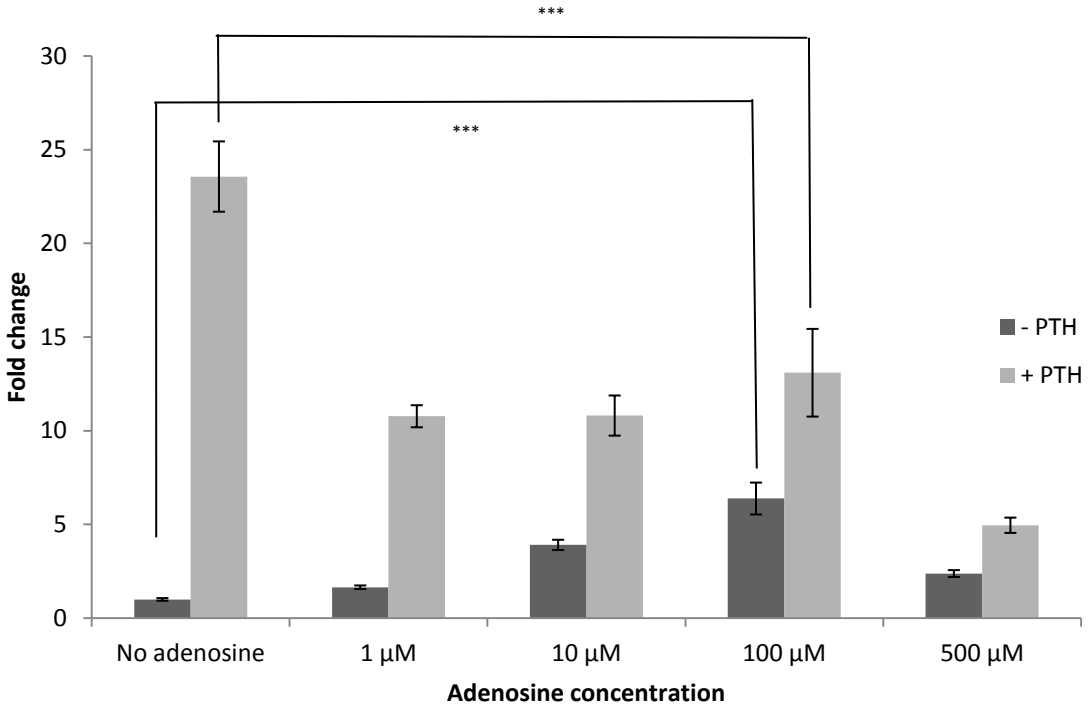

Figure 4.13. A dose response curve comparing *c-fos* transcription in SaOS-2 reporter cells with different adenosine concentrations when added with or without PTH (1 nM). Results represent fold change compared to no adenosine and no PTH. n=6. Error bars = S.E.

Figure 4.13 shows a 23.6 fold increase (+/- 3.2 S.E.) in PTH treated samples. When PTH was treated alongside 1 µM and 10 µM of adenosine this decreased by 55%, with 100 µM a decrease of 45% and with 500 µM a decrease of 80% was observed. All of these values were significant ($p<0.001$). Adenosine alone can increase *c-fos* transcription significantly at concentrations of 100µM.

4.4 Discussion

It is clear that adding ATP alongside PTH causes a synergistic increase in *c-fos* expression (Fig 4.1) and therefore the beginning of this chapter focused on what else could cause synergy. As shown in the previous chapter, mechanical strain, in the form of medium displacements, can cause an increase in the amount of ATP present in the extracellular medium. Therefore attempts were made to see if medium displacements with PTH added at the end caused an increase in synergy. This was not the case as is seen in Fig 4.2. However it would be wrong to presume that this rules out mechanical strain as the source of ATP *in vivo*. It is fairly accepted that the concentrations seen after mechanical stimulation *in vitro* are much smaller than what would occur *in vivo* [217], as the cells are bathed in much more fluid *in vitro* than *in vivo*. Fig 4.3 shows that GIP, a hormone from the GI tract can synergise with ATP to increase *c-fos* expression. This again shows evidence of the importance of ATP, a locally released factor, has on focusing system wide hormones to specific areas that are highly loaded. ATP release may therefore account for the phenomenon that is Wolff's law. i.e. an increase in bone mass in higher loaded areas of the skeleton. Finally experiments were run to see whether osteoclast treated supernatants could synergise with either ATP or ADP (Fig 4.4). Interestingly the addition of osteoclast supernatant did increase the *c-fos* expression, thus suggesting that factors can signal to osteoblasts to proliferate/differentiate and increase bone remodelling. There are a lot of potential factors that could be involved, for example osteoclasts release BMP 2, 4, 6 and 7 [218] and ephrin B2 which binds to EphB4 on the osteoblasts [219]. All of these can cause osteoblast recruitment, proliferation and differentiation and thus lay down more bone. When the osteoclast supernatant was added with ATP or ADP there was no significant increase in *c-fos* expression. This was not too surprising, as it is not incorporating a systemic factor with a local one, it is merely combining two local factors and therefore the ATP is not acting to focus the action of a system wide hormone to a highly loaded area

The next area of investigation was to look at whether these local and systemic hormones had to be present at the membrane at the same time. Both ATP and PTH are only transiently present, ATP has a half life of 10.5 minutes *in vitro* and PTH has an *in vivo* half life of 4 minutes. With such short half

lives for both it was decided to investigate whether ATP could sensitise the osteoblast to the effect of PTH. Fig 4.6 shows that when adding ATP up to 9 hours before PTH and 1 hour after PTH there is still synergy between them. This suggests that a mechanism exists whereby the cells are able to have a 'memory' of mechanically stressed areas. Thus whenever PTH binds to its receptor in these strained areas it increases *c-fos* expression and thus bone remodelling, in fact in one test it appeared beneficial to have ATP present before the PTH was there. The GIP time course was the opposite, GIP and ATP do synergise with each other to cause an increase in *c-fos*, however if ATP is added before GIP no increase in *c-fos* is observed over adding ATP alone. There may be a few reasons for this, the most obvious being that perhaps GIP has a longer half life than PTH, therefore the need of ATP to sensitise the osteoblast has never evolved. Or perhaps GIP and ATP are not enough to cause a serious bone remodelling effect alone.

To confirm that this synergy wasn't just affecting *c-fos* the effect ATP and PTH had on RANKL and OPG mRNA expression was examined. As stated previously *c-fos* is a master regulator gene that causes transcription of other genes thus it can increase RANKL and decrease its decoy receptor OPG. Fig 4.8 shows that PTH alone causes an increase in RANKL production and a decrease in OPG. When ATP and PTH are added simultaneously again a greater increase in RANKL, and a greater decrease in OPG, is observed. This again confirms that ATP and PTH work together to cause a greater response in these cells. ATP added 7, 5 and 3 hours before PTH still showed a synergistic increase in RANKL levels compared to PTH alone. ATP added 7, 5 or 3 hours before PTH caused a decrease in OPG levels compared to PTH alone, with 5 hours being the lowest, interestingly this was the measurement of RANKL that was also the lowest, showing a strong correlation between the two. However it must be pointed out that ATP had a large effect when added on its own for a longer period of time. These results provide further evidence that ATP and PTH synergy does exist, that it effects bone remodelling due to the fact the synergy can still be seen downstream of *c-fos* and that ATP can sensitise the cells to the action of PTH.

Given that ATP can be added hours before PTH and still have an effect, the next question was how does this happen. It has previously been shown, as alluded to in the Introduction, that ATP can

synergise with PTH in different ways, depending on the cell type. In UMR-106 cells it is said to act through P2Y1 receptors and acts with PTH to massively increase the intracellular release of Ca^{2+}. This then goes on to act on the Ca/CRE part of the c-fos promoter [160], however in SaOS-2 cells they act through different pathways. PTH, acting through the PKA pathway, causes phosphorylation of CREB, which acts on the Ca/CRE part of the *c-fos* promoter. However it has been shown that ATP acts on the SRE part of the *c-fos* promoter, by a yet unknown mechanism [159]. Neither of these pathways take into account the ability of ATP to create a 'memory' in which the cell can act to PTH. Initial investigations, therefore, looked into which of the two main ways ATP could sensitize the cells to PTH. ATP either acted to create a change within the cell or within the medium. Changes in the cell could include, for example, the fact that PTH has been shown to increase the intracellular store of Ca^{2+} for ATP to act on this larger store [220], perhaps ATP could play a similar role? Or ATP could increase how sensitive the intracellular stores were to PTH, for example by increasing the number of IP_3 receptors on the membrane. Alternatively ATP could even act to increase the number of PTH receptors on the membrane. However it is also known that ATP can cause a release of compounds into the medium, or ATP breakdown products may themselves act to synergise with PTH or release factors into the medium. The prime candidate for such a factor appears to be PGE_2, this is a lipid compound that, like ATP, acts in an autocrine or paracrine manner. It has been shown to be released by many different cell types in response to ATP binding to P2 receptors. These include osteoblasts [221], vas deferens epithelial cells [222], macrophages [223] and spinal cord astrocytes [224]. Further to this PGE_2 has also been proven to increase the transcription of *c-fos* by acting on the exact same pathway as PTH, i.e. it acts through PKA to increase CREB phosphrylation at ser 133 [225]. ATP could also be causing release of AA which is then broken down to PGE_2 using PGE synthase [226].

Tests were ran to determine whether the synergy is conferred in the medium by adding ATP to the medium 2 hours before PTH, then removing it at different time points as is shown in Fig 4.9. 2 hours was chosen as this was the highest point of synergy (Fig 4.6 A)). After the medium was removed, there was no longer any observed synergy, at any time point. Medium that was left on and then had PTH added to it showed synergy, this therefore suggests ATP affects the medium.

To further confirm this another test was run which comprised of adding ATP to one set of cells 2 hours before PTH. This medium was removed, replaced with untreated medium (which PTH was then added to), and added to a second set of cells (Fig 4.10). The cells the medium was added to had a synergistic increase in *c-fos* expression similar to controls that didn't have medium removed and that had ATP and PTH added at the same time. Furthermore the cells that the medium was removed from and had PTH added to did not increase *c-fos* levels compared to PTH alone. This again suggests that ATP sensitizes osteoblasts to PTH and that it does this through the medium. Finally a parallel test was run to determine the amount of ATP present in the medium after two hours. The results of this showing an average of 80 nM of ATP.

To confirm that 80 nM of ATP would not be sufficient to synergise with PTH different ATP concentrations were tested with PTH to determine the level of *c-fos* expression. As shown in Fig 4.11 10 nM, 100 nM and 1 μM of ATP with PTH had no synergistic increase in *c-fos*. Thus the sensitisation affect is not simply ATP working at low concentrations.

Finally we tested whether the sensitisation effect was due to ATP breakdown products. As shown already ADP can synergise to some extent [159], however there is only ever a maximum of 20% of the total amount of ATP that was placed in. Also ADP has completely disappeared after 30 minutes [227]. Thus the effect of AMP and adenosine on *c-fos* synergy were looked at. Interestingly both AMP and adenosine did not increase *c-fos* expression, in fact both inhibited the action of PTH on *c-fos* at 10 μM and below. Therefore the effect ATP is having on the medium has to be large enough to overcome this inhibition as it is inevitable that AMP and adenosine will be present at some point as ATP is broken down. Adenosine and its A1 receptor has been shown in neurones to inhibit the PKA/CREB pathway and is a possible explanation for the inhibition seen in these osteoblasts [228]. In conclusion it seems likely that ATP is releasing other, longer lasting, factors into the medium which synergise with PTH with PGE_2 or AA being the most likely candidates.

5. The effect of BL-1249 on osteoblasts

5.1 Introduction

Previous work has shown that when BL-1249, a K^+ channel activator, was added with ATP and PTH it causes a complete inhibition of the *c-fos* expression. Osteoblasts have been shown to express different types of K^+ channels, including BK_{Ca} [229, 230], inward rectifier K^+ (K_{IR}) [231] and ATP-sensitive K^+ (K_{ATP}) channels [171]. More recently, TREK-1, a two pore domain K^+ (K_{2P}) channel, has been found in primary human osteoblasts and MG-63 cells [169], as well as SaOS-2 and Te-85 (unpublished). K^+ channels have been implicated in a variety of functional responses of osteoblasts, including mechano-transduction [232], the ability to regulate the volume of the cell [161], secretion of osteogenic factors, such as osteocalcin [233], and regulating their response to hormones, for example PTH and PGE_2 [234]. Opening K^+ channels causes cell hyperpolarisation as K^+ will move out of a cell down its concentration gradient, at this stage the concentration pull of the K^+ is so great it will cause K^+ efflux even against its electrical gradient, eventually the forces will even out and no net movement of ions will occur, this constitutes the equilibrium potential. As BL-1249 activates K^+ channels it will, therefore, likely hyperpolarise cells.

There is still some debate as to what specific channel BL-1249 acts upon. The Tertyschnikova paper [172] proposed BL-1249 as an activator of TREK-1 channels because, firstly, voltage clamp studies showed that BL-1249 activated a current that reversed at the equilibrium potential for K^+. The current was insensitive to normal K^+ channel blockers (e.g. glyburide, tetraethylammonium, iberiotoxin, 4-aminopyridine, apamin, and Mg^{2+}), but it was inhibited by extracellular barium (Ba^{2+}). Thus it was assumed that it modulated TREK-1. Recent studies in our lab have suggested that this is not the case. The currents show an increased outward current at +80 mV but not -120 mV and thus is more likely to be that of a strongly voltage dependent K^+ channel. Tetraethylammonium (TEA) and penitrem A are BK_{ca} channel inhibitors. When TEA or penitrem A were added alongside BL-1249 they inhibited the outward current, therefore suggesting that BL-1249 acts on BK_{ca} channels. These channels respond to

increases in intracellular Ca^{2+} and therefore usually act as a negative feedback loop, as Ca^{2+} usually enters when cells become depolarized.

Investigations initially focused on the role BL-1249 has on *c-fos* expression, *c-fos* is a proto-oncogene and thus plays a major role in proliferation and differentiation of osteoblasts [210]. Then tests were carried out to attempt to discover how BL-1249 inhibits *c-fos*. Primarily the need was to make sure BL-1249 wasn't simply toxic to the cells after 4 hours of treatment, as 4 hours is the length of time BL-1249 is left on in the *c-fos* experiments. Finally experiments were run to determine the effect of BL-1249 on different cell types

5.2 Methods

5.2.1 *c-fos* assays

These were carried out using the transfected SaOS-2 cells reporter cells. Cells were seeded until 90% confluent and then serum starved for 24 hours prior to experiment. The cells in all experiments were treated with 1 nM PTH for 4 hours and incubated at 37^{o}C and 5% CO_2, before cell lysis. BL-1249 (Sigma-Aldrich, UK) was dissolved in DMSO and was added to cells at concentrations of 1, 10, or 100 µM, whilst ATP was used at concentrations ranging from 10 µM-10 mM. 5% FCS was used in experiments. sp-cAMP (Sigma-Aldrich, UK) treatments ranged from 10-100 µM. Finally, experiments that used KT-5752, which was dissolved in DMSO, (Sigma-Aldrich, UK) were preincubated with it for 1 hour prior to treatment with ATP and PTH. NS-1619 and TEA (both obtained from Sigma-Aldrich, UK) were dissolved in DMSO prior to application on cells.

5.2.2 Cell counts

When cells in 24 well plates were ready to be counted the DMEM was removed, they were washed X2 PBS then had 500 µl of trypsin added. When the cells had lifted 2 ml of DMEM with 5% FCS was added. The cell mixture was agitated by a pipette to ensure there were no clumps of cells, then 10 µl was added to 10 µl of trypan blue to distinguish between alive and dead cells. The cell mixture was then vortexed and 10 µl was added to a disposable haemocytometer. The count was taken from each corner of the square and an average was taken so that the total cell number could be calculated. The primary cell counts were undertaken with the help of Mrs. Jane Dillon. Cells were photographed using an Olympus microscope and camera

5.2.3 Western Blot

Cells were treated with different combinations of forskolin (Sigma-Aldrich, UK), PTH and BL-1249 after being serum starved for 24 hours. For the western blot the BL-1249 was preincubated for 15 minutes before any other treatment for it to have maximal effect. Treatments were left on for 20 minutes before protein extraction. The anti-phopsho-CREB (ser133, Millipore, USA) rabbit

polyclonal antibody was incubated overnight at 4^{o}C. The anti-rabbit horseradish peroxidise-linked secondary antibody was incubated at room temperature for 90 minutes. Exposures of 30 seconds and 5 minutes were carried out.

5.3 Results

5.3.1 BL-1249 inhibits ATP and PTH induced *c-fos* expression

Fig 5.1 shows that when BL-1249 was added with ATP and PTH it causes a complete inhibition of *c-fos* expression. Fig 5.2 shows that this was not due to BL-1249 being toxic to the cells as the cell counts were similar between BL-1249 treated cells and non-treated cells.

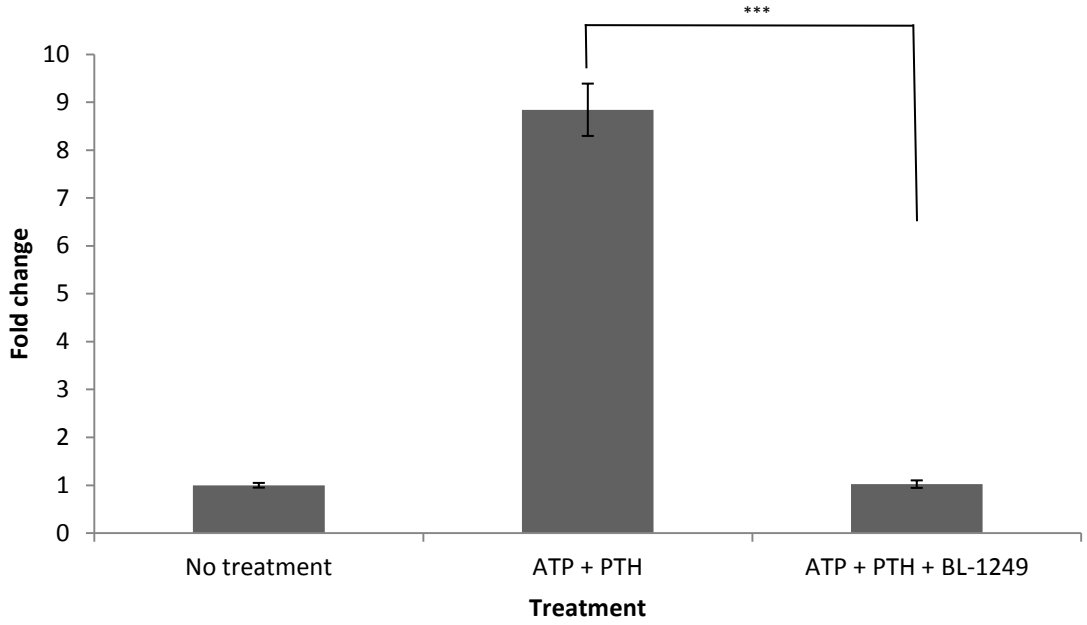

Figure 5.1. The effect of BL-1249 on ATP+PTH induced *c-fos* transcription in SaOS-2 reporter cells. The data are represented as fold changes compared to no treatment. Cells were treated with 10 µM ATP, 1 nM PTH and 10 µM BL-1249. n=6. Error bars represent S.E.

Fig 5.1 shows that ATP added with PTH causes an 8.5 fold increase (+/- 1.2 S.E.) in *c-fos* levels over basal expression. ATP and PTH co-treated with BL-1249 caused a massive inhibition of the ATP + PTH induced *c-fos* signal, with only a 1.1 fold increase (+/- 0.06 S.E.) over basal levels. This decrease in *c-fos* signal was significant ($p<0.001$).

A

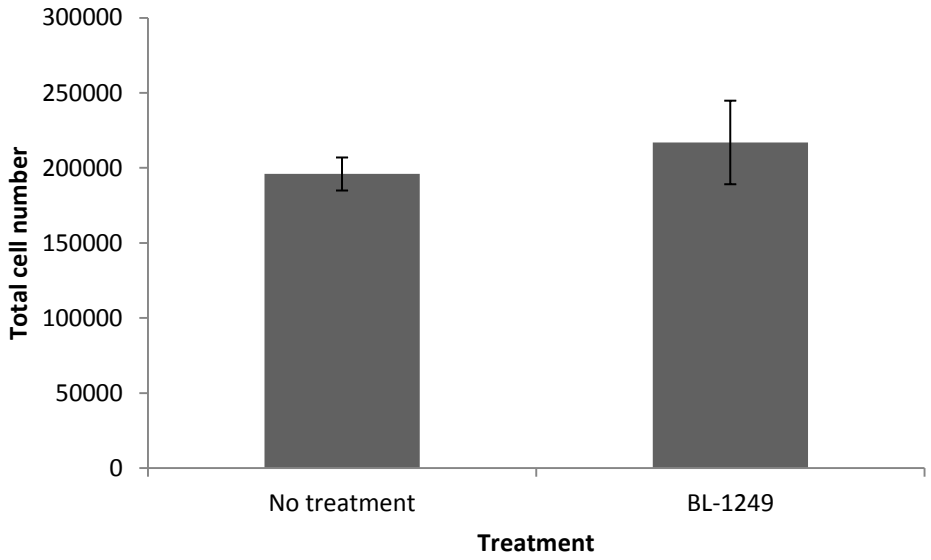

B

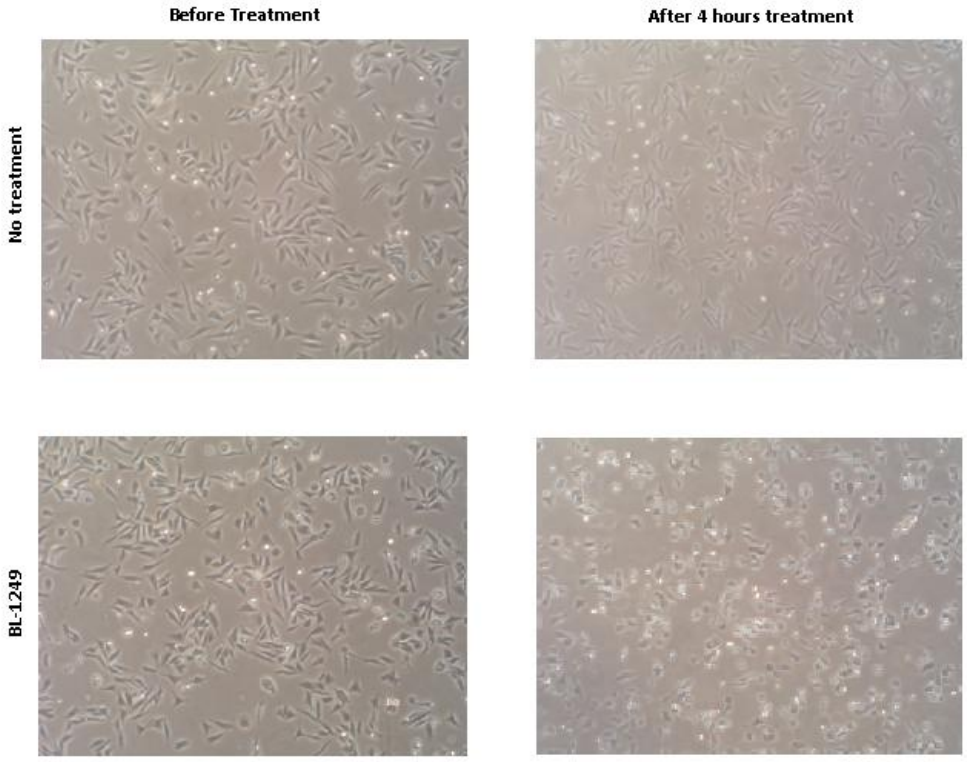

Figure 5.2. A) The effect of 4 hours of BL-1249 treatment on SaOS-2 cell number. n=4. Error bars = S.D. **B) Photomicrographs of SaOS-2 cells before and after 4 hours of BL-1249 treatment.**

Fig 5.2 A) shows 4 hours treatment of BL-1249 does not affect the total number of SaOS-2 cells alive in culture as there was no significant difference between the two cell counts. Photomicrographs were taken before BL-1249 was added and after 4 hours of treatment (Fig 5.2 B)). These photomicrographs confirm that the cells are alive after 4 hours treatment, however it is apparent that the cells have dramatically changed shape. The treated cells no longer have as many, or as well defined, processes as the control cell.

5.3.2 BL-1249 effect not due to opening of K^+ channels

The next experiment, shown in Fig 5.3, uses high extracellular K^+ to prevent hyperpolarisation of cells. To make this, $KHCO_3$ was substituted for $NaHCO_3$ when preparing the HEPES buffered medium. This ensured that the water potential stayed the same whist causing an extracellular K^+ concentration of 40 mM. Membrane hyperpolarisation to BL-1249 would likely be less in an extracellular solution containing 40 mM K^+ than in one containing 5 mM K^+, as K^+ would not move out down its concentration gradient [229, 235]. Therefore the experiment below tested whether BL-1249 was inhibiting *c-fos* via its effect on K^+ channels. The results suggested that BL-1249 did not inhibit *c-fos* via an opening of K^+ channels. These results were confirmed by Fig 5.4, which used a known K^+ opener, NS-1619, and showed no affect on *c-fos* expression.

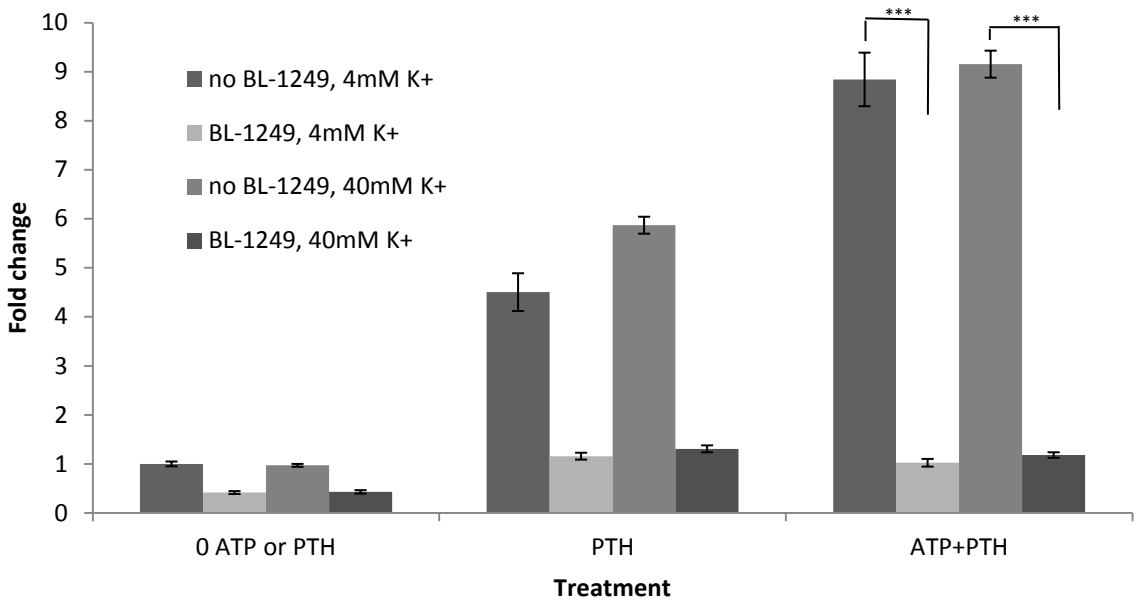

Figure 5.3. The effect of high extracellular K^+ on BL-1249 inhibition of ATP+PTH induced *c-fos* transcription in SaOS-2 reporter cells. The data are represented as fold changes in *c-fos* compared to basal levels (0 ATP or PTH, no BL and 4 mM K^+). Concentrations used were 1 nM PTH, 10 µM ATP and 10 µM BL-1249. n=6. Error bars represent S.E.

Fig 5.3 shows that BL-1249 can decrease basal levels of *c-fos* with a 50% reduction in the signal. The control of high external K^+ medium with no other treatment showed that this alone did not affect *c-fos* levels. Consistent with previous experiments, treatments of PTH and ATP + PTH with BL-1249 show a significant inhibition of the signal with a 3 and 8 fold decrease respectively. Treating cells with BL-1249 in high extracellular K^+ did not reverse the inhibition of *c-fos* ($p<0.001$). Importantly BL-1249 with PTH or ATP+PTH continued to inhibit the expression of *c-fos* as there was no significant difference with or without 40 mM K^+.

A

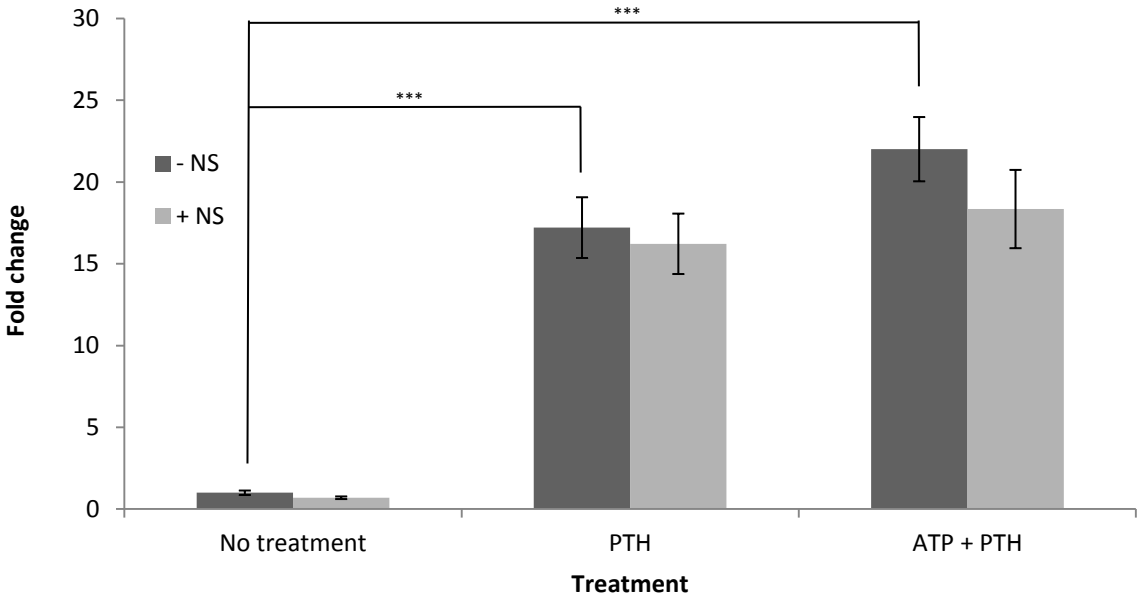

B

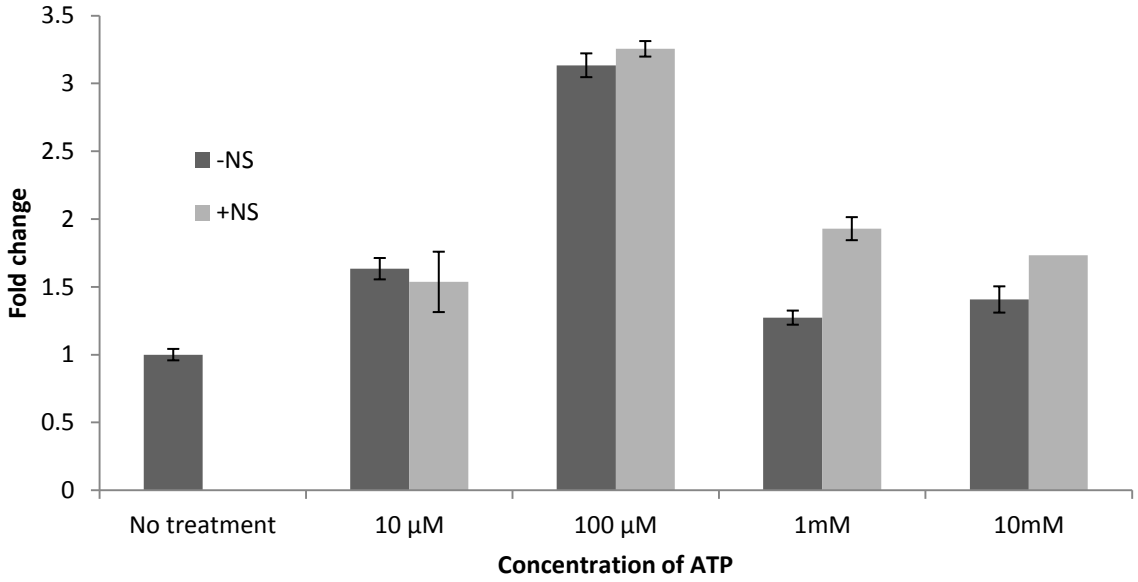

Figure 5.4. The effects of ATP and NS-1219 treatment on *c-fos* transcription in SaOS-2 reporter cells. The data are represented as fold changes compared to basal levels (No treatment, -NS-1619). A) PTH concentration was 1 nM, ATP and NS-1619 concentrations were 10 µM. B) concentrations of ATP ranged from 10 µM to 10 mM, with NS-1619 constant at 10 µM. n=18. Error bars represent S.E.

Fig 5.4 shows a 17 fold increase (+/- 3.5 S.E.) in PTH over basal levels whilst a 22 fold increase (+/- 3.3 S.E) was observed when ATP and PTH were added together. When NS-1619 was added with either PTH, ATP, ATP + PTH or alone there was no significant difference between the equivalent of not adding NS-1619.

5.3.3 BL-1249 acts on the PKA pathway to inhibit *c-fos* production

As K^+ channels do not influence BL-1249s inhibitory effect, the next investigations looked at what signalling pathways BL-1249 worked on. This series of experiments looked at different agonists of *c-fos* expression to see if BL-1249 has an effect, and therefore the pathway it inhibits can be determined. Fig 5.5 shows that BL-1249 inhibits ATP induced *c-fos* expression, however as it is still unclear how ATP and PTH synergise it is hard to learn anything from this. Fig 5.6 shows that FCS induced *c-fos* expression is not affected by BL-1249. As BL-1249 affects PTH and not FCS this points towards BL-1249 having an effect on the PKA pathway [142, 236] and not causing activation of the MAPK pathway. To confirm whether PTH does act on the PKA pathway Fig 5.7 shows SaOS-2 cells treated with KT-5752, a PKA inhibitor, and PTH to see if KT-5752 inhibited PTH. It showed that KT-5752 did inhibit PTH induced *c-fos* thus providing more evidence that PTH does act on the PKA pathway. Fig 5.8 shows an experiment were Sp-cAMP, which is a cAMP analogue, was used to provide more evidence that BL-1249 acts on the PKA pathway. It also suggests BL-1249 acts downstream of cAMP, i.e. it is not an adenylate cyclase inhibitor. Fig 5.9 showed attempts to determine if BL-1249 had any effect on the phosphorylation of CREB. Although open to interpretation, BL-1249 did not affect the levels of phosphorylation between non-treated and treated samples, suggesting BL-1249's effect may in fact be downstream of this.

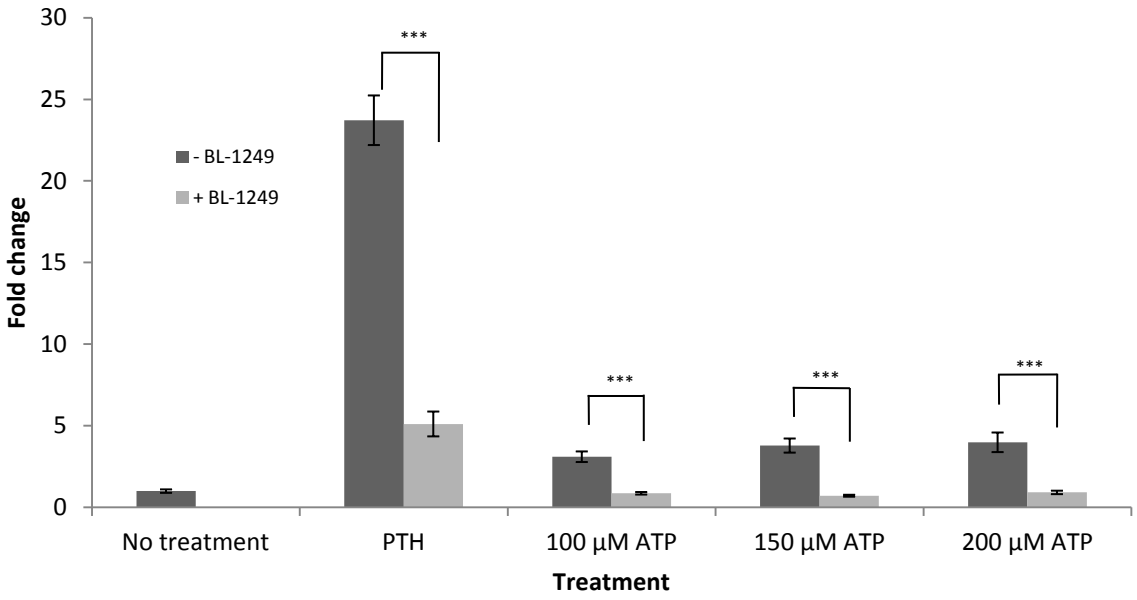

Figure 5.5. The effect of ATP and PTH treatment with BL-1249 on *c-fos* transcription in SaOS-2 reporter cells. The data are represented as fold changes compared to no treatment. Cells were treated with 1 nM PTH or 100 to 200 µM ATP with 10 µM BL-1249. n=6. Error bars represent S.E.

Figure 5.5 shows that PTH treatment caused a 23.7 fold increase (+/- 2.2 S.E.) in *c-fos* over basal levels. When PTH and BL-1249 were added together this caused a massive inhibition of the PTH induced *c-fos* signal, with levels reduced to only 5 fold over basal levels (+/- 0.7 S.E.), this inhibition was significant ($p<0.001$). The majority of experiments in the thesis use ATP at a concentration of 10 µM, and this causes a very small, usually insignificant increase in *c-fos* expression, however these larger ATP concentrations did cause an increase in *c-fos* over basal levels. A 3.1 (+/- 0.2 S.E.), 3.7 (+/- 0.7 S.E) and 3.9 (+/- 1 S.E.) fold increase was observed respectively. When the cells were treated with both ATP and BL-1249 this again caused a decrease in *c-fos* expression, in fact *c-fos* levels were measured below basal levels at 0.8 (+/- 0.01 S.E.), 0.7 (+/- 0.01) and 0.9 (+/- 0.02) respectively. In all cases this decrease was significant ($p>0.001$).

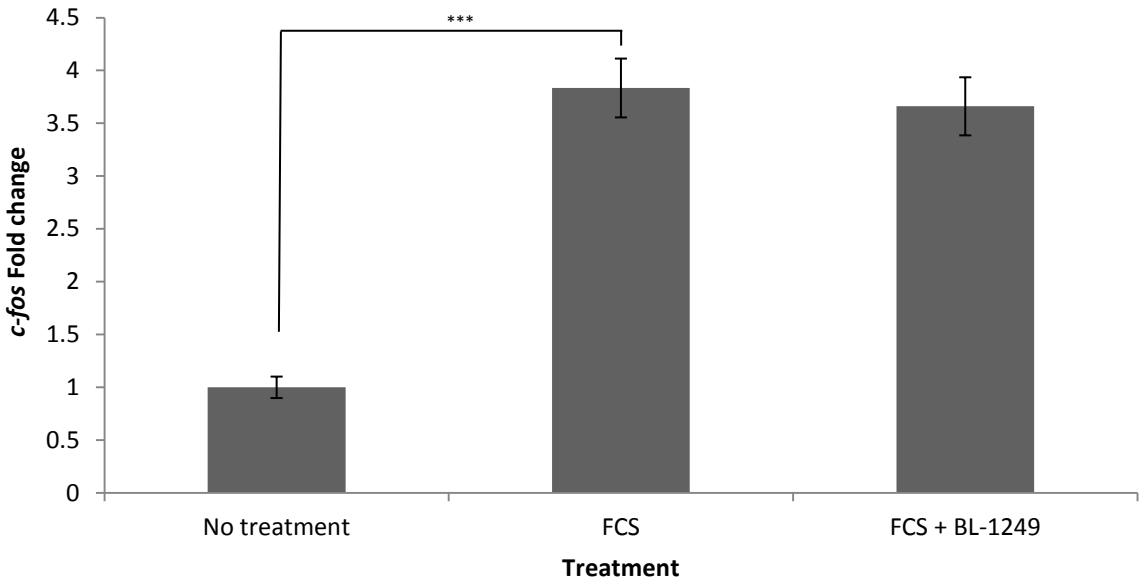

Figure 5.6. The effect of FCS treatment with BL-1249 on *c-fos* transcription in SaOS-2 reporter cells. The data are represented as fold change compared to no treatment. 5% FCS medium was added to cells, then either treated with 10 µM BL-1249 or left alone. n=12. Error bars represent S.E.

The results in Fig 5.6 show that adding 5% FCS medium and leaving for 4 hours causes a 3.8 fold increase (+/- 0.45 S.E.) in *c-fos* transcription over basal levels which was significant ($p<0.001$). Treating FCS medium with 10 µM BL-1249 caused no inhibition of the *c-fos* signal as this also had a 3.6 fold increase (+/- 0.4 S.E.) over basal levels. There was no significant difference between FCS and FCS+BL-1249.

A

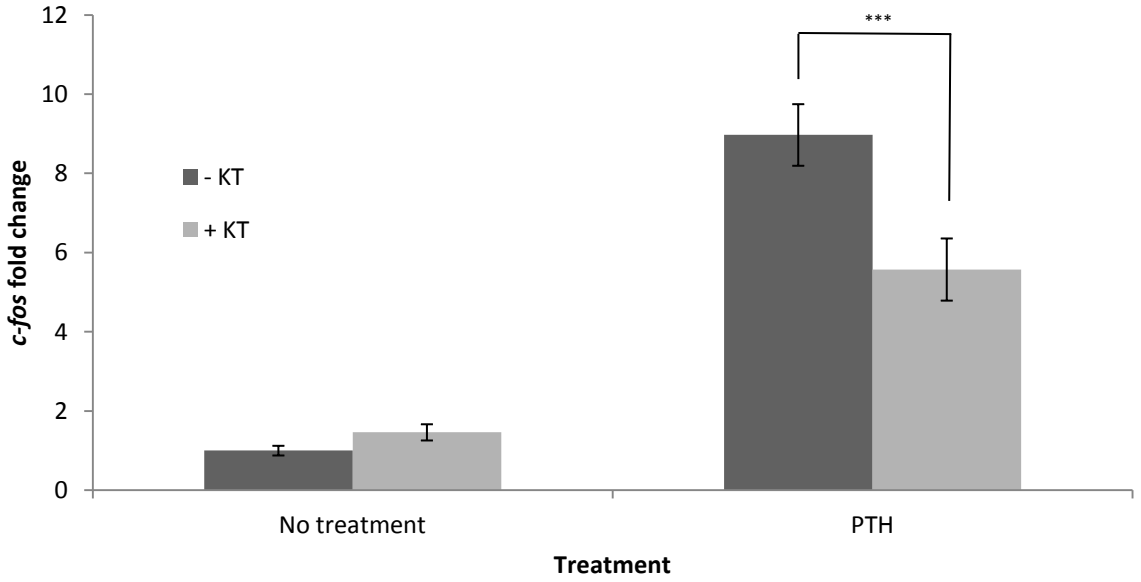

B

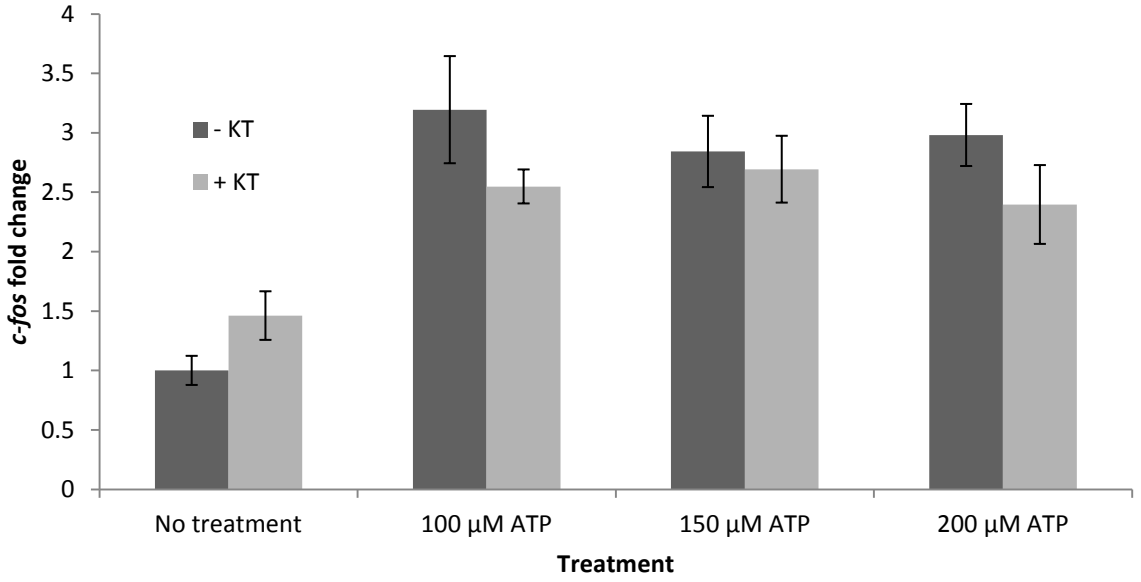

Figure 5.7. The effects of A) PTH and B) ATP treatment with KT-5752 on *c-fos* transcription in SaOS-2 reporter cells. The data are represented as fold changes compared to basal levels (no treatment, -KT-5752). + KT-5752 cells were pre-treated with 5 µM of KT-5752 1 hour before either adding 1 nM PTH (A), 100-200 µM ATP (B) or adding nothing (A and B). n=6. Error bars represent S.E.

These results (Fig 5.7) show a 9 fold increase (+/- 0.9 S.E.) in *c-fos* expression with PTH treatment. However when treated with the PKA-inhibitor KT-5752 there was a significant ($p<0.001$) reduction in the *c-fos* expression, as that only had a 5 fold increase (+/- 0.9 S.E.) over basal levels. An increase was measured in basal *c-fos* levels after KT-5752 treatment, but this was not significant. Fig 5.7 (B) shows a similar experiment but this time with ATP. 100 μM of ATP gave the highest expression of *c-fos* with an increase of 3.2 fold over basal levels (+/- 0.5 S.E.), 150 and 200 μM were of similar value. A very small decrease was measured in all ATP treatments that had KT-5752 pre-treatment. However these decreases were not significant.

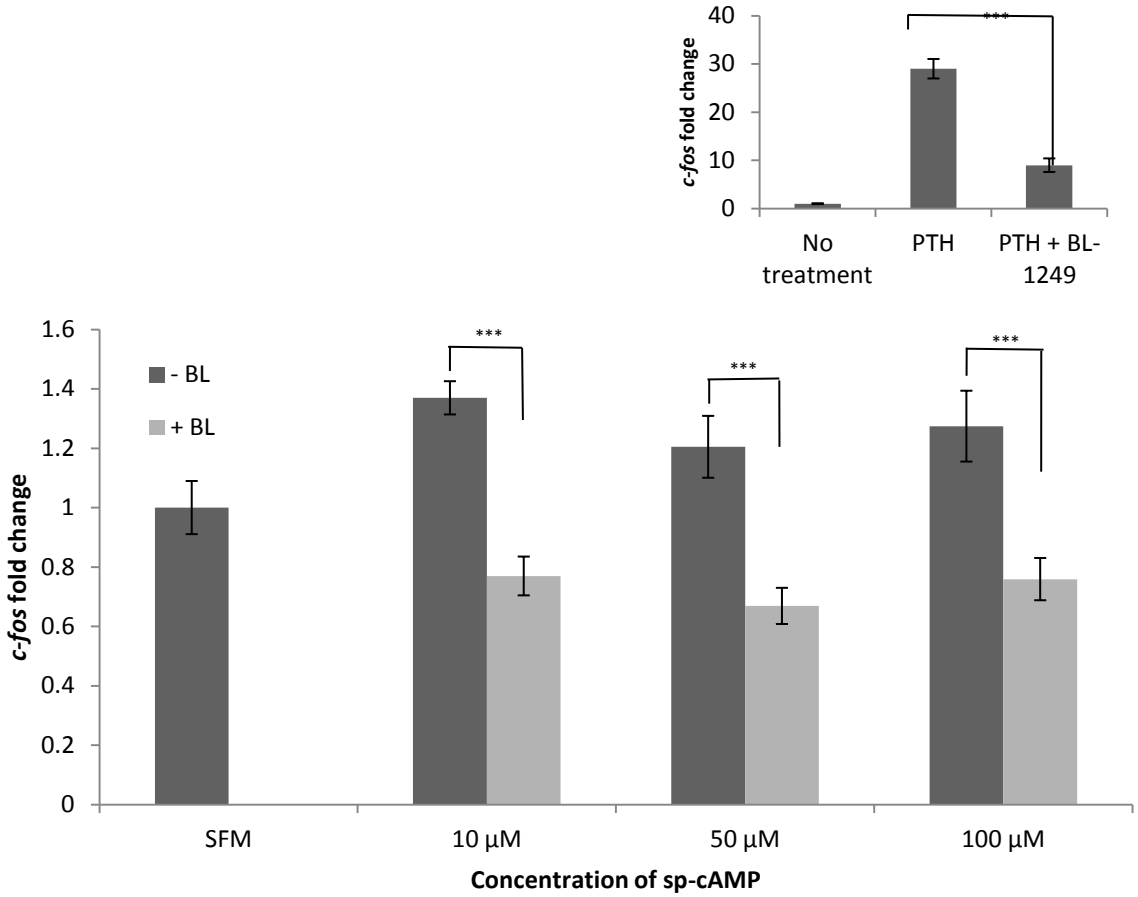

Figure 5.8. The effects of sp-cAMP treatment with BL-1249 on *c-fos* transcription in SaOS-2 reporter cells. The data are represented as fold changes in *c-fos* compared to no treatment. Inlaid graph shows cells were treated with PTH (1 nM) or PTH+BL-1249 (10 µM). Main graph shows concentration of sp-cAMP ranged from 10 to 100 µM and either treated alone or with BL-1249. n=6. Error bars represent S.E.

The inlaid graph in Fig 5.8 is the positive control test that was used for the main graph. It confirms that BL-1249 is still causing its inhibitory effect, as it is significantly lower than PTH alone, with only a 10 fold increase on no treatment. The main graph shows a significant increase in all treatments of the cAMP analogue sp-cAMP compared to no treatment. With 10 µM sp-cAMP showing a 1.37 (+/- 0.06 S.E.) fold increase, 50 µM sp-cAMP showing a 1.2 fold (+/- 0.1 S.E.) increase and 100 µM sp-cAMP showing a 1.27 fold increase (+/- 1.2 S.E.). When treated alongside BL-1249 they all show a massive decrease in the *c-fos* signal that is produced. 10 µM is 0.7 fold (+/- 0.08 S.E.) compared to no

treatment, 50 μM is 0.67 fold (+/- 0.08 S.E.) and 100 μM is 0.7 fold (+/- 0.08 S.E.) compared to no treatment. These are all significantly different to their none BL-1249 treated counterparts ($p<0.001$).

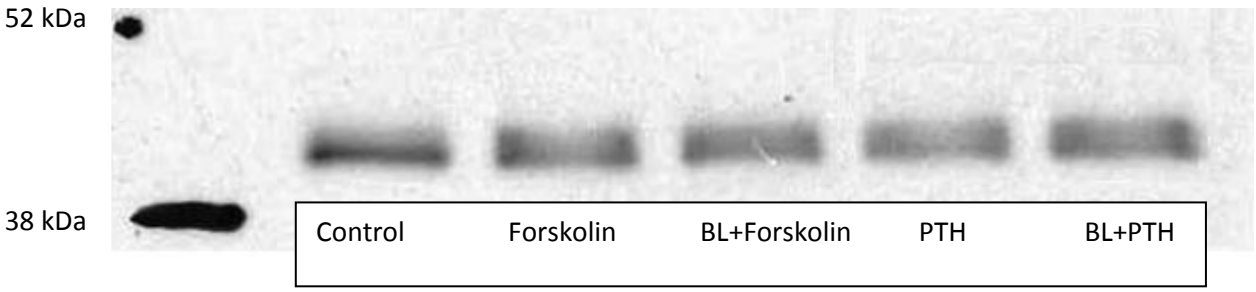

Figure 5.9 Western blot of phosphorylated CREB.

The western blot in Fig 5.9 is inconclusive due to the fact that the negative control group, which had no treatments added to it, appeared to have high levels of phosphorylated CREB. However it could be argued that each sample has two bars, and that the antibody doesn't distinguish between phosphorylated and unphosphorylated CREB. If that is the case then the lower bar for the control (the presumed non phospophylated CREB, has a molecular weight of 43 kDa) is darker than the rest and has a lighter upper bar (the phosphophylated CREB). If it is taken that the upper bar is phospho CREB ,which is in the correct position at 46.5 kDa, then there appears to be very little difference in the amount of phosphorylated CREB between PTH and PTH+BL-1249.

5.3.4 BL-1249 is toxic to osteosarcoma cells at 100 µM but not the primary osteoblast cell line MA16.

Fig 5.10 shows BL-1249 is toxic to cells at a 100 µM for 48 hours of treatment. The same is true for Te-85 and MG-63 cells shown in Fig 5.11, and 5.12 respectively. Photomicrographs, shown in Fig 5.12 C) were taken of the MG-63 cells showing the decreased number of cells in the 100 µM group compared to the other two. The decrease in cell number was not limited to osteosarcoma cells, in Fig 5.13 it was also shown in the breast cancer cell line T47D. However in the primary osteoblasts MA16 (taken from proximal tibia) BL-1249 did not cause a decrease in *c-fos* signalling. Suggesting that in fact BL-1249, acting through either its effect on *c-fos* expression, or its effect on K^+ channels can target its cytotoxicity effects to cancer like cells.

A

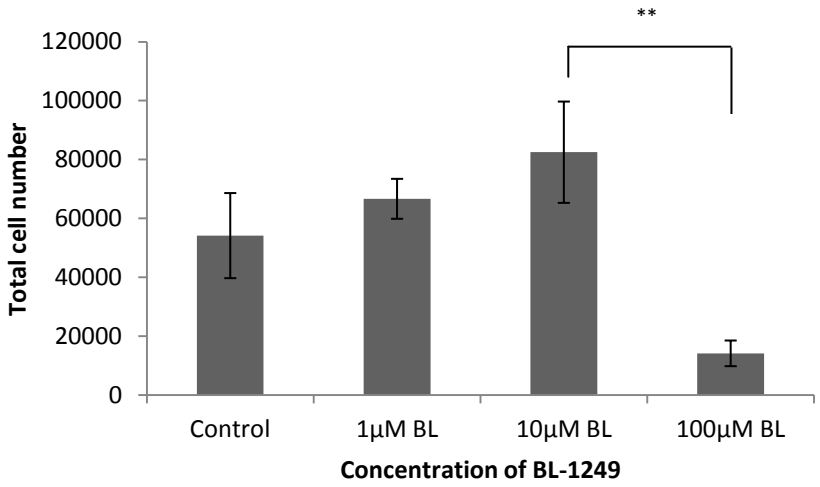

B

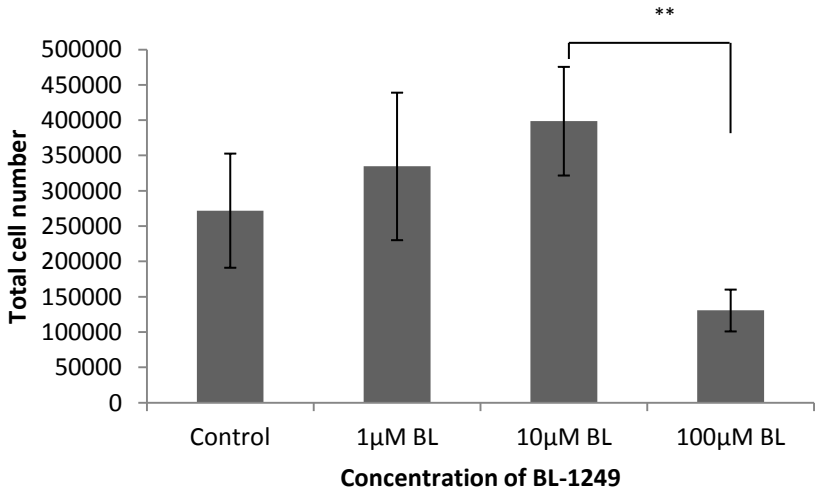

Figure 5.10. The effect of 48 hours of BL-1249 treatment on SaOS-2 cell number. A) Cells were seeded at a density of 40,000 cells. B) cells were seeded at a density of 250,000 cells. Both experiments were left overnight before BL-1249 was added. n = 4. Error bars = S.E.

The graphs in Fig 5.10 show that treating SaOS-2 cells with 1 µM or 10 µM of BL-1249 for 48 hours has no significant effect on the amount of cells present within the well. However, SaOS-2 cells treated with 100 µM of BL-1249 had a huge decrease in cell number, with Fig 5.10 A) showing an 80% reduction and Fig 5.10 B) showing a 70% reduction compared to 10 µM BL-1249. This was due to cytotoxicity as cell numbers were below the amount of cells that were seeded. In both experiments the reduction was significant ($p<0.001$).

A

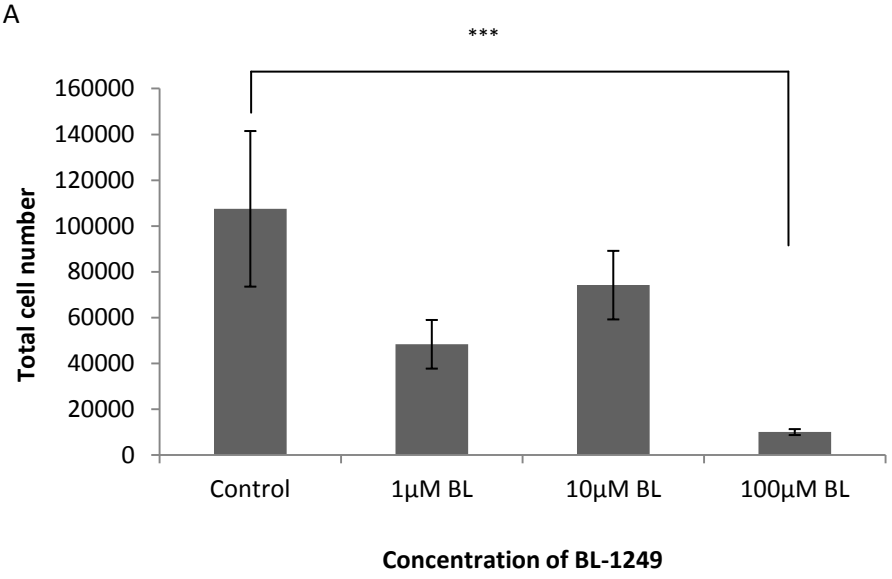

B

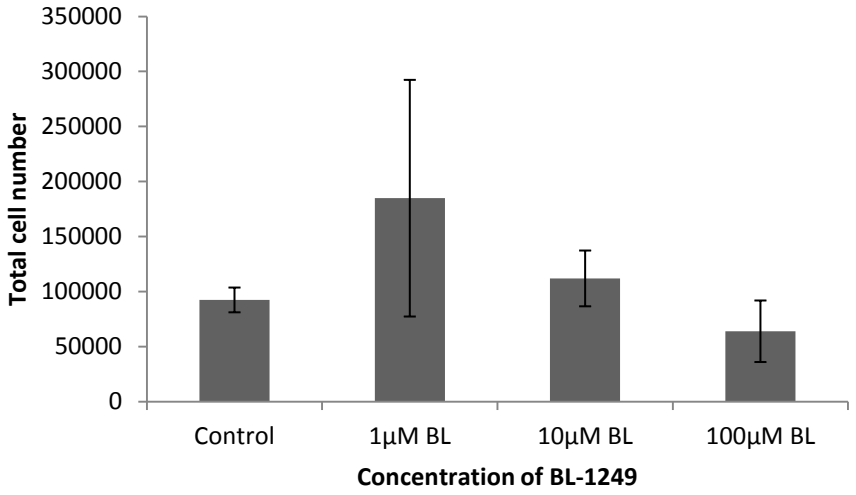

Figure 5.11. The effect of 48 hours of BL-1249 treatment on Te-85 cell number. A) cells were seeded at a density of 40,000 cells. B) cells were seeded at a density of 250,000 cells. Both experiments were left overnight before treatment started. n = 4. Error bars = S.E.

Fig 5.11 Both A) and B) show a decrease in Te-85 cell numbers when treated for 48 hours with 100 µM BL-1249. This was significant in A) but not in B), although perhaps a larger sample size will cause it to be significant. This again suggests that this concentration of BL-1249 for 48 hours kills the cell.

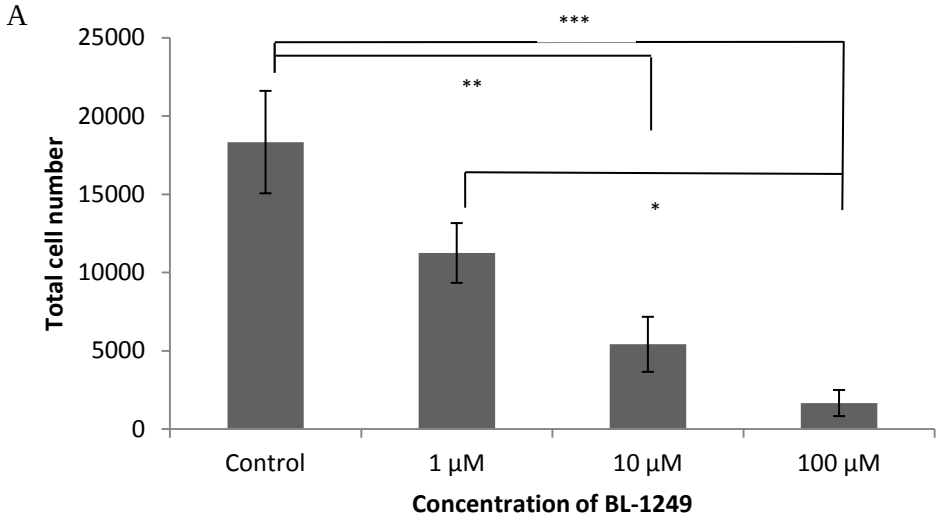

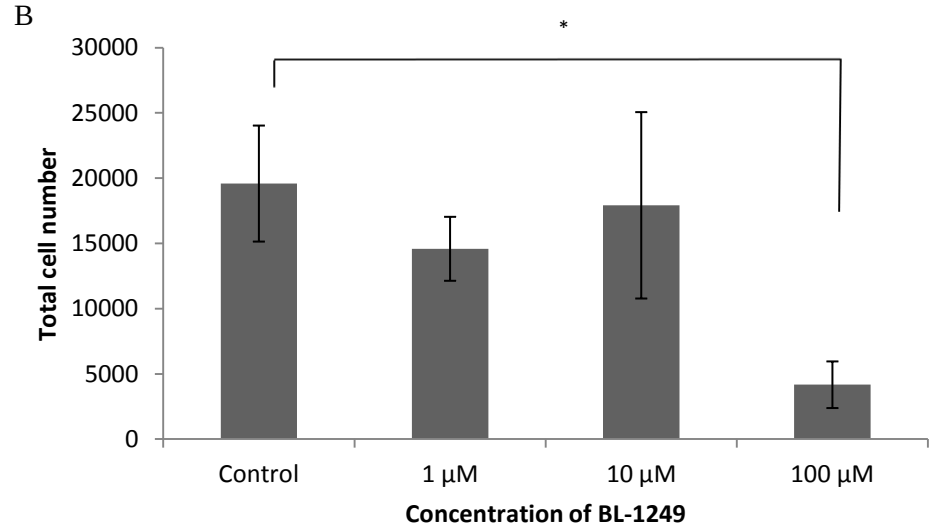

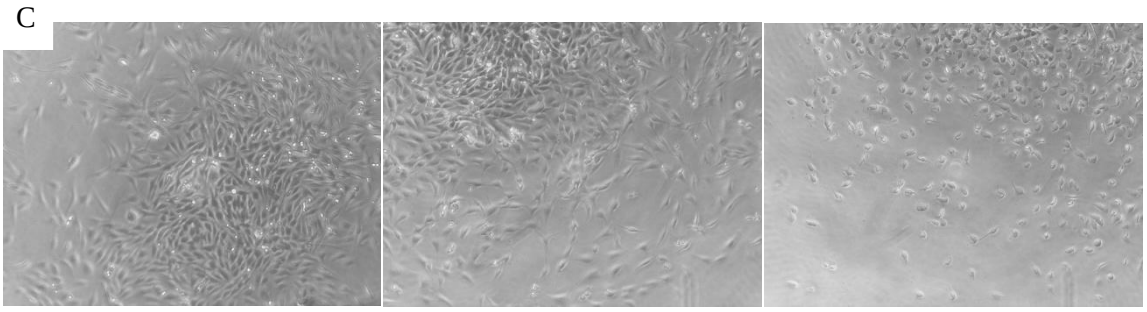

1µM BL-1249 10µM BL-1249 100µM BL-1249

Figure 5.12. The effect of 48 hours of BL-1249 treatment on MG-63 cell number. A) Cells were seeded at a density of 10,000 cells. B) Cells were seeded at a density of 15,000. Both experiments were left overnight before treatment started. n = 4. Error bars = S.E. C) Photomicrographs of MG-63 cells taken after 48 hours treatment of treatment.

Fig 5.12 A) shows a decrease of MG-63 cell number when cells were treated with 10 µM BL-1249 for 48 hours compared to when treated with 1 µM BL -1249 for 48 hours, with counts of 5400 (+/- 1700 cells S.E.) and 18000 (+/- 8000 cells S.E.) respectively. There is then a further decrease in the amount of MG-63 cells present when treated with 100 µM BL-1249 for 48 hours, having a count of 2000 cells (+/- 1000 cells S.E.). Both of these decreases were significant. Fig 5.12 B) shows no significant difference between 1 µM and 10 µM treatments, although once again when treated with 100 µM BL-1249 for 48 hours the cell number decreased massively to 5000 cells (+/- 2000 cells S.E.). This decrease was again significant and due to cytotoxicity.

Fig 5.12 C) Shows photomicrographs taken from the cells after their 48 hour treatments of BL-1249. The 1 µM and 10 µM treatments contain similar cell numbers. However it is apparent that in the 10 µM treatment the cells look different. They are smaller in size due to the fact that they have smaller processes. The 100 µM treatment cells look markedly different, as well as having a decreased amount of cells the morphology has changed dramatically as they appear to have lost their processes and now appear almost spherical.

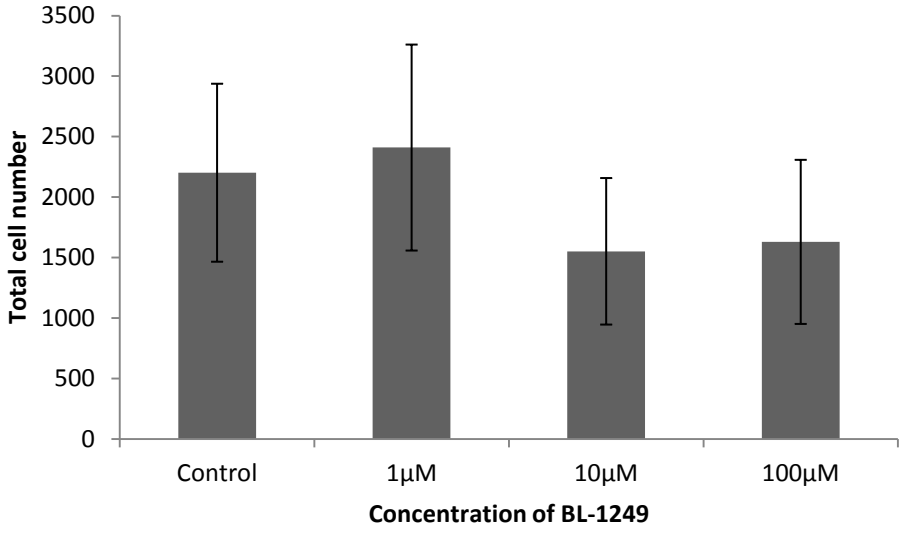

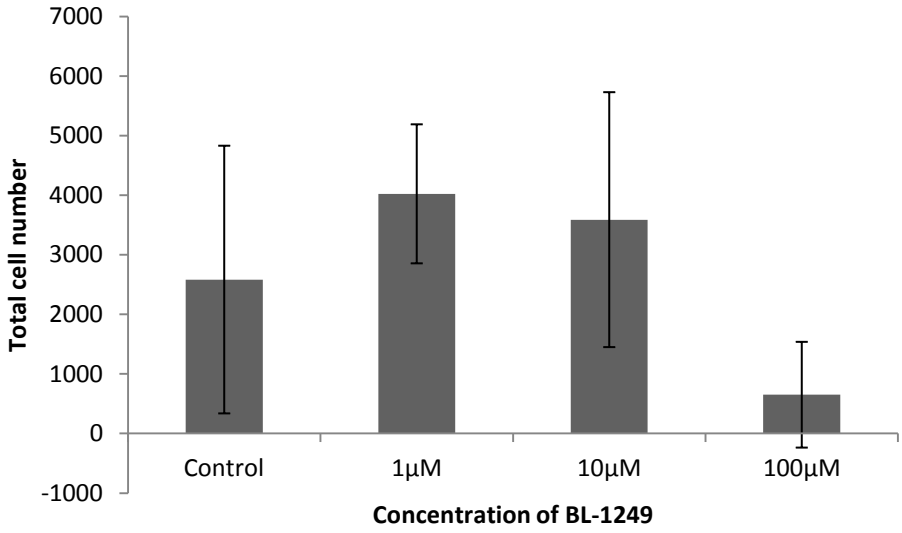

Figure 5.13. The effect of 48 hours of BL-1249 treatment on T47D cell number. Both experiments were seeded at 2000 total cells. Left to settle overnight before the treatment started. n=4. Error bars = S.D**.**

Fig 5.13 A) shows that between the non treated control and 1 µM BL-1249 there was no difference between the total cell number of these T47D breast cancer cells. However between the control and 10 µM BL-1249 and the control and 100µM BL-1249 there was a significant decrease in the amount of cells that were present. Fig 5.13 B) has no significance between the control and other treatments, due to the large standard deviation seen in the control. Both 1 µM and 10 µM were not decreased in

respect to the control, in fact a slight increase was observed and 100 µM, like A), showed a decrease in cell number compared to the control.

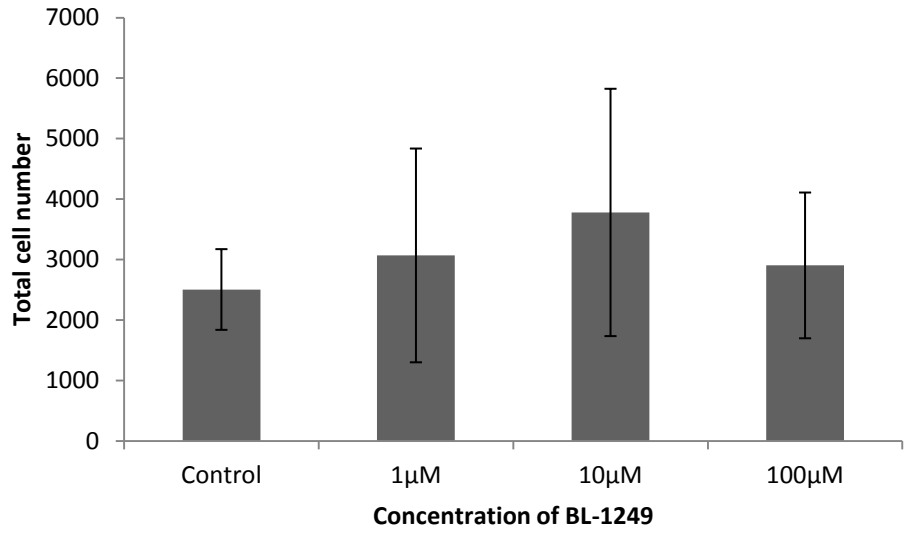

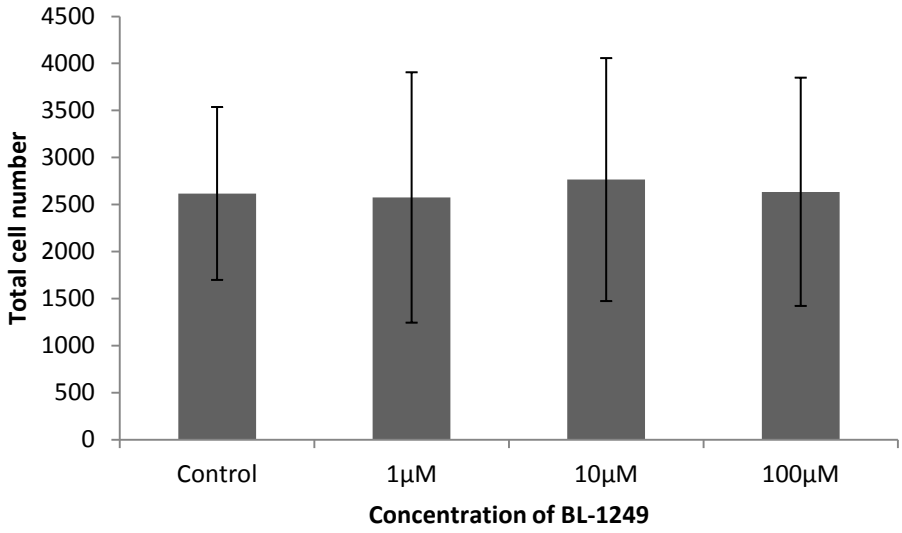

Figure 5.14. The effect of 48 hours of BL-1249 treatment on MA-16 cell number. Both experiments were seeded at 2000 cells. n= 4.Error bars = S.D.

These cell counts were performed on primary cells named MA16. They were taken from a knee joint at the proximal end of the tibia. Fig 5.14 (A) shows no significant difference between the non treated control and the BL-1249 treated wells. There was a slight increase with 1 µM and 10 µM but it is unlikely to be a real effect, just natural variation. Similar results were seen in Fig 5.14 (B) as no difference in the cell numbers between the control and 1 µM, 10 µM or 100 µM of BL-1249 was observed.

5.3.5 BL-1249 toxic effect is, in part, due to stimulation of K^+ channels.

Next, as with the inhibition of *c-fos*, tests were carried out to determine if the difference in cell number was due to BL-1249s reported effect on K^+ channels. It is known that K^+ channel activation can cause cell apoptosis [162, 237, 238]. Therefore using TEA, a K^+ channel inhibitor, investigation were made to determine if the cell number would decrease when treated with 100 µM BL-1249. Fig 5.15 shows an increased cell number with TEA, suggesting that activation of K+ channels may play a role in BL-1249s effect on cell number.

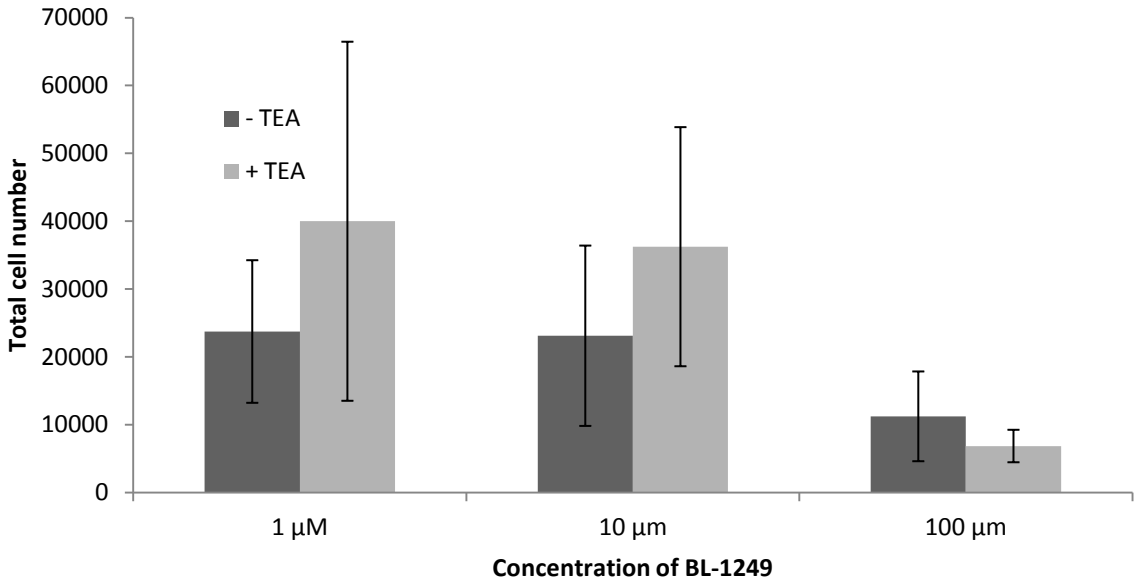

Figure 5.15. The effect of BL-1249 and TEA treatment on SaOS-2 cell number. Cells were seeded at a density of 20000 and left overnight. 2 mM of TEA was used. n=4. Error bars = S.E.

This graph (Fig 5.15) shows no significant change in any of the variables measured, however there are perhaps suggestions that with a higher n number both 1µM and 10µM of TEA with BL-1249 may increase cell number than with BL-1249 alone.

5.3.6 BL-1249 effects on cell morphology

Finally experiments looked more closely at the cell morphology change seen with normal (i.e. 10 μM) concentrations of BL-1249 after 4 hours. Firstly sub confluent cells were treated with BL-1249 to see if the effect could be seen more clearly (Fig 5.16), and finally the BL-1249 was taken off after 4 hours to determine if the effect was reversible (Fig 5.17).

A

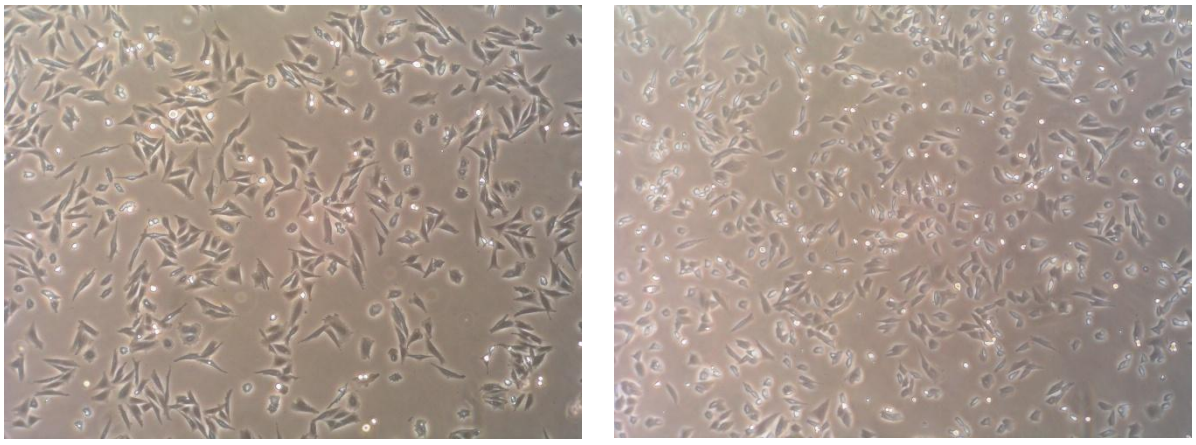

Before BL

After BL

B

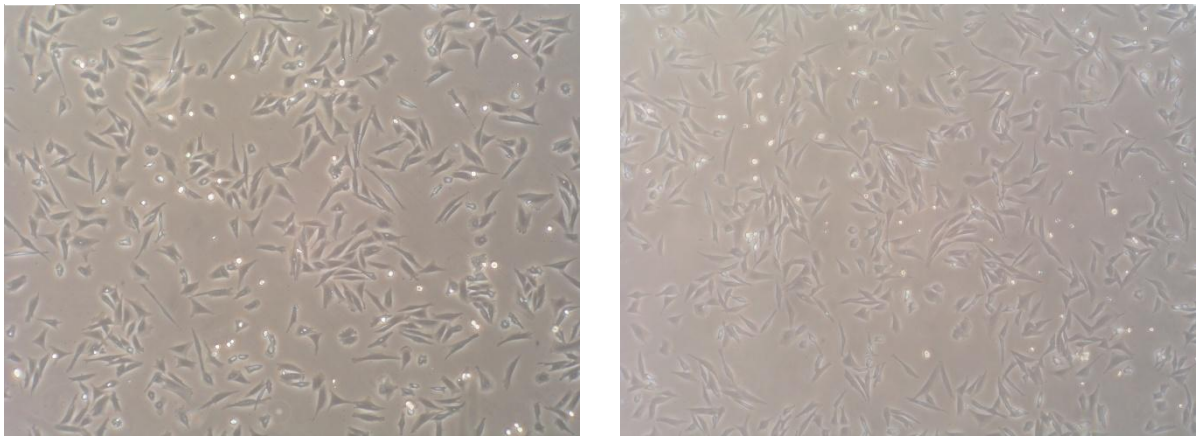

Before

After 4 hours no treatment

Figure 5.16. Photomicrographs of SaOS-2 cells treated with BL-1249 for 4 hours. A) Photomicrographs showing subconfluent SaOS-2 cells treated with 10 µM of BL-1249 for 4 hours. B) shows cells not treated with BL-1249 taken at the same time points as A).

These photomicrographs (Fig 5.16) show that treating SaOS-2 cells with 10 µM BL-1249 for 4 hours changes the shape of the cell dramatically. Before treatment SaOS-2 cells have long thin processes, however, after treatment these processes have disappeared and the cells appear much more spherical. This is not the case in the time matched experiment where BL-1249 was not added where the cells after 4 hours look very similar to the ones before (Fig 5.16 B)).

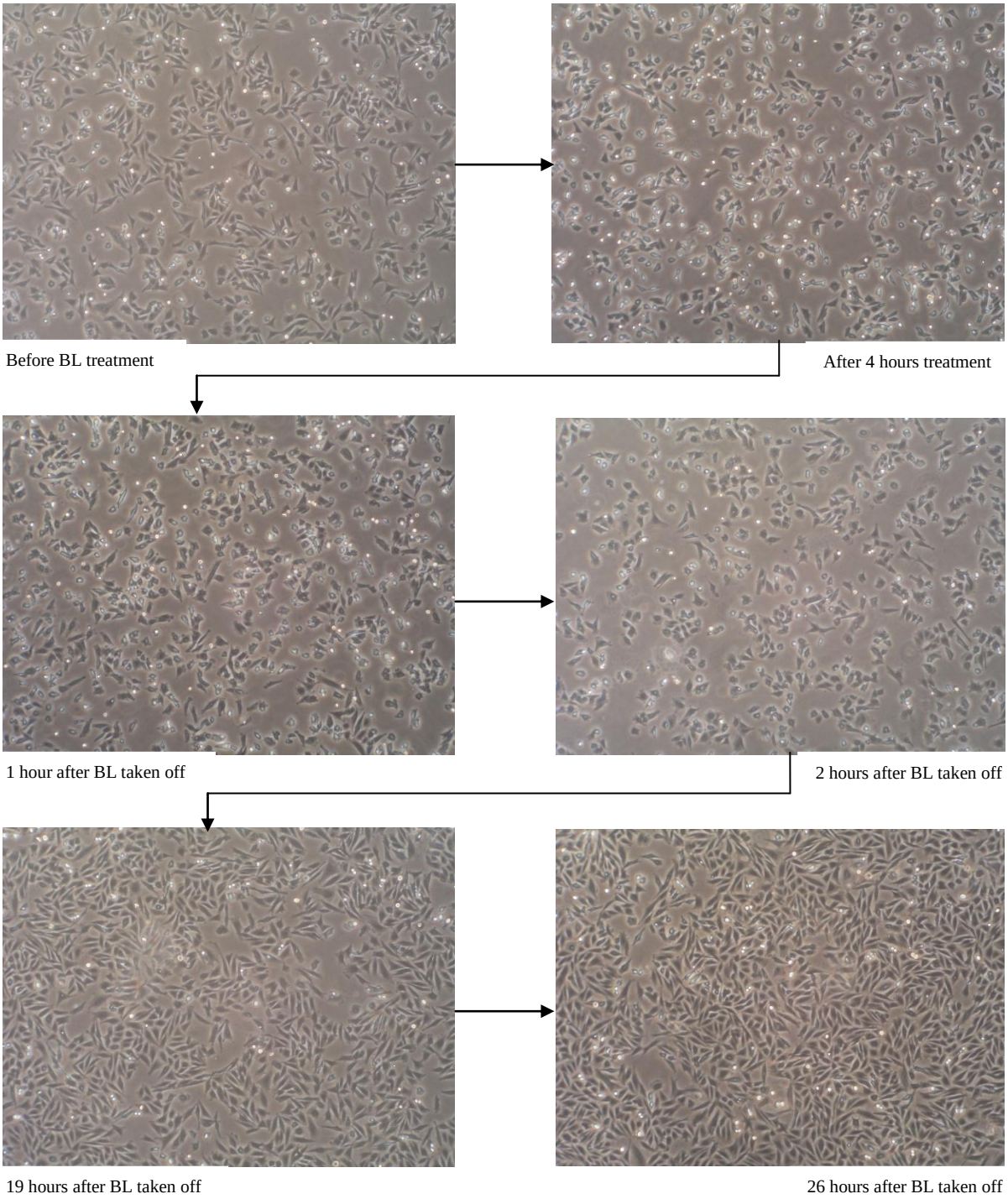

Figure 5.17 Photomicrographs of SaOS-2 cells treated with 10 µM BL-1249 for 4 hours. Photomicrographs were taken before treatment, at 4 hours after treatment, then the medium, including the BL-1249, was removed and replaced with new medium, Photomicrographs were then taken 1, 2, 19 and 26 hours after the medium was replaced.

These photographs (Fig 5.17) are one example of a set of 6 wells that all show similar results. Once again treatment of SaOS-2 cells with BL-1249 caused a change in the shape of the cell, with them

having less well defined and smaller processes after 4 hours treatment. However this effect could be reversed. There was no noticable recovery in the shape of the cells after 1 or 2 hours of 10 μM BL-1249 being taken off. However, after 19 and 26 hours the cells appear to be fully recovered, as they have regained thier processes and are proliferating well.

5.4 Discussion

Intial experiments looked at the effect BL-1249 had on *c-fos* expression. Fig 5.1 shows the preliminary discovery that BL-1249 inhibited ATP+PTH induced *c-fos* expression. BL-1249 could be decreasing *c-fos* expression by killing the cells, thus a 6 well plate was seeded at 150000 cells and left overnight to become confluent. The next day half the cells were treated with BL-1249 and counted. As the results show a very similar number of cells it is unlikely that cells are dying as a result of exposure to 10 µM BL-1249 for 4 hours. However given the fact that they have altered morphology and that with a higher concentration of BL-1249 there are fewer cells it seems likely that a reversable apoptotic effect has taken place either causing, or as a result of a decrease, of *c-fos* expression.

BL-1249 causes K^+ channels to open, whether this is through TREK-1 channels or BK_{ca} channels is still open for debate, but nevertheless BL-1249 causes K^+ currents to be observed [172]. Therefore BL-1249s effect on K^+ channels was examined to determine why *c-fos* expression was decreasing. To do this HEPES medium high in extracellular K^+ was used, thus when BL-1249 acted on K^+ channels, the K^+ would not leave, as it normally does, down its concentration gradient[229, 235]. Therefore the cell would not hyperpolarise. Thus if BL-1249s effect on *c-fos* was through K^+ channel opening, this experiment would inhibit the effect of BL-1249. As Fig 5.3 shows this was not the case, the high K^+ medium did not reverse the effects of BL-1249. A further experiment was carried out to look at K^+ channel involvement, which used the compound NS-1619. This is a well documented BK_{ca} channel opener [239, 240], thus if BL-1249 was exerting its effects via BK_{ca} channels NS-1619 would likely have the exact same effect. Fig 5.4 shows again that NS-1619 did not cause any inhibition of the *c-fos* signal. Taken together these two results strongly suggest that BL-1249 does not inhibit *c-fos* expression via opening of K^+ channels.

As BL-1249 was not exerting its inhibitory effect through K^+ channels, experiments were carried out to determine what pathway BL-1249 was acting on. As the molecular pathways that allow ATP and PTH to synergise are still under investigation ATP and PTH were looked at separately. Fig 5.5 shows that PTH increased *c-fos* expression, but when treated with BL-1249 its effects on *c-fos* were

inhibited. To confuse matters the same happened with ATP, all concentrations of ATP showed an increase in *c-fos* signalling over basal levels, but when treated with BL-1249 at the same time the effect was inhibited. Next the effects of BL-1249 on serum induced *c-fos* expression was looked at. Serum causes transcription of *c-fos* through the SRE region of the promotor. As Fig 5.6 shows cells treated with FCS had an increase in *c-fos* expression, and was not inhibited by BL-1249, suggesting that BL-1249 does not inhibit the MAPK pathway that acts on the serum responsive element of the *c-fos* promotor.

Knowing that BL-1249 could inhibit PTH, attention was turned to its pathway. The literature suggests that PTH acts on the PKA pathway to increase *c-fos* expression [142, 236], To confirm that PTH does activate PKA a test using KT-5752 was carried out. KT-5752 is a PKA inhibitor and thus should reduce *c-fos* expression when treated with PTH. Fig 5.7 shows that KT-5752 did decrease the *c-fos* signal when treated with PTH thus suggesting PTH does act through the PKA pathway. Interestingly the KT-5752 did not decrease the signal completely, this may be becuase KT-5752 is an ineffective PKA inhibitor or that PTH can act through other pathways simultaneously to transcribe *c-fos* [236].

Nevertheless it was decided to study BL-1249 and its effects on the PKA pathway. Firstly by using sp-cAMP (Fig 5.8) which is a cAMP analogue. The results show that sp-cAMP, as expected, caused an increase in *c-fos* expression, interestingly when treated with BL-1249 the expression was inhibited. This suggests that BL-1249, at the very least, effects the PKA pathway and it also suggests that it doesn't effect adenylate cyclase as this is upstream of PKA. It has to, therefore, be either a PKA inhibitor or alternatively something downstream of PKA. To determine the amount of phosporylated CREB compared to non phosphorylated CREB after BL-1249 treatment a western blot was used (Fig 5.9). This experiment was inconclusive, mainly due to the fact that the negative control had a signal. However it could be argued that the antibody could not distinguish between phosphorylated and non phosphorylated CREB, and that infact there are two bands in every lane. If that is the case then the upper band is in the correct place (46.5 kDa) for the phosphorylated band , and the experiment suggests that BL-1249 does not affect the phosphorylation of CREB as there appears to be no difference between PTH and PTH+BL-1249. So, for example, it may prevent the translocation of

CREB to the nucleus by inhibiting the importins designed to get CREB into the nucleus [241]. Perhaps looking at the location of CREB under a confocal microscope would be a useful way to determine whether BL-1249 does effect the movement of it.

Fig 5.10 is a cell count for SaOS-2 cells and clearly shows that there is a massive drop in the amount of cells after 100 µM BL-1249 treatment. This concentration of BL-1249 was then tried on other osteosarcoma cell lines. Both Te-85 and MG-63 were killed at this concentration of BL-1249. Experiments were then carried out to look at the primary osteoblasts MA16. At 100µM BL-1249 caused no significantly different cell counts. Thus it appears that BL-1249, either through its effects on *c-fos* expression, or acting through K^+ channel opening, can selectively cause cell death of osteosarcoma cells and not primary cells. Treating the cells with the K^+ channel inhibitior, TEA, caused larger cell counts at the lower concentrations of BL-1249 (Fig 5.15). It has been proposed that activation of K^+ channels can cause apoptosis through reduced cell volume [242], and given the fact that TEA managed to increase cell number over normal levels it suggests that K^+ channels are important for SaOS-2 cell survival. However it is unlikely that this is solely responsible for the reduction in cell number. The fact that primary osteoblastic cells survived when treated with BL-1249 suggests that a reduction in *c-fos* acting with K^+ channels causes the massive cell number decrease seen with 100 µM BL-1249.

Finally experiments were undertaken to look more closely at the morphology change seen in cells treated with 10 µM BL-1249. This morphology change may be closely related to the cytotoxicity effect of BL-1249 as it has been documented in different cell types that activation of K^+ channels can cause cell shrinkage and apoptosis [237, 238]. This is mainly due to the fact that as K^+ leaves the cell it will draw the water with it. For this experiment cells were seeded at 40000 and left for a day. Thus when BL-1249 was added they were subconfluent, and their shape change more easily identifiable. Fig 5.16 shows clearly that BL-1249 treatment of SaOS-2 cells shifts their morphology from one of a cell with sharp, long processes to a more rounded cell type. It is also shown that this change is reversable as it can change back, suggesting that this shrinkage may be responsible for the switching on of apoptosis.

To conclude, BL-1249 inhibits the expression of basal and agonist-induced *c-fos* expression. It is unlikely that this is achieved through its known effects on K^+ channels, or through the pathway that leads to the SRE of the *c-fos* promoter. Early evidence points to BL-1249 acting on part of the PKA pathway shown through the use of sp-cAMP. In addition to its effect on *c-fos* expression it was noticed that BL-1249 also affected the shape of the cells. It is likely that this is the first stages of apoptosis as a higher concentration of BL-1249 caused cell death. Activation of K^+ channels can cause a decrease in cell volume and apoptosis, thus, given that TEA can increase cell survival it is likely that K^+ channels do influence this process. However this is likely in conjunction with a decrease in *c-fos* as it was noted that primary cells did not die when subjected to the same concentrations of BL-1249.

6. P2 expression and bone morphology of SOD1-/- mice

6.1 Introduction

The work carried out in this thesis so far has examined the role of P2 receptors in normal physiology. However, occasionally, the role of genes only becomes apparent in situations of environmental stress or pathologies etc, therefore it was appropriate to investigate P2 expression in a diseased state. For this purpose, due to the link between SOD mutations, ATP signalling and an altered bone phenotype it was decided to examine P2 signalling in SOD1-/- mice.

SOD1 is an enzyme responsible for the dismutation of superoxide ions. These superoxide ions cause oxidative damage within a cell and therefore SOD1 is thought to be one of the mechanisms responsible for protecting against oxidative damage. One of the theories of why we age is that over time the accumulation of this oxidation damage causes disease. Numerous age related diseases have been implicated in free radical accumulation such as diabetes [175], Alzheimer's disease [176], atherosclerosis [177], and arthritis [178]. Interestingly, mutations in the SOD1 enzyme have been linked to P2 signalling as it has been proposed that astrocytes are more sensitive to the neurotoxic action of ATP, through P2X7, when they have SOD1 mutations, and it is this that may contribute to ALS [186].

SOD1-/- mice have previously had their phenotype examined and, overall, show age related disorders early on in life. The muscle phenotype shows that at 3-4 months they are 20% smaller than their WT counterparts. By 20 months the hind limb muscles were measured to be 50% less than normal, with a 40% observed reduction in the use of their exercise wheel. The older SOD1-/- mice also had tremors and were unable to walk properly [181]. The bone phenotype has briefly been examined and showed a shortening of the femur, a decreased BMD and a decreased bone stiffness [183].

To examine the relationship between SOD1 and P2 signalling SOD1 -/- mice were obtained and their hindlimbs were examined in a μCT scanner to better understand the phenotype of these bones. Also

the calvarial cells were cultured and tested for normal osteoblast bone markers as well as investigating changes in P2 receptor type.

6.2 Methods

6.2.1 Calvarial cell cultures

The calvarium of each mouse was cut into small sections and placed in DMEM. Cells would then migrate out of these bone chips to attach to the Petri dish. When these cells were confluent the bone chips were placed in another Petri dish and dissected into smaller pieces to allow more cells to migrate out of them. The cells were either frozen down in liquid nitrogen or had tri-reagent added to lyse them for mRNA extraction.

6.2.2 P2 expression in SOD1-/- calvarial cells

The expression of P2Y1, P2Y2, P2X7 and P2X4 in the mouse calvarial cells was examined. P2Y1, P2Y2 and P2X7 were chosen due to the fact they are expressed in mouse osteoblasts and are known to play a part in the bone response to ATP [243], furthermore the P2X7 receptor is highly implicated in ALS in humans. P2X4 was also tested as this is the most highly expressed P2 receptor in mouse osteoblasts and therefore warranted further investigation [243]. The details of the mRNA extraction, cDNA generation and PCR reaction can be found in Materials and Methods section 2.4 and 2.5.

6.2.3 µCT analysis of mouse hindlimbs

The proximal tibia and fibula of 4 SOD1 -/- mice and 4 age-matched WT mice where scanned as laid out in the Materials and Methods. The analysis of the scan was carried out using the Skyscan Nrecon software. Firstly the cortical bone width was measured by using the proximal growth plate as a landmark, the slice 1mm distal to this was measured and every subsequent 10 slices distal to this until 5 slices had been measured. Each slice had the cortical width measured in 3 areas (see Fig 6.1 (A)), these were averaged and the 2 sets compared to each other. For the trabecular analysis the area that was measured had to be standardised between bones. To do this a region of interest (ROI) had to be set using the Skyscan analysis software. Again, the proximal end of the growth plate was taken as marker from which all measurements could be taken. The 15 slices above the growth plate on all bones were taken and the ROI was drawn around the inside of the cortical bone (see Fig 6.1 (B)). This could then be analysed for the trabecular bone parameters outlined in the results.

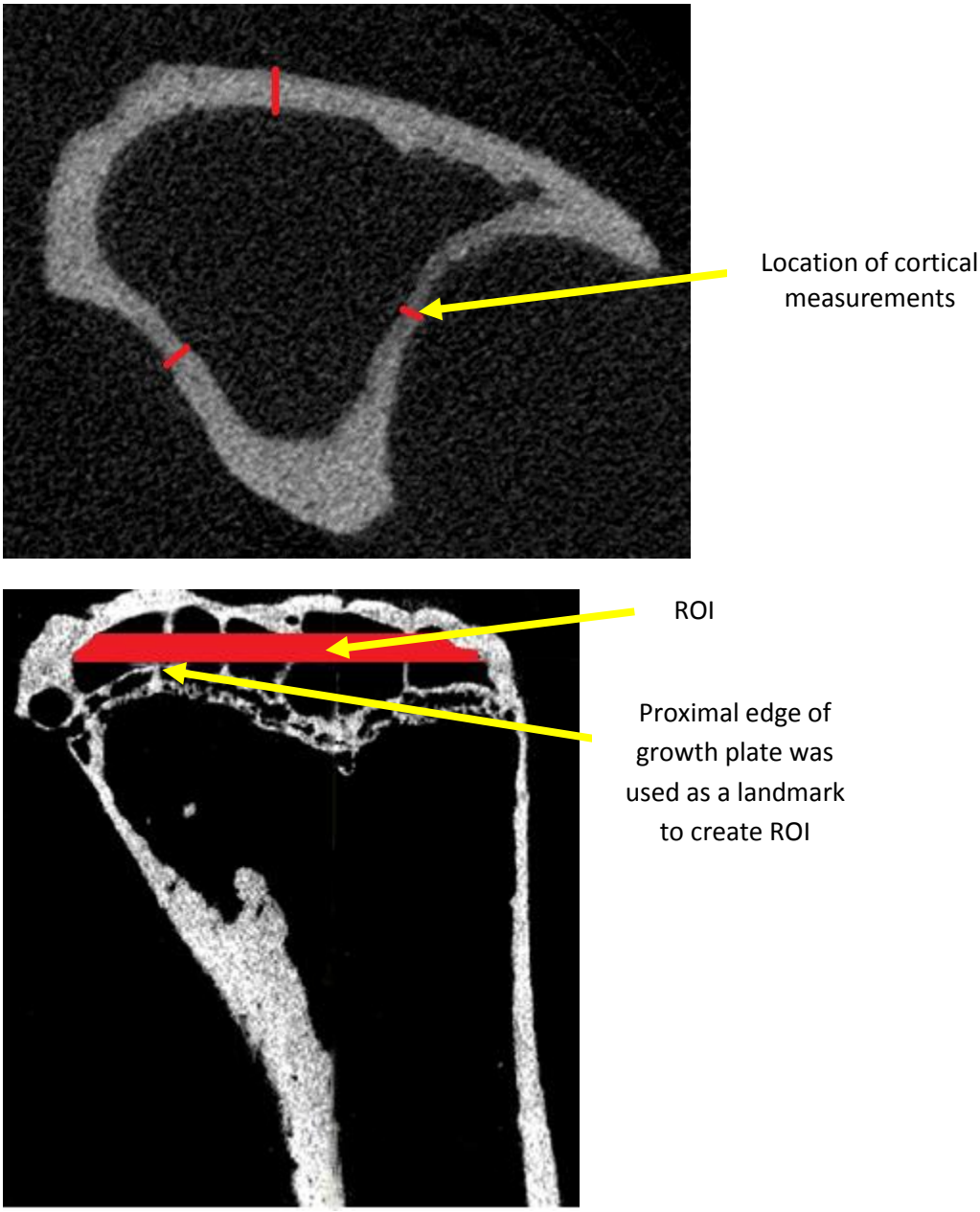

Fig 6.1 A) An example of the location of the cortical width measurements in WT and SOD 1 -/- mice. The areas measured are marked in red. **B) The location of the ROI in the WT and SOD1 -/- bones.**

6.2.4 Details of mice used

Name	Phenotype	Sex	Age (months)
SOD 1	SOD1 -/-	F	17.9
SOD 2	SOD1 -/-	F	18.4
SOD 3	SOD1 -/-	F	18.6
SOD 4	SOD1 -/-	F	18.9
WT 1	SOD1 +/+	F	18.2
WT 3	SOD1 +/+	M	20.5
WT 5	SOD1 +/+	F	20.8
WT 7	SOD1 +/+	M	20.8

Table 6.1 The phenotype, sex and age of mice analysed

To summarise:- there are 4 SOD1-/- that are all female with ages that range between 17.9 and 18.9 months. There are 4 WT mice that are age matched (ranging from 18.2 to 20). Of these there are 2 are male and 2 are female

6.3 Results

6.3.1 Comparison of P2 receptor expression between SOD1-/- and WT calvarial cells

The relative levels of P2 receptor expression between WT and SOD1-/- was examined to determine if there was any difference between the two. Fig 6.2 (A) shows a decrease in P2Y1 receptor expression, but this was not significant. Fig 6.2 (B) shows that SOD1-/- mice had an increase in P2Y2 receptor expression by more than 50%. Fig 6.2 (C) and (D) both show a decrease of P2X7 and P2X4 respectively in the SOD1-/- mice. The melt curves for these PCR reactions can be found inlaid in each graph, they confirm that the correct products were being amplified.

A

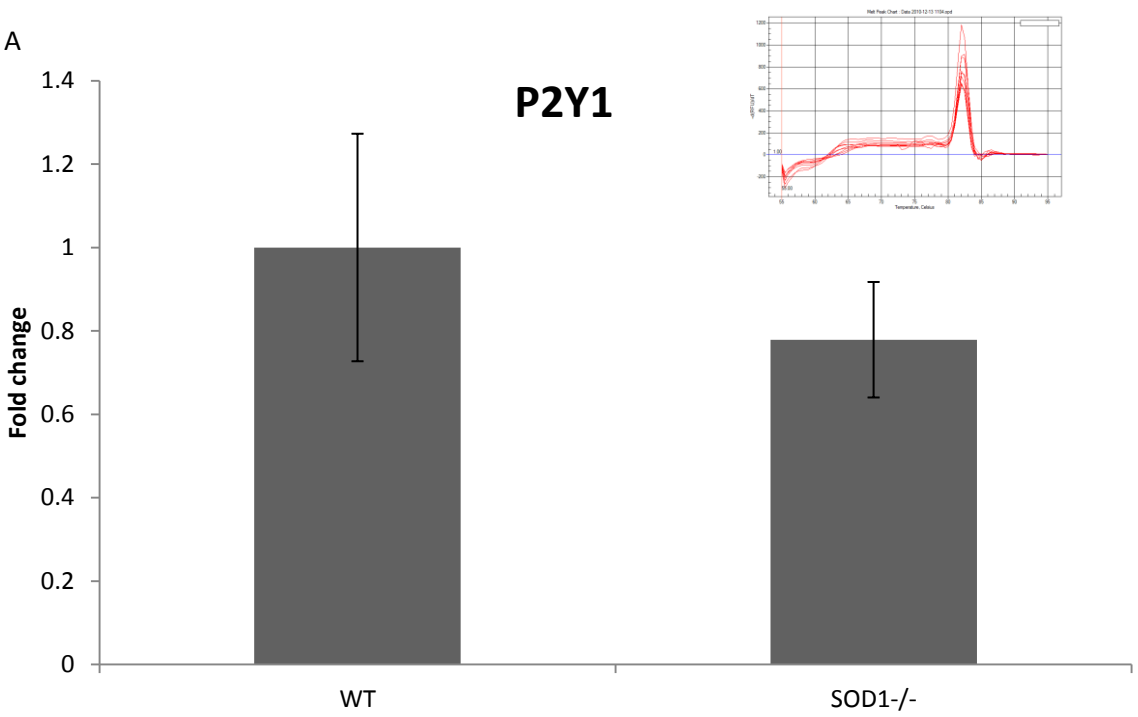
P2Y1
Fold change
1.4
1.2
1
0.8
0.6
0.4
0.2
0
WT
SOD1-/-

B

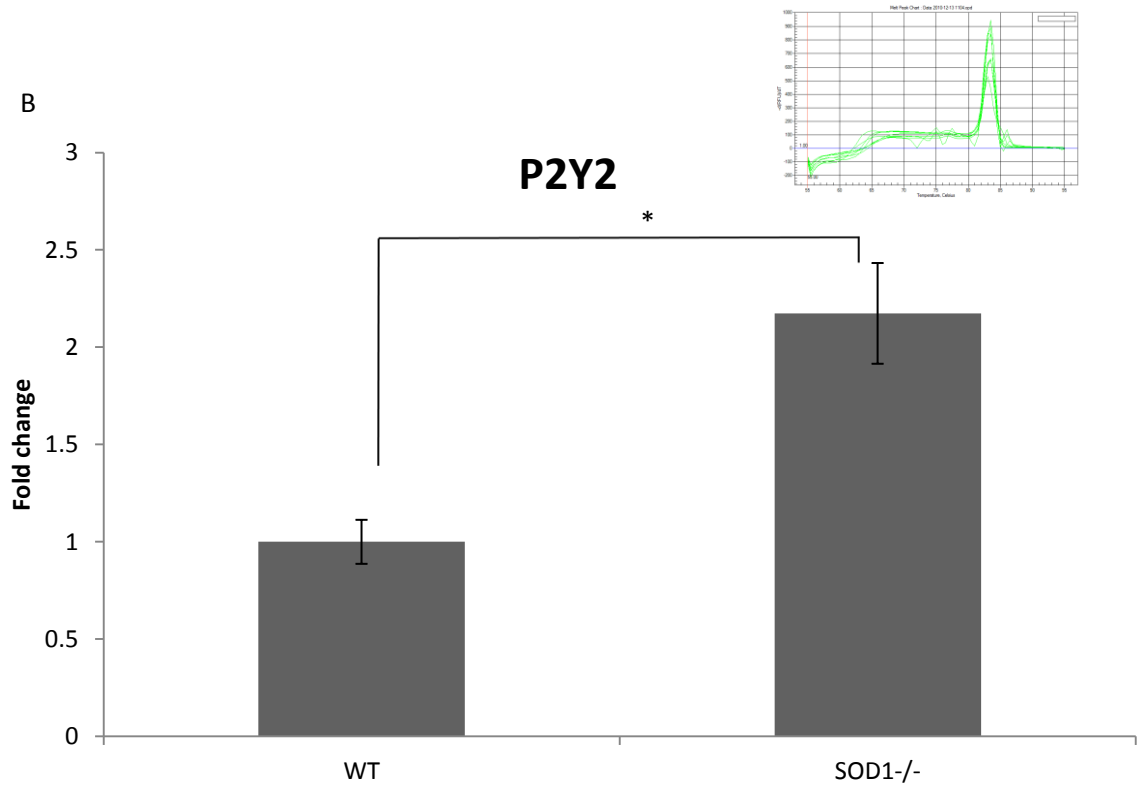
P2Y2
*
Fold change
3
2.5
2
1.5
1
0.5
0
WT
SOD1-/-

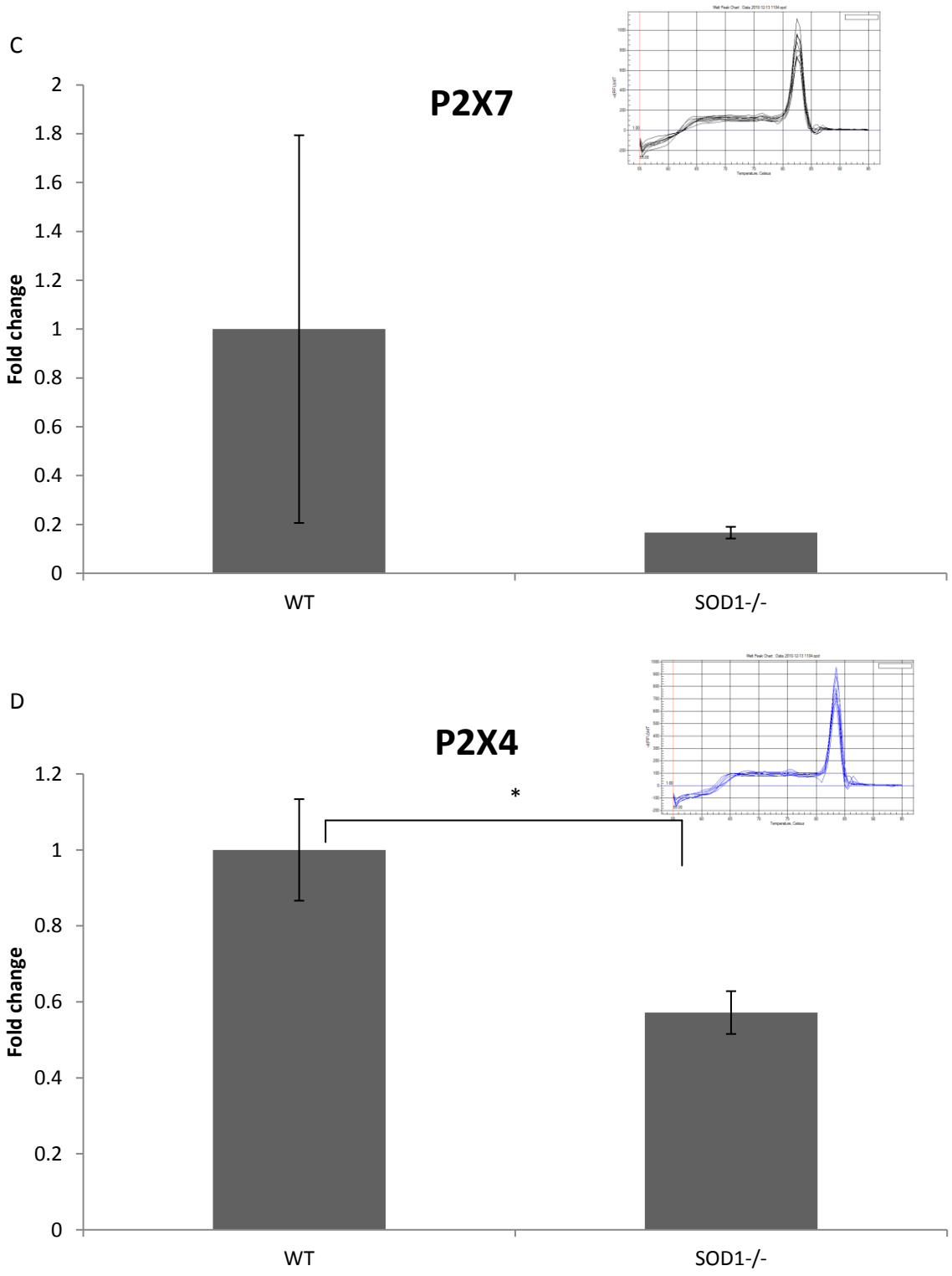

Fig 6.2 Relative expression of P2 receptors in mouse calvarium cells. (A) P2Y1 receptor (B) P2Y2 receptor (C) P2X7 receptor and (D) P2X4 receptor. All genes normalised to beta-actin. n=3-6. Error bars = S.D.

Fig 6.2 shows the results of investigations into the relative expression of P2 receptors in mouse calvarium cells. Overall, WT P2X4 had the highest expression, with SOD1-/- P2Y1 receptors having the lowest expression out of the P2 receptors that were measured. (A) shows that there was no significant difference between WT mice and SOD1-/- mice with respect to the P2Y1 receptor. (B) shows the largest difference between the WT mice and the SOD1-/- mice with a significant increase of over 50% in the SOD1-/- mice. (C) shows a decrease of P2X7 in the SOD1-/- however this was not significant due to the large difference between WTs. (D) Shows a significant decrease in P2X4 receptors in SOD1-/- mice.

The inlaid graphs are the melt curves for each respective primer set. They show that, as there is only one peak, there is no primer dimerisation, and because the melting point for each product corresponds to its expected melting point, determined by the products GC% content and length, it suggests that the primers are recognising the correct sequence.

6.3.2 Comparison of SOD1-/- and WT osteoblast markers

The calvarial cells were analysed for their osteoblast markers to determine what effect a SOD1 knockout would have on them. Interestingly, Fig 6.3 (A), (B) and (C) shows that ALP, Collagen 1A (Col1A) and osteocalcin are all increased in SOD1 knockout cells. However none of these were significant.

A

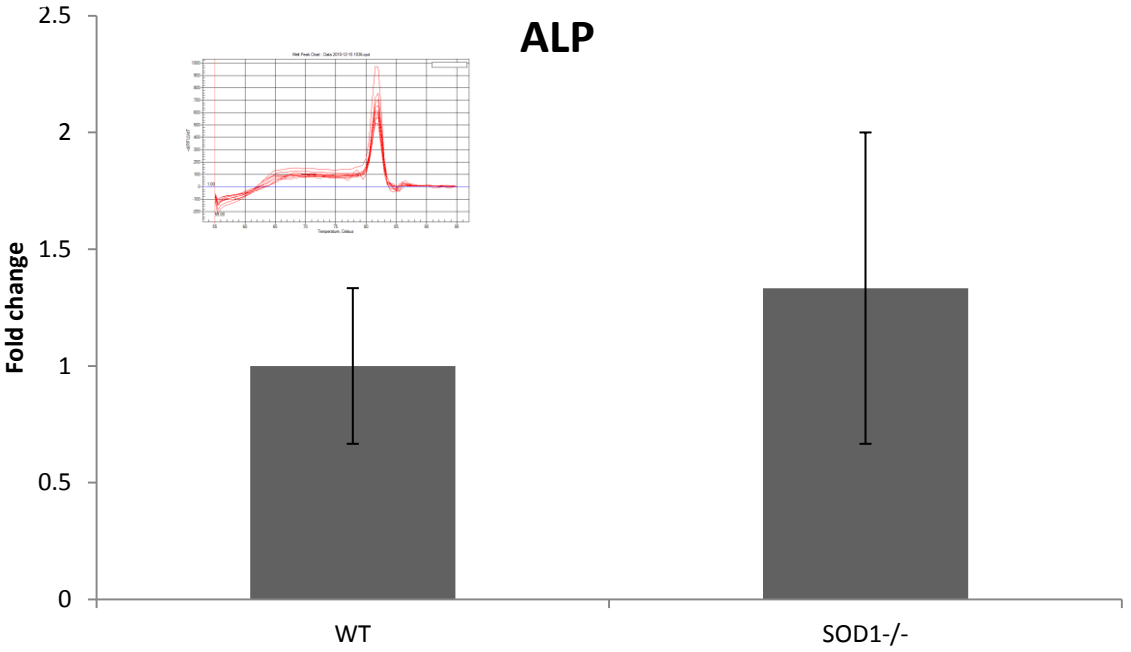
ALP
Fold change
2.5
2
1.5
1
0.5
0
WT
SOD1-/-

B

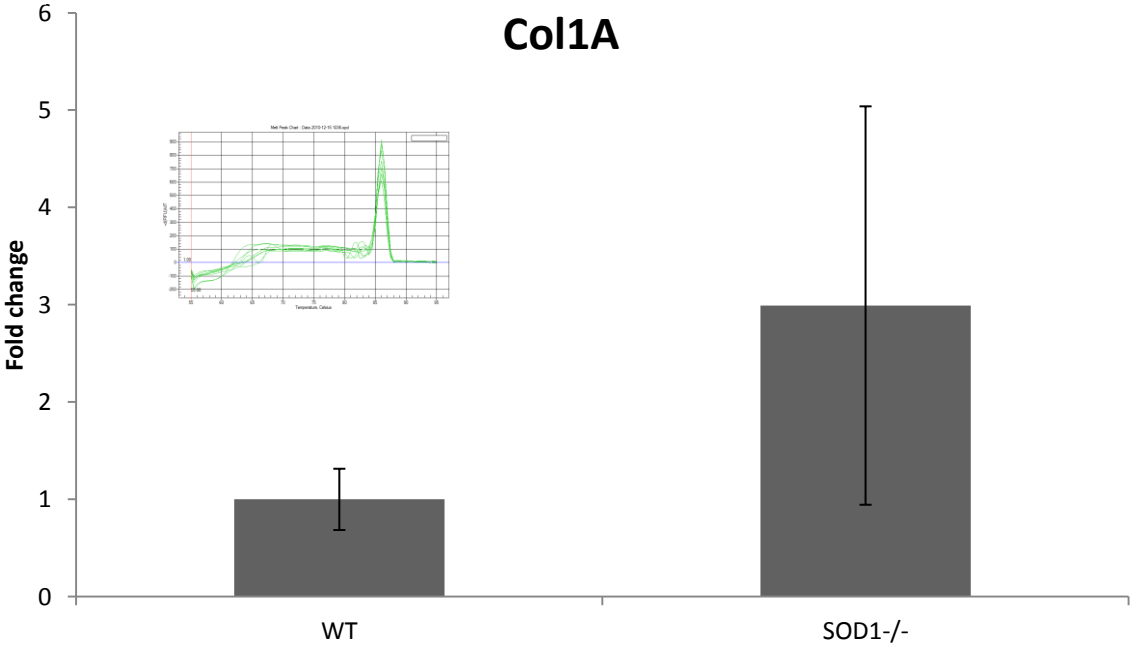
Col1A
Fold change
6
5
4
3
2
1
0
WT
SOD1-/-

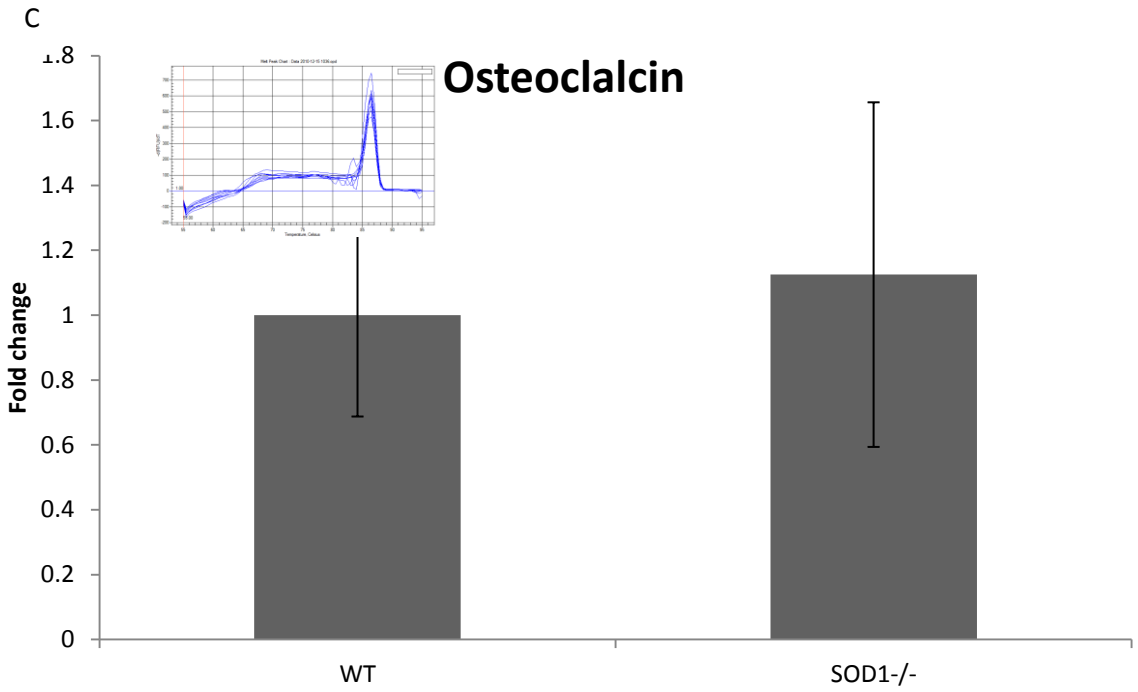

Fig 6.3 The relative expression of (A) ALP, (B) Col1A and (C) osteocalcin in mouse calvarial cells. All genes normalised to beta actin. n=3-6. Error bars = S.D.

Col1A is the most highly expressed of the markers with a relative expression of 0.04 (+/- 0.02 S.D.) in the SOD1-/- mice. ALP is the least expressed with a relative expression of 0.0004 (+/- 0.0002 S.D.). The expression of Col1A appears to have the largest difference between WT and SOD1 -/- which has 66% higher expression than the WT counterpart. The osteocalcin expression is similar whilst there is a small increase in ALP mRNA in the SOD1 -/- cells. However none of these differences were significant.

These melt curves confirm that the products measured were the correct ones according to their melting temperatures and that the products measured were not those of primer dimers.

6.3.3 µCT analysis of SOD1 -/- bones

Firstly the cortical bone was measured throughout the length of the proximal tibias. Slices were chosen, as described in above in section 6.2.3, throughout the stack and 3 measurements were taken to be averaged. Fig 6.4 shows that there appears to be no difference between the WT and SOD1-/- bones.

The trabecular bone of the samples were analysed using a number of parameters. Fig 6.5 shows the results for the tissue volume, which constitutes the entire volume in the ROI, the bone volume, which is the volume of bone in the ROI, and the percentage of tissue that was bone. It can be seen that there was no significant difference in any of these 3 measurements.

The surface of tissue was also measured, which represents the circumference of the ROI and can therefore be classed as the inner surface area of the cortical bone. It can be seen in Fig 6.6 that there is no difference between the WT and SOD1 -/- mice. The total surface of the trabecular bone was also measured, although a slight decrease in SOD1 -/- is observed this was nowhere near significance. From the bone surface and bone volume data the ratio between these two were calculated and is shown in Fig 6.7 (C), these measurements displayed no differences.

Finally Fig 6.8 shows the results for the thickness of the trabecular, on average how far apart these trabecular were and the number of trabecular that were measured. Again no significant difference was measured.

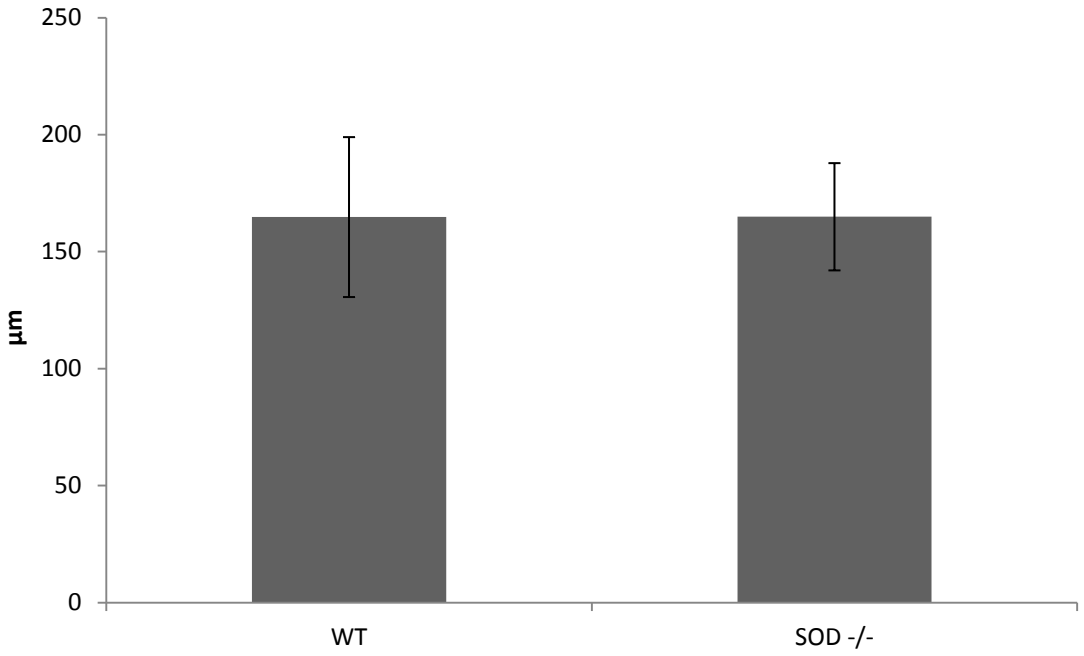

Fig 6.4 Cortical width of SOD1-/- and WT mice tibias. Width of cortex was measured in 5 different slices throughout the length of the tibia. These measurements were added together and an average taken. n=4. Error bars = S.D.

These results show the average width of the cortex for wild type mice measured at 164.7 µm across (+/- 40 µM S.D.). In the SOD1 -/- mice the average was 164.9 µm (+/- 30 µM S.D.). There was no significant difference between the two types of tibia.

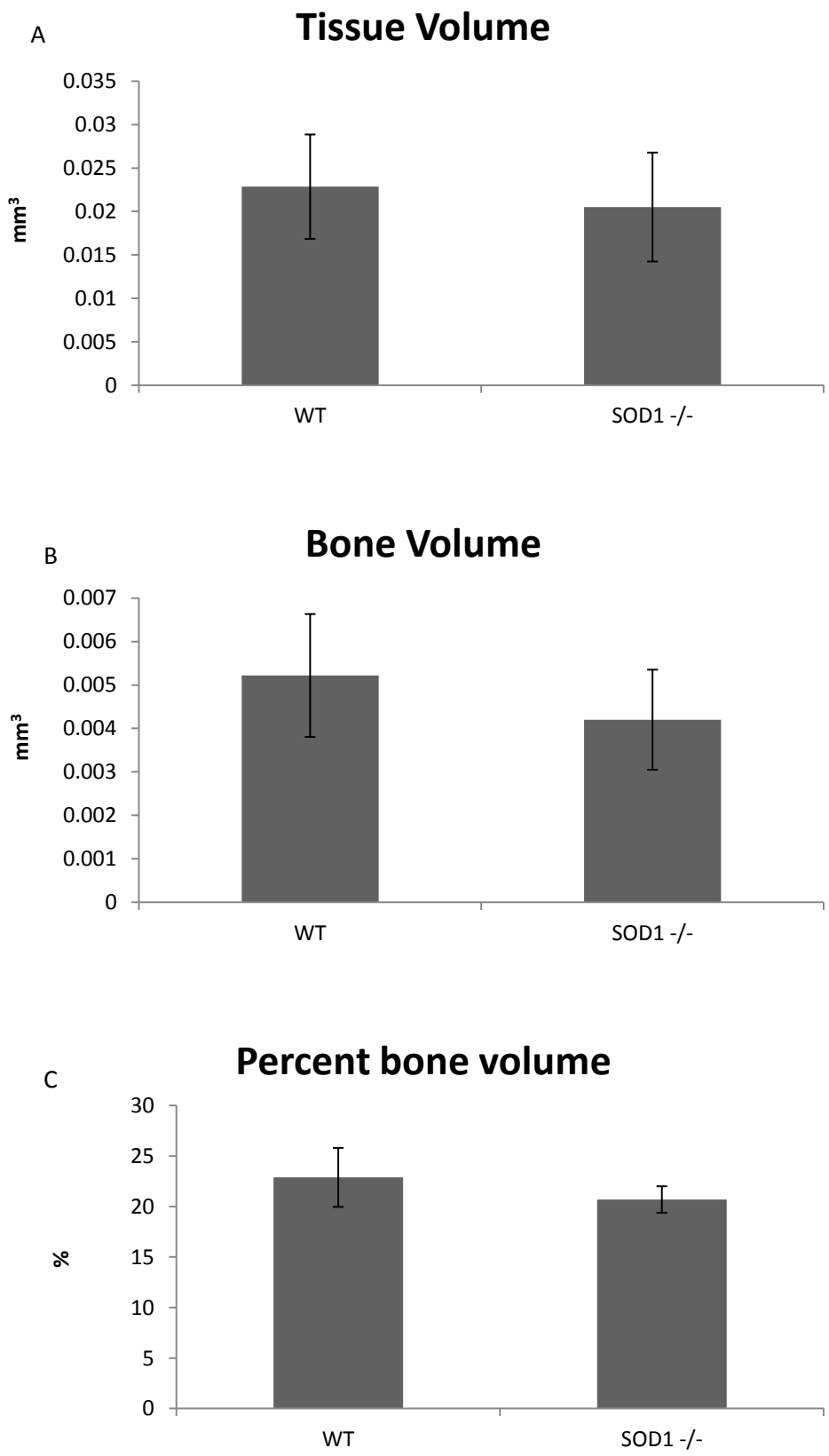

Fig 6.5 µCT volume measurements of SOD1-/- trabecular bone. (A) The total volume of the tissue measured. (B) The volume of bone present in the measured area. (C) The percentage of bone compared to tissue in each sample. n=4. Error bars represent S.D.

Fig 6.5 (A) Shows the tissue volume of both the WT and SOD1 -/- mice. The tissue volume constitutes the whole ROI, the larger it is the more volume exists between the cortical bone. In this case there is no difference between the WT and SOD1-/- mice. Fig 6.5 (B) shows the bone volume and again no significant difference between the two mice was observed. Finally Fig 6.5 (C) shows the amount of bone present in relation to the amount of tissue present, the percent bone volume. A higher reading may constitutes an increased amount of bone or a decreased amount of tissue. Although SOD1-/- mice appear to have a lower ratio this again is not significant.

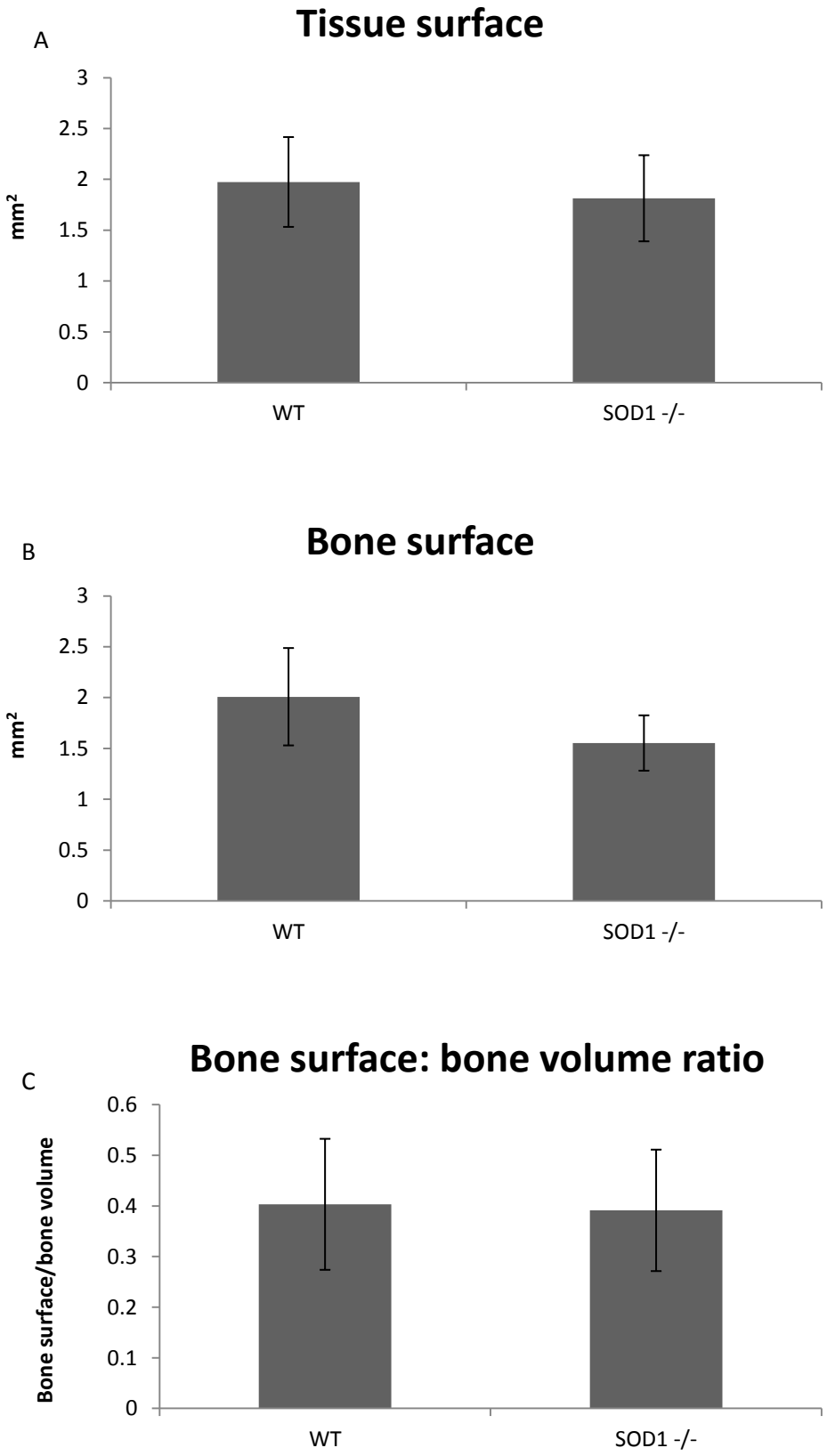

Fig 6.6 Surface measurements of SOD1-/- trabecular bone. (A) Surface area of tissue. (B) Surface of the bone (C) Bone surface to volume ration. n=4. Error bars = S.D.

Fig 6.6 (A) represents the results for the tissue surface. This is the circumference of the ROI, a larger amount would represent an increased surface area of cortical bone, however there was no difference between the two sets of mice. The bone surface measurements shown in Fig 6.6 (B) is the total surface of the trabecular bone throughout the ROI. It shows a slightly decreased value for SOD1 -/- mice, however this was not significant. Using the bone volume (Fig 6.5 (B)) and the surface of the bone (Fig 6.6 (B)) the ratio of the two was calculated, which is shown in Fig 6.6 (C), there was no significant difference between the two.

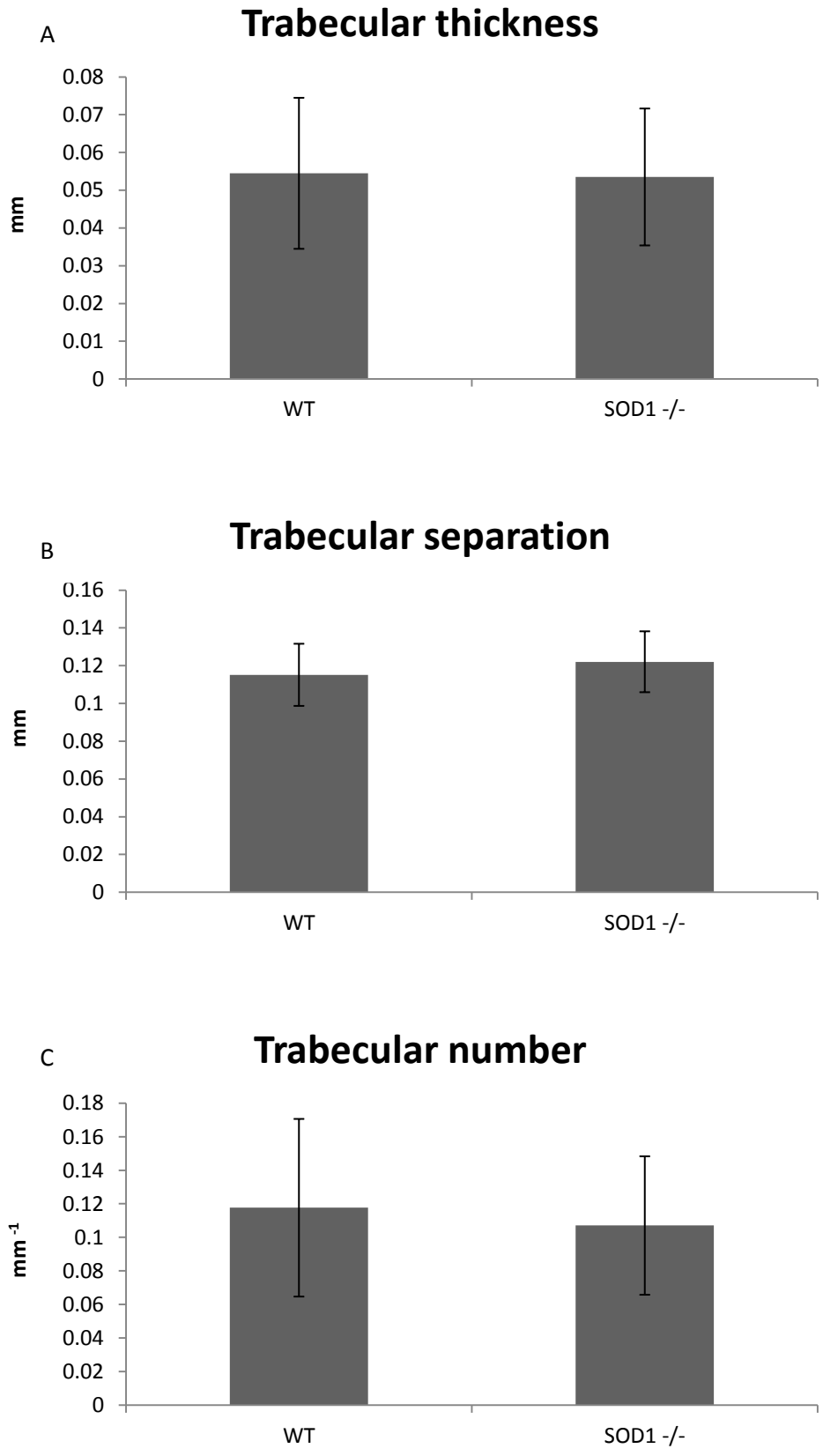

Fig 6.7 Trabecular measurements of SOD1 -/- mice. (A) The average thickness of the trabecular bone. (B) The trabecular separation. (C) The number of trabecular in each sample. n=4. Error bars = S.D.

Fig 6.7 represents some specific trabecular measurements obtained from the μCT scan. The average thickness of the trabecular from each specimen, how far apart the trabecular were from each other and the number of trabecular from each sample was calculated. It can be seen that in all measurements there was no difference in the trabecular bone between WT bones and SOD1-/- bones.

6.4 Discussion

The basis of this chapter was to further investigate the P2 expression and bone morphology of SOD1-/- mice. This was in part due to evidence that mutations of this gene in humans can lead to ALS. The mechanism behind this is unknown, however it appears that the astrocytes are more sensitive to the neurotoxic action of ATP. The bones of SOD1-/- mice have also been analysed previously in strength tests and were shown to be much weaker. Therefore the investigative approach to these mice were carried out in 3 ways, firstly the most highly expressed P2 receptors in the osteoblasts were analysed to determine if sensitization came about due to any alterations in the expression of P2 receptors. The bones would also be analysed to determine any changes in osteoblastic bone cell markers, and finally µct would be employed to look at the structure of these bones.

Section 6.3.1 shows the top four P2 receptors that are expressed in mouse bones [243], these being P2Y1, P2Y2, P2X7 and P2X4. Interestingly SOD1-/- mice were significantly different in 2 of the 4 receptors, and given the small sample number it is likely that all 4 would be significant given more numbers. There was no significant change in the expression of P2Y1 receptor between SOD1 -/- mice and WT mice. P2Y1 is involved, in humans, with the expression of the proto oncogene *c-fos* [33, 199]. This allows increased bone remodelling as well as increased proliferation and differentiation of osteoblasts, thus the net result would be a gain in bone. P2Y2 is known to inhibit bone mineralisation through inhibition of ALP [69], thus an increase of P2Y2, which is what has been observed in these tests, would again suggest a decrease of bone mineralisation and therefore bone strength. Although stimulation of P2X7 can lead to apoptosis it has also been shown that stimulation at lower concentrations can have an anabolic response to bone [73, 74], thought to be through the release of PGE_2. Indeed P2X7 knockout mice have a decrease in periosteal bone formation and cultured osteoblasts taken from these mice had reduced osteogenesis and ALP activity [75, 76]. It can be seen in Fig 6.2 (C) that whilst there was a decrease in P2X7 expression in these mice the changes were not siginificant. This provides further evidence that the deletion of SOD1 may be decreasing bone formation via its effects on P2 receptors. The case with P2X4 is less distinct, mainly due to the fact

that a clear role of P2X4 has not been examined in bone, but again, a reduced expression suggests that SOD1 may affect it, and therefore, the formation of bone.

The next part investigated the expression of osteoblast cell markers to determine if they had been altered as a result of the SOD1 deletion. Although there were differences between the SOD1-/- and WT mice these were not significant which suggests that there were no changes to the function of the osteoblasts in these mice.

Finally the next test was to examine the structure of the bone to better understand the results seen when these bones were placed under physical strain. That is they were found to be less stiff, probably due to a decrease in BMD. To do this the cortical bone was measured for thickness along set points on the tibia. To measure the trabecular bone a ROI was produced, this was taken at the proximal end of the growth plate and the following 15 slices moving in a proximal direction. The cortical bone was excluded by drawing around the inside edge of it. Fig 6.5 shows the total volume of the measured area, the total bone volume and the bone as a percentage of the total volume. In all 3 cases the SOD1 -/- mice had very small decreases, however these were not significant and are unlikely to be anything of value. Thus it appears that this is in conflict with published data and the P2 receptor expression outlined in this chapter. A similar story was found with the surface area measurements of the trabecular bone, with no significant difference between the tissue volume, the bone volume, the bone volume:surface ratio and the density of the bone surface. It should be noted that in all these cases the SOD1-/- had lower values and given a greater n number may become significant. Finally the thickness of the trabeculae, the separation between them and the number showed no significance between SOD1 -/- and the WT mice.

The results in this chapter are quite intriguing as the change in P2 mRNA expression is in line with the literature, specifically that the increase of P2Y2 transcript would suggest a loss of bone mineralization that is seen in the Wang paper [183]. However with no significant differences in Col1A, ALP and osteocalcin it suggest that these mice have experienced no difference in their bone phenotype. Further to this the µCT scans also showed no difference between mice. Cleary work still

needs to be carried out to determine the effect a SOD1-/- knockout has on these bones. One drawback of the experimental procedure was the lack of young mice. The SOD1-/- and WT mice that were obtained were old at 20 months, these mice were so old that the trabecular bone in the diaphysis was no longer present which is traditionally used to measure trabecular bone in μCT analysis. To truly determine whether an ageing phenotype was present it would have been beneficial to look at much younger mice. This may explain the lack of difference between the scans as the WT mice had 'caught up' age wise. Therefore the next step in any investigation would be to carry out the exact same experiments on much younger mice.

7. General discussion

7.1 ATP release from osteoblasts

For ATP to be an effective local hormone in bone it needs to be released from bone cells. SaOS-2, HOBIT, Te-85 and MG-63 osteoblast cells have all been shown to release ATP both basally and in response to mechanical stimulation [64, 100, 101]. The mechanism involved in ATP release has still to be elucidated, however 4 methods have been postulated. These being ATP release through gap hemichannels, the P2X7 formed pore, ABC transporters and exocytosis. The latter is very likely to be at least partly involved as inhibition of exocytosis prevented hypoxic ATP release in osteoblasts, also quinicrine staining displayed ATP presence in vesicles [82]. However these exocytosis inhibitors were unable to completely block ATP release [82] and work carried out in our lab showed that NEM was unable to stop basal release (Fig 3.14). Thus it appears to be more than just exocytosis that causes ATP release in osteoblasts.

To study this further a standardised test needed to be implemented. Thus work was undertaken to design a standardised fluid perturbation protocol that would allow for consistent ATP release data (see appendix), currently this was not the case as the ATP release data that was collected had a lot of variation in and between experiments.

The most obvious source of variation in the medium displacement experiments was the inherent human error involved in pipetting. It is impossible to displace with the same force and the same speed between repeats and certainly impossible between investigators. Work that looked at finding standardized fluid perturbation methods in vibrating and rocking the plate showed no increase in ATP release. This suggests that osteoblasts only react specifically to the type of fluid flow seen in medium displacement experiments. This specificity to certain flow types has been seen before in 3D scaffold experiments [102] and may also account for the increase in ATP release seen on dentine (Fig 3.18 and Fig 3.19). Attempts to standardize medium displacement experiments using multichannel pipettes, to ensure the same speed and force was being used, still had a lot of variation, which suggests that this wasn't the main source of variation.

The kinetics of the luciferase enzyme was also examined to better understand how the protocol could be changed to get the maximal efficiency from it. It can be seen that small changes in pH or temperature caused a large difference in the light readings that were produced in the luminometer, thus experiments were now performed in HEPES buffered medium and only 5 samples at a time were measured to ensure samples loaded early on would not heat up.

When sampling from multiple areas of the well it also became apparent that the ATP was massively different in a single well both basally and following on from medium displacements. This was most likely due to the slow diffusion rate of ATP which was demonstrated in Fig 3.17. The decision was made to sample multiple times from the same well before and after any tests to get a better average of ATP across the well. Previous to this, one well had been taken as the standard basal level and the other wells manipulated. Given the difference in basal levels in a single well and across different wells this was no longer feasible. Also a 6-well plate lid was designed and manufactured that allowed the same area of the wells to be sampled from, and at the same depth.

By using mtDNA analysis in conjunction with NEM (Fig 3.14) it was shown that ATP release is not due to the damage of the cell membrane. This is consistent with previous data using the less sensitive measure of LDH (unpublished). It does, however, suggest that cells may be lifted off the bottom and therefore taken up with the sample which may contribute towards variation.

7.2 ATP synergy with systemic hormones

ATP has previously been shown to synergise with other factors to cause an increased response. This was shown in MC3T3 cells were it synergised with PDGF to increase DNA synthesis and has also been shown in fibroblasts and porcine smooth muscle cells [65, 157, 158]. In both SaOS-2 and UMR-106 cells the addition of nucleotides with PTH massively up regulated the *c-fos* expression in these cells. *c-fos* is a master regulator gene and the expression of which signifies a switching on of bone remodelling as it causes the activation of osteoclasts and causes osteoblasts to proliferate. It has been known since Wolff proposed it in the 19th century that an increase in loading causes an increase in

bone mass in these areas. Therefore the fact ATP could be released upon mechanical strain suggests that ATP may target the action of the PTH to these specific highly loaded areas.

It was also shown that ATP can sensitise osteoblast to the action of PTH. Given the short half life of both (9 minutes *in vitro* for ATP and 4 minutes *in vivo* for PTH) this strengthens the argument that it plays a major role on osteoblast physiology. The synergy of ATP and PTH was shown in *c-fos* expression (Fig 4.1, Fig 4.8), the up-regulation of RANKL and the down regulation of OPG.

It is not clear how this fits in to current opinion on how the synergy is achieved, as they do not allow for such a sensitisation mechanism. In UMR-106 cells the synergy is obtained by a potentation of the Ca^{2+} release, which would disappear quickly. In SaOS-2 cells, although not completely clear, it is through the combination of transcription factors, of which one is the short lived phosphorylated CREB, acting on different parts of the *c-fos* promoter. It therefore appears that the sensitisation effect is by another mechanism as removing ATP treated medium and then adding PTH causes no synergy to be observed (Fig 4.9, Fig 4.10), and therefore ATP must be altering something within the medium and thus not having an effect on the known mechanisms of synergy. Given the fact that ADP and AMP are so transient in the medium and that adenosine has an inhibitory affect on PTH it seems sensible to assume that ATP must cause the release of another longer lasting paracrine factor. A prime candidate for this would be PGE_2 as this has been shown to be released from osteoblasts and it has also been shown to increase the transcription of *c-fos* in these osteoblasts. Why a cell would chose to release another paracrine factor remains unclear. These 'paracrine loops' have been observed in osteoblasts, an example being FGF-2 causing release of VEGF in MC3T3 cells [244]. It could be that in this system the compound has a longer half life and that is why the need exists to release another paracrine factor into extracellular environment. In addition to this another hypothesis is that is its acts to amplify the ATP signal. For instance if the mechanical strain is only sensed by one or two cells these will release a small amount of ATP that acts on nearby cells, perhaps ten or more. These may all release the next paracrine factor which perhaps acts on a hundred cells, all of which can now respond to PTH with a greater effect from only a few cells detecting the strain.

7.3 The effect of BL-1249 on osteoblasts

Previously in our lab it has been shown that the putative K^+ channel opener BL-1249 caused a decrease in ATP + PTH induced *c-fos* synergy. As *c-fos* is a master regulator gene that is involved in the proliferation and differentiation of osteoblasts, an overexpression of *c-fos* can lead to uncontrolled growth and osetosarcoma development. A drug that appears to inhibit the expression of *c-fos* is therefore worth investigating.

Initial experiments were designed to elucidate how BL-1249 was inhibiting c-*fos*. It was proven not to be either through cell death or its advertised effects on K^+ channels (Fig 5.2, Fig 5.3). This was displayed by tests that were run in high extracellular K^+ which would prevent the hyperpolarisation should the K^+ channels open [229, 235]. Also NS-1619, a known BK channel opener, did not cause the same effect.

Attention therefore was turned to its effects on signalling pathways. Given the fact that BL-1249 inhibited both ATP induced and PTH induced *c-fos* it was not obvious what this pathway could be, unless current opinion on how ATP causes an increase in *c-fos* is flawed. Experiments using sp-cAMP suggest that BL-1249 affects the PKA pathway. Whether this is through inhibition of CREB phosphorylation is still unclear, if not it is likely to be downstream of this. So for example it may prevent the translocation of CREB to the nucleus, by inhibiting the importins designed to get CREB into the nucleus [241]. Alternatively it may directly inhibit the binding of CREB to the Ca/CRE domain of the promoter.

Interestingly BL-1249 also caused cell death at high concentrations when left on for 48 hours. It was noted that the morphology of cells treated with 10 μM BL-1249 for 4 hours was changed, with a decrease in cell processes. It is likely that these two are linked as there is evidence that opening K^+ channels causes cell shrinkage and if enough open, or are left open for a long period this would lead to apoptosis in these cells. This data was backed up by the fact that TEA (a K^+ channel blocker) slightly reversed the BL-1249 effect on cell number. However BL-1249 did not cause a decrease in the primary cell line MA16, it is unknown whether these cells express BK channels, however this is

likely given that other osteoblast lines express it. Therefore this suggests that it targets survival pathways in the osteoblast, perhaps on top of the activation of K^+ channels.

7.4 The bone phenotype and P2 expression of SOD1-/- mice

Given that mutations of SOD1 have been linked with ALS, through a P2 dependent manner, and SOD1 -/- mice have been reported to have a lower BMD it was decided to investigate this further. To do this the mRNA expression of P2 receptors and osteoblast cell markers was investigated, and for the first time the structure of the bone was examined using µct scanning

The results of the P2 receptor expression tests appeared to suggest that a SOD1 deletion would lead to a decreased bone mass. This is due to the fact that there was a decrease of P2Y1 and P2X7 expression. These have both been linked to aiding the formation of mineralized bone. Also a massive increase in P2Y2 expression was observed. This again has been implicated in increasing bone formation and thus a decrease in its expression would have the opposite effect.

The bone marker results were interesting as the mRNA expression of both ALP and Col1A appeared to be higher, suggesting an increase of bone formation. However, these results were not significant and therefore cannot be assigned great value.

Finally µct scans were performed on the proximal tibia and fibula of each mouse. There were no significant differences in any of the parameters that were tested, suggesting the increased ALP and Col1A expression was not sufficient to cause an increase BMD in the SOD1 -/- mice. These being cortical bone width, tissue and bone volume, tissue and bone area trabecular width, separation and number. Again given the data that has already been published this was unexpected. The most likely explanation of this is the fact that the mice that were obtained were already ‘old’. As mentioned in the introduction SOD1 is an antioxidant and thus the deletion of which will produce more oxidative damage. As oxidative damage accumulates with age the highest differences are likely to be when the two sets of mice are younger.

7.5 Future perspectives

Given that the reading of ATP in supernatant has now been standardized work can focus on how ATP is released. Future work should investigate the exact mechanism of release in different states (i.e. basal release, release following medium displacements). The best way to achieve this is likely through siRNA inhibition. For example siRNA can be used to inhibit the SNARE complex that allows vesicle fusion to the membrane. Another avenue of investigation is to look at the real time release of ATP. This may be possible by using a PMEluc, which is a membrane bound version of NMR. It has been developed in order to read ATP near the cell surface and if placed under a confocol microscope could give real time data. Live imaging would be a great insight into the characteristics of ATP release following medium displacements.

Further work needs to be undertaken to elucidate the mechanism behind the ATP sensitisation of osteoblasts to PTH. If not PGE_2 then a proteonomic analysis of the medium needs to take place to determine what possible proteins are present within the medium. Any that are present need to be tested for synergy with PTH and confirmed that it is released upon ATP treatment.

The method by which BL-1249 inhibits *c-fos* expression still needs to be completely illuminated. It appears to be downstream of PKA and thus either effects the phosphorylation of CREB or the subsequent movement and binding of CREB to the *c-fos* promoter. Work should initially focus on determining the phosphorylation state of CREB following on from BL-1249 treatment with PTH.

As stated previously work on investigating the SOD1 -/- should continue in the same vein but younger mice need to be examined to see if these are consistent with the findings for the mice examined in this thesis.

The work in this thesis are the first steps to understanding how ATP arrives in the extracellular space and how it relates to other hormones that are present in the extracellular space. Once fully understood drugs can be developed to target these mechanisms in an aid to modulate the BMD. Work here has also looked a novel drug that inhibited *c-fos* expression. Again if fully understood this has the potential to decrease the proliferation of osteosarcoma cells. Finally it can be seen that increased

superoxide ions may alter the expression of P2 receptors. This is vital information when investigating purinergic signalling in age related diseases.

Bibliography

1. NHS. *Osteoporosis*. [Web page] 8/5/12 [cited 2013 25/3/13]; Available from: http://www.nhs.uk/Conditions/Osteoporosis/Pages/Introduction.aspx.
2. Body, J.J., *How to manage postmenopausal osteoporosis?* Acta Clin Belg, 2011. **66**(6): p. 443-7.
3. Hannan, E.L., et al., *Mortality and locomotion 6 months after hospitalization for hip fracture: risk factors and risk-adjusted hospital outcomes.* JAMA, 2001. **285**(21): p. 2736-42.
4. Martini, F.H., *Anatomy and Physiology*. 7 ed2006, San Fransico, U.S.A.: Peason eduction Inc.
5. Bonewald, L.F., *Osteocytes.* Primer on the Metabolic Bone Diseases and Disorders of Mineral Metabolism. The American society for bone and mineral research., 2008: p. 22-27.
6. Fogh, J., J.M. Fogh, and T. Orfeo, *One hundred and twenty-seven cultured human tumor cell lines producing tumors in nude mice.* J Natl Cancer Inst, 1977. **59**(1): p. 221-6.
7. Rodan, S.B., et al., *Characterization of a human osteosarcoma cell line (Saos-2) with osteoblastic properties.* Cancer Research, 1987. **47**(18): p. 4961-6.
8. Clover, J. and M. Gowen, *Are MG-63 and HOS TE85 human osteosarcoma cell lines representative models of the osteoblastic phenotype?* Bone, 1994. **15**(6): p. 585-91.
9. Hill, P.A., *Bone remodelling.* Br J Orthod, 1998. **25**(2): p. 101-7.
10. Gallagher, J.A. and J.P. Dillon, *Bone remodelling*. 2 ed. Encylopedia of human biology. Vol. 2. 1997.
11. Wolff, J., *The law of bone remodelling*1986, Berlin, Heidelberg, New York: Springer.
12. Dalen, N., et al., *The effect of athletic activity on the bone mass in human diaphyseal bone.* Orthopedics, 1985. **8**(9): p. 1139-41.
13. Collet, P., et al., *Effects of 1- and 6-month spaceflight on bone mass and biochemistry in two humans.* Bone, 1997. **20**(6): p. 547-51.
14. Frost, H.M., *Dynamics of bone remodelling*. Bone Biodynamics, ed. H.M. Frost1964, Boston, U.S.A.: Little Brown.
15. Wagner, E.F., *Functions of AP1 (Fos/Jun) in bone development.* Ann Rheum Dis, 2002. **61 Suppl 2**: p. ii40-2.
16. Suda, T., N. Udagawa, and N. Takahashi, *Cells of bone: osteoclast generation*. Principles of bone biology, ed. J.P. Bilezikian, L.G. Raisz, and G.A. Rodan1996, San Diego, U.S.A.: Academic press.
17. Roodman, G.D., *Advances in bone biology: the osteoclast.* Endocr Rev, 1996. **17**(4): p. 308-32.
18. Anderson, C.M., J.P. Bergher, and R.A. Swanson, *ATP-induced ATP release from astrocytes.* J Neurochem, 2004. **88**(1): p. 246-56.
19. Lakkakorpi, P.T., et al., *Vitronectin receptor has a role in bone resorption but does not mediate tight sealing zone attachment of osteoclasts to the bone surface.* Journal of Cell Biology, 1991. **115**(4): p. 1179-86.
20. Martin, T.J. and K.W. Ng, *Mechanisms by which cells of the osteoblast lineage control osteoclast formation and activity.* Journal of Cellular Biochemistry, 1994. **56**(3): p. 357-66.
21. Matsuo, K. and N. Irie, *Osteoclast-osteoblast communication.* Archives of Biochemistry and Biophysics, 2008. **473**(2): p. 201-209.
22. Pfeilschifter, J., L. Bonewald, and G.R. Mundy, *Characterization of the Latent Transforming Growth Factor-Beta Complex in Bone.* Journal of Bone and Mineral Research, 1990. **5**(1): p. 49-58.
23. Mundy, G.R., et al., *Unidirectional migration of osteosarcoma cells with osteoblast characteristics in response to products of bone resorption.* Calcif Tissue Int, 1982. **34**(6): p. 542-6.

24. Hill, P.A., A. Tumber, and M.C. Meikle, *Multiple extracellular signals promote osteoblast survival and apoptosis.* Endocrinology, 1997. **138**(9): p. 3849-3858.
25. Knowles, J.R., *Enzyme-catalyzed phosphoryl transfer reactions.* Annu Rev Biochem, 1980. **49**: p. 877-919.
26. Drury, A.N. and A. Szent-Gyorgyi, *The physiological activity of adenine compounds with especial reference to their action upon the mammalian heart.* J Physiol, 1929. **68**(3): p. 213-37.
27. Burnstock, G., et al., *The effects of drugs on the transmission of inhibition from autonomic nerves to the smooth muscle of the guinea pig taenia coli.* Biochem Pharmacol, 1963. **12**(S): p. 134-135.
28. Burnstock, G., *Evolution of the autonomic innervation of visceral and cardiovascular systems in vertebrates.* Pharmacol Rev, 1969. **21**(4): p. 247-324.
29. Burnstoc.G, et al., *Evidence That Adenosine Triphosphate or a Related Nucleotide Is Transmitter Substance Released by Ono-Adrenergic Inhibitory Nerves in Gut.* British Journal of Pharmacology, 1970. **40**(4): p. 668-&.
30. Burnstock, G., *Purinergic nerves.* Pharmacol Rev, 1972. **24**(3): p. 509-81.
31. Burnstock, G., et al., *The birth and postnatal development of purinergic signalling.* Acta Physiol (Oxf), 2010. **199**(2): p. 93-147.
32. Burnstock, G. and V. Ralevic, *New Insights into the Local-Regulation of Blood Flow by Perivascular Nerves and Endothelium.* British Journal of Plastic Surgery, 1994. **47**(8): p. 527-543.
33. Burnstock, G., *Introduction: P2 receptors.* Curr Top Med Chem, 2004. **4**(8): p. 793-803.
34. Yerxa, B.R., *Therapeutic use of nucleotides in respiratory and ophthalmic diseases.* Drug Development Research, 2001. **52**(1-2): p. 196-201.
35. Burnstock, G., *Purinergic P2 receptors as targets for novel analgesics.* Pharmacol Ther, 2006. **110**(3): p. 433-454.
36. Di Virgilio, F., et al., *Purinergic P2X(7) receptor: A pivotal role in inflammation and immunomodulation.* Drug Development Research, 1998. **45**(3-4): p. 207-213.
37. Agteresch, H.J., et al., *Adenosine triphosphate - Established and potential clinical applications.* Drugs, 1999. **58**(2): p. 211-232.
38. Burnstock, G., *Purinergic receptors.* J Theor Biol, 1976. **62**(2): p. 491-503.
39. Burnstock, G., *A basis for distinguishing two types of purinergic receptor.* Cell Membrane Receptors for Drugs and Hormones: A Multidisciplinary Approach, ed. R.W. Straub and L. Bolis1978, New York, U.S.A.: Raven Press.
40. Burnstock, G. and C. Kennedy, *Is there a basis for distinguishing two types of P2-purinoceptor?* Gen Pharmacol, 1985. **16**(5): p. 433-40.
41. Abbracchio, M.P. and G. Burnstock, *Purinoceptors: are there families of P2X and P2Y purinoceptors?* Pharmacol Ther, 1994. **64**(3): p. 445-75.
42. Burnstock, G., *Purine and pyrimidine receptors.* Cell Mol Life Sci, 2007. **64**(12): p. 1471-83.
43. North, R.A., *Molecular physiology of P2X receptors.* Physiol Rev, 2002. **82**(4): p. 1013-1067.
44. Burnstock, G., *Introduction:ATP and its metabolites as potent extracellular agonists*. Current Topics in Membranes, ed. E.M. Schwiebert. Vol. 54. 2003, San Diego, U.S.A.: Academic Press.
45. Luttrell, L.M. and R.J. Lefkowitz, *The role of beta-arrestins in the termination and transduction of G-protein-coupled receptor signals.* Journal of Cell Science, 2002. **115**(3): p. 455-465.
46. Abbracchio, M.P., et al., *Update and subclassification of the P2Y G protein-coupled nucleotide receptors: from molecular mechanisms and pathophysiology to therapy.* Pharmological review, 2006. **58**: p. 281 – 341.
47. Abbracchio, M.P., et al., *Characterization of the UDP-glucose receptor (re-named here the P2Y14 receptor) adds diversity to the P2Y receptor family.* Trends Pharmacol Sci, 2003. **24**(2): p. 52-5.

48. Waldo, G.L. and T.K. Harden, *Agonist binding and Gq-stimulating activities of the purified human P2Y1 receptor.* Molecular Pharmacology, 2004. **65**(2): p. 426-36.
49. Burnstock, G. and G.E. Knight, *Cellular distribution and functions of P2 receptor subtypes in different systems.* International Review of Cytology - a Survey of Cell Biology, Vol. 240, 2004. **240**: p. 31-+.
50. Weick, M., et al., *P2 receptors in satellite glial cells in trigeminal ganglia of mice.* Neuroscience, 2003. **120**(4): p. 969-977.
51. Xu, J., et al., *Prostaglandin E2 production in astrocytes: regulation by cytokines, extracellular ATP, and oxidative agents.* Prostaglandins Leukot Essent Fatty Acids, 2003. **69**(6): p. 437-48.
52. Seye, C.I., et al., *Functional P2Y2 nucleotide receptors mediate uridine 5'-triphosphate-induced intimal hyperplasia in collared rabbit carotid arteries.* Circulation, 2002. **106**(21): p. 2720-6.
53. Robaye, B., et al., *Loss of nucleotide regulation of epithelial chloride transport in the jejunum of P2Y4-null mice.* Molecular Pharmacology, 2003. **63**(4): p. 777-83.
54. Lazarowski, E.R., et al., *Cloning and functional characterization of two murine uridine nucleotide receptors reveal a potential target for correcting ion transport deficiency in cystic fibrosis gallbladder.* J Pharmacol Exp Ther, 2001. **297**(1): p. 43-9.
55. Communi, D., et al., *Cotranscription and intergenic splicing of human P2Y11 and SSF1 genes.* Journal of Biological Chemistry, 2001. **276**(19): p. 16561-6.
56. Foster, C.J., et al., *Molecular identification and characterization of the platelet ADP receptor targeted by thienopyridine antithrombotic drugs.* Journal of Clinical Investigation, 2001. **107**(12): p. 1591-1598.
57. Andre, P., et al., *P2Y12 regulates platelet adhesion/activation, thrombus growth, and thrombus stability in injured arteries.* Journal of Clinical Investigation, 2003. **112**(3): p. 398-406.
58. Birnbaumer, L., *Signal transduction by G proteins: basic principles, molecular diversity, and structural basis of their actions.* Handbook of Cell Signaling, ed. R.A. Bradshaw and E.A. Dennis2004, Boston, U.S.A: Academic.
59. Wettschureck, N. and S. Offermanns, *Mammalian G proteins and their cell type specific functions.* Physiol Rev, 2005. **85**(4): p. 1159-1204.
60. Bastepe, M., et al., *Receptor-mediated adenylyl cyclase activation through XLalpha(s), the extra-large variant of the stimulatory G protein alpha-subunit.* Molecular Endocrinology, 2002. **16**(8): p. 1912-9.
61. Sunahara, R.K., C.W. Dessauer, and A.G. Gilman, *Complexity and diversity of mammalian adenylyl cyclases.* Annual Review of Pharmacology and Toxicology, 1996. **36**: p. 461-480.
62. Exton, J.H., *Regulation of phosphoinositide phospholipases by hormones, neurotransmitters, and other agonists linked to G proteins.* Annu Rev Pharmacol Toxicol, 1996. **36**: p. 481-509.
63. Buhl, A.M., et al., *G alpha 12 and G alpha 13 stimulate Rho-dependent stress fiber formation and focal adhesion assembly.* Journal of Biological Chemistry, 1995. **270**(42): p. 24631-4.
64. Buckley, K.A., et al., *Release and interconversion of P2 receptor agonists by human osteoblast-like cells.* Faseb Journal, 2003. **17**(11): p. 1401-1410.
65. Shimegi, S., *ATP and adenosine act as a mitogen for osteoblast-like cells (MC3T3-E1).* Calcified Tissue International, 1996. **58**(2): p. 109-113.
66. Nakamura, E., et al., *ATP activates DNA synthesis by acting on P2X receptors in human osteoblast-like MG-63 cells.* Am J Physiol Cell Physiol, 2000. **279**(2): p. C510-9.
67. Jones, S.J., et al., *Purinergic transmitters inhibit bone formation by cultured osteoblasts.* Bone, 1997. **21**(5): p. 393-399.
68. Hoebertz, A., et al., *ATP and UTP at low concentrations strongly inhibit bone formation by osteoblasts: a novel role for the P2Y2 receptor in bone remodeling.* Journal of Cellular Biochemistry, 2002. **86**(3): p. 413-9.

69. Orriss, I.R., et al., *Extracellular Nucleotides block bone mineralization in vitro: Evidence for dual inhibitory mechanisms involving both P2Y(2) receptors and pyrophosphate.* Endocrinology, 2007. **148**(9): p. 4208-4216.
70. Orriss, I., et al., *MicroCT analysis of P2Y1 and P2Y2 receptor knockout mice demonstrates significant changes in bone phenotype.* Purinergic Signal, 2008. **4**: p. S176-S176.
71. Rassendren, F., et al., *The permeabilizing ATP receptor, P2X7. Cloning and expression of a human cDNA.* Journal of Biological Chemistry, 1997. **272**(9): p. 5482-6.
72. Gartland, A., et al., *Expression of a P2X7 receptor by a subpopulation of human osteoblasts.* Journal of Bone and Mineral Research, 2001. **16**(5): p. 846-56.
73. Panupinthu, N., et al., *P2X7 receptors on Osteoblasts couple to production of lysophosphatidic acid: A novel signaling axis promoting osteogenesis.* Journal of Bone and Mineral Research, 2007. **22**: p. S95-S95.
74. Panupinthu, N., et al., *P2X7 nucleotide receptors mediate blebbing in osteoblasts through a pathway involving lysophosphatidic acid.* Journal of Biological Chemistry, 2007. **282**(5): p. 3403-3412.
75. Ke, H.Z., et al., *Deletion of the P2X7 nucleotide receptor reveals its regulatory roles in bone formation and resorption.* Molecular Endocrinology, 2003. **17**(7): p. 1356-67.
76. Okumura, H., et al., *P2X7 receptor as sensitive flow sensor for ERK activation in osteoblasts.* Biochemical and Biophysical Research Communications, 2008. **372**(3): p. 486-490.
77. Ihara, H., et al., *ATP-stimulated interleukin-6 synthesis through P2Y receptors on human osteoblasts.* Biochemical and Biophysical Research Communications, 2005. **326**(2): p. 329-334.
78. WatanabeTomita, Y., et al., *Arachidonic acid release induced by extracellular ATP in osteoblasts: role of phospholipase D.* Prostaglandins Leukotrienes and Essential Fatty Acids, 1997. **57**(3): p. 335-339.
79. Johnson, K.A., et al., *Osteoblast tissue-nonspecific alkaline phosphatase antagonizes and regulates PC-1.* American Journal of Physiology-Regulatory Integrative and Comparative Physiology, 2000. **279**(4): p. R1365-R1377.
80. Genetos, D.C., et al., *Fluid shear-induced ATP secretion mediates prostaglandin release in MC3T3-E1 osteoblasts.* Journal of Bone and Mineral Research, 2005. **20**(1): p. 41-49.
81. Rumney, R.M.H., et al., *ATPase activity and ATP release in osteoblast cultures.* Calcified Tissue International, 2009. **85**: p. 158-201.
82. Orriss, I.R., et al., *Hypoxia Stimulates Vesicular ATP Release From Rat Osteoblasts.* Journal of Cellular Physiology, 2009. **220**(1): p. 155-162.
83. Gartland, A., et al., *Blockade of the pore-forming P2X7 receptor inhibits formation of multinucleated human osteoclasts in vitro.* Calcif Tissue Int, 2003. **73**(4): p. 361-9.
84. Penolazzi, L., et al., *N-Arylpiperazine modified analogues of the P2X7 receptor KN-62 antagonist are potent inducers of apoptosis of human primary osteoclasts.* J Biomed Sci, 2005. **12**(6): p. 1013-20.
85. Masin, M., et al., *Expression, assembly and function of novel C-terminal truncated variants of the mouse P2X7 receptor: re-evaluation of P2X7 knockouts.* Br J Pharmacol, 2012. **165**(4): p. 978-93.
86. Ohlendorff, S.D., et al., *Single nucleotide polymorphisms in the P2X7 gene are associated to fracture risk and to effect of estrogen treatment.* Pharmacogenet Genomics, 2007. **17**(7): p. 555-67.
87. Jorgensen, N.R., et al., *Single-nucleotide polymorphisms in the P2X7 receptor gene are associated with post-menopausal bone loss and vertebral fractures.* Eur J Hum Genet, 2012. **20**(6): p. 675-81.
88. Gartland, A., et al., *Polymorphisms in the P2X7 receptor gene are associated with low lumbar spine bone mineral density and accelerated bone loss in post-menopausal women.* Eur J Hum Genet, 2012. **20**(5): p. 559-64.

89. Korcok, J., et al., *Extracellular nucleotides act through P2X7 receptors to activate NF-kappaB in osteoclasts.* Journal of Bone and Mineral Research, 2004. **19**(4): p. 642-51.
90. Armstrong, S., et al., *Activation of P2X7 receptors causes isoform-specific translocation of protein kinase C in osteoclasts.* Journal of Cell Science, 2009. **122**(1): p. 136-144.
91. Jorgensen, N.R., et al., *Intercellular calcium signaling occurs between human osteoblasts and osteoclasts and requires activation of osteoclast P2X7 receptors.* Journal of Biological Chemistry, 2002. **277**(9): p. 7574-7580.
92. Hazama, R., et al., *ATP-induced osteoclast function: the formation of sealing-zone like structure and the secretion of lytic granules via microtubule-deacetylation under the control of Syk.* Genes to Cells, 2009. **14**(7): p. 871-884.
93. Korcok, J., et al., *P2Y6 nucleotide receptors activate NF-kappa B and increase survival of osteoclasts.* Journal of Biological Chemistry, 2005. **280**(17): p. 16909-16915.
94. Genetos, D.C., et al., *Oscillating fluid flow activation of gap junction hemichannels induces ATP release from MLO-Y4 osteocytes.* Journal of Cellular Physiology, 2007. **212**(1): p. 207-14.
95. Bodin, P. and G. Burnstock, *Purinergic signalling: ATP release.* Neurochem Res, 2001. **26**(8-9): p. 959-69.
96. Koop, A. and P.H. Cobbold, *Continuous Bioluminescent Monitoring of Cytoplasmic Atp in Single Isolated Rat Hepatocytes during Metabolic Poisoning.* Biochemical Journal, 1993. **295**: p. 165-170.
97. Bowler, W.B., et al., *ATP released into the extracellular environment by osteoblasts regulates differentiation and apoptosis of bone cells.* Journal of Bone and Mineral Research, 2000. **15**: p. S476-S476.
98. WB Bowler, et al., *Release of ATP by osteoblasts: Modulation by fluid shear forces.* Bone Marrow Transplantation, 1998. **22**: p. 3S.
99. Beigi, R., et al., *Detection of local ATP release from activated platelets using cell surface-attached firefly luciferase.* American Journal of Physiology-Cell Physiology, 1999. **276**(1): p. C267-C278.
100. Romanello, M., et al., *Mechanically induced ATP release from human osteoblastic cells.* Biochemical and Biophysical Research Communications, 2001. **289**(5): p. 1275-1281.
101. Rumney, R.M.H., N. Wang, and A. Gartland, *The role of P2X(7) receptors in ATP release from osteoblasts.* Purinergic Signal, 2010. **6**(1): p. 129-129.
102. Weinbaum, S., S.C. Cowin, and Y. Zeng, *A Model for the Excitation of Osteocytes by Mechanical Loading-Induced Bone Fluid Shear Stresses.* Journal of Biomechanics, 1994. **27**(3): p. 339-360.
103. Gartland, A., *Regulation of ATP release from human osteoblasts: A calcium dependant, exocytotic vesicular mechanism.* Calcified Tissue International, 2006. **78**: p. S49-S49.
104. Mwaura, B.K., et al., *Release of ATP from human osteoblastic cell lines and primary osteoblasts occurs via exocytosis.* Bone, 2006. **38**(3): p. S11-S11.
105. RMH Rumney, et al., *ATPase activity and ATP release in osteoblast cultures.* Calcified Tissue International, 2009. **85**: p. 158-201.
106. Romanello, M., et al., *Autocrine/paracrine stimulation of purinergic receptors in osteoblasts: Contribution of vesicular ATP release.* Biochemical and Biophysical Research Communications, 2005. **331**(4): p. 1429-1438.
107. Larsen, W.J., *Biological Implications of Gap Junction Structure, Distribution and Composition - a Review.* Tissue & Cell, 1983. **15**(5): p. 645-671.
108. Stout, C.E., et al., *Intercellular calcium signaling in astrocytes via ATP release through connexin hemichannels.* Journal of Biological Chemistry, 2002. **277**(12): p. 10482-10488.
109. Cotrina, M.L., et al., *Connexins regulate calcium signaling by controlling ATP release.* Proceedings of the National Academy of Sciences of the United States of America, 1998. **95**(26): p. 15735-15740.

110. Huang, Y.J., et al., *The role of pannexin 1 hemichannels in ATP release and cell-cell communication in mouse taste buds.* Proceedings of the National Academy of Sciences of the United States of America, 2007. **104**(15): p. 6436-6441.
111. Baranova, A., et al., *The mammalian pannexin family is homologous to the invertebrate innexin gap junction proteins.* Genomics, 2004. **83**(4): p. 706-716.
112. Abraham, E.H., et al., *The Multidrug Resistance (Mdr1) Gene-Product Functions as an Atp Channel.* Proceedings of the National Academy of Sciences of the United States of America, 1993. **90**(1): p. 312-316.
113. Lovas, K., et al., *Glucocorticoid replacement therapy and pharmacogenetics in Addison's disease: effects on bone.* Eur J Endocrinol, 2009. **160**(6): p. 993-1002.
114. Shead, E.F., et al., *Cystic fibrosis transmembrane conductance regulator (CFTR) is expressed in human bone.* Thorax, 2007. **62**(7): p. 650-651.
115. Le Heron, L., et al., *Cystic fibrosis transmembrane conductance regulator (CFTR) regulates the production of osteoprotegerin (OPG) and prostaglandin (PG) E2 in human bone.* J Cyst Fibros, 2010. **9**(1): p. 69-72.
116. Suadicani, S.O., C.F. Brosnan, and E. Scemes, *P2X7 receptors mediate ATP release and amplification of astrocytic intercellular Ca2+ signaling.* Journal of Neuroscience, 2006. **26**(5): p. 1378-85.
117. Li, J., et al., *The P2X7 nucleotide receptor mediates skeletal mechanotransduction.* Journal of Biological Chemistry, 2005. **280**(52): p. 42952-9.
118. Poole, K.E. and J. Reeve, *Parathyroid hormone - a bone anabolic and catabolic agent.* Curr Opin Pharmacol, 2005. **5**(6): p. 612-7.
119. Partridge, N.C., et al., *Inhibitory effects of parathyroid hormone on growth of osteogenic sarcoma cells.* Calcif Tissue Int, 1985. **37**(5): p. 519-25.
120. Dempster, D.W., et al., *Anabolic actions of parathyroid hormone on bone.* Endocr Rev, 1993. **14**(6): p. 690-709.
121. Schiller, P.C., et al., *Anabolic or catabolic responses of MC3T3-E1 osteoblastic cells to parathyroid hormone depend on time and duration of treatment.* Journal of Bone and Mineral Research, 1999. **14**(9): p. 1504-12.
122. Dobnig, H. and R.T. Turner, *The effects of programmed administration of human parathyroid hormone fragment (1-34) on bone histomorphometry and serum chemistry in rats.* Endocrinology, 1997. **138**(11): p. 4607-12.
123. Sone, T., et al., *A small dose of human parathyroid hormone(1-34) increased bone mass in the lumbar vertebrae in patients with senile osteoporosis.* Miner Electrolyte Metab, 1995. **21**(1-3): p. 232-5.
124. Brommage, R., et al., *Daily treatment with human recombinant parathyroid hormone-(1-34), LY333334, for 1 year increases bone mass in ovariectomized monkeys.* J Clin Endocrinol Metab, 1999. **84**(10): p. 3757-63.
125. Dobnig, H. and R.T. Turner, *Evidence That Intermittent Treatment with Parathyroid-Hormone Increases Bone-Formation in Adult-Rats by Activation of Bone Lining Cells.* Endocrinology, 1995. **136**(8): p. 3632-3638.
126. Swarthout, J.T., et al., *Stimulation of extracellular signal-regulated kinases and proliferation in rat osteoblastic cells by parathyroid hormone is protein kinase C-dependent.* Journal of Biological Chemistry, 2001. **276**(10): p. 7586-7592.
127. Verheijen, M.H. and L.H. Defize, *Parathyroid hormone activates mitogen-activated protein kinase via a cAMP-mediated pathway independent of Ras.* Journal of Biological Chemistry, 1997. **272**(6): p. 3423-9.
128. Cole, J.A., *Parathyroid hormone activates mitogen-activated protein kinase in opossum kidney cells.* Endocrinology, 1999. **140**(12): p. 5771-5779.

129. Siddhanti, S.R., J.E. Hartle, 2nd, and L.D. Quarles, *Forskolin inhibits protein kinase C-induced mitogen activated protein kinase activity in MC3T3-E1 osteoblasts.* Endocrinology, 1995. **136**(11): p. 4834-41.
130. Verheijen, M.H.G. and L.H.K. Defize, *Parathyroid-Hormone Inhibits Mitogen-Activated Protein-Kinase Activation in Osteosarcoma Cells Via a Protein-Kinase a-Dependent Pathway.* Endocrinology, 1995. **136**(8): p. 3331-3337.
131. Jilka, R.L., et al., *Increased bone formation by prevention of osteoblast apoptosis with parathyroid hormone.* Journal of Clinical Investigation, 1999. **104**(4): p. 439-446.
132. Turner, P.R., et al., *Apoptosis mediated by activation of the G protein-coupled receptor for parathyroid hormone (PTH)/PTH-related protein (PTHrP).* Molecular Endocrinology, 2000. **14**(2): p. 241-254.
133. Juppner, H., *Receptors for parathyroid hormone and parathyroid hormone-related peptide: Exploration of their biological importance.* Bone, 1999. **25**(1): p. 87-90.
134. Jobert, A.S., et al., *Expression of alternatively spliced isoforms of the parathyroid hormone (PTH)/PTH-related peptide receptor messenger RNA in human kidney and bone cells.* Molecular Endocrinology, 1996. **10**(9): p. 1066-1076.
135. Swarthout, J.T., et al., *Parathyroid hormone-dependent signaling pathways regulating genes in bone cells.* Gene, 2002. **282**(1-2): p. 1-17.
136. Babich, M., et al., *Thrombin and Parathyroid-Hormone Mobilize Intracellular Calcium in Rat Osteosarcoma Cells by Distinct Pathways.* Endocrinology, 1991. **129**(3): p. 1463-1470.
137. Yamaguchi, D.T., C.R. Kleeman, and S. Muallem, *Protein kinase C-activated calcium channel in the osteoblast-like clonal osteosarcoma cell line UMR-106.* Journal of Biological Chemistry, 1987. **262**(31): p. 14967-73.
138. Yamaguchi, D.T., et al., *Parathyroid hormone-activated calcium channels in an osteoblast-like clonal osteosarcoma cell line. cAMP-dependent and cAMP-independent calcium channels.* Journal of Biological Chemistry, 1987. **262**(16): p. 7711-8.
139. Tyson, D.R., J.T. Swarthout, and N.C. Partridge, *Increased osteoblastic c-fos expression by parathyroid hormone requires protein kinase A phosphorylation of the cyclic adenosine 3 ',5 '-monophosphate response element-binding protein at serine 133.* Endocrinology, 1999. **140**(3): p. 1255-1261.
140. Fiol, C.J., et al., *A secondary phosphorylation of CREB341 at Ser129 is required for the cAMP-mediated control of gene expression. A role for glycogen synthase kinase-3 in the control of gene expression.* Journal of Biological Chemistry, 1994. **269**(51): p. 32187-93.
141. Tyson, D.R., et al., *PTH induction of transcriptional activity of the cAMP response element-binding protein requires the serine 129 site and glycogen synthase kinase-3 activity, but not casein kinase II sites.* Endocrinology, 2002. **143**(2): p. 674-82.
142. Clohisy, J.C., et al., *Parathyroid-Hormone Induces C-Fos and C-Jun Messenger-Rna in Rat Osteoblastic Cells.* Molecular Endocrinology, 1992. **6**(11): p. 1834-1842.
143. Koe, R.C., et al., *Parathyroid hormone versus phorbol ester stimulation of activator protein-1 gene family members in rat osteosarcoma cells.* Calcif Tissue Int, 1997. **61**(1): p. 52-8.
144. McCauley, L.K., et al., *Parathyroid hormone stimulates fra-2 expression in osteoblastic cells in vitro and in vivo.* Endocrinology, 2001. **142**(5): p. 1975-81.
145. Ruther, U., et al., *C-Fos Expression Induces Bone-Tumors in Transgenic Mice.* Oncogene, 1989. **4**(7): p. 861-865.
146. Johnson, R.S., B.M. Spiegelman, and V. Papaioannou, *Pleiotropic effects of a null mutation in the c-fos proto-oncogene.* Cell, 1992. **71**(4): p. 577-86.
147. Wang, Z.Q., et al., *Bone and haematopoietic defects in mice lacking c-fos.* Nature, 1992. **360**(6406): p. 741-5.
148. Grigoriadis, A.E., et al., *C-Fos - a Key Regulator of Osteoclast-Macrophage Lineage Determination and Bone Remodeling.* Science, 1994. **266**(5184): p. 443-448.

149. Otto, F., et al., *Cbfa1, a candidate gene for cleidocranial dysplasia syndrome, is essential for osteoblast differentiation and bone development.* Cell, 1997. **89**(5): p. 765-771.
150. Lee, B., et al., *Missense mutations abolishing DNA binding of the osteoblast-specific transcription factor OSF2/CBFA1 in cleidocranial dysplasia.* Nature Genetics, 1997. **16**(3): p. 307-10.
151. Partridge, N.C., et al., *Collagenase production by normal and malignant osteoblastic cells.* Frontiers of Osteosarcoma Research, ed. J.F. Novak and J.H. McMaster1993, Seattle U.S.A: Hogrefe and Huber.
152. Gack, S., et al., *Phenotypic Alterations in Fos-Transgenic Mice Correlate with Changes in Fos/Jun-Dependent Collagenase Type-I Expression - Regulation of Mouse Metalloproteinases by Carcinogens, Tumor Promoters, Camp, and Fos Oncoprotein.* Journal of Biological Chemistry, 1994. **269**(14): p. 10363-10369.
153. Johansson, N., et al., *Collagenase-3 (MMP-13) is expressed by hypertrophic chondrocytes, periosteal cells, and osteoblasts during human fetal bone development.* Developmental Dynamics, 1997. **208**(3): p. 387-397.
154. Lavoie, J.N., et al., *Cyclin D1 expression is regulated positively by the p42/p44MAPK and negatively by the p38/HOGMAPK pathway.* Journal of Biological Chemistry, 1996. **271**(34): p. 20608-16.
155. Weber, J.D., et al., *Sustained activation of extracellular-signal-regulated kinase 1 (ERK1) is required for the continued expression of cyclin D1 in G1 phase.* Biochemical Journal, 1997. **326 (Pt 1)**: p. 61-8.
156. Rosen, C.J. and J.P. Bilezikian, *Clinical review 123: Hot topic - Anabolic therapy for osteoporosis.* Journal of Clinical Endocrinology & Metabolism, 2001. **86**(3): p. 957-964.
157. Huang, N.H., D.J. Wang, and L.A. Heppel, *Extracellular ATP is a mitogen for 3T3 cell, 3T6-cell, and A-431 cell and acts synergistically with other growth factors.* Proc Natl Acad Sci, 1989. **86**: p. 7904-7908.
158. Wang, D.J., N.N. Huang, and L.A. Heppel, *Extracellular Atp and Adp Stimulate Proliferation of Porcine Aortic Smooth-Muscle Cells.* Journal of Cellular Physiology, 1992. **153**(2): p. 221-233.
159. Bowler, W.B., et al., *Signaling in human osteoblasts by extracellular nucleotides - Their weak induction of the c-fos proto-oncogene via Ca2+ mobilization is strongly potentiated by a parathyroid hormone/cAMP-dependent protein kinase pathway independently of mitogen-activated protein kinase.* Journal of Biological Chemistry, 1999. **274**(20): p. 14315-14324.
160. Buckley, K.A., et al., *Parathyroid hormone potentiates nucleotide-induced [Ca2+](i) release in rat osteoblasts independently of G(q) activation or cyclic monophosphate accumulation - A mechanism for localizing systemic responses in bone.* Journal of Biological Chemistry, 2001. **276**(12): p. 9565-9571.
161. Weskamp, M., W. Seidl, and S. Grissmer, *Characterization of the increase in [Ca-i(2+]) during hypotonic shock and the involvement of Ca2+-activated K+ channels in the regulatory volume decrease in human osteoblast-like cells.* Journal of Membrane Biology, 2000. **178**(1): p. 11-20.
162. Henney, N.C., et al., *A large-conductance (BK) potassium channel subtype affects both growth and mineralization of human osteoblasts.* Am J Physiol Cell Physiol, 2009. **297**(6): p. C1397-408.
163. Hoffmann, E.K., I.H. Lambert, and S.F. Pedersen, *Physiology of Cell Volume Regulation in Vertebrates.* Physiol Rev, 2009. **89**(1): p. 193-277.
164. Doyle, D.A., et al., *The structure of the potassium channel: molecular basis of K+ conduction and selectivity.* Science, 1998. **280**(5360): p. 69-77.
165. Patel, A. and E. Honore, *The TREK two P domain K+ channels.* Journal of Physiology-London, 2002. **539**(3): p. 647-647.
166. Shieh, C.C., et al., *Potassium channels: Molecular defects, diseases, and therapeutic opportunities.* Pharmacol Rev, 2000. **52**(4): p. 557-593.

167. Reimann, F. and F.M. Ashcroft, *Inwardly rectifying potassium channels.* Curr Opin Cell Biol, 1999. **11**(4): p. 503-8.
168. Lesage, F., *Pharmacology of neuronal background potassium channels.* Neuropharmacology, 2003. **44**(1): p. 1-7.
169. Hughes, S., et al., *Expression of the mechanosensitive 2PK+channel TREK-1 in human osteoblasts.* Journal of Cellular Physiology, 2006. **206**(3): p. 738-748.
170. Yellowley, C.E., et al., *Whole-cell membrane currents from human osteoblast-like cells.* Calcif Tissue Int, 1998. **62**(2): p. 122-32.
171. Kawase, T., et al., *Calcitonin gene-related peptide rapidly inhibits calcium uptake in osteoblastic cell lines via activation of adenosine triphosphate-sensitive potassium channels.* Endocrinology, 1996. **137**(3): p. 984-90.
172. Tertyshnikova, S., et al., *BL-1249 [(5,6,7,8-tetrahydro-naphthalen-1-yl)-[2-(1H-tetrazol-5-yl)-phenyl]-amine] : a putative potassium channel opener with bladder-relaxant properties.* J Pharmacol Exp Ther, 2005. **313**(1): p. 250-9.
173. Tainer, J.A., et al., *Structure and mechanism of copper, zinc superoxide dismutase.* Nature, 1983. **306**(5940): p. 284-7.
174. Borgstahl, G.E., et al., *The structure of human mitochondrial manganese superoxide dismutase reveals a novel tetrameric interface of two 4-helix bundles.* Cell, 1992. **71**(1): p. 107-18.
175. Davi, G., A. Falco, and C. Patrono, *Lipid peroxidation in diabetes mellitus.* Antioxid Redox Signal, 2005. **7**(1-2): p. 256-68.
176. Nunomura, A., et al., *Involvement of oxidative stress in Alzheimer disease.* J Neuropathol Exp Neurol, 2006. **65**(7): p. 631-41.
177. Van Gaal, L.F., I.L. Mertens, and C.E. De Block, *Mechanisms linking obesity with cardiovascular disease.* Nature, 2006. **444**(7121): p. 875-80.
178. Hitchon, C.A. and H.S. El-Gabalawy, *Oxidation in rheumatoid arthritis.* Arthritis Res Ther, 2004. **6**(6): p. 265-78.
179. Conwit, R.A., *Preventing familial ALS: A clinical trial may be feasible but is an efficacy trial warranted?* Journal of the Neurological Sciences, 2006. **251**(1-2): p. 1-2.
180. Al-Chalabi, A. and P.N. Leigh, *Recent advances in amyotrophic lateral sclerosis.* Curr Opin Neurol, 2000. **13**(4): p. 397-405.
181. Muller, F., et al., *Absence of Cu,Zn-Sod causes severe oxidative stress and acceleration of age-dependent skeletal muscle atrophy.* Free Radical Biology and Medicine, 2005. **39**: p. S127-S127.
182. Elchuri, S., et al., *CuZnSOD deficiency leads to persistent and widespread oxidative damage and hepatocarcinogenesis later in life.* Oncogene, 2005. **24**(3): p. 367-80.
183. Wang, X., et al., *Knockouts of Se-glutathione peroxidase-1 and Cu,Zn superoxide dismutase exert different impacts on femoral mechanical performance of growing mice.* Mol Nutr Food Res, 2008. **52**(11): p. 1334-9.
184. Phillis, J.W., M.H. O'Regan, and L.M. Perkins, *Adenosine 5'-triphosphate release from the normoxic and hypoxic in vivo rat cerebral cortex.* Neuroscience Letters, 1993. **151**(1): p. 94-6.
185. Melani, A., et al., *ATP extracellular concentrations are increased in the rat striatum during in vivo ischemia.* Neurochem Int, 2005. **47**(6): p. 442-8.
186. Gandelman, M., et al., *Extracellular ATP and the P2X7 receptor in astrocyte-mediated motor neuron death: implications for amyotrophic lateral sclerosis.* J Neuroinflammation, 2010. **7**: p. 33.
187. Gartland, A., et al., *Isolation and culture of human osteoblasts.* Methods Mol Med, 2005. **107**: p. 29-54.
188. Livak, K.J. and T.D. Schmittgen, *Analysis of relative gene expression data using real-time quantitative PCR and the 2(-Delta Delta C(T)) Method.* Methods, 2001. **25**(4): p. 402-8.

189. Karlen, Y., et al., *Statistical significance of quantitative PCR.* BMC Bioinformatics, 2007. **8**: p. 131.
190. Nolan, T., R.E. Hands, and S.A. Bustin, *Quantification of mRNA using real-time RT-PCR.* Nature Protocols, 2006. **1**(3): p. 1559-1582.
191. Holton, P., *The liberation of adenosine triphosphate on antidromic stimulation of sensory nerves.* J Physiol, 1959. **145**(3): p. 494-504.
192. Abood, L.G., S. Miyamoto, and K. Koketsu, *Outflux of Various Phosphates during Membrane Depolarization of Excitable Tissues.* American Journal of Physiology, 1962. **202**(3): p. 469-&.
193. Detwiler, T.C. and R.D. Feinman, *Kinetics of the thrombin-induced release of adenosine triphosphate by platelets. Comparison with release of calcium.* Biochemistry, 1973. **12**(13): p. 2462-8.
194. Bergfeld, G. and T. Forrester, *Efflux of Adenosine-Triphosphate from Human-Erythrocytes in Response to a Brief Pulse of Hypoxia.* Journal of Physiology-London, 1989. **418**: p. P88-P88.
195. Maugeri, N., E. Bermejo, and M.A. Lazzari, *Adenosine-Triphosphate Released from Human Mononuclear-Cells.* Thrombosis Research, 1990. **59**(5): p. 887-890.
196. Queiroz, G., et al., *A study of the mechanism of the release of ATP from rat cortical astroglial cells evoked by activation of glutamate receptors.* Neuroscience, 1999. **91**(3): p. 1171-1181.
197. Lalevee, N., et al., *Acute effects of adenosine triphosphates, cyclic 3 ',5 '-adenosine monophosphates, and follicle-stimulating hormone on cytosolic calcium level in cultured immature rat Sertoli cells.* Biology of Reproduction, 1999. **61**(2): p. 343-352.
198. Graff, R.D., et al., *ATP release by mechanically loaded porcine chondrons in pellet culture.* Arthritis and Rheumatism, 2000. **43**(7): p. 1571-1579.
199. Bowler, W.B., et al., *Extracellular ATP enhances parathyroid hormone induced c-fos expression in human osteoblasts.* Journal of Bone and Mineral Research, 1997. **12**: p. F357-F357.
200. Nakamura, E., et al., *ATP activates DNA synthesis by acting on P2X receptors in human osteoblast-like MG-63 cells.* American Journal of Physiology-Cell Physiology, 2000. **279**(2): p. C510-C519.
201. Hoebertz, A., et al., *Extracellular ADP is a powerful osteolytic agent: evidence for signaling through the P2Y(1) receptor on bone cells.* Faseb Journal, 2001. **15**(7): p. 1139-1148.
202. Panupinthu, N., et al., *P2X7 receptors on osteoblasts couple to production of lysophosphatidic acid: a signaling axis promoting osteogenesis.* Journal of Cell Biology, 2008. **181**(5): p. 859-871.
203. Gartland, A., et al., *Purinergic signalling in osteoblasts.* Front Biosci, 2012. **17**: p. 16-29.
204. Wood, C. and J.A. Gallagher, *Tornado F3 conversion of publications data to AECMA (Association Europeenne des Constructeurs de Materiel Aerospatial) 1000D - A case study.* Sgml Europe '97 - Conference Proceedings, 1997: p. 27-30.
205. Smalt, R., et al., *Induction of NO and prostaglandin E2 in osteoblasts by wall-shear stress but not mechanical strain.* American Journal of Physiology, 1997. **273**(4 Pt 1): p. E751-8.
206. Basso, N. and J.N. Heersche, *Characteristics of in vitro osteoblastic cell loading models.* Bone, 2002. **30**(2): p. 347-51.
207. Thompson, W.R., C.T. Rubin, and J. Rubin, *Mechanical regulation of signaling pathways in bone.* Gene, 2012. **503**(2): p. 179-93.
208. Cui, Y., et al., *Lrp5 functions in bone to regulate bone mass.* Nature Medicine, 2011. **17**(6): p. 684-91.
209. Scheven, B.A., D. Marshall, and R.M. Aspden, *In vitro behaviour of human osteoblasts on dentin and bone.* Cell Biology International, 2002. **26**(4): p. 337-46.
210. Grigoriadis, A.E., Z.Q. Wang, and E.F. Wagner, *Fos and Bone Cell-Development - Lessons from a Nuclear Oncogene.* Trends in Genetics, 1995. **11**(11): p. 436-441.

211. Lee, S.K. and J.A. Lorenzo, *Parathyroid hormone stimulates TRANCE and inhibits osteoprotegerin messenger ribonucleic acid expression in murine bone marrow cultures: Correlation with osteoclast-like cell formation.* Endocrinology, 1999. **140**(8): p. 3552-3561.
212. Rodan, G.A. and T.J. Matin, *Role of Osteoblasts in Hormonal-Control of Bone-Resorption - a Hypothesis.* Calcified Tissue International, 1981. **33**(4): p. 349-351.
213. Pacheco-Pantoja, E.L., et al., *Expression of gut hormone receptors in different stages of osteoblastic development.* Calcified Tissue International, 2008. **82**: p. S114-S114.
214. Sanchez-Fernandez, M.A., et al., *Osteoclasts Control Osteoblast Chemotaxis via PDGF-BB/PDGF Receptor Beta Signaling.* Plos One, 2008. **3**(10).
215. Kreja, L., et al., *Non-Resorbing Osteoclasts Induce Migration and Osteogenic Differentiation of Mesenchymal Stem Cells.* Journal of Cellular Biochemistry, 2010. **109**(2): p. 347-355.
216. Teitelbaum, S.L., *Bone resorption by osteoclasts.* Science, 2000. **289**(5484): p. 1504-1508.
217. Arnett, T.R., et al., *Hypoxia Stimulates Vesicular ATP Release From Rat Osteoblasts.* Journal of Cellular Physiology, 2009. **220**(1): p. 155-162.
218. Garimella, R., et al., *Expression and synthesis of bone morphogenetic proteins by osteoclasts: A possible path to anabolic bone remodeling.* Journal of Histochemistry & Cytochemistry, 2008. **56**(6): p. 569-577.
219. Hui, D., et al., *Development and test of 10.5 kV/1.5 kA HTS fault current limiter.* Ieee Transactions on Applied Superconductivity, 2006. **16**(2): p. 687-690.
220. Short, A.D. and C.W. Taylor, *Parathyroid hormone controls the size of the intracellular Ca2+ stores available to receptors linked to inositol trisphosphate formation.* Journal of Biological Chemistry, 2000. **275**(3): p. 1807-1813.
221. Genetos, D.C., H.J. Donahue, and R.L. Duncan, *Fluid flow-induced ATP release occurs by a vesicular mechanism and mediates prostaglandin release.* Journal of Bone and Mineral Research, 2004. **19**: p. S237-S237.
222. Ruan, Y.C., et al., *Regulation of smooth muscle contractility by the epithelium in rat vas deferens: role of ATP-induced release of PGE(2).* Journal of Physiology-London, 2008. **586**(20): p. 4843-4857.
223. Ulmann, L., H. Hirbec, and F. Rassendren, *P2X4 receptors mediate PGE2 release by tissue-resident macrophages and initiate inflammatory pain.* Embo Journal, 2010. **29**(14): p. 2290-2300.
224. Xia, M.S. and Y. Zhu, *Signaling Pathways of ATP-Induced PGE2 Release in Spinal Cord Astrocytes are EGFR Transactivation-Dependent.* Glia, 2011. **59**(4): p. 664-674.
225. Fitzgerald, J., T.J. Dietz, and M. Hughes-Fulford, *Prostaglandin E-2-induced up-regulation of c-fos messenger ribonucleic acid is primarily mediated by 3 ',5 '-cyclic adenosine monophosphate in MC3T3-E-1 osteoblasts.* Endocrinology, 2000. **141**(1): p. 291-298.
226. Gerritsen, M.E., et al., *Arachidonic-Acid Metabolism by Cultured Bovine Corneal Endothelial-Cells.* Investigative Ophthalmology & Visual Science, 1989. **30**(4): p. 698-705.
227. Schofl, C., et al., *Evidence for P2-purinoceptors on human osteoblast-like cells.* Journal of Bone and Mineral Research, 1992. **7**(5): p. 485-91.
228. Carruthers, A.M., et al., *Adenosine A(1) receptor-mediated inhibition of calcitonin gene-related peptide release from rat trigeminal neurones.* British Journal of Pharmacology, 2001. **133**: p. U27-U27.
229. Dixon, S.J., J.E. Aubin, and J. Dainty, *Electrophysiology of a clonal osteoblast-like cell line: evidence for the existence of a Ca2+-activated K+ conductance.* J Membr Biol, 1984. **80**(1): p. 49-58.
230. Hirukawa, K., et al., *Electrophysiological Properties of a Novel Ca2+-Activated K+ Channel Expressed in Human Osteoblasts.* Calcified Tissue International, 2008. **83**(3): p. 222-229.
231. Yellowley, C.E., et al., *Whole-cell membrane currents from human osteoblast-like cells.* Calcified Tissue International, 1998. **62**(2): p. 122-132.

232. Chen, X., et al., *Stretch-induced PTH-related protein gene expression in osteoblasts.* Journal of Bone and Mineral Research, 2005. **20**(8): p. 1454-61.
233. Moreau, R., et al., *Pharmacological and biochemical evidence for the regulation of osteocalcin secretion by potassium channels in human osteoblast-like MG-63 cells.* Journal of Bone and Mineral Research, 1997. **12**(12): p. 1984-92.
234. Moreau, R., et al., *Activation of maxi-K channels by parathyroid hormone and prostaglandin E2 in human osteoblast bone cells.* J Membr Biol, 1996. **150**(2): p. 175-84.
235. Civitelli, R., et al., *Membrane-Potential and Cation Content of Osteoblast-Like Cells (Umr-106) Assessed by Fluorescent Dyes.* Journal of Cellular Physiology, 1987. **131**(3): p. 434-441.
236. Murrills, R.J., et al., *Parathyroid hormone synergizes with non-cyclic AMP pathways to activate the cyclic AMP response element.* Journal of Cellular Biochemistry, 2009. **106**(5): p. 887-95.
237. Beauvais, F., L. Michel, and L. Dubertret, *Human Eosinophils in Culture Undergo a Striking and Rapid Shrinkage during Apoptosis - Role of K+ Channels.* Journal of Leukocyte Biology, 1995. **57**(6): p. 851-855.
238. Krick, S., et al., *Activation of K+ channels induces apoptosis in vascular smooth muscle cells.* American Journal of Physiology-Cell Physiology, 2001. **280**(4): p. C970-C979.
239. Olesen, S.P., et al., *Selective activation of Ca(2+)-dependent K+ channels by novel benzimidazolone.* European Journal of Pharmacology, 1994. **251**(1): p. 53-9.
240. Edwards, G., et al., *Ion channel modulation by NS 1619, the putative BKCa channel opener, in vascular smooth muscle.* Br J Pharmacol, 1994. **113**(4): p. 1538-47.
241. Forwood, J.K., M.H.C. Lam, and D.A. Jans, *Nuclear import of CREB and AP-1 transcription factors requires importin-beta 1 and Ran but is independent of importin-alpha.* Biochemistry, 2001. **40**(17): p. 5208-5217.
242. Henney, N.C., et al., *A large-conductance (BK) potassium channel subtype affects both growth and mineralization of human osteoblasts.* American Journal of Physiology-Cell Physiology, 2009. **297**(6): p. C1397-C1408.
243. Qi, J., et al., *ATP reduces gel compaction in osteoblast-populated collagen gels.* Journal of Applied Physiology, 2007. **102**(3): p. 1152-1160.
244. Yamauchi, J., et al., *Tacrolimus but not cyclosporine A enhances FGF-2-induced VEGF release in osteoblasts.* Int J Mol Med, 2009. **23**(2): p. 267-72.

Appendix

Given the changes that have been implicated as a result of this investigation a new protocol for ATP measurement after fluid perturbation in 6 well plates has been written and is shown below:-

Remove DMEM from wells, wash twice in PBS and add HEPES buffered medium.

Leave at 37^{o}C for one hour for basal levels of ATP to be reached (as ATP is released upon medium changing).

Take out NMR from -20^{O}C and defrost.

Pipette out enough NMR into luminometer tubes for a 10:1 reaction with supernatant.10µl will usually be enough as it is standard to remove 100µl.

Place tubes with NMR on ice to cool.

Using the 6-well lid with holes in sample 3 times (100µl) from each well to get an average basal ATP reading.

To perform a medium displacement first take up medium from centre of well. For a 6 well use 1000 µl although this can be changed as you see fit. Then displace the medium against the side wall of the well to ensure there isn't a large 'blast' on a certain section of cells. This will cause a wave across the well. It is important not to touch the bottom of the well with the pipette tip as this may damage the cells.

Perform the number of medium displacements you need. Given the fact that to reduce the variation multiple repeats of the same number would be needed it would be wise to just do the same number of medium displacements across the whole well rather than staggering it.

As soon as the medium displacements have ended in one well sample 3 times (100 µl) from the medium.

When finished with sampling, take tubes still on ice and start the luminometer.
No matter how many tubes are present take 5 out of the ice and place in luminometer for 4 minutes, then read.

Do this for all samples and then put together the results. This ensures tubes are at the same temperature when read.